

## INFORMATION TO USERS

This manuscript has been reproduced from the microfilm master. UMI films the text directly from the original or copy submitted. Thus, some thesis and dissertation copies are in typewriter face, while others may be from any type of computer printer.

**The quality of this reproduction is dependent upon the quality of the copy submitted.** Broken or indistinct print, colored or poor quality illustrations and photographs, print bleedthrough, substandard margins, and improper alignment can adversely affect reproduction.

In the unlikely event that the author did not send UMI a complete manuscript and there are missing pages, these will be noted. Also, if unauthorized copyright material had to be removed, a note will indicate the deletion.

Oversize materials (e.g., maps, drawings, charts) are reproduced by sectioning the original, beginning at the upper left-hand corner and continuing from left to right in equal sections with small overlaps. Each original is also photographed in one exposure and is included in reduced form at the back of the book.

Photographs included in the original manuscript have been reproduced xerographically in this copy. Higher quality 6" x 9" black and white photographic prints are available for any photographs or illustrations appearing in this copy for an additional charge. Contact UMI directly to order.

# UMI

A Bell & Howell Information Company  
300 North Zeeb Road, Ann Arbor MI 48106-1346 USA  
313/761-4700 800/521-0600

**IRON OXIDE MINERALOGY OF SOILS DERIVED FROM VOLCANIC  
ROCKS IN THE PARANÁ RIVER BASIN, BRAZIL**

**DISSERTATION**

Presented in Partial Fulfillment of the Requirements for the  
Degree Doctor of Philosophy in the Graduate School of  
The Ohio State University

By

Antonio Carlos Saraiva da Costa, M.S.

\* \* \* \* \*

The Ohio State University

1996

Dissertation Committee:

Dr. Jerry M. Bigham

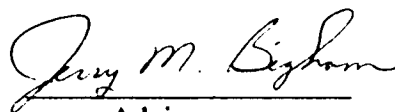
Dr. Neil E. Smeck

Dr. George F. Hall

Dr. Samuel J. Traina

Dr. Gunter Faure

Approved by:



Adviser

Graduate Program in Agronomy

UMI Number: 9630874

Copyright 1996 by  
Costa, Antonio Carlos Saraiva da

All rights reserved.

---

UMI Microform 9630874  
Copyright 1996, by UMI Company. All rights reserved.

This microform edition is protected against unauthorized  
copying under Title 17, United States Code.

---

**UMI**  
300 North Zeeb Road  
Ann Arbor, MI 48103

## **ABSTRACT**

Soils derived from volcanic rocks in the Paraná River Basin were studied to evaluate the influence of various soil forming factors on the genesis and distribution of iron oxides and clay minerals. These minerals were identified and characterized using chemical dissolution procedures, magnetic susceptibility, X-ray diffraction and thermal analysis techniques. The soils were formed from two different types of rocks, including basic rocks (basaltic-andesite and transitional basalt) with SiO<sub>2</sub> contents less than 53% and acid/intermediate rocks (latite, rhyodacite and dacite) with SiO<sub>2</sub> contents greater than 53%. The silicate clay mineralogy was always dominated by kaolinite, but variable amounts of 2:1 clay minerals (vermiculite and/or smectite) were also present depending upon the landscape position and the associated degree of soil weathering. The 2:1 clay minerals in young soils derived from basalt (Brunizem Avermelhado, Solos Litólicos) were often interstratified with kaolinite or halloysite. Less interstratification but more hydroxy-Al-interlayering was observed in 2:1 minerals from the highly weathered profiles (Terra Roxa, Terra Bruna, Latossolo). On comparable landscape positions and at similar stages of weathering, the acid/intermediate rock soils usually contained more kaolinite than those soils derived from basic rocks.

The percentage of gibbsite in the basic rock soils was correlated with soil chemistry and the degree of weathering.

The type and distribution of iron oxide minerals were also strongly influenced by the parent rock and the degree of soil weathering. Hematite and maghemite were the dominant iron oxide minerals in the highly weathered soils formed from basic rocks; maghemite comprised almost 50% of the total iron oxides in some Latossolo. Significant amounts of goethite were found in very young profiles and in saprolites formed from basalt. Goethite was also the dominant iron oxide in all soils developed on acid/intermediate rocks. Comparisons of well drained Latossolo profiles formed from basalt showed that regional climatic gradients in mean annual temperature and excess water were not the primary factors influencing the distribution of iron oxide minerals. Hematite and maghemite were always the dominant phases, and some samples contained no X-ray detectable goethite. The soil iron oxides exhibited Al-for-Fe substitutions that were within the ranges defined by earlier investigators. Aluminum substitution was not significantly influenced by the parent rock material and was only weakly correlated with the soil pH and percentage of gibbsite.

**Este trabalho é dedicado a meu pai Sr. Antonio Saraiva da Costa e a minha mãe  
Sra. Arcelina Figueiredo da Costa como forma de agradecimento por tudo  
aquilo que vocês fizeram e representam para mim**

**In special, I dedicate this work to my wife Norma and our kids, Maria Clara and Daniel  
for the last 10 years and more to come**

## ACKNOWLEDGMENTS

I greatly appreciate the orientation, encouragement, ideas and support provided by my advisor, Dr. Jerry M. Bigham during my stay at the Ohio State University. I deeply appreciate Dr. Bigham for the last quarter for helping me to bring my “portuguenglish” writing to what I consider a fine final dissertation. I would like also to thank Dr. George F. Hall, Dr. Gunter Faure, Dr. Sam J. Traina and Dr. Neil E. Smeck and Dr Rodney T. Tettenhorst for their help throughout this period. During the last 5 years several other people were really important for this achievement. To my professors Dr. Luiz I. Demattê and Dr. Rafael R. Aloisi the early help filling out forms for my application and the discussion of what should be done. To Dr. J. L. I. Demattê a special thanks for telling me so incisively “Olhe para a rocha”. I thank my colleagues at the Universidade Estadual de Maringá for their support in laboratory and paper work. Special thanks to Sr. Cassio A. Tormena and my father-in-law Sr. Carlos José de Melo for spending their time with my documents, contracts and correspondences in Brazil. Thanks to the people from our soil fertility lab (FUEM) for the basic soil characterization data. I also thank colleagues and their employees from COAMO, IAPAR, EMATER and FUEM who helped me digging pits, cleaning up profiles during the soil sampling in 1993 throughout the state of Paraná.

I thank the colleagues that sent me soil materials and those who kindly let me characterize their soils. I also thank Dr. Fred Rhoton for letting me use his magnetic susceptibility meter at the facilities of the USDA - Oxford, MI and Dr. Donald F. Post (The University of Arizona) for letting me use his color meter. At the Ohio State special thanks to Mr. Sandy F. Jones for the total carbon analysis and being always open to discuss topics related and not related to soil science and helping me with several chemical and physical characterizations. Thanks to Mr. Ubaldo Soto for the total chemical analysis of my soil clays. In the last 5 years I have shared the classroom and lab space with very nice people who helped me with my “portuguenglish” and to pass through labs and finals. I had a lot of fun. Thanks to Mr. Randy Fowler, and the other colleagues of the fourth floor at Kottman Hall for the good time. I would like also to thank my university, Fundação Universidade Estadual de Maringá, for granting me leave of absence during my studies at the Ohio State University. Financial support for my studies were provided by CAPES - Brazil (Coordenadoria de Aperfeiçoamento de Pessoal de Nível Superior) and the Ohio State in the last six months is greatly appreciated. For all Americans (Latinos and non Latinos) friends and the other colleagues in this rather cosmopolitan environment who shared their family time with us I'd like to finish saying that may God (whoever you conceive Him to be) give you in double what you gave us. Thanks.

## **VITA**

- September 1, 1959                      **Born - São Paulo - Brazil**
- February , 1982                        **B.Sc., Escola Superior de Agricultura “Luiz de Queiroz”  
Universidade de São Paulo - USP, Piracicaba-SP-Brazil**
- September, 1986                        **M.S., Escola Superior de Agricultura “Luiz de Queiroz”  
Universidade de São Paulo - USP, Piracicaba-SP-Brazil**
- 1985 - 1987                                **Instituto Agronômico do Paraná-IAPAR  
Seção de Solos - Soil Researcher, Londrina - Pr - Brazil**
- 1988                                         **Escola Superior de Agricultura “Luiz de Queiroz”  
Universidade de São Paulo  
Assistant Professor - Departamento de Solos  
Piracicaba - SP - Brazil**
- 1989 - nd                                    **Fundação Universidade Estadual de Maringá - FUEM  
Assistant Professor - Departamento de Agronomia - DAG  
Maringá - Pr - Brazil**
- 1996                                         **Graduate Research Associate  
Department of Agronomy  
The Ohio State University  
Columbus-OH-USA**

## **PUBLICATIONS**

- Costa, A. C. S.; J. M. Bigham, and S. J. Traina. 1995. Mineralogy of oxisols after application of sequential dissolution procedure. Proceedings of the V. M. Goldschmidt Conference. Abstracts p. 39.
- Maurice, P., S. J. Traina, and A. C. S. Costa. 1995. From atoms to oxisols: AFM of hydrous Fe(III) oxides. Proceedings of the V. M. Goldschmidt Conference. Abstracts p. 709.
- Costa, A. C. S., J. M. Bigham, G. F. Hall, and S. J. Traina. 1994. Mineralogy of soils developed from basalts under isoclimatic conditions in southern Brazil. Agronomy Abstracts p. 408.

## **FIELDS OF STUDY**

Major Field: Agronomy

Specialization : Soil Mineralogy

Studies in Soil Science. Professors J. M. Bigham; G. F. Hall; S. J. Traina.

Studies in Geology and Mineralogy. Professors G. Faure, R. T. Tettenhorst.

Studies in Chemistry. Professors J. Parson, A. A. Wojciki, E. P. Schram.

## TABLE OF CONTENTS

	<u>Page</u>
ABSTRACT.....	ii
DEDICATION.....	iv
ACKNOWLEDGMENTS.....	v
VITA.....	vii
LIST OF TABLES.....	xii
LIST OF FIGURES.....	xv
Chapters .....	
1. INTRODUCTION AND OBJECTIVES.....	1
2. DESCRIPTION OF THE STUDY AREA.....	5
2.1. Geology of the Paraná River Basin.....	5
2.2. Physiography and geology of Paraná state.....	11
2.3. Climate.....	14
2.4. Vegetation.....	17
2.5. Soils.....	18
3. LITERATURE REVIEW.....	23
3.1. Iron oxide minerals: structure and composition.....	24
3.2. Iron oxide minerals: magnetic properties.....	31
3.3. Iron oxides in soils.....	35
3.4. Iron oxides : influence on soil characteristics.....	38
3.5. Iron oxides : factors of soil formation.....	46
4. MATERIALS AND METHODS.....	52
4.1. Rock samples.....	53
4.2. Soil samples.....	55
4.2.1. Soil toposequences.....	55
4.2.2. Soil climosequences.....	58
4.3. Rock characterization.....	60
4.3.1. Total chemical analysis.....	60
4.3.2. X-ray diffraction.....	60
4.3.3. Magnetic susceptibility.....	61

4.3.4. Thin section.....	62
4.4. Soil characterization.....	63
4.4.1. Profile description and sampling.....	63
4.4.2. Particle size distribution.....	63
4.4.3. Total carbon content.....	64
4.4.4. pH, exchangeable cations, and exchangeable acidity.....	64
4.4.5. Magnetic susceptibility.....	65
4.4.6. Color.....	66
4.5. Mineralogy of the clay fraction.....	66
4.5.1. Sample fractionation.....	66
4.5.2. Na-citrate-bicarbonate-dithionite extraction.....	67
4.5.3. Acid ammonium oxalate extraction.....	68
4.5.4. Magnetic susceptibility.....	68
4.5.5. Color.....	68
4.5.6. Silicate clay mineralogy.....	69
4.5.6.1. X-ray diffraction.....	69
4.5.6.2. Thermal analysis.....	70
4.5.6.3. Magnetic Susceptibility.....	72
4.6. Iron oxide mineralogy.....	72
4.6.1. Boiling 5M NaOH procedure.....	72
4.6.2. Selective dissolution of maghemite.....	73
4.6.3. X-ray diffraction analysis.....	74
4.6.4. Magnetic susceptibility.....	76
4.7. Mass balance of the clay fraction.....	76
<b>5. RESULTS AND DISCUSSION.....</b>	<b>76</b>
5.1. The parent rock material.....	78
5.2. Soil toposequences.....	89
5.2.1. Morphological characteristics and landscape relationships.....	89
5.2.2. Physical and chemical characteristics.....	95
5.2.3. Magnetic properties of the soil fractions.....	100
5.2.4. Classification of the soils.....	104
5.3. Clay mineralogy of the toposequence soils.....	106
5.3.1. Quantitative analysis of major mineral groups.....	106
5.3.2. The 1:1 clay minerals.....	120
5.3.3. The 2:1 clay minerals.....	126
5.3.4. Gibbsite.....	131
5.4. Iron oxide mineralogy.....	134
5.4.1. Selective dissolution of the iron oxides.....	135
5.4.2. Identification of iron oxides in the soil clay fraction.....	138
5.4.3. Quantification of iron oxides minerals in the soil clay fraction by XRD.....	140
5.4.4. Quantification of maghemite using magnetic susceptibility.....	144
5.4.5. Iron oxides and clay color.....	151

5.4.6. Al-substitution in the soil oxides.....	155
5.4.7. The influence of lithology on iron oxide mineralogy.....	170
5.4.8. Iron oxides and degree of soil weathering (Basalt soils).....	178
5.4.9. The influence of climate on iron oxide mineralogy.....	184
<b>6. CONCLUSIONS.....</b>	<b>189</b>
<b>LIST OF REFERENCES.....</b>	<b>196</b>
<b>APPENDICES.....</b>	
<b>APPENDIX A. Soil morphological descriptions.....</b>	<b>221</b>
<b>APPENDIX B. Soil chemical, physical and mineralogical data.....</b>	<b>241</b>

## LIST OF TABLES

Table	Page
2.1. Petrography of the three major types of volcanic rocks from the Paraná continental flood volcanism (Piccirillo et al., 1988).....	9
2.2. Color , Ki value, magnetic attraction and Fe <sub>2</sub> O <sub>3</sub> contents of the main soils derived from rocks of the Paraná flood volcanism (EMBRAPA, 1984)...	20
2.3. Classification of soils according to the U.S. Taxonomy (Soil Survey Staff, 1975) and the Brazilian system (EMBRAPA, 1984). Major changes in the U.S. system have since been made (Soil Survey Staff, 1994).....	20
2.4. Distribution of soils according to climate and physiographic region on the third plateau of the state of Paraná (EMBRAPA, 1984).....	22
3.1. List of materials / minerals according to their magnetic character, chemical formula, iron content and magnetic susceptibility. Modified from Dearing (1994).....	33
3.2. Distribution of single and multidomain particles according to their frequency dependent magnetic susceptibility ( $\chi_{fd}\%$ ).After Dearing (1994).....	35
3.3. Mass specific ( $\chi_{tr}$ ) and volumetric ( $\kappa$ ) magnetic susceptibility for selected parent rock materials.....	42
3.4. Magnetic susceptibility ( $10^{-8} \bullet m^3/Kg$ ) of soils and soil fractions derived from different parent materials. ....	44
3.5. Specific surface area ( $m^2/g$ ) of soil Fe-oxides (Schwertmann, 1988).....	46
4.1. Location and source of parent rock materials analyzed in this study.....	55
4.2. Profile, location, parent material and classification of soil profiles.....	57

4.3. Altitudes, climatic conditions, and climatic classification according to the Koeppen system for the climosequence sites in the states of Paraná (IAPAR, 1994) and São Paulo (Setzer, 1966).....	59
4.4. Influence of saturating cation, solvating agent, and thermal treatment on diagnostic d-spacings of the most important clay minerals, quartz and gibbsite	71
5.1. Total chemical analysis of the parent rock material and classification according to De La Roche (1980).....	83
5.2. Average values of major and minor elements from Table 5.1. and from Bellieni et al. (1984b). Numbers of samples given in parentheses. Acid and basic rock data from Bellieni et al. (1984b) are for rhyodacites and basaltic andesites, respectively.....	84
5.3. Magnetic susceptibility ( $\chi_{lf}$ ) of the ground rock samples.....	88
5.4. Summary of important soil chemical and physical attributes in the toposequences sampled.....	97
5.5. Classification of the toposequence soils according to the Brazilian (Camargo et al., 1987) and U. S. (Soil Survey Staff, 1994) systems of soil classification .....	105
5.6. Magnetic susceptibility ( $\chi_{lf}$ ) of selected CBD - treated clay samples.....	107
5.7. Proportions of minerals in clays from the toposequence soils. $Fe_2O_3$ determined by CBD extraction. Kao and Gb determined by TGA analysis.....	109
5.8. Width at half height (WHH) and position of diagnostic XRD peaks for the CBD - treated clays.....	122
5.9. Temperature of diagnostic DTA peaks for the clay size fraction gibbsite and kaolinite.....	125
5.10. CBD-extractable iron ( $Fe_d$ ) and aluminum ( $Al_d$ ), oxalate-extractable iron ( $Fe_o$ ) and aluminum ( $Al_o$ ) and total iron ( $Fe_t$ ) in clays from the toposequence soils.....	136

5.11. Average values (AV) and standard deviation (SD) for CBD - extractable iron (Fed) and aluminum (Ald), oxalate-extractable iron (Feo) and aluminum (Alo), and total iron extraction (Fet) in clays from the highly weathered (LR, LB, TR, TB) and less weathered soils (BAv, R, C) of the five toposequences.....	137
5.12. Proportion of maghemite (Mm); goethite (Gt); hematite (Hm) in the 5 NaOH concentrates as measured by X-ray diffraction peak area.....	143
5.13. Mole % Al substitution in goethite, hematite and maghemite determined from XRD peak positions.....	161

## LIST OF FIGURES

Figure	Page
2.1. The Paraná River Basin in South America Modified from Petri and Fúlfaro (1983).....	6
2.2. The Paraná River Basin within the southern region of Brazil, showing the states of Mato Grosso do Sul (MS), Mato Grosso (Mt), Goiás (Go), Minas Gerais (MG), São Paulo (SP), Paraná (Pr), Santa Catarina (SC), and Rio Grande do Sul (RS).....	7
2.3. Distribution of volcanic rocks in the states of Goiás (Go), Minas Gerais (MG), Mato Grosso do Sul (MS), São Paulo (SP), Paraná (Pr), Santa Catarina (SC), and Rio Grande do Sul (RS). Modified from Piccirillo et al. (1988).....	10
2.4. Major stratigraphic units in Paraná. Modified from Mineropar (1986).....	12
2.5. Physiographic regions of Paraná. Modified from EMBRAPA (1984).....	13
2.6. Distribution of the Koeppen climatic types in Paraná. Terms defined in section 2.3. Modified from IAPAR (1994).....	16
4.1. Toposequences sampled in Paraná state.....	54
4.2. Distribution of all sampling sites and previous work in the Paraná River Basin.....	56
5.1. Thin sections of the acid / intermediate (Tamarana) and basic rock (Ibiporã). Frame width 13.4 mm.....	80
5.2. Representative XRD patterns from the acid/intermediate (Tamarana) and basic (Ibiporã and Londrina) rock samples. Ch=chlorite; Pl=plagioclase feldspar; Qz=quartz; Py=pyroxene; Mg=magnetite; Uv=ulvöspinel.....	81

5.3. Distribution of volcanic rocks in the Paraná River Basin using the classification diagram of De La Roche et al. (1980) from Bellieni et al. (1984b).....	85
5.4. Distribution of volcanic rocks collected in the current study using the De La Roche et al. (1980) diagram.....	86
5.5. Cross section of the five soil toposequences.....	93
5.6. Relationship between magnetic susceptibility ( $\chi_{lf}$ ) of the 2 mm fraction with the silt, sand and clay size fractions of the basic rock soils.....	101
5.7. Relationship between frequency dependent magnetic susceptibility ( $\chi_{fd}\%$ ) of the 2mm fraction with the silt, sand and clay size fractions of the basic rocks.....	102
5.8. Magnetic susceptibility ( $\chi_{lf}$ ) of the 2mm fraction and percentage of maghemite in the clay fraction from basic and acid / intermediate volcanic rock soils.....	103
5.9. X-ray diffraction patterns from selected CBD-treated clays.....	110
5.10. DTA patterns from selected CBD-treated clays.....	117
5.11. Correlation between percentages of kaolinite, gibbsite, and 2:1 clay fraction minerals determined by XRD and TGA.....	119
5.12. Relationship between the cation exchange capacity (T value) and the percentage 2:1 clay fraction minerals in the subsurface horizons from the toposequences soils.....	130
5.13. Relationship between soil pH (CaCl <sub>2</sub> ) and gibbsite content.....	132
5.14. Effect of the boiling 5M NaOH procedure on the dissolution of kaolinite and gibbsite in the Latossolo Roxo-Bw2 and Brunizem Avermelhado-Bt clay fractions from Ibiporã.....	139
5.15. X-ray diffraction patterns for synthetic hematite, goethite and maghemite prepared according to the methods of Schwertmann and Cornell, (1993).....	141

5.16. Magnetic susceptibility vs. percentage maghemite determined by XRD peak area in the total clays from both the acid and basic rock soils.....	145
5.17. Magnetic susceptibility ( $\chi_{ir}$ ) of artificial mixtures of synthetic maghemite, hematite and goethite.....	147
5.18. Calculated magnetic susceptibility ( $\chi_{ir}$ ) of the soil and synthetic maghemites.	149
5.19. Relationship between the mass of maghemite measured by XRD and by magnetic susceptibility using a value of 50000 ( $10^{-8} \cdot \text{m}^3/\text{Kg}$ ) for the magnetic susceptibility of soil maghemite.....	150
5.20. Relationship between the redness rating of the dry soil clays and the percentage hematite.....	153
5.21. Relationship between redness rating of the dry soil clays and the percentage hematite and maghemite.....	154
5.22. XRD patterns from synthetic hematite and goethite compared to that from a residue of the 5M NaOH and the 1.8M H <sub>2</sub> SO <sub>4</sub> treatments (TRd - Cruzmaltina).....	156
5.23. Sequential XRD patterns from 5M NaOH residues (LR - Cascavel and LR - Londrina) following exposure to 1.8M H <sub>2</sub> SO <sub>4</sub> (75°C) for up to 7.5 hr.....	158
5.24. Al and Fe in the 1.8M H <sub>2</sub> SO <sub>4</sub> (75°C) extracts expressed as percentages of the CBD-extractable Al and Fe as a function of dissolution time.....	159
5.25. Representative XRD patterns from the 5M NaOH and 5M NaOH plus 1.8M H <sub>2</sub> SO <sub>4</sub> residues (TRd- Cruzmaltina).....	163
5.26. Relationship between Al-substitution in hematite and goethite measured by XRD vs. dissolution using the CBD procedure (maghemite previously removed by dissolution with 1.8M H <sub>2</sub> SO <sub>4</sub> ).....	164
5.27. Relationship between Al substitution in maghemite measured by XRD peak area vs. extraction with 1.8M H <sub>2</sub> SO <sub>4</sub> .....	167
5.28. Relationship between soil pH (CaCl <sub>2</sub> ) and Al substitution in soil hematites, goethites, and maghemites measured by XRD.....	168

5.29. Relationship between % gibbsite and Al substitution in soil hematites, goethites, and maghemites by XRD peak area.....	169
5.30. Relationship between Hm/(Hm+Gt) ratios and % SiO <sub>2</sub> in the parent rock material.....	171
5.31. Relationship between soil pH and the Hm/(Hm+Gt) ratios for the highly weathered soils (LR-LB-TR-TB).....	173
5.32. Relationship between soil carbon content and the Hm/(Hm+Gt) ratios for the highly weathered soil (LR-LB-TR-TB).....	174
5.33. Relationship between Hm/(Hm+Gt) ratios and the % maghemite in the highly weathered soils (LR-LB-TR-TB).....	175
5.34. Relationship between Al-substitution in goethite, hematite and maghemite in the highly weathered soils (LR-LB-TR-TB) and SiO <sub>2</sub> content of the parent rocks.....	177
5.35. Relationship between soil pH and the Hm/(Hm+Gt) ratios of both the highly weathered (LR-TR) and the less weathered soils (BAv-R) derived from basic rocks.....	181
5.36. Relationship between total C and the Hm/(Hm+Gt) ratios of both the highly weathered (LR-TR) and the less weathered soils (BAv-R) derived from basic rocks.....	182
5.37. Relationship between gibbsite and maghemite contents in clays from the basalt soils.....	183
5.38. Relationship between mean annual temperature and the Hm/(Hm+Gt) ratios of Latossolo investigated by Kämpf (1981); Palmieri (1986) and Fontes (1988).....	186
5.39. Relationship between mean annual temperature and the Hm/(Hm+Gt) ratios of Latossolo Roxo derived from basalt.....	187
5.40. Relationship between excess water (P-ETp) and the Hm/(Hm+Gt) ratios of Latossolo Roxo derived from basalt.....	188

## **Chapter 1**

### **INTRODUCTION AND OBJECTIVES**

The Paraná River Basin is a large and important agricultural area in the east corner of South America. It is a sedimentary basin elongated in a NE-SW direction that includes both sedimentary and volcanic rocks. The Paraná River cuts the Basin north to south through Brazil and forms part of the border between Brazil, Argentina, Paraguay, and Uruguay. Most of the Basin is located in Brazil where fertile soils have formed from the weathering of the volcanic rocks. These rocks, in Brazil, comprise the Serra Geral Formation or "Derrame do Trapp". Recent research on the geochemistry of the volcanic rocks has shown that both basic (mostly basalt - andesite) and acid/intermediate varieties (mostly rhyolite - dacite) occur within the Basin. The distribution of these rocks follows a defined pattern with the acid/intermediate rocks (10 % in volume) occurring mostly at high altitudes on the eastern and southern sides of the basin and the basic rocks (90% in volume) occupying the western and northern regions.

The management of soils formed in the volcanic rocks has been intensively studied in the last 20 yr but few studies have dealt with the genesis of minerals in the clay size fraction. The clay mineralogy of these soils is usually considered to be monotonous because only a few minerals make up more than 90% of the clay fraction (Schwertmann and Herbillon, 1992).

Nevertheless, a wide range in mineralogical characteristics influences the fertility of the soils. Kaolinite and hydroxy-Al-interlayered vermiculite are the most common and dominant clay minerals while smectite and vermiculite have been found in young profiles (Moniz and Jackson, 1967; Moniz et al., 1994; Demattê et al., 1991; Demattê and Marconi, 1991). Gibbsite is the only aluminum oxide found, and it is abundant in the most highly weathered, acid soils. Iron oxides, recognized by purple to brown soil colors, are represented by hematite, maghemite, and goethite. Characterization of these minerals has shown that they present different degrees of crystallinity and display isomorphous substitution within their crystal structures that may be related to the specific environment in which they form (Schwertmann and Taylor, 1989). Most previous work with the iron oxides has involved a qualitative evaluation of their presence, distribution, and relationship with important soil chemical and physical characteristics (Resende, 1976; Resende et al., 1986; Fasolo, 1978; Rauen, 1980; Kämpf, 1981; Curi, 1983; Palmieri, 1986; Fontes, 1988; Castro Fo, 1988; Peixoto, 1995). A detailed quantification of the iron oxide mineralogy has only been done in the states of Minas Gerais (Curi, 1983; Fontes, 1988), Rio Grande do Sul (Kämpf, 1981) and Santa Catarina (Palmieri, 1986). In these previous studies, some authors recognized that parent rock (Resende, 1976; Resende et al., 1986; Fontes, 1988) and previous drainage conditions (Curi, 1983) were important factors associated with the distribution of the iron oxides, while others (Kämpf, 1981; Palmieri, 1986) put emphasis on the bioclimatic factor as the driving force for the formation of these minerals. The latter authors made comparisons of the iron oxide mineralogy of soils formed not only under different climatic conditions but also from different parent rock materials and with different degrees of weathering. In addition, they only evaluated the properties and

distribution of hematite and goethite; maghemite was not considered even though the authors noticed that the soils presented different degrees of magnetic attraction. In no case has there been an attempt to systematically evaluate the impact of selected factors of soil formation (parent rock material, climate, time, topography, organisms) on the genesis and properties of iron oxides in soils of the Paraná River Basin while excluding or limiting potentially confounding effects from other parameters.

Therefore, the hypothesis of this dissertation is that the clay mineralogy of soils developed from the weathering of volcanic rocks in the Paraná River Basin is mainly determined by differences in the mineralogical and chemical characteristics of the parent rock material, position in the landscape, and degree of soil weathering rather than climatological conditions. In order to test this hypothesis, two sampling procedures were used. First, soil materials were sampled from eighteen profiles comprising five toposequences formed under isoclimatic conditions in the northern section of Paraná state. These soils represented different chemical environments and were developed from different parent rocks. Second, the distribution of iron oxides in a climatic gradient was studied with selected samples from highly weathered soils (Latossolo Roxo) formed only from basic rocks.

The specific objectives of this study were to evaluate:

1 - the distribution of iron oxides and clay minerals in eutrophic versus dystrophic/allic soils formed from the weathering of basic versus acid/intermediate rocks under similar climatic conditions; and

2 - the distribution and properties of iron oxides in highly weathered profiles formed from basic rocks under a climatic gradient, using a combination of magnetic susceptibility measurements, chemical dissolution procedures, and X-ray diffraction analysis.

## Chapter 2

### DESCRIPTION OF THE STUDY AREA

#### 2.1. Geology of the Paraná River Basin

The Paraná River Basin is a sedimentary basin located in the east portion of South America (Fig. 2.1). It has an area of 1,600,000 km<sup>2</sup> and is distributed between Brazil (1,000,000 km<sup>2</sup>), Argentina (400,000 km<sup>2</sup>), Uruguay (100,000 km<sup>2</sup>) and Paraguay (100,000 km<sup>2</sup>) (Petri and Fúlfaro, 1983). In Brazil, the Paraná River Basin includes portions of São Paulo (SP), Minas Gerais (MG), Goiás (Go), Mato Grosso (Mt) and Mato Grosso do Sul (MS) states and most of Paraná (Pr), Santa Catarina (SC), and Rio Grande do Sul (RS) (Fig. 2.2). The basin contains a sequence of Paleozoic sedimentary rocks deposited on metamorphic and acid magmatic rocks of the Brazilian Cycle (700–450 my). The different environments of sedimentation (marine, lacustrine, aeolian) produced a wide variety of sedimentary rocks whose total thickness approaches 5,000 m at some points. At the beginning of the Cretaceous period, these sedimentary rocks were covered ( $\cong$  70% of the area) by extrusive rocks from the Paraná continental flood volcanism (PFV) (greatest thickness = 1723 m).

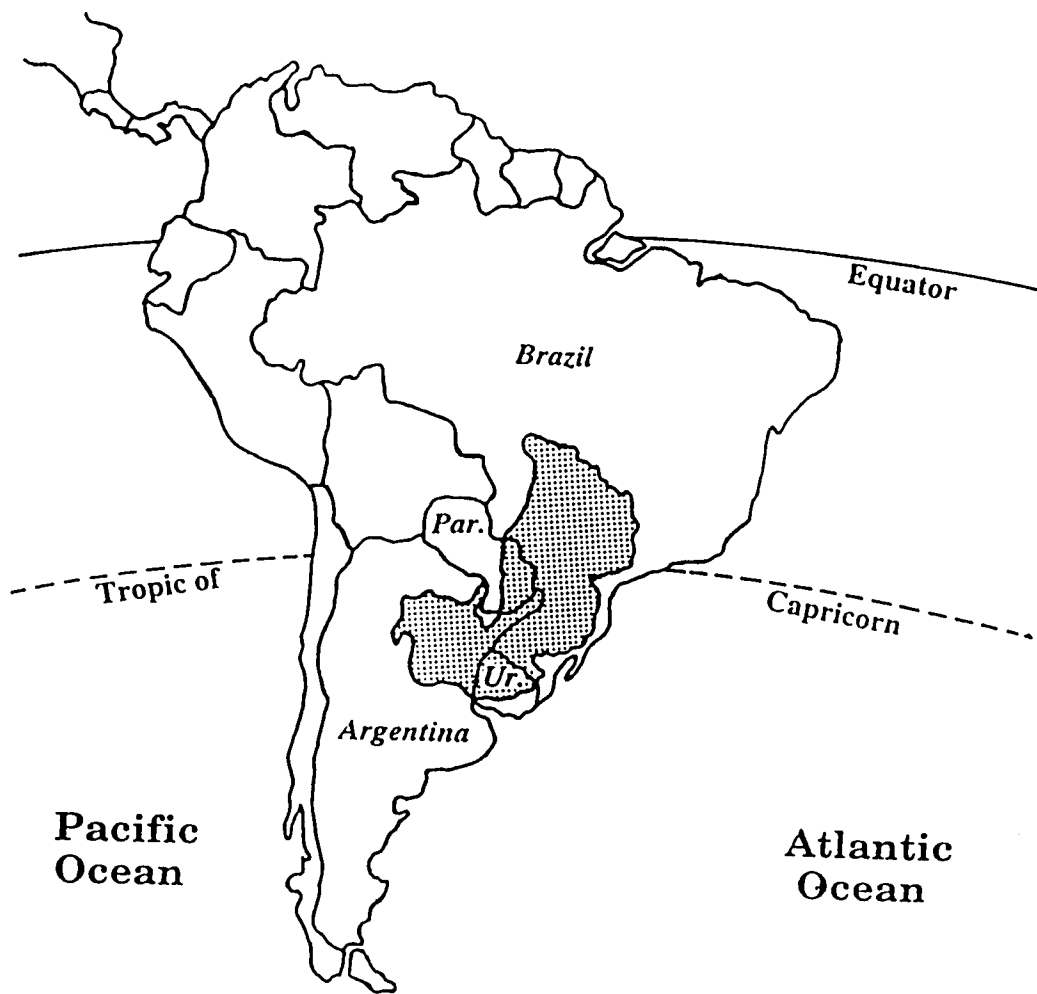


Figure 2.1. The Paraná River Basin in South America. Modified from Petri and Fúlfaro (1983).

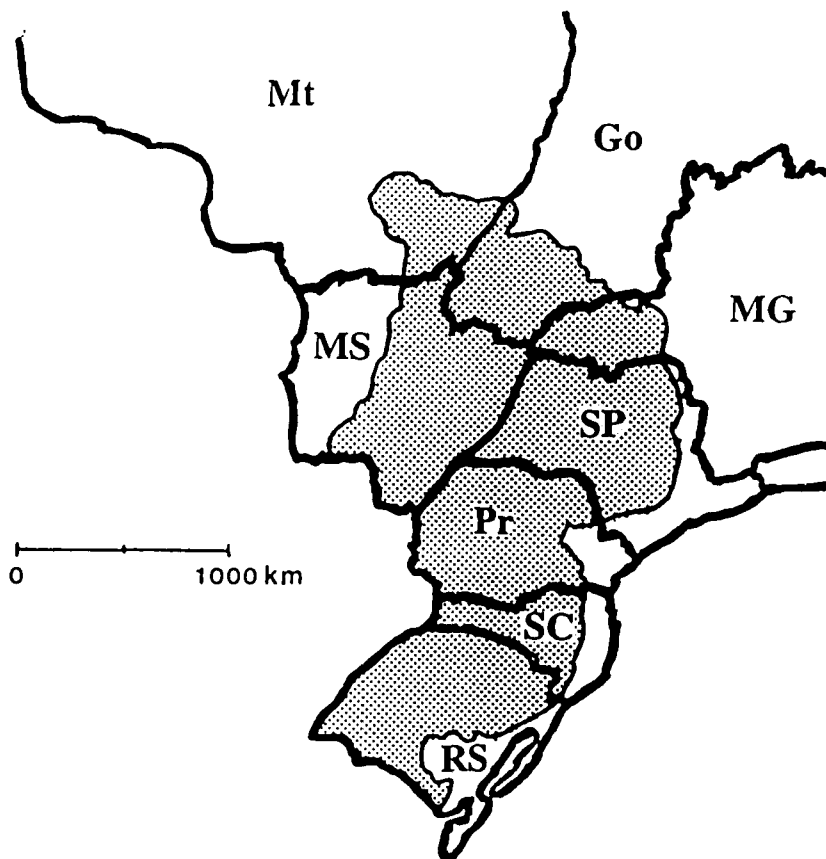


Figure 2.2. The Paraná River Basin within the southern region of Brazil, showing the states of Mato Grosso (Mt), Mato Grosso do Sul (MS), Goiás (Go), Minas Gerais (MG), São Paulo (SP), Paraná (Pr), Santa Catarina (SC), and Rio Grande do Sul (RS).

Radiometric dating using K/Ar and Rb/Sr indicates that the lavas were deposited mostly between 140 and 120 m.y. ago (Amaral et al., 1966; Melfi, 1966; Sartori et al., 1975; Cordani et al., 1980). During deposition of these flood basalts, the regional climate changed from marine to a continental desert condition. At the end of the Cretaceous, a new period of aeolian deposition occurred overlaying extensive areas of the lava flows with sandy deposits. Extrusive rocks of the PFV comprise the Serra Geral Formation or "Derrame do Trapp". The Serra Geral Formation is considered the product of one of the biggest volcanic eruptions of continental origin on the surface of the earth. An enormous volume of lava (around 780,000 km<sup>3</sup>) that covered an area of more than 1,200,000 km<sup>2</sup> was expelled through numerous fissures. Rocks of the PFV extend from the states of Minas Gerais and Goiás in the north to the state of Rio Grande do Sul in the south and also reach into the countries of Paraguay, Argentina and Uruguay to the south and west. The PFV has an average thickness of 650 km (Leinz et al., 1966).

Early geological maps of the PFV showed only the presence of basaltic rocks (Brasil, 1977, Mineropar, 1986) even though several authors had already recognized the existence of acid and intermediate flows as well (Leinz, 1949; Schneider, 1964; Szubert et al., 1978; Sartori and Gomes, 1980). In 1981, a systematic study of rocks comprising the PFV was undertaken, and 1,500 samples from throughout the basin were subsequently analyzed. As a result, recent maps (Fig. 2.3) provide a much more accurate description of rocks comprising the PFV (Bellieni et al., 1984a and b; Hawksworth et al., 1988; Piccirillo et al., 1988). From these studies, basic volcanic materials ( $\leq 53\%$  SiO<sub>2</sub>) comprise around 90% of the total volume of rocks in the PFV, whereas 3% are acid

( $\geq 63\%$  SiO<sub>2</sub>) and 7% are intermediate in composition. The basic rocks are usually very uniform in composition, mainly aphyric to subaphyric, and can be classified mostly as tholeiitic basalts and tholeiitic basaltic andesites. The intermediate rocks, also aphyric to subaphyric, include mostly tholeiitic andesites, lati-andesites and latites. The acid rocks constitute the Nova Prata Formation and occur mostly along the eastern flank of the "Derrame do Trapp" mostly at elevations above 800 m (Fig. 2.3). These acid rocks are mostly porphyritic with varying degrees of crystallinity and are virtually devoid of obsidian. They are subdivided into two groups that include the Chapecó (quartz-latite, rhyodacites, rhyolites) and Palmas (rhyodacites and rhyolites) types. A general description of the petrography of rocks comprising the PFV is provided in Table 2.1 (Piccirillo et al., 1988).

Basic Rock Types SiO <sub>2</sub> ≤ 53%	Intermediate Rock Types 53 < SiO <sub>2</sub> < 63 %	Acid Rock Types SiO <sub>2</sub> ≥ 63%
<b>Phenocrystals</b>		
mostly augite, plagioclase, pigeonite, minor Ti-magnetite, sporadic olivine	mostly augite, pigeonite, plagioclase, and Ti-magnetite	mostly plagioclase, augite, pigeonite, orthopyroxene, and Ti-magnetite
<b>Ground Mass</b>		
mostly plagioclase, augite, pigeonite, abundant Ti-magnetite and ilmenite	mostly plagioclase, augite, pigeonite, Ti-magnetite, ilmenite and quartz	mostly quartz, alkali-feldspar, plagioclase, pyroxenes, Ti-magnetite and ilmenite

Table 2.1. Petrography of the three major types of volcanic rocks from the Paraná continental flood volcanism (Piccirillo et al., 1988).

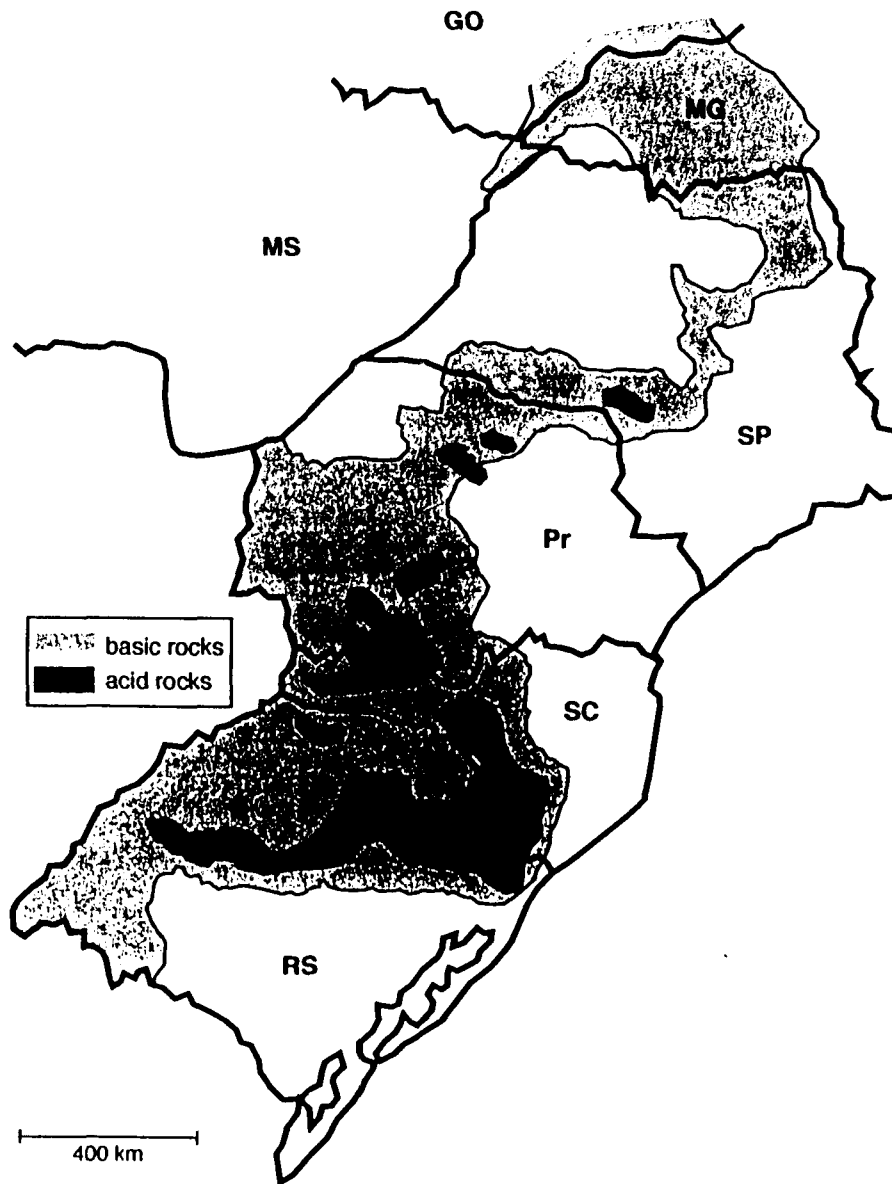


Figure 2.3. Distribution of volcanic rocks in the states of Goiás, (Go), Minas Gerais (MG), Mato Grosso do Sul (MS), São Paulo (SP), Paraná (Pr), Santa Catarina (SC), and Rio Grande do Sul (RS). Modified from Piccirillo et al. (1988).

## **2.2. Physiography and geology of Paraná state**

Paraná state is located between 22° 29' 30" and 26° 42' 59" south latitude and between 48° 02' 24" and 54° 37' 38" west longitude. The state has an area of 199,218 km<sup>2</sup> and represents 2,35% of the total land area in Brazil. Paraná shares its borders with the Brazilian states of São Paulo to the north, Santa Catarina to the south, and Mato Grosso do Sul to the northwest. The Republic of Paraguay is located to the west and Argentina is to the southwest. The main stratigraphic divisions of Paraná include a Crystalline Complex, Epimetamorphic Rocks of the Acungui Group, Sedimentary Rocks, Effusive Basic and Intermediate Rocks, Pre-Gondwanic Rocks, and Extrusive Basic and Acid/Intermediate Rocks of the Serra Geral Formation (EMBRAPA, 1984) (Fig. 2.4). These stratigraphic units are distributed over five physiographic regions, including a seaboard, coastal highlands, and three inland plateaus (Fig. 2.5). The area of interest in this study is the third plateau, which is a simple physiographic region that has been cut into a series of blocks or sub-plateaus by the major rivers (Tibagi, Ivai, Piquiri and Iguaçú Rivers) in response to tectonic movements and changes in weather conditions. The major landforms delimited by these rivers include the sub-plateaus of Cambará, Apucarana, Campo Mourão, Guarapuava and Palmas (EMBRAPA, 1984) (Fig. 2.5).

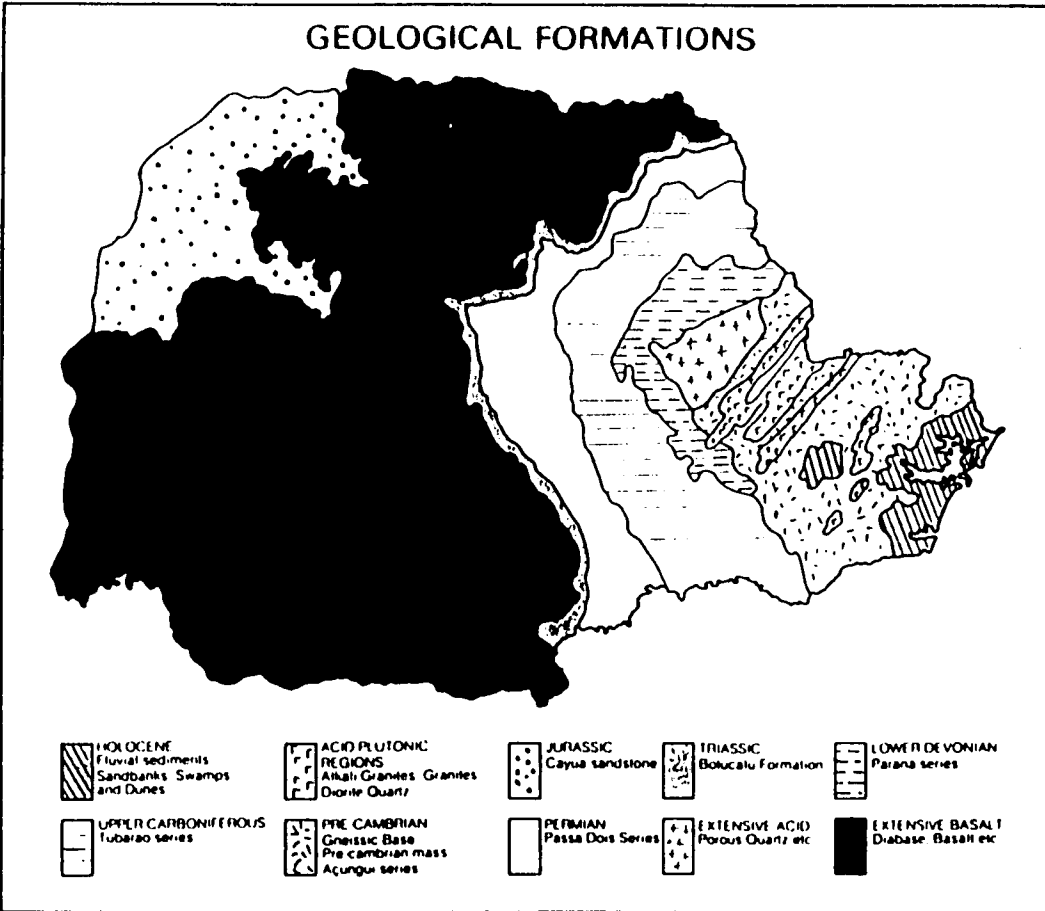
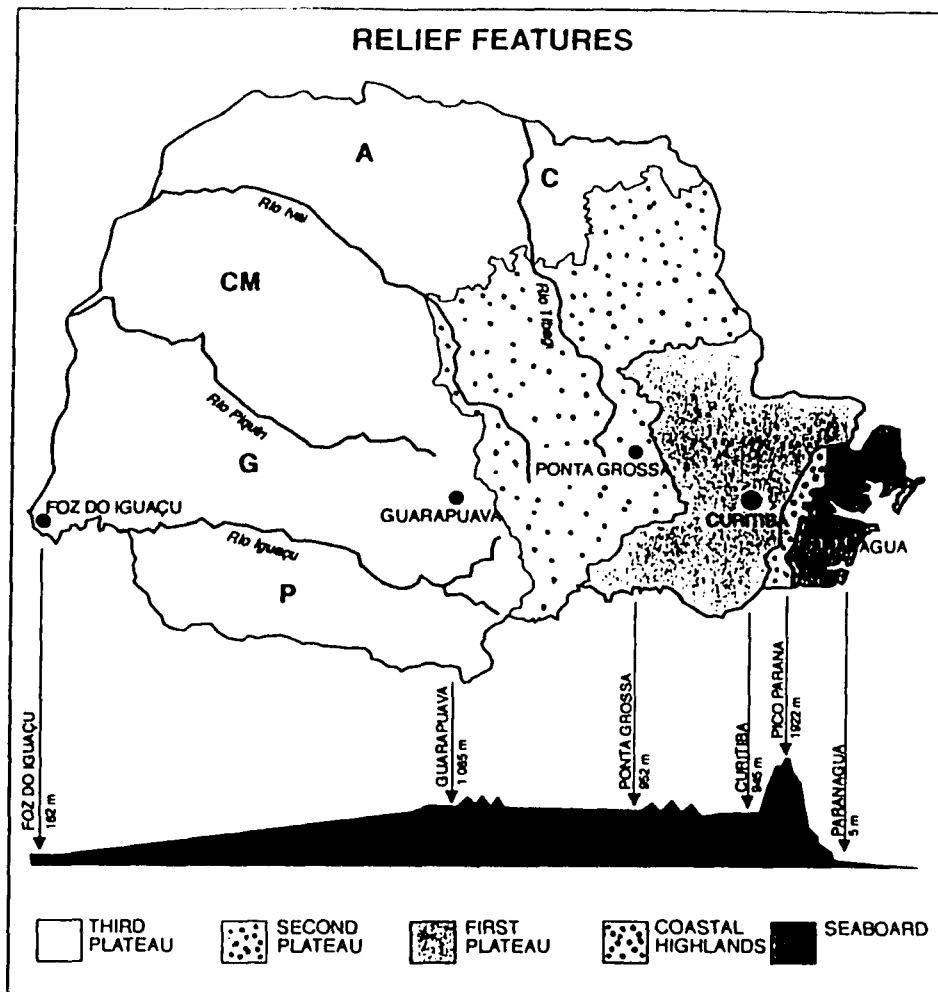


Figure 2.4. Major stratigraphic units in Paraná. Modified from Mineropar (1986).



Subplateaus : C = Cambará  
 A = Apucarana  
 CM = Campo Mourão  
 G = Guarapuava  
 P = Palmas

Figure 2.5. Physiographic regions of Paraná. Modified from EMBRAPA (1984).

### **2.3. Climate**

An important aspect of the climate of Paraná is its transitional character. The state is cut by the Tropic of Capricorn at a latitude of 23°30' south. This line subdivides the state into two “distinct” climatic zones. To the north the climate is warmer, drier and evapotranspiration is greater than in the south. The rainfall is also strongly seasonal, being distributed mainly between September and February. To the south, the average annual temperature and evapotranspiration decreases, while precipitation increases and is well distributed throughout the year. According to the Koeppen classification system, the state has a predominance of Af, Cfa, Cfa(h), and Cfb climatic regimes (Fig. 2.6) (IAPAR, 1994). The Af zone is restricted to the eastern seaboard and is a perhumid environment. The climatic type Cfa is a subtropical humid mesothermic climate, without a dry season and with hot summers. The precipitation usually is concentrated in the summer period (December through February) with the average temperature in the warmest month exceeding 22° C. The climatic type Cfa(h) is similar to Cfa, but there is a dry period during the winter season. The Cfb regime is characteristic of a mesothermic climate, usually humid to perhumid, without a dry season but with an average temperature in the warmest month that is less than 22° C. In the state of Paraná, the Cfb climatic zone is characterized by frequent and severe frosts in the winter (EMBRAPA, 1984; IAPAR, 1994).

The third plateau is influenced by the Cfa, Cfa(h), and Cfb climatic regimes. The Cfa and Cfa(h) zones include the Cambará, Apucarana, Campo Mourão, and the western portion of the Guarapuava sub-plateaus.

The average annual temperature of the third plateau is almost constant at 20 - 21°C, but there is a steady increase in precipitation from the northeast (Cambará) to the southwest (Foz do Iguaçu). In the area close to the city of Cambará, the average annual precipitation is 1371 mm as compared to 1833 mm at Foz do Iguaçu. In addition, the decreasing altitude (Fig. 2.5) creates an increase in the relative air humidity (IAPAR, 1994). The average temperature in the coldest month is 10° C near the city of Palmas (EMBRAPA, 1984).

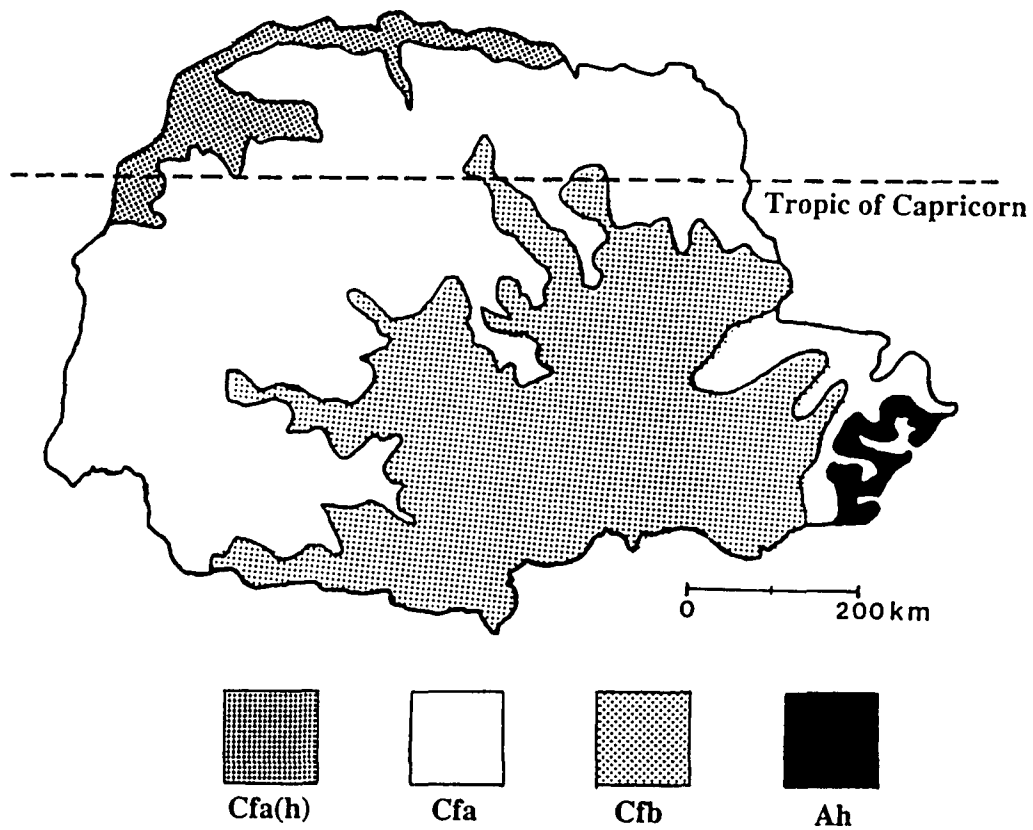


Figure 2.6. Distribution of the Koeppen climatic types in Paraná. Terms defined in section 2.3. Modified from IAPAR (1994).

## 2.4. Vegetation

The diversity of climatic conditions in Paraná gave rise to a variety of different types of native forests (Maack, 1968). These original forests were mostly removed during several agricultural cycles (tea, coffee, sugar, wheat, soybeans, corn, pasture) that the state of Paraná has gone through in the last century. Much of the area now supports cultivated crops and secondary forests (pinus and eucalyptus) needed to produce food, grain, fiber and energy (EMBRAPA, 1984). Remnants of the original vegetation are still found in state and federal parks, such as the Tropical Evergreen Forest preserved in the National Park of Foz do Iguaçu at the border of Brazil, Paraguay and Argentina.

The native forests can be subdivided into different classes according to plant composition. The most important subtypes are those in which the trees are either evergreen or semi-evergreen. The primary evergreen forest is the typical Araucaria forest, or Brazilian pine (Araucaria angustifolia), which is also the state tree of Paraná. Other important evergreen species are the Aspidosperma sp. (“peroba”), Gallesia gorazema (“pau d’alho”), Ocotea porosa (“imbuia”), Parapiptadenia rigida (“angico-vermelho”), and Cordia trichotoma (“louro-pardo”). Examples of semi-evergreen species include Cedrella fissilis (“cedro-branco”), Nectandra sp., and Arecastrum romanzoffianum. Both types of forests have rich subforest communities dominated by epiphytes and mosses. Other varieties of vegetation originally present in the state included secondary (“capoeiras” and “reflorestamentos”) forests, xeromorphic savannas (“cerradão” and “cerrado”), tropical grasslands (anthropic and wetlands), and subtropical grasslands (natural grasslands, anthropic, and wetlands) (EMBRAPA, 1984).

Evergreen and semi-evergreen forests originally covered the third plateau physiographic region except for the eastern portion of the Guarapuava sub-plateau. In the vicinity of the city of Guarapuava, the native vegetation was a subtropical grassland that was more or less continuous except for forested areas adjacent to the rivers. These grasslands were composed of short grasses and were usually concentrated on very acid soils at high altitudes where several species of Andropogon, Aristida, Paspalum, Panicum, and Eragrostis flourished. Associated with the grasses were some small trees with roots or bulbs that are resistant to frost and frequent burning (Maack, 1968).

## 2.5. Soils

The soils of interest to this dissertation are those formed from rocks of the PFV in the Cambará, Apucarana, Campo Mourão, Guarapuava and Palmas sub-plateaus. These soils are popularly called *raxos* (purple soils) due to the presence of iron oxides that impart red to purple colors. In the Brazilian System of Soil Classification (Camargo et al., 1987) the amount of iron oxides is used to separate classes of soils at the highest level (Table 2.2). The purple soils with high to intermediate amounts of iron oxides, are mainly from the Latossolo Roxo (Oxisols) and Terra Roxa Estruturada (Alfisols, Ultisols) classes. Soils with lesser amounts of iron oxides include the soils from the Brunizem Avermelhado (Mollisols), Solos Litólicos (Inceptisols), Cambissolo (Mollisols and Inceptisols), and Vertissolo (Vertisols) classes. A more detailed comparison of the classifications of these soils according to both the Brazilian (EMBRAPA, 1984) and the US systems (Soil Survey Staff, 1975) is given in Table 2.3.

The soils of the third plateau often form a typical catena or toposequence wherein Latossolo Roxo occupy the summits or most stable portions of the landscape in association with Terra Roxa Estruturada on the shoulder or upper backslope positions. Soils of the Brunizem class usually occur on the lower backslope positions adjacent to Solos Litólicos on the footslope. If present, Vertissolo will occur on the toeslopes. Of the soils formed from rocks of the PFV in Paraná, 17.4% are Latossolo Roxo, 13.8% are Terra Roxa Estruturada, 16.1% are Solos Litólicos, 2.4% are Cambissolo and 0.8% are Terra Bruna Estruturada (EMBRAPA, 1984). A general description of the major characteristics of these soils (Table 2.2) shows that as weathering increases the soil color becomes redder, the Ki values ( $\text{SiO}_2 / \text{Al}_2\text{O}_3$ ) decrease, and the magnetic attraction increases with the Fe oxides content.

The clay mineralogy of the most highly weathered soils (Oxisols, Alfisols and Ultisols) is usually considered to be simple (Table 2.2). Kaolinite-halloysite, hydroxy-Al-interlayered vermiculite, and small amounts of vermiculite and smectite are the most common silicate clay minerals. Kaolinite may comprise 60 to more than 90% of the total clay. The percentage of 2:1 clay minerals tends to be greater in less weathered profiles (Mollisols, and Inceptisols), but kaolinite-halloysite still dominates the clay fraction. The other major mineral components in these soils are the oxides, hydroxides and oxyhydroxides of aluminum and iron.

Soil Class	Munsell Hue	Ki Value	Magnetic Attraction	Mineralogy <2mm Fraction	Fe <sub>2</sub> O <sub>3</sub> (%)
LR (1)	10R - 5YR	0.6-1.8	STRONG	Kao>Gb>HIV>Hm>Gt (2)	18-40
TR	10R - 5YR	1.7-2.4	STRONG	Kao>Mi>Gb>VeCl	> 15
LB	5YR - 5YR	0.7-1.9	SMALL	Kao>HIV.Gb>Go	> 11
TB	10YR - 7.5YR	1.7-2.0	NONE	Kao>Gb>Gt>Hm	> 10
BAv	10R - 2.5YR	> 2.0	STRONG	Kao>Mo>Mi>V	VARIES
C	5YR - 7.5YR	> 1.0	STRONG	Kao>AMO>Mi>Mo>V>Gb	VARIES
R	2.5YR - 5YR	> 2.0	STRONG	Kao>Mo>Mi>V>Gb	VARIES

(1) LR = Latossolo Roxo; TR = Terra Roxa Estruturada; LB = Latossolo Bruno; TB = Terra Bruna Estruturada; BAv = Brunizem Avermelhado; C = Cambissolo; R = Solos Litólicos.

(2) Kao = kaolinite; Gb = gibbsite; HIV = hydroxy-Al-interlayered vermiculite; Hm = hematite; Gt = goethite; Mi = mica; AMO = amorphous; V = vermiculite.

Table 2.2. Color, Ki value, magnetic attraction and Fe<sub>2</sub>O<sub>3</sub> contents of the main soils derived from rocks of the Paraná flood volcanism (EMBRAPA, 1984).

Brazilian	U. S. Soil Taxonomy (1975)
Latossolo Roxo	Eutrorthox, Acrorthox, Haplorthox, Acrohumox, Umbriorthox, Haplohumox
Latossolo Bruno	Acrohumox
Terra Roxa Estruturada	Paleudoll, Paleudalf, Paleudult, Rhodudalf, Argiudoll, Rhodudult,
Terra Bruna Estruturada (1)	Dystrochrepts, Haplohumox
Brunizem Avermelhado	Argiudoll
Cambissolo	Hapludoll, Haplumbrept, Sombriotropept
Solos Litólicos	Hapludoll, Haplustoll, Haplumbrept

(1) Palmieri (1986)

Table 2.3. Classification of soils according to the U.S. Soil Taxonomy (Soil Survey Staff, 1975) and the Brazilian system (EMBRAPA, 1984). Major changes in the U.S. system have since been made (Soil Survey Staff, 1994).

Gibbsite,  $\text{Al}(\text{OH})_3$ , is the most common Al mineral, especially in the most acid soils where it may represent as much as 30% of the clay fraction. Iron is also not a very mobile element and accumulates as weathering proceeds; therefore, the Latossolo Roxo may have as much as 40% iron oxide in the total soil, while young soils (Inceptisols and Mollisols) may have less than 1% reductant-soluble  $\text{Fe}_2\text{O}_3$ . The reductant - soluble  $\text{Fe}_2\text{O}_3$  represents mostly the presence of crystalline Fe oxides because “amorphous” materials are almost never present except in some Cambissolo. Hematite ( $\alpha\text{-Fe}_2\text{O}_3$ ), maghemite ( $\gamma\text{-Fe}_2\text{O}_3$ ) and goethite ( $\alpha\text{-FeOOH}$ ) are the most important crystalline Fe oxides found in these soils. Lepidocrocite ( $\gamma\text{-FeOOH}$ ) may be present in hydromorphic soils, but these constitute a very small percentage of the soils of the state and are not yet well characterized. The Fe and Al oxides affect not only soil physical conditions such as aggregation, color, and permeability but also chemical properties such as anion sorption and charge balance. Most soils on the third plateau have a very low cation exchange capacity (CEC), and more than 60% of the CEC can be attributed to organic matter (Pavan et al., 1985).

Soils with near neutral pH, base saturation  $\geq 50\%$  (eutrophic), and low organic matter contents usually occur in the northern region of the third plateau (Cambará sub-plateau) where the landscape is more dissected, the climate is warmer and there is less precipitation to leach basic cations from the profile (Table 2.4). By contrast, soils formed in the southern region (Guarapuava and Palmas plateaus) are very acid ( $\text{pH} < 5$ ), allic (Al saturation  $\geq 50\%$ ), and rich in organic matter. Such properties reflect a greater intensity

of weathering where desilication and allitization are the most important soil forming processes. Soils of the Apucarana and Campo Mourão subplateaus tend to be intermediate in soil chemistry and are usually dystrophic (base saturation < 50%); some are also allic.

Subplateau	Soils (1)	Climate
Cambará	LRe, TRe, BAv, Re	Cfa to Cfa (h)
Apucarana	LRd, LRe, TRe, BAv, Re	Cfa
Campo Mourão	LRa, LRd, LRe, BA, Re	Cfa
Guarapuava	LRa, LRd, LRe, Ra, Rd, Re	Cfa and Cfb
Palmas	LRa, LRd, LRe, TRd, TRe, TRa, Ra, Rd, Re, Ce, Cd, Ca, TBa, LBa	Cfb

(1) LR = Latossolo Roxo; TR = Terra Roxa Estruturada; BAv = Brunizem Avermelhado; R = Solos Litólicos; C = Cambissolo; TB = Terra Bruna Estruturada; LB = Latossolo Bruno; a = allic character; d = dystrophic character, e = eutrophic character.

Table 2.4. Distribution of soils according to climate and physiographic region on the third plateau of the state of Paraná (EMBRAPA, 1984).

## **Chapter 3**

### **LITERATURE REVIEW**

The proper use, management and conservation of a soil should be based on a knowledge of its intrinsic attributes, including mineralogical, morphological, physical, chemical and biological characteristics. Soils of the temperate and subtropical regions have been intensively studied and their characteristics are often well known. Soils of the tropical region have only recently been the subjects of systematic research (e.g., Mohr and van Baren, 1954; Mohr et al., 1973; Sanchez, 1976; Uehara and Gillman, 1981; Theng, 1981; van Wambeke, 1992).

This bibliographic review will mostly deal with the Fe oxide mineralogy of tropical soils. It is intended to summarize some important aspects of recent work done on the characterization of Fe oxides (hereafter, the term Fe oxides is used in a collective sense to refer to all oxides, hydroxides, and oxyhydroxides of iron) and relationships between their properties and the factors (parent material, topography, time, organisms, and drainage), and processes (additions, losses, translocations, redistribution and transformations) of soil formation. A number of major review articles are available on these topics, and the reader should refer to these works for additional information (e.g., Schwertmann and

Taylor, 1989; Mullins, 1977; Schwertmann, 1985; Murad and Johnston, 1987; Stucki et al, 1985; Maher, 1986; Dzomback and Morel, 1990; Schwertmann and Cornell, 1991; Schwertmann, 1991; Bigham and Ciolkosz, 1993).

### **3.1. Iron oxides: structure and composition**

Iron is the fourth most abundant element (7.06 wt. %) in the earth's crust, after O, Si, and Al (Faure, 1991). In soils, iron is present in the soil solution (dissolved or organically complexed iron) and inside the crystal structures of a wide variety of minerals (mostly silicates and metal oxides). Probably the best description of the Fe oxides is that they are composed of close-packed sheets of oxygen with Fe ions filling the interstices. The  $\text{Fe}(\text{O}, \text{OH})_6$  octahedron is the basic structural element and combinations of Fe(III), Fe(II), O, and OH determine the different Fe oxide phases (Schwertmann and Taylor, 1989). In total, fifteen different Fe oxides have been identified but six of these phases, including  $\text{Fe}(\text{OH})_2$ ,  $\text{Fe}(\text{OH})_3$ , FeO,  $\beta\text{-Fe}_2\text{O}_3$ ,  $\epsilon\text{-Fe}_2\text{O}_3$  and a high pressure  $\text{FeOOH}$ , are not common or do not exist under natural conditions (Schwertmann and Cornell, 1991).

The Fe oxides occur in either hexagonal (hcp or  $\alpha$ -form) or cubic close-packed (ccp or  $\gamma$ -form) arrangements. The common feature among all is the presence of an Fe-Fe interatomic distance across edge-shared octahedra that ranges from 0.295 to 0.305 nm and the (1010) and (1120) planes of the hcp system ranging from 0.250 to 0.256 nm and 0.148 to 0.154 nm. Hematite ( $\alpha\text{-Fe}_2\text{O}_3$ ) and goethite ( $\alpha\text{-FeOOH}$ ) are the most common hcp minerals, and maghemite ( $\gamma\text{-Fe}_2\text{O}_3$ ) and lepidocrocite ( $\gamma\text{-FeOOH}$ ) are the most

common ccp phases. Magnetite ( $\text{Fe}_3\text{O}_4$ ) and maghemite also include Fe in tetrahedral coordination. Other Fe oxides of potential interest include ilmenite ( $\text{FeTiO}_3$  - hexagonal) and ferrihydrite (nominally  $\text{Fe}_5\text{HO}_8 \cdot 4\text{H}_2\text{O}$  - hexagonal).

**Magnetite:** Magnetite is a well crystallized mineral that is usually not considered to be pedogenic in origin; however Murray (1983), as cited by Curi (1983), states that pedogenic magnetite can be formed from the oxidation of Fe(II) in solution, and there have been recent reports of bacterial magnetites in soils (Fassbinder et al., 1990). In basic volcanic rocks, magnetite is usually associated with titanomagnetites ( $\text{Fe}_{3-x}\text{Ti}_x\text{O}_4$ ) wherein the amount of Ti is largely determined by the cooling temperature of the magma (Wechsler et al., 1984). Magnetite belongs to the cubic crystal system ( $a = 0.8391$  nm) and has an inverse spinel structure with 1/3 of the total Fe occurring as Fe(III) in the tetrahedral sites, 1/3 as Fe(III) in octahedral coordination, and 1/3 as Fe(II) in octahedral coordination. Magnetite forms a solid solution with hercynite ( $\text{Fe(II)Al}_2\text{O}_4$ ), making possible Al for Fe substitution within the crystal structure. There is still some disagreement on the extent of Al substitution within magnetite. Some authors argue that there is unlimited miscibility between the two minerals (Dehe et al., 1975 cited by Wolska and Wolniewicz, 1987), but others report that Al can only substitute for up to 10 mole % Fe (Wolska and Wolniewicz, 1987).

With heating ( $t \approx 250^\circ\text{C}$ ) under oxidizing conditions, magnetite forms maghemite (Schwertmann and Taylor, 1989). Soil magnetites may exist in a fairly wide range of particle sizes and, according to Galhagher et al. (1968), small particles ( $<0.2\mu\text{m}$ ) form hematite rather than maghemite upon heating. The transformation of magnetite to

maghemite is accompanied by a reduction in the unit cell volume due to the replacement of Fe(II) with an ionic radius of 0.074 nm by Fe(III) with an ionic radius of 0.065 nm.

**Maghemite:** Maghemite is a common ferrimagnetic mineral in soils developed from basic volcanic rocks, and can be easily detected in the field with a hand magnet (Resende et al., 1986). It is commonly thought to form by oxidation of the Fe(II) in magnetite during weathering or by burning of other Fe oxides in the presence of organic matter (Schwertmann and Taylor, 1989). Recently, however, maghemite was identified in association with primary minerals in basalts from the northern hemisphere (Steinhorsson et al., 1992; Helgason et al., 1994) and in a tuffite deposit from Brazil (Fabris et al., 1995) using Moessbauer spectroscopy.

Maghemite belongs to the cubic or tetragonal crystal system and has a defect spinel structure related to that of magnetite. When magnetite is oxidized to form maghemite, either the addition of O or the ejection of Fe appears to occur with the net result that an average of only 21.33 Fe(III) ions (2.66 vacancies) are distributed among 8 tetrahedral and 16 octahedral sites per unit cell. The occurrence of both tetragonal and cubic maghemites is a result of the distribution of these vacancies. Unit cell dimensions vary from  $a = 0.834$  nm (cubic system) to  $a = 0.8338$  and  $c = 2.501$  nm (tetragonal system). As with magnetite, part of the Fe(III) in maghemite may be replaced by other ions such as Al (Wolska and Schwertmann, 1989), Mg, Ti, or Cr (Fabris et al., 1995). Aluminum is probably the most common foreign ion and appears to change the vacancy ordering (Wolska and Schwertmann, 1989). The Al distribution within the crystal structure is apparently not uniform so that about 90% of the Al is located in the octahedral

positions (Wolska and Schwertmann, 1989). Schwertmann and Fechter (1984) observed that Al for Fe(III) substitution in maghemites could be up to 20 mole %. These authors observed a systematic decrease in the  $a_0$  unit cell dimension with an increase in degree of Al substitution and derived the relationship.

$$a_0 = 0.8343 - 2.22 \cdot 10^{-4} \text{ mole \% Al} \quad (3.1)$$

The differentiation of maghemite and magnetite occurring in the same sample may be rather complicated because of their similar physical (magnetic) and structural properties. Selective dissolution techniques have been applied to separate them. Hunt et al. (1995) successfully used a modification of the Na-citrate-bicarbonate-dithionite procedure (Mehra and Jackson, 1960) in conjunction with magnetic susceptibility and its frequency dependence (Dearing, 1994) to distinguish pedogenic maghemite (ca. < 1mm) from lithogenic magnetite (ca. > 1 mm). Schwertmann and Taylor (1989) have also shown that upon exposure to heat ( $t > 500^\circ\text{C}$ ), maghemite forms hematite and loses its magnetic properties. By contrast, magnetite is initially transformed to maghemite.

**Ferrihydrite:** Ferrihydrite is a poorly-ordered hydrous oxide with a hexagonal closed packed structure ( $a_0 = 0.508$  and  $c_0 = 0.94$  nm) involving sheets of  $\text{O}^{2-}$ ,  $\text{OH}^-$ , and  $\text{H}_2\text{O}$  with Fe(III) occupying the octahedral positions. Ferrihydrite has a hematite-type structure, but details remain controversial (Eggleton and Fitzpatrick, 1988; Drits et al., 1993). The best crystalline specimens usually yield XRD patterns with six broad peaks at 0.254, 0.224, 0.198, 0.173, 0.152, and 0.147 nm.

Ferrihydrite is often found as a precipitate from Fe-bearing waters (Carlson and Schwertmann, 1981) and is commonly associated with other Fe oxides such as goethite,

lepidocrocite and hematite. In soils, ferrihydrite is usually difficult to identify by direct methods of analysis due to its low concentration, small particle size and poor crystallinity. A combination of techniques such as differential x-ray diffraction (DXRD) (Schulze, 1981), selective dissolution treatments (e.g., acid ammonium oxalate extraction; Schwertmann, 1973), and Moessbauer spectroscopy is commonly required for positive identification (Schwertmann et al., 1982b). Unless ferrihydrite is stabilized by organic matter or sorbed Si it appears to convert rapidly to other mineral species (Schwertmann, 1985).

Ferrihydrite is considered to be a required precursor for hematite formation, a process that is thought to involve the coalescence and dehydration of ferrihydrite particles (Schwertmann and Taylor, 1989). The transformation of ferrihydrite to hematite has been observed in laboratory experiments involving the heating of synthetic ferrihydrites at modest temperatures for different time periods and observing the gradual evolution of the hematite XRD pattern (Johnson and Lewis, 1983). Goethite may also form from ferrihydrite, but the process is thought to proceed via a dissolution and reprecipitation pathway (Schwertmann and Taylor, 1989). In soils, the formation of ferrihydrite seems to be related to the rate or intensity with which Fe is released by the weathering of primary minerals. Ferrihydrite will form only if the rate of Fe release is rapid so that the activity of Fe in solution exceeds its solubility product ( $\log K_{SO} = 3.0 - 5.0$ ). Hematite may then form by dehydration - recrystallization reactions. Otherwise, goethite will preferentially form due to its lower  $K_{sp}$  ( $\log K_{SO} = -1.0$ ) (Schwertmann and Taylor, 1989; Kämpf and Schwertmann, 1983).

**Lepidocrocite:** Lepidocrocite belongs to the orthorhombic crystal system ( $a_0 = 0.388$ ;  $b_0 = 1.254$ ; and  $c_0 = 0.307$  nm) and has a ccp structure of the boehmite ( $\gamma$ -AlOOH) type. The structure of lepidocrocite is composed of double chains of  $\text{Fe}(\text{O},\text{OH})_6$  octahedra oriented parallel to [001] and linked to other double chains by sharing of edges. Lepidocrocite can be formed by the oxidation of green rust (Schwertmann and Fechter, 1994), and it is commonly found in redoximorphic soils as orange-yellow segregations (Schwertmann, 1993). Upon heating, lepidocrocite decomposes initially to maghemite ( $t = 200 - 300$  °C) and subsequently to hematite ( $t = 500^\circ\text{C}$ ) (Gehring and Hofmeister, 1994).

**Goethite:** Goethite is the most common of the Fe oxides, and it occurs in almost all pedogenic environments. It has an hcp structure with oxygen and hydroxyls forming planes parallel to [001] in the sequence ABABA and with Fe(III) occupying the octahedral sites in double chains of octahedra. Goethite belongs to the orthorhombic crystal system and has unit cell dimensions of  $a_0 = 0.4608$ ;  $b_0 = 0.9956$  and  $c_0 = 0.30215$  nm (Schwertmann and Taylor, 1989). The mineral is isostructural with groutite ( $\alpha$ -MnOOH) and diaspore ( $\alpha$ -AlOOH) and commonly forms a partial solid solution with Al. Aluminum substitutions of up to 33 mole % have often been reported (Schwertmann and Carlson, 1994).

Schulze (1984) described an XRD procedure to determine the amount of Al substitution in goethite by using the positions of the (110), (111) and (130) peaks. These peaks are displaced to higher angles (lower d values) with increasing Al due to the smaller size of the Al ion as compared to Fe(III). The  $c_0$  unit cell dimension is the most sensitive

to Al substitution; therefore, Schulze (1984) suggested the following relationship between  $c_0$  and mole % Al in goethite:

$$\text{Al (\%)} = 1730 - 572.0 \cdot c_0 \quad (3.2)$$

This relationship has been frequently used in other studies of both synthetic and natural goethites (e.g., Kämpf, 1981; Palmieri, 1986; Schwertmann and Lathan, 1986; Fontes 1988; Schwertmann and Carlson, 1994).

With heating, goethite transforms to hematite at  $t = 250 - 350$  °C (Schwertmann and Taylor, 1989). If a source of organic matter is present, goethite will form magnetite at  $t \sim 250$ °C. With further heating, the magnetite transforms to maghemite via a three-step reaction (Murad and Johnston, 1987).

**Hematite:** Hematite has an hcp structure ( $a_0 = 0.5034$ ;  $c_0 = 1.3752$  nm) wherein each  $\text{FeO}_6$  octahedron contains one shared and one unshared face in the upper and lower basal planes. Hematite is isostructural with corundum ( $\alpha\text{-Al}_2\text{O}_3$ ) and partial solid solutions involving up to 16 mole % Al have been observed in both synthetic and natural hematites (Kämpf and Schwertmann, 1983; Palmieri, 1986; Schwertmann and Taylor, 1989). From table 1 (page 106) in Schwertmann et al. (1979) it is possible to obtain a relationship between the  $a_0$  dimension and the amount of Al substitution in hematites synthesized at 70°C. The linear regression equation ( $R^2 = 0.97133$ ) relates the degree of Al substitution and the  $a_0$  dimension by:

$$\text{Al \%} = 3076.8 - 610.7 \cdot a_0 \quad (3.3)$$

Schwertmann and Lathan (1986) derived a similar relationship using the  $a_0$  unit cell parameter and the mole % Al substitution of hematites synthesized at 25°C; however, they found that the data from a group of New Caledonian soils could best be described by the relationship:

$$\text{Al \%} = 678 \bullet (5.0418 - a_0) \quad (3.4)$$

Recently, Stanjek and Schwertmann (1992) reported that hydroxyl ions may also substitute for  $O^{2-}$  inside the crystal structure of hematite. The authors synthesized a series of hematites and measured the amount of Al for Fe(III) and OH for  $O^{2-}$  substitution by using chemical dissolution and thermal analysis (weight loss) techniques. Ideally, hematite is thermally inert, but small quantities of  $H_2O$  are evolved with heating when  $OH^-$  is present in the structure. They found a good correlation between the  $a_0$  and  $c_0$  dimensions and the volume ( $V$ ) of the unit cell with the amount of Al and OH present in the samples. Besides Al, other metals can substitute for Fe(III) (Murad and Johnston, 1987) such as Rh (Morrish and Eaton, 1971), Mn (Vandenberghe et al., 1986); Ga, Cr, In, (Sváb and Kren, 1979), and Ti (Curry et al., 1965).

### **3.2. Iron oxides : magnetic properties**

Magnetism is an important property of materials. In minerals, magnetism is usually associated with the amount of Fe present in the structure. Iron is the only element among the nine major elements in the earth's crust that has a magnetic moment. A magnetic moment arises through the summation of the spin angular momentum of unpaired

electrons and their orbital angular momentum. The easiest way of measuring the degree of magnetization of a material is to expose it to a magnetic field (Coey, 1985).

There are then five types of magnetic behavior that are commonly recognized (Coey, 1985): ferromagnetism, ferrimagnetism, antiferromagnetism (or canted ferrimagnetism), paramagnetism and diamagnetism (Table 3.1). Ferromagnetism occurs with pure substances (Fe, Co, Ni) where each atom behaves as a single magnet. Exposure to a magnetic field aligns all magnetic moments so that the total magnetization is the summation of millions of magnetic moments associated with each electron present in each metal atom. Ferrimagnetic materials also display a strong magnetic susceptibility. However, ferrimagnetic substances (magnetite, hematite, pyrrhotite) have two out of three magnetic moments aligned in one direction with the third oriented in the opposite direction, thereby decreasing the net total magnetization. Some substances/minerals such as goethite and hematite have adjacent atomic magnetic moments aligned in opposite directions so that a net positive or zero magnetization is achieved; these materials are said to be antiferromagnetic. Antiferromagnets are thus similar to paramagnetic materials wherein the thermal motion of the atoms constantly overrides the alignment of magnetic moments resulting in a small, net positive magnetization. Examples of paramagnetic minerals are olivine, biotite, vermiculite and smectite. Finally, diamagnetic minerals have no magnetic moment when exposed to an external magnetic field. They are composed of atoms that have no magnetic moment because the various orbital and spin components cancel each other. Consequently, there is a net negative magnetic susceptibility.

Mineral / Material	Chemical Formula	Fe (%)	$\chi$ *
<b>Ferromagnetic</b>			
Iron	Fe	100	27600000
Cobalt	Co	0	20400000
Nickel	Ni	0	6885000
<b>Ferrimagnetic</b>			
Magnetite (0.012-0.069 um)	Fe <sub>3</sub> O <sub>4</sub>	72	44000 - 111600
Magnetite (1-250um)	Fe <sub>3</sub> O <sub>4</sub>	72	39000 - 71600
Maghemite	$\gamma$ -Fe <sub>2</sub> O <sub>3</sub>	70	28600 - 41000
Titanomagnetite	Fe <sub>3</sub> O <sub>4</sub> -Fe <sub>2</sub> TiO <sub>4</sub>	varied	16900 - 29000
Titanohematite	Fe <sub>3</sub> O <sub>4</sub> -FeTiO <sub>3</sub>	varied	28100 - 31500
<b>Canted Anti-ferromagnetic</b>			
Hematite	$\alpha$ - Fe <sub>2</sub> O <sub>3</sub>	70	27 - 169
Goethite	$\alpha$ -FeOOH	63	35 - 125
<b>Paramagnetic</b>			
Ilmenite	FeTiO <sub>3</sub>	37	170 - 200
Olivine	(Mg,Fe)•2SiO <sub>4</sub>	<55	1 - 130
Biotite	Mg,Fe,Al silicate	31	5-95
Lepidocrocite	$\gamma$ -FeOOH	63	50 - 75
Vermiculite	Mg,Fe,Al silicate	varied	15
Smectite	Mg,Fe,Al silicate	varied	2.7-5
<b>Diamagnetic</b>			
Quartz	SiO <sub>2</sub>	0	-0.58
Organic matter	C,H,O,N	varied	-0.9
Water	H <sub>2</sub> O	0	-0.9
Kaolinite	Al <sub>4</sub> Si <sub>4</sub> O <sub>10</sub> (OH) <sub>8</sub>	0	-1.9

\* Magnetic susceptibility ( $10^{-8} \bullet m^3/Kg$ )

Table 3.1. List of materials / minerals according to their magnetic character, chemical formula, iron content and magnetic susceptibility. Modified from Dearing (1994).

Examples of diamagnetic minerals include quartz and kaolinite. Isomorphous substitution and particle size are both major factors influencing the magnetic susceptibility of a mineral.

The replacement of Fe by a diamagnetic element (Al, Mg) decreases the degree of magnetization of the mineral (Coey, 1985). Small particles (<1mm), with restricted volumes have only one magnetic domain whereas larger, multi-domain particles may have multiple zones with different magnetization. For example, primary magnetites that are commonly present in the coarse fractions of soils usually have multi-domain structures. In contrast, pedogenic maghemites are commonly found in the finest particle-size fractions (< 2mm) and have single domain character. Multi - and single-domain particles respond differently when exposed to a magnetic field. Single domain particles are superparamagnetic. After being exposed to a magnetic field, they lose their induced magnetization very rapidly (1/10000 s) because intrinsic thermal agitation overcomes the induced magnetic alignments. Multi-domain particles have a much longer demagnetization time. Measurements of magnetic susceptibility for single and multi-domain particles under the influence of different magnetic fields can therefore be used to determine the presence and relative amount of superparamagnetic particles. A low frequency field (0.46 kHz) brings single and multi-domain particles to complete magnetization whereas a high frequency (4.6 kHz) field shifts the domain boundary to smaller crystal sizes and decreases the magnetic induction. The percentage of frequency-dependent magnetic susceptibility ( $\chi_{fd}$  %) can be defined by:

$$\chi_{fd}\% = 100 \cdot (\kappa_{lf} - \kappa_{hf}) / \kappa_{lf} \quad (3.5)$$

where  $\kappa$  is the mass specific susceptibility (Dearing, 1994).

Dearing (1994) attempted to evaluate the distribution of single and multidomain particles in samples according to  $\chi_{fd}\%$  as shown in Table 3.2.

$\chi_{fd}\%$	Distribution Single and Multidomain Particles
< 2%	Superparamagnetic minerals
2-10%	Mixture of superparamagnetic, coarse single domain and multidomain grains
10-14%	virtually only superparamagnetic grains (>75%)
>14%	anisotropy, weak sample, metal contamination

Table 3.2. Distribution of single and multidomain particles according to their frequency dependent magnetic susceptibility ( $\chi_{fd}\%$ ). After Dearing (1994)

### 3.3. Iron oxides in soils

The Fe oxides are the most abundant of the metallic oxides. They are present in dusts, sediments, rocks, and soils in particle sizes ranging from colloidal to macroscopic. In soils, the Fe oxides mainly occur as small particles that are dispersed throughout the soil matrix (Bigham et al., 1978a; Hendershot and Lavkulich, 1981) but may also form microaggregates, segregations, concretions and cemented horizons. The nature and distribution of Fe oxides in the soil profile are used in many classification systems to help define soil taxa (e.g., McKeague, 1967; McKeague et al., 1971). In Brazil, the amount of Fe oxides extracted with  $H_2SO_4$  ( $d=1.47$ ) is used in the distinction of the "Latossolo" class (Camargo et al., 1987) even though Rodrigues (1984) does not consider the absolute amount of Fe oxides to be an important indicator of pedogenetic processes.

In some literature, the soil Fe oxides are referred to as "free" iron oxides to differentiate them from the Fe bound within the structure of clay minerals such as nontronite. Soil Fe oxides may include primary (lithogenic) minerals associated with the parent material (e.g., magnetite) but are more commonly viewed as secondary (pedogenic) minerals that result from the weathering of primary silicates (e.g., olivine, pyroxenes) or the oxidation of other Fe(II)-bearing oxides (e.g., magnetite => maghemite). The various types of "secondary" Fe oxides usually reflect the environment (pH, Eh, temperature, moisture, rate of iron release, organic matter) in which they are formed and are therefore good instruments to investigate the genesis and evolution of soils (Schwertmann, 1985).

Until rather recently, the soil Fe oxides were considered to be amorphous materials because they could not be easily identified or distinguished using normal mineralogical techniques. Difficulties with identification and characterization by XRD techniques were usually related to low concentrations, very small particle size, and the overlap of low intensity diffraction peaks with those from better crystalline phases. Selective or preferential dissolution techniques using complexing or reducing agents were the primary tools by which the Fe oxides were studied. For example, the acid ammonium oxalate dissolution procedure (Schwertmann, 1973) is fairly specific for organically complexed Fe and poorly crystalline inorganic phases (e.g., ferrihydrite); whereas, the citrate - bicarbonate - dithionite procedure (Mehra and Jackson, 1960) dissolves crystalline phases (e.g., goethite and hematite) as well. The difference between these two values is therefore commonly taken as the amount of crystalline Fe oxide in the sample, and the ratio of Fe

extracted by the two methods has been used as an indicator of the degree of weathering (Resende, 1976; Fasolo, 1978; Kämpf, 1981; Palmieri, 1986; Fontes, 1988). Selective dissolution techniques provide much useful information, but there is usually a desire to obtain greater mineralogical detail.

In Oxisols derived from basic or ultrabasic rocks that are rich in Fe, it is sometimes possible to distinguish various Fe-oxide weathering products using conventional XRD techniques (Curi and Franzmeier, 1987; Schwertmann and Lathan, 1986), but the same is not always true for younger soils (Alfisols, Ultisols and Inceptisols) where the amount of Fe oxides is very low (Volkoff, 1977; Demattê et al., 1977). In these cases, detailed mineralogical analysis of the Fe oxides require the application of advanced analytical techniques such as Moessbauer spectroscopy (Bigham et al., 1978a), visible spectroscopy (Kosmas et al., 1984), or differential x-ray diffraction (Schulze, 1981). Methods have also been developed to concentrate the Fe oxides prior to analysis using, for example, density gradient centrifugation (Jaynes and Bigham, 1986a) or chemical dissolution procedures that selectively remove matrix minerals. The 5M NaOH technique for selective dissolution of kaolinite and gibbsite (Norrish and Taylor, 1961; Kämpf and Schwertmann, 1983) has been widely applied in the study of tropical soils.

With these recent improvements, two things have become clear with respect to the Fe oxide minerals occurring in soils. First, they are usually not amorphous but do present a wide range of crystallinity. Secondly, the soil Fe oxides are often solid solutions created by the isomorphous replacement of Fe by other metal ions. Degree of crystallinity and isomorphous substitution may, in fact, be related properties because the replacement of Fe

by a smaller or larger element will usually deform the unit cell and affect crystal growth (Schulze, 1981; Schwertmann and Kämpf, 1985). Numerous studies have now documented the effects of metal substitution on the properties of the Fe oxides; elements studied to date include Al (Norrish and Taylor, 1960), Ni (Cornell., 1991), V (Nalovic et al., 1975), Ti (Fitzpatrick et al., 1978), Zn (Lim-Nunez and Gilkes, 1987), Cu (Thiry and Sornein, 1983), Ge (Bernstein and Waychunas, 1987), Cr (Schwertmann et al., 1989), and Mn (Cornell and Giovanoli, 1987).

#### **3.4. Iron oxides : influence on soil characteristics**

**Soil color:** Soil color is dependent in large part on the solid-phase composition of the soil. Therefore, important relationships may exist between soil color, temperature, and physical-chemical behavior (Barrow, 1992). There are two primary methods for measuring soil color. Historically, color has been evaluated in the field by visual comparisons with color charts like those produced by the Munsell Color Co. (Munsell Color Co., 1975). More recently, spectrophotometers or spectrophotoradiometers have been used in the laboratory to quantify soil color (Torrent and Barron, 1993; Post et al., 1993). Field measurements of soil color are usually taken from fresh samples in an aggregated state. In the laboratory, most measurements are performed on perturbed samples that have been dried, ground and sieved so that color characteristics are likely modified to some degree from the field state (Barrón and Torrent, 1986; Fernández and Schulze, 1987).

The most common approach to color evaluation is the Munsell System that is based on the principle that color is a combination of three parameters: hue, value and chroma. Hue is related to the perception of primary color elements (red, green, yellow, blue). Value defines the gradient between white and black, and chroma defines the degree of color saturation relative to a gray scale. Spectrophotometers convert the visible portion of the spectrum reflected from the surface of an object or sample into X, Y and Z tristimulus values by means of wavelength functions defined by the 1931 Commission Internationale de L'Eclairage (CIE, 1931). These tristimulus values may then be converted to the Munsell system of color measurement.

Soils often exhibit striking differences in color that can usually be related to the presence (or absence) of one or more common pigmenting agents. General correlations have been defined between soil color and organic matter (Alexander, 1969; Schulze et al., 1993), moisture (Leger et al., 1979), and Fe oxides (Schwertmann, 1993). Soils developed under intense hydromorphic conditions or on Fe-depleted rocks such as granite may also exhibit colors that can be related to the matrix silicate minerals. For many tropical soils, the Fe oxides are particularly important pigmenting agents. Numerous studies have now documented that the type of Fe oxide is more significant than the quantity in determining soil color. Goethite is present in most soils and (in the absence of hematite) imparts a brown to yellow hue (Resende, 1976, Fasolo, 1978, Bigham et al., 1978a, Rauen, 1980; Kämpf, 1981; Santana, 1984; Palmieri, 1986, Fontes, 1988). Hematite is a less common but more effective pigmenting agent. Resende (1976), for example, observed that the hue of a yellow Oxisol changed from 10YR to 5YR when only

1% hematite was added to the soil. Color has, in fact, been used to quantitatively determine the hematite/goethite ratio in soils. Torrent et al. (1980) modified a color index originally developed by Hurst (1977) to derive a so-called “redness rating” (RR) defined by:

$$RR = [(10 - H) \cdot C] / V \quad (3.6)$$

where H, C and V are the hue, chroma and value of the Munsell notation. Correlations of the redness rating with hematite/goethite ratios obtained by XRD analysis have since been demonstrated in several studies (Torrent et al., 1983; Torrent and Cabedo, 1986; Boero and Schwertmann, 1987). Torrent et al. (1983) found that the relationship

$$RR = -0.1 + 2.6 \cdot (\% \text{ hematite}) \quad (3.7)$$

had a high correlation coefficient ( $r^2 = 0.814$ ) for several European soils. A different and less statistically significant relationship ( $r^2 = 0.760$ ) was obtained by Kämpf (1981) for soils developed on basalt in Brazil where:

$$RR = 2.45 + 0.82 \cdot (\% \text{ hematite}) \quad (3.8)$$

These results suggest that there is no general equation to represent the correlation of color and the content of hematite in soils or soil clays; however, the work of Kämpf (1981) may have been confounded by the presence of undetected maghemite. Maghemite imparts a reddish brown color (Schwertmann and Taylor, 1989) and is commonly associated with hematite in Brazilian soils (Resende, 1985). At present, no attempt has been made to modify the redness rating or to develop any other color index that would consider the presence of maghemite.

**Magnetic properties:** The magnetic properties of soils and sediments are highly correlated with the presence of Fe-bearing minerals such as the Fe oxides. Magnetic susceptibility has been successfully used for the identification, separation and grouping of rocks (Floyd and Trench, 1988), ore deposits (Mares, 1984), soils (Singer and Fine, 1989), glacial drift deposits (Bjork et al., 1982) and sediments (Dearing, 1992; Walling et al., 1979). The magnetic properties of rocks have been widely studied by geophysicists, and an extensive literature in this area has already been published. Rock magnetic susceptibility (Table 3.3) is highly correlated with the presence of magnetite, maghemite, Ti-magnetite and Ti-maghemite. Basic rocks like basalts, diabase, and dolerite are well known to contain significant concentrations of magnetite and/or maghemite. Magnetite is a primary mineral formed during the process of cooling and oxidation of the magma. The temperature and the degree of oxidation of the Fe affect the formation of this mineral. Rapid cooling with temperatures below 400°C leads to the formation of Ti-maghemites while cooling at temperatures above 600°C mostly forms magnetite and Ti-magnetites (Dearing, 1994).

The application of magnetic properties to the study of soils and sediments has been much less intense, probably due to the difficulty of correlating values of magnetic susceptibility to the actual amounts of magnetic minerals present in a sample. Once again, the ferrimagnetic minerals (maghemite, magnetite, Ti-magnetite, and Ti-maghemite) determine most of the magnetic behavior of soils and sediments. Other ferrimagnetic minerals such as the iron sulfides (pyrrhotite, greigite) are less common in soils but may be important in some sedimentary environments.

Rock	$\chi_{tr}$ ( $10^{-8} \bullet m^3/Kg$ ) (1)	$\kappa$ (dimension less)
Andesite	46	5 - 1000
Basalt	856 - 1260	2 - 1450
Diabase	1110	
Granite	7 - 220	0 - 400
Limestone	2	0.2 - 2.8
Rhyolite	161 - 525	2 - 300
Schist	17	2.5 - 24
Shale	3	0.5 - 14.8
Siltstone	5	

1. Lovejoy unpub. data cited by Dearing (1994); Brown (1990), Mooney and Bleifus (1953) cited by Mullins (1977)

Table 3.3. Mass specific ( $\chi_{tr}$ ) and volumetric ( $\kappa$ ) magnetic susceptibility for selected parent rock materials

Dearing (1994) estimates that 0.5 wt% of ultrafine magnetite will produce a magnetic susceptibility of 500 ( $10^{-8} \bullet m^3/Kg$ ), which is higher than the magnetic susceptibility of pure hematite, goethite or any other iron oxide (except maghemite) or clay mineral that might be present in a sample.

Several studies have shown that there is a strong effect of the parent rock material as well as particle size (Resende, 1975; Resende et al., 1985; Singer and Fine, 1989, Curi, 1983, Fontes, 1988), intensity of weathering (Santana, 1984) and drainage condition (Curi, 1983) on the magnetic susceptibility of the soil or soil fractions (Table 3.4). Singer and Fine (1989) studied numerous California soils and observed that the magnetic susceptibility of the soils were related mostly to the parent material rather than to climate or time of formation. They also observed that the magnetic susceptibility increased toward

the surface of the profiles. This phenomenon has been termed magnetic enhancement and can be attributed to different processes. For example, burning of surface vegetation and roots is well known to enhance the magnetic susceptibility of soils. This process involves the reduction of minerals such as goethite and hematite in the presence of organic matter to form magnetite that is reoxidized to maghemite (Maher, 1986). An important aspect of the process is that, after burning, magnetite and maghemite will normally retain any isomorphous substitution which was present in the original oxide (Dearing, 1994). Magnetic enhancement of topsoils may also be caused by the accumulation of primary magnetic minerals (e.g., coarse-grained magnetite) resistant to weathering, by atmospheric fall-out of industrial materials or other magnetic dust particles (Hunt, 1986), or by the production of magnetic minerals by soil bacteria (Fassbinder et al., 1990).

Soil	Rock Type	2mm	2-0.05mm	50-2µm	<2µm	Reference
IIIRCC-7	Basalt	7296	9932	12797	2885	a
8ISCW-7	Basalt		17471	12438	4238	b,h
III RCC-6	Basalt	5886	14465	2546	1046	a
III RCC-11	Basalt	803	4525	2222	458	a
G1	Basalt	212		410	165	b,e,g
G2	Basalt	232		337	185	b,e,g
G3	Basalt	347		428	382	b,e,g
G4	Basalt	601		612	603	b,e,g
G5	Basalt	946		810	904	b,e,g
G6	Basalt	756				i
IIIRCC-5	Claystone	565	573	448	642	a
	Diabase	1020				i
IIIRCC-2	Gneiss	10	27	125	13	a
IIIRCC-1	Itabirite	7353	12970	4078	2535	a
MQ	Itabirite	28327		12389	13271	c,d,b
8ISCW-20	Metapellit		779	152	59	b,h
8ISCW-19	Metapellit		4617	183	15	b,h
	Metasedimentary	55				i
IIIRCC-3	Migmatite	48	114	290	23	a
IIIRCC-14	Migmatite	218	946	90	9	a
8ISCW-22	Pellitic		603	249	169	b,h
IIIRCC-8	Sandstone	67	71	643	118	a
8ISCW-3	Sandstone		219	461	55	b,h
8ISCW-10	Sandstone		230	538	53	b,h
	Sandstone	608				i
8ISCW-9	Schists		230	538	53	b,h
8ISCW-18	Schists		1043	193	24	b,h
	Siltstone	45				i
IIIRCC-4	Tertiary Sediments	11	18	253	23	a
F7	Tuffite	1845	4990	3419	2247	b,f
F9	Tuffite	3612	4365	15848	2356	b,f
F2	Tuffite	816	3129	1093	1034	b,f
F3	Tuffite	1064	2981	1633	1577	b,f
F4	Tuffite	1332	2952	1810	1624	b,f
F5	Tuffite	1359	3822	2232	1839	b,f
F6	Tuffite	1494	4707	2359	1901	b,f
	Limestone	18-110				j
	Limestone	10-630				k

a. Resende et al. (1985), b. Resende et al.(1986), c. Fontes et al. (1985), d. Curi (1983), e. Curi and Franzmeier (1984), f. Santana (1984), g. Gualberto (1984), h. Camargo et al. (1986), i. Singer and Fine (1989), j. Tite and Mullins (1971), k. Tite and Linington (1986).

Table 3.4. Magnetic susceptibility ( $10^{-8} \bullet m^3 / Kg$ ) of soils and soil fractions derived from different parent materials.

**Surface area:** As mentioned by Schwertmann and Taylor (1989), soil Fe oxides usually occur as small particles that present very reactive surfaces to the soil solution. Hence, the Fe oxides are efficient sorbents for inorganic anions (phosphate, silicate, molybdate), dissolved organic compounds (biocides, humic and fulvic acids), and metals (Al, Cu, Pb, V, Zn, Co, Cr, Ni). Another important surface phenomenon associated with the soil Fe oxides is their ability to aggregate (affecting the structure of soils) and to cement particles leading to the formation of crusts, nodules, plinthite, laterite, ortstein, and bog iron ores.

In general, tropical soils are expected to have low specific surface areas because their clay mineralogy is dominated by kaolinite; however, the presence of Fe and Al oxides with different degrees of crystallinity and crystal shape may produce unexpectedly high reactivity. Values of specific surface area for Fe oxides obtained by different methods (mostly indirect) from different soils range from 47 to 1154 m<sup>2</sup>/g (Table 3.5). These values are much higher than for most clay minerals and show why the oxides are primarily responsible for microstructure development, soil water behavior, and surface reactions occurring in these soils.

Several studies suggest that soil hematites typically have lower specific surface areas than goethite (Bigham et al., 1978b; Curi and Franzmeier, 1984; Palmieri, 1986). By contrast, Gallez et al., (1976) reported that the specific surface areas of Fe oxides (mostly hematite) in Nigerian soils derived from basaltic rocks averaged 300 m<sup>2</sup>/g as compared to 50 m<sup>2</sup>/g for the iron oxides (mostly goethite) derived from acid rocks. The lower values in the second case were attributed to a strong association between kaolinite

and the Fe oxides resulting in a blockage of effective surface area. As a result, phosphorus sorption in the soils derived from acid rocks was lower than that in the soils derived from the basaltic rocks (Juo and Fox, 1977).

Fraction	Soils	#	SSA(1)	AV	SD	Reference
DCB- Fe <sub>2</sub> O <sub>3</sub>	Red Soils-Australia	7	101-410	267	101	Deshpande et al., 1968
DCB- Fe <sub>2</sub> O <sub>3</sub>	Ultisols-Alfisols-Nigeria	4	47-324	168	131	Gallez et al., 1976
DCB- Fe <sub>2</sub> O <sub>3</sub>	Oxisols-Brazil	6	629-1154	929	175	Curi and Franzmeier, 1984
DCB-EDTA-Fe <sub>2</sub> O <sub>3</sub>	Tasmania	10	79-336	173	82	Borggaard, 1983
EDTA- Fe <sub>2</sub> O <sub>3</sub>	Tasmania	11	268-658	446	136	Borggaard, 1983
DCB weigh loss	Oxisols-Brazil	4	60-93	76	15	Bigham et al., 1978b
DCB weigh loss	Petroferric material	16	77-278	146	55	Ibanga et al., 1983

SSA = specific surface area (m<sup>2</sup>/g); AV = average value; SD = standard deviation

Table 3.5. Specific surface area (m<sup>2</sup>/g) of soil Fe-oxides (Schwertmann, 1988)

### 3.5. Iron oxides : factors of soil formation

Iron oxide minerals are distributed in various proportions through different soils depending on the weathering intensity (Pena and Torrent, 1984; Boero and Schwertmann, 1987), climatic regime (Kämpf and Schwertmann, 1983), vegetation, drainage conditions, and type of parent material (Resende, 1976; Curi, 1983; Resende et al., 1986; Fontes, 1988). These soil forming factors determine specific soil characteristics (pH, Eh, cations and anions present, osmotic pressure, temperature) that change over time and, with different intensities, guide the formation of various Fe oxides. The simulation of the effect

of each of these factors on the genesis of these minerals can best be performed under laboratory conditions.

**Hematite/goethite:** Two of the most studied iron oxides under controlled conditions are hematite and goethite. In very general terms, laboratory syntheses of hematite and goethite have suggested that the presence of organics, soluble Si, slow Fe release, low temperatures (Schwertmann, 1985), pH extremes (both low and high) (Schwertmann and Murad, 1983), high water activity (Torrent et al., 1982), and Na and K in solution (Torrent and Guzman., 1982) favor the formation of goethite over hematite.

These laboratory experiments have helped to explain many of the field occurrences of these two minerals. In soils from Tasmania, Taylor and Graley (1967) observed a decrease in the amount of goethite relative to hematite with decreasing altitude from 575 m to sea level. This decrease corresponded to a temperature increase from 9 to 12°C and a decrease in the precipitation from 1650 to 1080 mm/year. These results are similar to those found by Schwertmann et al. (1982a) in the southern region of Germany and Bui et al. (1990) in Niger. Interpretations of data collected along altitudinal climatic gradients in the Paraná River Basin, Brazil, (Kämpf and Schwertmann, 1983; Palmieri, 1986) have also suggested that the proportions of hematite and goethite are largely a function of climate (temperature, precipitation, and evapotranspiration). Once again, goethite was the dominant Fe oxide in soils at high elevations (high precipitation and low temperature) and hematite contents increased as elevation decreased (temperature increases and precipitation decreases). However, recent detailed studies (Bellieni et al., 1984a, 1984b) of the flood basalts indicate that acid/intermediate extrusive rocks also occur in the Paraná

River Basin. The acid/intermediate rocks (mostly rhyolites, dacites, latites, and andesites) cover about 10% of the area but are concentrated on the east side of the basin and at high altitudes, whereas the basic rocks (mostly latite-basalts, andesite-basalts and subalkaline basalts) are concentrated on the west side of the basin at lower altitudes. Thus, the interpretations of previous studies in Brazil are potentially confounded by changes in rock chemistry.

Schwertmann et al. (1982a) detected small amounts of hematite in Alfisols from southern Germany with average annual temperatures as low as 8°C. Water deficits (low relative humidity) also appear to increase the formation of hematite. In laboratory experiments, Torrent et al. (1982) observed an increase in the formation of hematite from ferrihydrite with a decrease in the relative humidity from 99 to 70%. Moisture and solution gradients in toposequences of soils are well known and may explain previous reports of color variations where climatic gradients and changes in parent material are not factors. Moniz et al. (1982), for example, found hematite to be the predominant Fe oxide mineral in soils from the upper (drier) portion of a typical Brazilian soil landscape, whereas goethite was more abundant in downslope soils where conditions were more humid and organic matter was abundant. Similar observations were made by Willians and Coventry (1979) in England and Curi and Franzmeier (1984) in Brazil. In contrast, Macedo and Bryant (1987) studied the morphology and mineralogy of Oxisols from central Brazil and found that hematite was concentrated in the wetter segments of the landscape. They concluded that the hematite was a relict of former, drier climates and had not been transformed to goethite (Fey, 1983) due to the lack of an energy source for

microorganisms to reduce the Fe(III) in hematite. This was later confirmed (Macedo and Bryant, 1989) in laboratory experiments wherein sugar was added and hematite was rapidly converted to goethite. This result is also consistent with the idea that organic complexes favor the formation of goethite (Kämpf and Schwertmann, 1983) by preventing ferrihydrite precipitation as a necessary precursor to hematite (Schwertmann and Taylor, 1989).

As noted previously, foreign ions may be incorporated into both the goethite and hematite structures during the precipitation process. Anand and Gilkes (1987), for example, found significant quantities of Co, Ni, Cr, V, Cu, Zn and Mn in Fe oxides from lateritic profiles in Australia. Aluminum, however, is easily the most common foreign ion in hematite and goethite (Norrish and Taylor, 1961; Davey et al., 1975), and its presence may have significance with regard to the environment of formation (Fitzpatrick and Schwertmann, 1982). Rodrigues (1984), working with "Terra Bruna Estruturada" soils formed from alkaline rocks in Poços de Caldas, Brazil, found values of Al substitution in goethite exceeding 35 mole %. By contrast, the maximum Al substitution in hematite appears to be around 16 mole % (Bigham et al., 1978a). Maximum Al substitutions in goethites (over 32% mole percent) have usually been reported from allic soils where intense weathering has provided an ample supply of Al in the soil solution. Goethites formed under hydromorphic conditions and in mesotrophic soils (weakly acid) typically contain lower Al contents (up to 15 mole %).

The substitution of foreign ions for Fe not only affects the particle size and unit cell dimensions of goethite and hematite but may also influence their geochemical

stabilities. Fey (1983) used Gibbs free energy of formation data and the fact that the goethite structure may accommodate more Al substitution than that of hematite to predict that periodic reducing conditions may result in the preferential reduction and removal of hematite when both hematite and goethite are present in a soil. Bryant and Macedo (1990) subsequently used differential chemoreductive dissolution with sodium dithionite as the reducing agent to demonstrate that hematite would dissolve before goethite. They also found that increasing Al substitution decreased the rate of dissolution for both goethite and hematite.

**Maghemite:** Besides hematite and goethite, maghemite has also been found in tropical soils, especially those formed from basic volcanic rocks (Resende, 1976; Kämpf, 1981; Curi, 1983; Palmieri, 1986; Resende et al., 1986; Fontes, 1988). While detection is usually easy due to its magnetic character, further characterization of soil maghemites has been complicated by the same problems encountered with the other soil Fe oxides, i.e., small particle size, variable crystallinity and composition, and low concentrations. Density magnetic fractionation (Fontes, 1988) and the boiling 5M NaOH concentration procedure (Kämpf and Schwertmann, 1982), have been used with some success to beneficiate samples for further analysis. Most of the data related to maghemite are concerned with its magnetic properties and there have been few attempts to understand its genesis or pedogenic relationships to other Fe oxides. Bryant (1981), cited by Curi (1983), observed that periodic reducing conditions promoted the dissolution of maghemite and lowered the magnetic attraction of soils from Indiana. Curi (1983) observed similar results in a toposequence of soils developed on basalt in Brazil (profiles G1 to G6, Table

3.4). Hematite and maghemite formed under well drained conditions on the summit of the landscape (profiles G5 and G6) while soils on the footslope position (profiles G1 and G2) contained no maghemite and goethite was the dominant Fe oxide. Fontes (1988) evaluated the distribution of Fe oxides in Oxisols formed from different parent materials in the state of Minas Gerais, Brazil. He observed a strong association between magnetic susceptibility, the presence of maghemite and the type of parent material. Maghemite was only identified in the clay fraction of Oxisols formed from volcanic rocks and not in those formed from schist, sandstone and claystone. Using DXRD he was able to calculate the amount of Al substitution within the maghemite and observed values of 16 to 26 mole %. Resende et al. (1985) also studied the magnetic susceptibility of a set of Brazilian soils. Maghemite was identified in Oxisols developed on mafic, tuffitic, and itabirite rocks (Table 3.4), and the authors argued that Fe content, color and magnetic susceptibility were highly correlated and should be used as diagnostic criteria to classify tropical soils.

## Chapter 4

### MATERIALS AND METHODS

In order to evaluate the effects of parent material, intensity of weathering, landscape position, and chemical properties on the distribution of clay minerals and Fe oxides in soils of the PFV, sets of soil and rock samples were collected from five toposequences (Ibiporã, Tamarana, Faxinal, Campo Mourão and Cruzmaltina) within the same climatic regime (Cfa - Koepen type) in northern Paraná. The parent material for the toposequences at Ibiporã, Campo Mourão and Cruzmaltina was basalt; whereas those at Tamarana and Faxinal were formed from acid/intermediate extrusive volcanic rocks of the PFV (Fig. 4.1). All toposequences except that at Campo Mourão (Campo Mourão sub-plateau) occurred on the Apucarana sub-plateau .

To evaluate the regional effect of climate on the formation of Fe oxides during the weathering of basalt, Oxisol samples from the Ibiporã, Campo Mourão and Cruzmaltina toposequences were combined with similar samples collected throughout the third plateau of Paraná (and from northern São Paulo) as part of previous research studies (Castro F<sup>o</sup>, 1988; Alleoni and Camargo, 1994a and 1994b; Peixoto, 1995). These were further supplemented by samples collected at the institutional research stations of the Instituto

Agronômico do Paraná (IAPAR) in Cambará and Pato Branco and the Fundação Universidade Estadual de Maringá (FUEM) in Maringá, and by grab samples taken during a field trip in 1987 that involved members of the IAPAR and Ohio State University (OSU) staffs (Bigham, personal communication). In most cases, samples of the underlying basalt were also collected for analysis. The full distribution of sample sites is summarized in Fig. 4.2 , which also shows the locations of previous studies involving the characterization of Fe oxides in soils formed from rocks of the PFV (Kämpf, 1981; Curi, 1983; Palmieri, 1986; and Fontes, 1988). Samples from the latter sites were not available for use in the current study.

#### **4.1. Rock samples**

An important aspect of this dissertation is the influence of the parent rock on the genesis of soil Fe oxides. The parent rock materials were always collected close to (if not immediately beneath) the soil profiles of interest. Quarries, open pits, and road cuts were used depending upon the situation (Table 4.1). At each location, several pieces (50-250g) of fresh rock were sampled and saved in double plastic bags. At some locations, samples of saprolite and weathered rock were also collected for analysis.

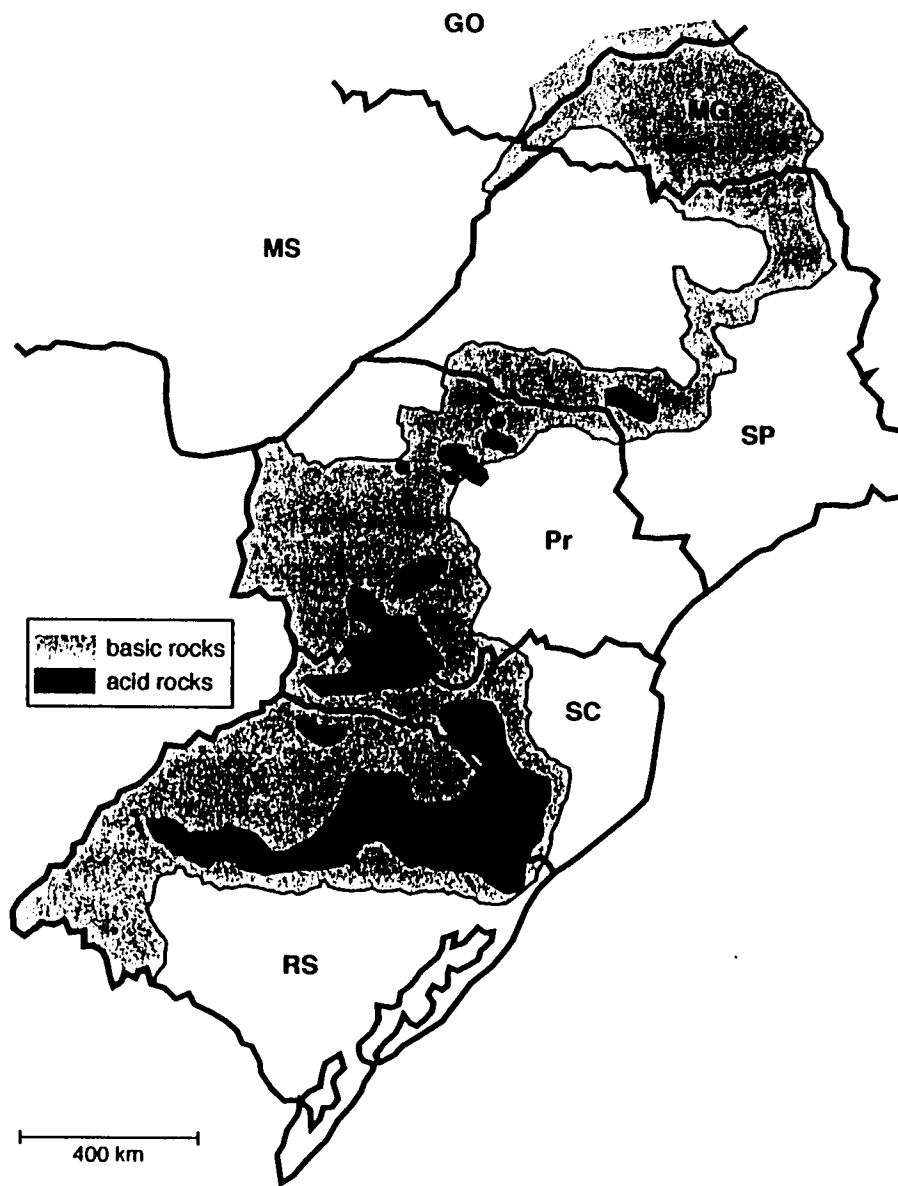


Figure 4.1. Toposequences sampled in Paraná state.

Site	Parent Material	Source	Collected by *
Cambará	Basalt	road cut, quarry	MAP and LAL
Campo Mourão	Basalt	quarry	ACSC
Faxinal	Basalt	road cut	ACSC and RTGP
Faxinal	Acid/intermediate	quarry	ACSC
Guarapuava	Acid/intermediate	road cut	JMB
Ibiporã	Basalt	quarry	ACSC
Londrina	Basalt	quarry	ACSC
Maringá	Basalt	quarry, road cut	CAT and JMB
Pato Branco	Basalt	road cut	AC and JMB
São Miguel do Iguaçú	Basalt	road cut	JMB
Tamarana	Basalt	road cut	ACSC
Tamarana	Acid/intermediate	road cut	ACSC
Toledo	Basalt	road cut	JMB
Vitória	Acid/intermediate	road cut	RTGP

\* MAP = Marcos Antonio Pavan (IAPAR), LAL = Luiz Antonio Lucchese (UFPr); ACSC = Antonio C. S. Costa (FUEM); JMB = Jerry M. Bigham (OSU); RTGP = Ricardo T.G. Peixoto(IAPAR); CAT = Cassio A. Tormena (FUEM); AC = Ademir Calegari (IAPAR)

Table 4.1. Location and source of parent rock materials analyzed in this study.

## 4.2. Soil samples

### 4.2.1. Soil toposequences

Each toposequence included at least two profiles occurring on the same landscape and developed from the same rock material. Profiles occupying sideslope and footslope positions may have been influenced by colluviation processes. A total of 18 profiles were described in the field using standard morphological terminology (Table 4.2).

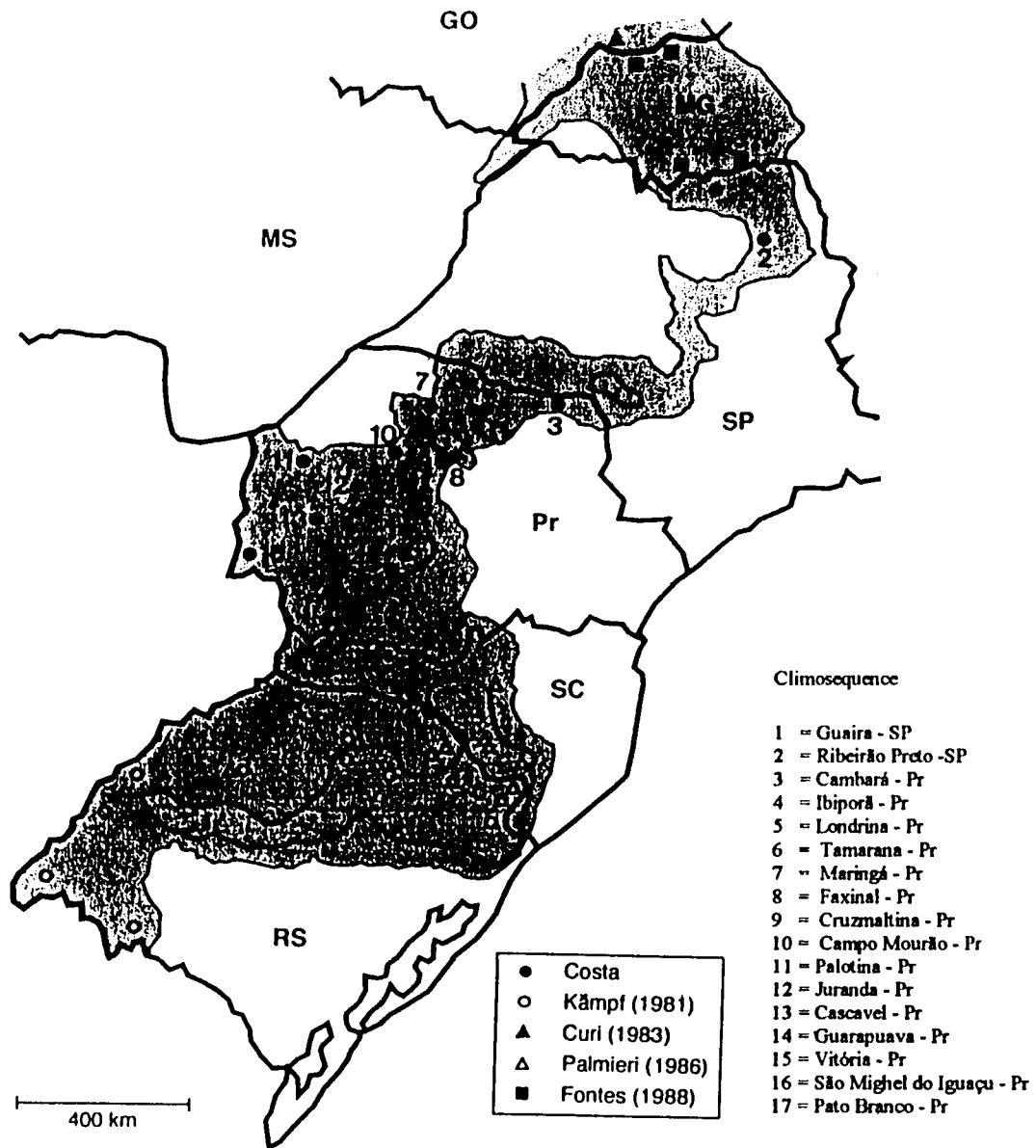


Figure 4.2. Distribution of all sampling sites and previous work in the Paraná river basin

Prof. #	Location	Brazil*	USA **	Parent Material ***
1.	Ibiporã	Terra Roxa Estruturada	Alfisol	Basalt
2.	Ibiporã	Solos Litólicos	Mollisol	Basalt
3.	Ibiporã	Brunizem Avermelhado	Mollisol	Basalt
4.	Ibiporã	Latossolo Roxo	Oxisol	Basalt
5.	Campo Mourão	Latossolo Roxo	Oxisol	Basalt
6.	Campo Mourão	Latossolo Roxo	Oxisol	Basalt
7.	Campo Mourão	Solos Litólicos	Entisol	Basalt
8.	Tamarana	Cambissolo	Inceptisol	Acid/intermediate rock
9.	Tamarana	Terra Bruna Estruturada	Ultisol	Acid/intermediate rock
10.	Tamarana	Terra Bruna Estruturada	Ultisol	Acid/intermediate rock
14.	Cruzaltina	Terra Roxa Estruturada	Ultisol	Basalt
15.	Cruzaltina	Solos Litólicos	Entisol	Basalt
16.	Cruzaltina	Latossolo Roxo	Oxisol	Basalt
17.	Cruzaltina	Latossolo Roxo	Oxisol	Basalt
18.	Faxinal	Latossolo Bruno	Oxisol	Acid/intermediate rock
19.	Faxinal	ND	ND	Acid/intermediate rock
20.	Faxinal	Solos Litólicos	Entisol	Acid/intermediate rock
21.	Faxinal	Solos Litólicos	Entisol	Acid/intermediate rock

ND-not determined (auger soil samples); \* = Camargo et al (1987), \*\* = Soil Survey Staff (1994), \*\*\* = Basalt (rocks with SiO<sub>2</sub> ≤ 53%) , Acid /intermediate rocks (rocks with SiO<sub>2</sub> > 53%)

Table 4.2. Profile, location, parent material and classification of soil profiles.

#### **4.2.2. Soil climosequence**

The samples used in this study were from surface and subsurface (A1 or Ap and Bo) horizons of highly weathered, freely-drained profiles (Oxisols) located on the most stable landscape positions (Table 4.3). Only the most highly weathered soils were used in order to represent near equilibrium conditions for the local pedochemical environment. All profiles were weathered from basalt and represented a wide range in soil chemical characteristics (allic to eutrophic). Two samples from the state of São Paulo were included because they permitted the climosequence to be extended to hotter and drier (Aw, Koeppen type of climate) conditions than can not be found in the state of Paraná.

Site	Altitude (m)	Average Annual T (°C)	Annual P (mm)	ETp (mm)	P-ETp (mm)	Koepfen Classif.
Cambará - Pr	450	21.1	1371	1342	29	Cfa
Campo Mourão - Pr	616	21.2	1700	1200	500	Cfa
Cascavel - Pr *	760	19.5	1937	1033	904	Cfa
Cruzmalina -Pr*	655	17.5	1750	1200	550	Cfa
Faxinal - Pr*	650	17.5	1750	1200	550	Cfa
Guaíra - SP	490	23.6	1250	1222	28	Aw
Ibiporã - Pr	510	21.8	1565	1358	207	Cfa
Juranda - Pr *	560	20.0	1650	1100	550	Cfa
Londrina - Pr	570	20.8	1603	1279	324	Cfa
Maringá -Pr	550	21.0	1600	1400	200	Cfa
Palotina - Pr	710	21.3	1649	998	651	Cfa
Pato Branco - Pr	760	18.7	2136	1020	1116	Cfa
Ribeirão Preto - SP	621	22.4	1534	1095	439	Aw
São Miguel do Iguaçu - Pr	180	21.3	1833	1000	833	Cfa
Tamarana - Pr*	640	20.0	1650	1200	450	Cfa

\* interpolated values. T = temperature, P = precipitation, Et<sub>p</sub> = evapotranspiration

Table 4.3. Altitudes, climatic conditions, and climatic classifications according to the Koepfen system for the climosequence sites in the states of Paraná (IAPAR, 1994) and São Paulo (Setzer, 1966)

### **4.3. Rock characterization**

#### **4.3.1. Total chemical analysis**

The rock specimens were cleaned with alcohol and, when weathering rinds were present, trimmed with a Hillquist rock saw to expose “unweathered” volumes for sampling. The subsamples were ground with a 800 Spex Mixer/Mill using a Tungsten carbide sample holder, for periods of 10 min until all material had passed a 100 mesh nylon sieve. Approximately 5 g of each sample were separated, placed in glass vials, and sent to XRAL-laboratories (Division of the Société Générale de Surveillance - SGS, 1885 Leslie St., Don Mills, Ontario, Canada M3B 3J4) for total chemical analysis by X-ray fluorescence (method XRF-101). One sample was sent in duplicate (Faxinal - acid / intermediate rock) and one internal standard obtained from CANMET (SY-2, syenite rock) was also sent for analysis in order to check the precision and accuracy of the results.

#### **4.3.2. X-ray diffraction**

A X-ray diffraction pattern was obtained from each of the powdered rock samples. The powdered material (~ 200 mg) was gently side-loaded into an aluminum holder using a glass slide to contain the sample and to avoid preferential orientation of the mineral grains. Diffraction patterns were recorded from 2 to 68 °2θ using Cu Kα radiation from a Philips Electronics PW 1316 / 90 wide range goniometer fitted with a theta-compensating slit, a 0.2 mm receiving slit, and a diffracted beam graphite monochromometer. Data were collected in a step scan mode (0.02 °2θ for 5 sec) and transferred from the detector to a computer using a Databox (Radix Instruments, 1990) interface and software.

### 4.3.3. Magnetic susceptibility

The magnetic susceptibility of each powdered rock sample was measured using a Bartington MS2 Magnetic Susceptibility System (Bartington Instruments LTD, Oxford, England) coupled with a MS2B sensor. This is a dual frequency meter that exposes the samples to a weak alternating magnetic field of approximately  $80 \text{ A}\cdot\text{m}^{-1}$ . The MS2 meter also has two range multipliers (0.1 and 1) that permit the analysis of a wide range of materials. The MS2B sensor is equipped with both low frequency (0.46 kHz) and high frequency settings (4.65 kHz) for the identification of fine grained paramagnetic or superparamagnetic materials.

Ten  $\text{cm}^3$  of sample were weighed into 20  $\text{cm}^3$  glass vials and placed in the appropriate sample holder. The volumetric magnetic susceptibility values ( $\kappa$ ) for samples with weak magnetic susceptibility were corrected ( $\kappa_c$ ) for the magnetic susceptibility of the background using the average measurement (in duplicate) of ten empty glass vials ( $\kappa_{\text{first air}}$ ,  $\kappa_{\text{second air}}$ ) at both high and low frequency (Dearing, 1994).

$$\kappa_c = \kappa_{\text{sample}} - [(\kappa_{\text{first air}} + \kappa_{\text{second air}}) / 2] \quad (4.1)$$

The mass specific magnetic susceptibility ( $\chi_{\text{lf}}$ ) was measured using the low frequency volumetric magnetic susceptibility as follows:

$$\chi_{\text{lf}} = \kappa \text{ or } \kappa_c / \rho \quad (4.2)$$

where  $\chi_{\text{lf}}$  = low frequency mass specific susceptibility ( $10^{-8} \cdot \text{m}^3 / \text{Kg}$ )

$\kappa$  = volumetric magnetic susceptibility (dimensionless)

$\rho$  = bulk density of the sample ( $\text{Kg}/\text{m}^3$ ).

Using S.I. units and keeping the volume of the samples at 10 cm<sup>3</sup>, one can rearrange eq. (4.2) to measure the mass specific magnetic susceptibility as:

$$\chi_{lf} = (\kappa \bullet 10 / m) \quad (4.3)$$

where  $\chi_{lf}$  = mass specific magnetic susceptibility (10<sup>-8</sup> • m<sup>3</sup> / Kg)

$\kappa$  = volumetric magnetic susceptibility (dimensionless)

m = mass of the basalt sample (g).

The presence of superparamagnetic minerals due to very small particle size (<0.03  $\mu$ m) could be determined from the dual frequency dependent magnetic susceptibility ( $\chi_{fd}$ ). In this determination, the volumetric magnetic susceptibility ( $\kappa$ ) was measured at the low frequency (0.46 kHz) setting ( $\kappa_{lf}$ ) and subsequently at the high frequency setting (4.6 kHz) ( $\kappa_{hf}$ ). The percentage dual frequency magnetic susceptibility ( $\chi_{fd}$  %) was then calculated by:

$$(\chi_{fd} \%) = 100 \bullet ((\kappa_{lf} - \kappa_{hf}) / \kappa_{lf}) \quad (4.4)$$

#### 4.3.4. Thin section

Samples of the fresh rocks (Table 4.1) were sent to Mineral Optics Laboratory (Wilder, VT) where were cut and fixed in glass slides for petrographic analysis.

#### **4.4. Soil characterization**

##### **4.4.1. Profile descriptions and sampling**

The morphologies of profiles 1 through 21 (Table 4.2) were recorded in the field using the methodology described by Lemos and Santos (1982) and the Soil Survey Manual (Soil Survey Staff, 1972). The horizon nomenclature was taken from the Soil Survey Manual and EMBRAPA (1988). Disturbed soil samples from each horizon (1 Kg) were placed in plastic bags and taken to the laboratory. Part of the soil material ( $\approx 500$  g) was dried in the shade for further chemical and physical ( $\approx 300$  g) characterization in the soil fertility laboratory of the Departamento de Agronomia - FUEM. The remaining dried ( $\approx 200$  g) and field-moist ( $\approx 500$  g) soil materials were carefully packed in triple plastic bags and double cardboard boxes and sent to OSU for clay mineralogical analysis.

##### **4.4.2. Particle size distribution**

Particle size distribution was determined according to the pipette method described by Camargo et al. (1986) with some modifications. First, the air dried soil material was passed through a 2-mm sieve (sieve n° 10) and the percentage of material passing the sieve was determined. Ten g of the the  $<2$ mm fraction was placed in a 1000-mL plastic bottle with 10 mL of 1M NaOH and 200 mL of distilled water and 10g of coarse clay to completely disperse the soil aggregates. The resulting suspension was shaken for 2 hr. The material was placed in a 1000-mL glass cylinder and shaken for 30 s. An aliquot of the silt fraction was pipetted at a depth of 10 cm after a settling time of 4 min and 30 sec

as determined by Stokes' Law. A similar aliquot of the clay fraction was pipetted after 4 hr at a depth of 5 cm. The sand content was then determined by difference.

#### **4.4.3. Total carbon content**

Total C content was determined using a dry combustion procedure (Soil Survey Staff, 1972). Approximately 10 g of the < 2mm fraction was accurately weighed into a ceramic boat and doped with MnO<sub>2</sub>. The sample was then inserted into a furnace (900 - 950 °C) under a continuous stream of O<sub>2</sub>. The CO<sub>2</sub> liberated by the combustion of the organic matter was trapped in a pre-weighed absorption bulb containing ascarite and determined gravimetrically. The total C (% TC) was calculated by:

$$\% \text{ TC} = ((S_A - S_B) / M_S) \cdot 27.2727 \quad (4.5)$$

where  $S_B$  = weight (g) of absorption bulb before ignition

$S_A$  = weight (g) of absorption bulb after ignition

$M_S$  = initial dry mass of the sample.

#### **4.4.4. pH, exchangeable cations, and exchangeable acidity**

Soil pH values in water (pH<sub>H<sub>2</sub>O</sub>) and in 0.01M CaCl<sub>2</sub> (pH<sub>CaCl<sub>2</sub></sub>) were determined from 1:2.5 soil solution mixtures. The mixtures were shaken for 15 min and allowed to settle for 30 min after which the pH was determined using a glass electrode.

Exchangeable cations (Ca, Mg, Al) were extracted with 1M KCl using a soil: solution ratio of 1:10 and determined using an EDTA procedure (EMBRAPA, 1979).

Potassium and P were extracted with a mixture of 0.0125M H<sub>2</sub>SO<sub>4</sub> and 0.05M HCl at a soil : solution ratio of 1:10. Potassium was determined in the extract by flame emission photometry and P was determined by colorimetry using ascorbic acid and reduced phosphomolybdate (EMBRAPA, 1979).

The exchangeable acidity (H + Al) was determined with 1M (CH<sub>3</sub>COO)<sub>2</sub>Ca at pH 7.0. Five g of air dried soil (<2mm fraction) was transferred to a 125-mL Erlenmeyer flask with 75 mL of 1M (CH<sub>3</sub>COO)<sub>2</sub>Ca at pH 7.0, shaken for 5 min, and filtered. Three drops of phenolphthalein was added to the filtrate and the solution was titrated with 0.025M NaOH.

Exchangeable cations and acidity are used in the Brazilian soil classification system to define several important soil chemical parameters (EMBRAPA, 1988). These include the S value or sum of bases ( $S = Ca + Mg + K$ ); the T value or CEC where  $T = CEC = S + Al + H$ ; the V value or percent base saturation ( $\% V = ( S / T ) \bullet 100$ ); and the percentage of Al saturation where  $\% Al = ( Al / (Al + S) \bullet 100$ ). With these parameters, it is possible to separate soils according to the % base and Al saturation into eutrophic ( $\% V \geq 50$ ), dystrophic ( $\% V < 50$ ), and allic ( $\% Al \geq 50$ ) groupings.

#### **4.4.5. Magnetic susceptibility**

Magnetic susceptibility was determined as in section 4.3.3. using the <2mm soil material.

#### **4.4.6. Color**

Color was measured in the field using Munsell soil color charts (Munsell Color Company, 1975) and in the laboratory with a Minolta CR-200 chroma meter (Post et al., 1993). The field determination was performed using moist aggregates from the soil profile. In the laboratory, the determination was performed on dried, powdered soil material. The chroma meter data were used to calculate a redness rating (RR) as proposed by Torrent et al. (1983):

$$RR = ((10 - H) \cdot C) / V \quad (4.6)$$

where H = 0 for 10YR and ranges to a numerical value of 10 for 10R

C = Munsell chroma

V = Munsell value.

### **4.5. Mineralogy of the clay fraction**

#### **4.5.1. Sample fractionation**

Approximately 50 g of < 2-mm soil material was fractionated into sand, silt and clay separates using the equipment described by Rutledge et al. (1967). The soil material was weighed into a 500-mL polyethylene flask, 250 mL of distilled water and 5 mL of 1M NaOH were added, and the suspension was shaken overnight on a horizontal shaker. No attempt was made to remove organic matter. After shaking, the pH was adjusted (8 - 9.5) and the sample was poured into a sample holder for automatic fractionation. The suspensions were stirred for 3 min and allowed to settle for 7 hr and 56 min. The < 2 $\mu$ m clay material was then separated by syphoning the suspension column to a depth of 10 cm

as calculated from Stokes' Law. This cycle was repeated 7-12 times depending on the clay content of the sample. The syphoned clay fraction was collected in a bucket, flocculated with 1M NaCl, and transferred to a 500-mL flask. The clay was then washed free of excess salt by repeated centrifugation with distilled water, frozen at  $-4^{\circ}$  C, and dried in a Labconco lyophilizer. Finally, the dried clays were gently crushed with an agate mortar and pestle and saved for further analysis. The residual sand and silt fractions were removed from the automatic fractionater and separated by wet sieving with a 300-mesh sieve.

#### **4.5.2. Na-citrate-bicarbonate-dithionite extraction**

The total, non-silicate Fe ( $Fe_d$ ) was determined by using the Na-citrate-bicarbonate-dithionite (CBD) procedure of Mehra and Jackson (1960) with slight modifications. One g of air dried clay was weighed into a 100-mL centrifuge tube. Forty mL of the citrate-bicarbonate solution (pH = 7.3) was added and the sample was placed in a water bath at  $80^{\circ}$  C for 30 min. During this time, the sample was mixed at least twice using a vortex mixer (120V - 50-60 cycles/min). Three, 1-g portions of Na-dithionite ( $Na_2S_2O_4$ ) were then added to the solution at 15-minute intervals. After 1 hr, the sample was centrifuged using an IEC centrifuge for 10 minutes at 2000 rpm, and the supernatant was transferred to a pre-weighed, 250 mL polyethylene flask. The solid residue was then mixed and re-equilibrated with 40-mL of Na-citrate-bicarbonate solution for 15 minutes at  $80^{\circ}$ C. The sample was again centrifuged, and the supernatant was combined with the original extract. The CBD-extracts were then diluted, and total Fe,

Mn, Al and Si were determined by atomic absorption spectroscopy using a Varian Techtron AA-6 Spectrophotometer. The CBD-treated clays were transferred to Spectrum dialysis tubes and equilibrated against double-distilled water until the electrical conductivity of the wash water was less than  $2 \mu\Omega$ . The clays were then quick frozen in liquid nitrogen and freeze-dried in the Labconco lyophilizer.

#### **4.5.3. Acid ammonium oxalate extraction**

Poorly crystalline Fe ( $\text{Fe}_2\text{O}_3$ ) and Al ( $\text{Al}_2\text{O}_3$ ) were determined by a modification of the acid ammonium oxalate procedure of McKeague and Day (1966). A 250-mg portion of the air-dried clay was quantitatively weighed into a 100-mL polypropylene tube wrapped with Al foil to exclude light because the reaction is photosensitive. The clay was then shaken with 50 mL of 0.2M ammonium oxalate ( $\text{pH} = 3$ ) for 4 hr and the suspension was centrifuged at 2,000 rpm for 5 min. The resulting extract was saved in a 125-mL, pre-weighed plastic bottle. An aliquot was then diluted to an appropriate concentration range, and Fe and Al were determined by atomic absorption spectrophotometry as described above.

#### **4.5.4. Magnetic susceptibility**

Magnetic susceptibility of the total clay, sand and silt fractions was determined as described in section 4.3.3.

#### **4.5.5. Color**

The dry color of the natural clays was determined as described in section 4.4.6. using the Minolta CR 200 chroma meter.

#### **4.5.6. Silicate clay mineralogy**

The mineralogy of the silicate clays was evaluated using the freeze-dried, CBD-treated clays.

##### **4.5.6.1. X-ray diffraction**

The CBD-clays were analyzed by X-ray diffraction following saturation with standard cations and thermal treatment. Duplicate, 250-mg samples of clay were weighed into 16-mL polypropylene centrifuge tubes. One subsample was saturated with Mg by multiple washings with 0.5M MgCl<sub>2</sub> and the other was saturated with K by washing with 1M KCl. In both cases, excess salt was removed by repeated washings with double-distilled water (IEC centrifuge; 2000 rpm, 5 min). The resulting clays were dispersed in water using an ultrasonic cell disruptor model W185 (Heat Systems - Ultrasonic, Inc.) operated for 30 sec at 90 watts. Oriented aggregates of Mg- and K-saturated clays were then prepared on standard petrographic microscope slides using the Millipore filter transfer method of Moore and Reynolds (1989).

The air-dried aggregates (Mg-25°C and K-25°C) were x-rayed from 2 to 20 °2θ using either a step interval of 0.05 °2θ and a stepping time of 5 sec or a 0.02 °2θ step interval with a counting time of 2 sec. The K-saturated clays were then heated to 350°C

for 4 hr (K-350°C), x-rayed, heated to 550°C for 4 hr (K-550°C), and x-rayed again. Expandable clay minerals were identified by x-raying the Mg-saturated clays after exposure to an atmosphere saturated with ethylene glycol (Mg-E.G.) at 60°C inside a closed chamber for at least 24 hr. Qualitative identification of various clay minerals was based on the position of appropriate diffraction peaks following each treatment. A summary of treatment effects for the most common minerals is given in Table 4.4.

#### **4.5.6.2. Thermal analysis**

The quantitative determination of kaolinite and gibbsite was accomplished by thermal analysis (Dixon, 1966; Karathanasis and Hajek, 1982; Mackenzie, 1964; and Tan and Hajek, 1977) of the CBD-clays using a Seiko 200 instrument fitted with a Pt-Pt Rh (13%) thermocouple, controlled by a Seiko SSC - 5020 disk station, and capable of simultaneous thermogravimetric (TG) and differential thermal analysis (DTA). A basic assumption of this analysis was that the only possible dehydration and dehydroxylation events within the temperature range of interest were those related to gibbsite and kaolinite (Resende, 1976, Curi, 1983, Palmieri, 1986, Fontes, 1988). An appropriate quantity of clay material (25-50 mg) was transferred to a Pt-pan and placed on the thermocouple of the TG/DTA unit. The sample was then heated from 50 to 800°C under a 200 mL/min flux of N<sub>2</sub>-gas. The heating rate was linear with time (20°C/min), and an empty Pt pan was used as a thermally inert reference material. The equipment recorded the initial sample weight, the weight loss with increasing temperature (TG), the derivative of the weight loss (DTG), and the change in temperature of the sample relative to the reference

material during heating (DTA). The amount of gibbsite was determined using the % weight loss of the sample within the 250 - 300°C region as compared to a calculated weight loss corresponding to complete dehydroxylation of a pure sample of gibbsite.

$$\% \text{ Gibbsite} = 100 \bullet (\text{WL}_S / \text{WLGb}) \quad (4.7)$$

where  $\text{WL}_S$  = % weight loss of sample (250 - 300°C)

$\text{WLGb}$  = % weight loss of pure gibbsite (i.e., 34.6%).

Mineral	Plane	Treatment				
		Mg-25°C	Mg-E.G.	K-25°C	K-350°C	K-550°C
		----- d (Å) -----				
Kaolinite	001	7.2	7.2	7.2	7.2	disappear
	002	3.6	3.6	3.6	3.6	disappear
Halloysite	001	7.2-10	7.2-10	7.2-10	7.2	disappear
Illite	001	10	10	10	10	10
	002	5	5	5	5	5
Vermiculite	001	14	14	10	10	10
Smectite	001	14	17-18	12	10	10
Chlorite	001	14.2	14.2	14.2	14.2	14.2
	002	7.1	7.1	7.1	7.1	7.1
H.I.V. *	001	14	14	14	12	11
H.I.S. **	001	14	15	14	12	11
Quartz	001	4.2	4.2	4.2	4.2	4.2
	101	3.3	3.3	3.3	3.3	3.3
Gibbsite	002	4.8	4.8	4.8	disappear	disappear

\*H.I.V. = hydroxy-Al-interlayered vermiculite; \*\*H.I.S. = hydroxy-Al-interlayered smectite.

Table 4.4. Influence of saturating cation, solvating agent, and thermal treatment on diagnostic d-spacings of the most important clay minerals, quartz, and gibbsite.

A similar approach was used for determining the kaolinite content based on the pronounced dehydroxylation event occurring within the 400 - 600°C region.

$$\% \text{ Kaolinite} = 100 \bullet (WL_S / WL_{Kao}) \quad (4.8)$$

where  $WL_S$  = % weight loss of sample (400 - 600°C)

$WL_{Kao}$  = % weight loss of pure kaolinite (i.e., 13.9%).

#### **4.5.6.3. Magnetic susceptibility**

Magnetic susceptibility of the CBD - treated clays was determined as described in section 4.3.3.

### **4.6. Iron oxide mineralogy**

The Fe oxide content of the natural clays ranged from 1 - 30%  $Fe_2O_3$  as determined by the CBD procedure. Further mineralogical characterization of the Fe oxides was initiated by selectively dissolving kaolinite, halloysite and gibbsite using the boiling 5M NaOH procedure of Norrish and Taylor (1961) as modified by Kämpf and Schwertmann (1982).

#### **4.6.1. Boiling 5M NaOH procedure**

One g of soil clay was transferred to a plastic bottle and 100 mL of boiling 5M NaOH were added. The suspension was brought to a boil in a sand bath and maintained at  $\approx 105^\circ C$  for 1 hr. The sample was removed from the sand bath, cooled with running water,

centrifuged (2000 rpm, 5 min), and the supernatant was discarded. The residues were then sequentially washed with cold 5M NaOH, 0.5M HCl (to dissolve sodalite), 0.5M (NH<sub>4</sub>)<sub>2</sub> CO<sub>3</sub> (to remove excess Na) and twice with distilled water. The washed residues were placed in crucibles and dried in an oven (110°C) for at least 12 hr to remove excess NH<sub>4</sub> and CO<sub>3</sub>. The dried residues were removed, ground with an agate mortar and pestle and saved for further analysis.

#### **4.6.2. Selective dissolution of maghemite**

Maghemite was found to be an important component of the Fe oxide fraction in those soils formed from basic rocks. It was easily detected by magnetic susceptibility measurements of the natural clays (section 4.5.4); however, its X-ray profile was similar to hematite and this created a problem for detailed XRD analysis of both phases. In particular, the d<sub>110</sub> and d<sub>300</sub> lines of hematite have routinely been used to determine the degree of Al substitution within the crystal structure (discussed later). Unfortunately, the d<sub>110</sub> of hematite and the d<sub>311</sub> line of maghemite both occur at approximately 35.6 °2θ. Likewise, the d<sub>300</sub> line of hematite and the d<sub>440</sub> line of maghemite both occur at approximately 63.9°2θ. In order to accurately determine both the positions and integrated intensities of these important peaks of hematite, it became necessary to selectively dissolve the maghemite component. This was accomplished using a modification of a procedure described by Schwertmann and Fechter (1984).

Duplicate, 100-mg samples of the 5M NaOH residues were weighed into 100-mL polypropylene tubes. The residues were washed once with Na-citrate-bicarbonate (75°C,

15 min) and once with distilled water to remove any readily soluble Fe and Al. The remaining materials received 20 mL of 1.8M H<sub>2</sub>SO<sub>4</sub> and were maintained at 75± 5°C in a water bath for 2 hr. The samples were then centrifuged, and the extracts saved in a pre-weighed 25-mL polyethylene bottle for chemical analysis of Fe and Al dissolved from maghemite. This procedure effectively removed most of the maghemite and further concentrated hematite and/or goethite. The solid residue from one tube was washed twice with distilled water, dried (110°C for 24 hr), and saved for XRD and magnetic susceptibility analysis. The other subsample was treated with CBD (described in section 4.5.2.), and the extract was saved to determine Fe and Al present in hematite and/or goethite.

#### **4.6.3. X-ray diffraction analysis**

The powdered residues from the 5M NaOH and 5M NaOH - 1.8M H<sub>2</sub>SO<sub>4</sub> dissolution procedures were analyzed by X-ray diffraction. About 100 mg of the residues were doped with 5% silicon as an internal standard and mixed thoroughly with an agate mortar and pestle. The mixture was placed in a silicon holder and gently compacted with a glass slide to avoid preferential orientation of the mineral grains. Step scanned (0.02 °2θ for 5 sec) patterns were obtained from 15 to 68 °2θ as described in section 4.5.6.1.

Semiquantitative estimates of hematite and goethite in the 5M NaOH residues were obtained from the areas of the d<sub>012</sub> peak (x 3.5) of hematite and the d<sub>110</sub> peak of goethite (Schwertmann and Lathan, 1986). The area of the d<sub>220</sub> diffraction peak (x 3.5) of maghemite was used in similar fashion because its chemical and mineralogical

properties are similar to those of hematite. A factor of 3.5 was used for the selected hematite and maghemite peaks because the relative intensities of these diffraction peaks are approximately 30% of the maximum, whereas the  $d_{110}$  peak is the most intense for goethite. Measurements of both peak position and peak area were made using the Grams 386 v. 2.0 software. Corrections for the goethite, hematite and maghemite peak positions were calculated using a polynomial equation developed from the measured and reported peak positions of the internal standard.

Aluminum substitutions within the crystal structures of hematite, maghemite and goethite were determined using published equations that relate unit cell parameters (XRD peak positions) to the Al content. For hematite, the equations developed by Schwertmann et al. (1979) and Schwertmann and Lathan (1986) were chosen. Schwertmann et al. (1979) determined the amount of Al substitution in hematite from the  $a_0$  dimension of the unit cell as obtained from either the  $d_{110}$  or  $d_{300}$  peak positions as follows:

$$\text{mol \% Al} = 3076.8 - 610.7 \cdot a_0 (\text{\AA}) \quad (4.9)$$

where  $a_0 = d_{110} \cdot 2$ , or  $a_0 = d_{300} \cdot 3.464$ .

Schwertmann and Lathan (1986) obtained a somewhat different relationship between Al substitution and the  $a_0$  unit cell dimension of hematites synthesized at 25°C. Using a value for  $a_0$  calculated from the  $d_{300}$  diffraction line, they found:

$$\text{mol \% Al} = 678 \cdot (5.0418 - a_0(\text{\AA})) \quad (4.10)$$

The percentage of Al substitution in goethite was determined by the methodology of Schulze (1981, 1984), who calculated the  $c_0$  dimension of the goethite unit cell using the positions of the  $d_{110}$  and  $d_{111}$  peaks. Then:

$$\text{mol \% Al} = 1730 - 572 \cdot c_0(\text{\AA}) \quad (4.11)$$

where  $c_0 = ((1 / d_{111})^2 - (1 / d_{110}^2)^{-1/2})$

Aluminum substitution within the maghemite structure was evaluated from the equation developed by Schwertmann and Fechter (1984) who used the  $d_{220}$  diffraction line to calculate  $a_0$ . Then:

$$\text{mol \% Al} = ((0.8343 - a_0(\text{\AA})) / 2.22 \cdot 10^{-4}) \quad (4.12)$$

#### 4.6.4. Magnetic susceptibility.

Magnetic susceptibility of both the 5M NaOH and 5M NaOH - 1.8M H<sub>2</sub>SO<sub>4</sub> residues was determined as described in section 4.3.3.

#### 4.7. Mass balance of the clay fraction

A quantitative analysis of clay mineralogy is difficult to achieve because no single method of analysis is suitable for all components. Nevertheless, reasonable estimates can be achieved for tropical soil clays by combining data from several sources. The complete clay mineralogy of such materials can be represented by the following equation:

$$\text{CF} = (1:1 \text{ and } 2:1 \text{ CM}) + \text{IO} + \text{Gb} + \text{Qt} + \text{TO} \quad (4.13)$$

where CF = clay fraction

1:1 and 2:1 CM = 1:1 and 2:1 clay minerals including kaolinite-halloysite (KH), vermiculite, smectite, hydroxy-Al-interlayered vermiculite (HIV) and smectite, and interstratified minerals,

IO= Fe oxides including hematite (Hm), maghemite (Mm), and goethite (Gt),

Gb = gibbsite,

Qt = quartz,

TO = titanium oxides including anatase and rutile.

In this study, the total Fe oxide contents of the clays were obtained by selective dissolution using the CBD procedure. The Fe oxide fraction was then partitioned to Hm, Gt, and Mm using a combination of XRD analysis of the 5M NaOH concentrates, magnetic susceptibility measurements, and chemical analysis. Semiquantitative analysis of KH and Gb were achieved by thermal analysis of the CBD-treated clays. In most instances, the only other major component left unaccounted for was HIV. This mineral was considered to comprise the bulk of the residue (together with other 2:1 minerals, quartz, anatase, and rutile) after other major components were accounted for and was, in essence, determined by difference. Therefore, the following working equation was used for semiquantitative analysis of the clay mineralogy.

$$CF = KH + Gb + Hm + Gt + Mm + HIV \quad (4.14)$$

where parameters are as previously defined.

## Chapter 5

### RESULTS AND DISCUSSION

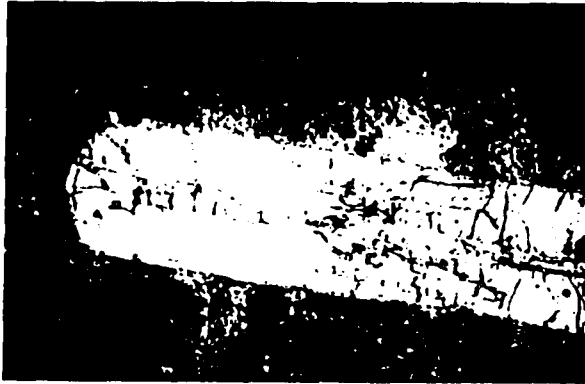
#### 5.1. The parent rock material

Early geologic studies on the volcanic rocks of the Paraná River Basin recognized the dominance of basic over acid/intermediate rocks. Maps published from these works (Brasil, 1973, Mineropar, 1986) only display the existence of basic volcanic rocks but the legends indicate the presence of acid / intermediate volcanic rocks as well (Leinz, 1949; Schneider, 1964; Sartori and Gomes, 1980). Recently, numerous geochemical studies have been conducted to determine the age (Fodor et al., 1989; Renne et al., 1992), petrology (Fodor et al., 1985; Piccirillo et al., 1988), and spatial distribution of extrusive rocks produced by the PFV (Bellieni et al., 1984a, 1984b, 1986). Maps prepared by Piccirillo et al. (1988) show significant inclusions of acid ( $\geq 63\%$  SiO<sub>2</sub>) and intermediate (53 - 63 % SiO<sub>2</sub>) rocks within the southern and eastern portions of the mostly basic ( $\leq 53\%$  SiO<sub>2</sub>) Paraná flood basalt (Fig. 2.3). In the state of Paraná, these rocks occur primarily at high elevations in the Apucarana, Guarapuava and Palmas subplateaus (Fig. 2.5) near the boundary of the PFV with sedimentary rocks of the second plateau. The presence of acid (3% by volume) and intermediate rocks (7%

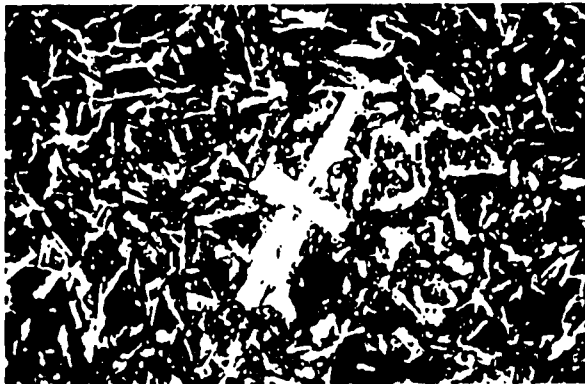
by volume) within the PFV may be related to the formation of “rhyodacite melts derived from basalts through low pressure crystal fractionation processes accompanied by crustal contamination” (Bellieni et al., 1984a, 1984b).

In the present study, rock materials were collected from a total of 14 locations (Table 4.1). Field investigations based on the map of Piccirillo et al. (1988) suggested that acid / intermediate rocks were exposed at three of the sites (Faxinal, Tamarana and Vitória). Intercalations of acid / intermediate and basic rocks were observed in Tamarana and Faxinal where sharp contacts were apparent between the proposed rock types. Differences in rock composition were associated with marked changes in soil color over lateral distances of only 1,000 and 5,000m, respectively. Differences in altitude were less than 100m. The acid rocks had a glassy matrix (Fig. 5.1), apparently produced by the rapid cooling of the magma, within which large plagioclase phenocrystals (less than 5% of the sample) could be identified with the naked eye. The basic rocks were darker and mostly microcrystalline with smaller plagioclase phenocrystals (Fig. 5.1).

Total chemical analysis of the rock samples support the field separations; however, the rock materials from Guarapuava and Vitória are intermediate in composition (Table 5.1). The basic rocks are enriched in Fe, Ca, and Mg due to the presence of magnetite, ulvöspinel, pyroxenes, and abundant plagioclase feldspars (Fig. 5.2). Secondary chlorite, probably altered from olivine (Bellieni et al., 1986) was observed in most thin sections as light green pleochroic aggregates of variable size. The acid / intermediate rocks display similar mineral suites but, in addition, contain abundant quartz in the ground mass of the rock.



a. Acid Rock - Tamarana



b. Basic Rock - Ibiporã

Figure 5.1. Thin sections of acid / intermediate (Tamarana) and basic rock (Ibiporã).

Frame width 13.4 mm.

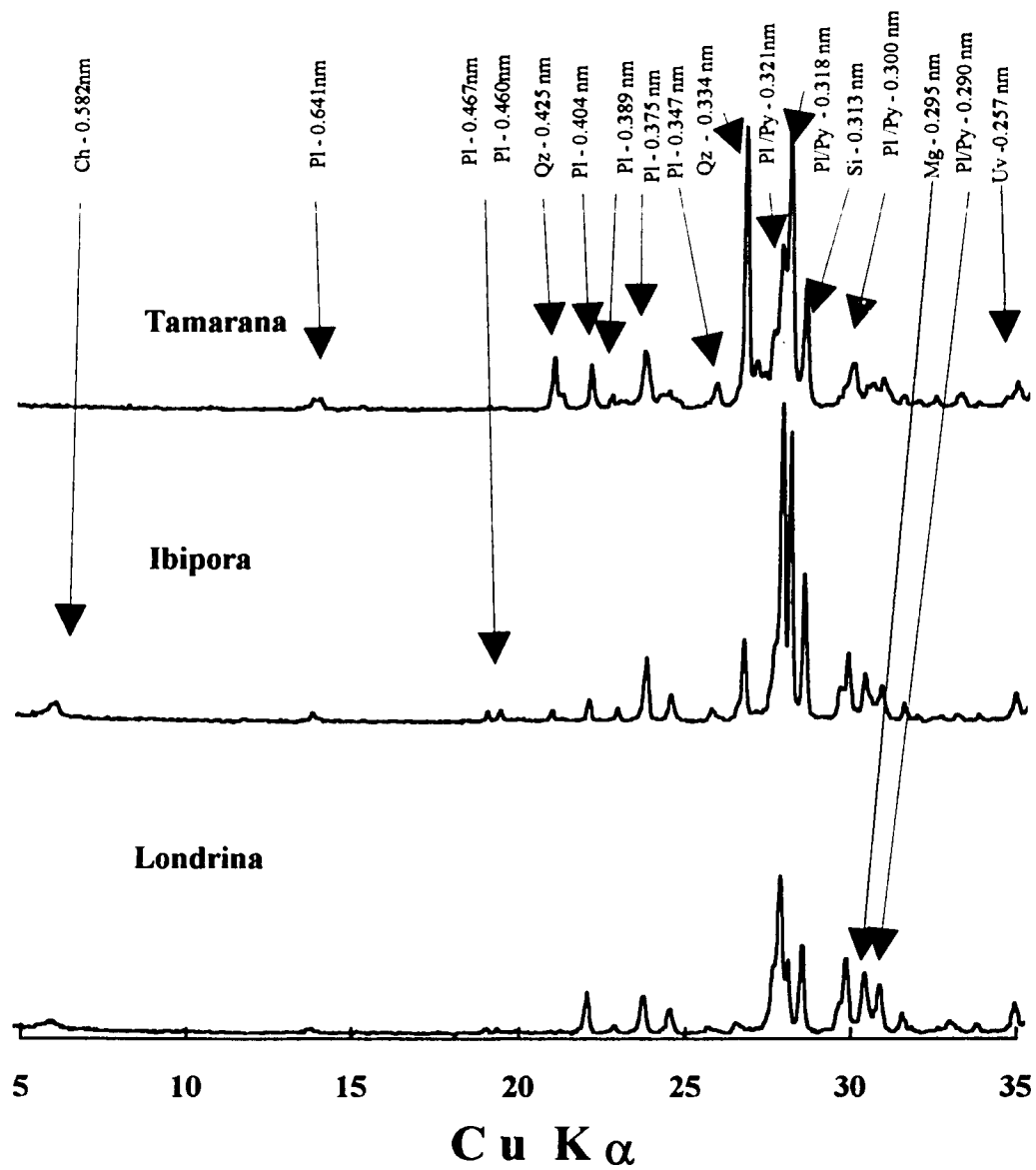


Figure 5.2. Representative XRD patterns from acid / intermediate (Tamarana) and basic (Ibiporã and Londrina) rock samples. Ch = chlorite; Pl = plagioclase feldspar; Qz = quartz; Py = pyroxene; Mg = magnetite; Uv = ulvöspinel.

Quartz was also detected in most of the basic rocks where its presence may be associated with crustal contamination of the emerging magma or to secondary formation (Faure, personal communication).

There are different approaches to classify volcanic rocks on the basis of their chemical composition. Silica is the major component and it is the common factor in most classification schemes. For example, Williams et al. (1982) separated volcanic and plutonic rocks into four broad groups based solely on the silica content. The proposed classes were acid ( $\text{SiO}_2 \geq 66\%$ ), intermediate (52 - 66%  $\text{SiO}_2$ ), basic (45 to 52%  $\text{SiO}_2$ ), and ultrabasic ( $\leq 45\%$   $\text{SiO}_2$ ). A more complex approach involves not only the amount of Si but also Na and K in a so-called total alkali-silica system (Bas et al., 1992). Recently, more than 1500 samples of volcanic rocks from the Paraná River Basin have been classified in a still more complex system (De La Roche et al., 1980) that accounts for most of the major elements (Si, Al, Fe, Mg, Ca, Ti, Na, K) (Bellieni et al., 1984a, 1984b; Bellieni, 1986; Piccirillo et al., 1988) (Fig. 5.3). According to the R1 x R2 diagram of De La Roche et al. (1980), the acid/intermediate rocks collected in the present study classify in the quartz-latitude and dacite/rhyodacite fields whereas the basic rocks are mostly basaltic-andesites or transitional-basalts (Fig. 5.4).

Basaltic andesites and rhyodacites have been identified as the two most common types of basic and acid / intermediate rocks, respectively, in the Paraná river basin (Comin - Chiaramonti et al., 1983; Bellieni et al., 1984a, 1984b; Bellieni et al., 1986; Piccirillo, 1988).

Location	Major Elements (%)										
	Na <sub>2</sub> O	MgO	Al <sub>2</sub> O <sub>3</sub>	SiO <sub>2</sub>	P <sub>2</sub> O <sub>5</sub>	K <sub>2</sub> O	CaO	TiO <sub>2</sub>	Cr <sub>2</sub> O <sub>3</sub>	MnO	Fe <sub>2</sub> O <sub>3</sub>
<b>Acid / Intermediate Rocks</b>											
1 - Tamarana	4.41	1.09	13.4	64.0	0.41	3.91	3.29	1.38	<0.01	0.18	7.60
2.1 - Faxinal	3.23	1.32	12.5	62.9	0.46	3.86	3.20	1.37	<0.01	0.15	7.06
2.2 - Faxinal	3.24	1.29	12.6	63.2	0.46	3.88	3.21	1.39	<0.01	0.15	7.14
3 - Vitória	3.83	1.53	13.1	62.3	0.43	3.99	3.18	1.39	<0.01	0.16	7.83
4 - Guarapuava	2.54	2.63	11.9	52.1	0.92	2.12	6.84	3.08	<0.01	0.20	15.2
<b>Basic Rocks</b>											
5 - Tamarana	2.49	5.05	13.1	50.3	0.39	1.25	8.95	2.67	<0.01	0.20	13.2
6 - Faxinal	2.50	4.36	12.6	49.8	0.52	1.49	8.34	2.90	<0.01	0.19	13.9
7 - Cambará	2.44	4.35	12.6	48.1	0.40	1.04	8.71	3.69	<0.01	0.19	15.4
8 - Ibiporã	2.30	4.73	12.4	50.3	0.28	1.17	9.03	2.30	<0.01	0.21	15.8
9 - Londrina	2.24	6.04	13.2	49.0	0.20	0.81	10.8	1.75	0.01	0.21	13.3
10 - Maringá	2.03	4.97	12.7	50.0	0.29	1.27	8.83	2.45	0.01	0.19	15.2
11 - Campo Mourão	2.45	4.62	12.4	50.7	0.28	1.06	9.03	2.28	<0.01	0.22	15.6
12 - São Miguel do Iguaçu	2.20	4.74	12.6	51.3	0.28	1.16	8.80	2.25	0.01	0.22	15.1
13 - Pato Branco	2.47	4.00	11.9	49.5	0.47	1.71	7.72	3.21	<0.01	0.21	15.2
14 - Toledo	2.57	5.16	12.2	50.4	0.30	1.04	9.58	2.56	<0.01	0.21	15.0

Location	Minor Elements (ppm)					<= ( %) =>		Classification
	Rb	Sr	Zr	Nb	Ba	LOI	Sum	
<b>Acid / Intermediate Rocks</b>								
1 - Tamarana	100	478	581	<10	1110	0.50	100.4	Quartz - Latite
2.1 - Faxinal	78	342	642	78	930	2.45	98.8	Dacite
2.2 - Faxinal	92	337	625	77	955	2.70	99.5	Rhyodacite
3 - Vitória	88	421	602	80	1050	1.55	99.6	Quartz - Latite
4 - Guarapuava	40	390	380	50	640	2.23	100.0	Lati - Andesite
<b>Basic Rocks</b>								
5 - Tamarana	35	465	214	25	400	1.45	99.2	Basaltic - Andesite
6 - Faxinal	31	462	246	47	463	2.05	98.8	Basaltic - Andesite
7 - Cambará	23	447	239	22	554	2.15	99.2	Basaltic - Andesite
8 - Ibiporã	33	200	163	21	298	1.10	99.7	Basaltic - Andesite
9 - Londrina	25	268	108	12	219	1.04	99.0	Transitional Basalt
10 - Maringá	50	180	170	20	310	1.23	100.3	Basaltic - Andesite
11 - Campo Mourão	<10	195	181	34	292	0.70	99.4	Basaltic - Andesite
12 - São Miguel do Iguaçu	50	200	150	30	320	1.00	99.8	Basaltic - Andesite
13 - Pato Branco	32	338	261	62	474	2.10	98.6	Basaltic - Andesite
14 - Toledo	12	207	186	36	245	0.90	100.0	Transitional - Basalt

Table 5.1. Total chemical analysis of the parent rock material and classification according to De La Roche (1980).

Hereafter, the parent rock materials will be separated for simplicity in acid / intermediate rocks (“acid rocks”) with  $\text{SiO}_2 > 53\%$  and the remaining basic rocks with  $\text{SiO}_2 \leq 53\%$ .

The average major element compositions of samples collected in the present study are in good agreement with the average results reported by Bellieni et al. (1984a) for these rock types (Table 5.2). The average minor element composition (Rb, Sr, Zr, Ba) are also consistent in most respects with previous results for these rocks (Table 5.2).

	Na <sub>2</sub> O	MgO	Al <sub>2</sub> O <sub>3</sub>	SiO <sub>2</sub>	P <sub>2</sub> O <sub>5</sub>	K <sub>2</sub> O	CaO	TiO <sub>2</sub>	Cr <sub>2</sub> O <sub>3</sub>	MnO	Fe <sub>2</sub> O <sub>3</sub>	Rb	Sr	Zr	Ba
	%											ppm			
Acid /Intermediate Rocks															
Average (5)	3.68	1.31	12.90	63.10	0.44	3.91	3.22	1.38	<0.01	0.16	7.41	90	395	613	1011
Bellieni (3)	3.21	1.47	12.81	66.93	0.31	3.54	2.99	0.97	<0.01	0.11	7.60	163	140	231	617
Basic Rocks															
Average (10)	2.38	4.60	12.51	50.14	0.39	1.28	8.78	2.65	0.01	0.20	14.81	33	305	209	383
Bellieni (49)	2.64	4.55	14.31	52.82	0.25	1.29	8.68	1.44	<0.01	0.17	13.85	55	241	151	429

Table 5.2. Average values of major and minor elements from Table 5.1 and from Bellieni et al., (1984b). Numbers of samples given in parentheses. Acid and basic rock data from Bellieni et al., (1984b) are for rhyodacites and basaltic andesites, respectively.

Bellieni et al., (1984a) observed that the basic rocks of the Paraná river basin might be further separated into high and low TiO<sub>2</sub> groups due, apparently, to heterogeneous mantle source magmas (Fodor, 1987). The high Ti rocks (above 3% TiO<sub>2</sub>) appear to be concentrated in the northern portion of the basin (São Paulo, Minas Gerais, Mato Grosso states), whereas the low Ti rocks (< 1% TiO<sub>2</sub>) are most abundant in the southern region (Santa Catarina and Rio Grande do Sul states, Fig. 2.3).

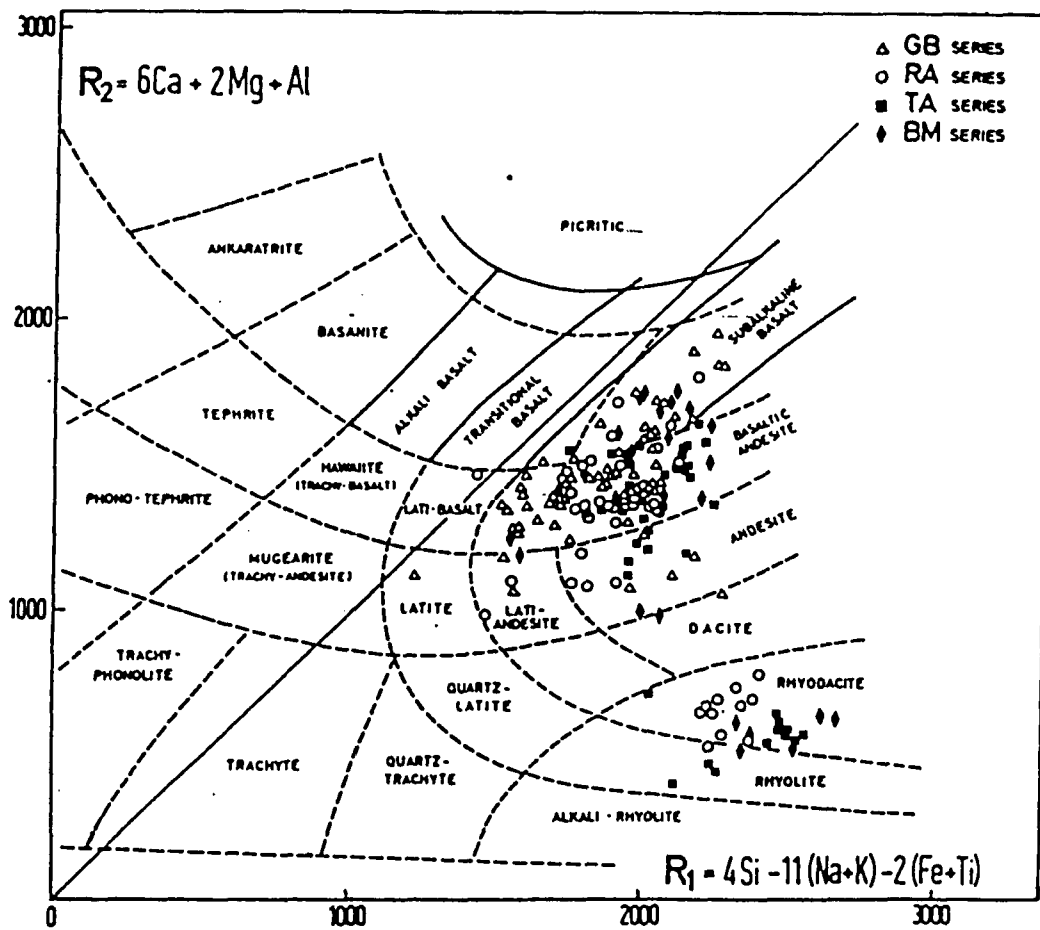
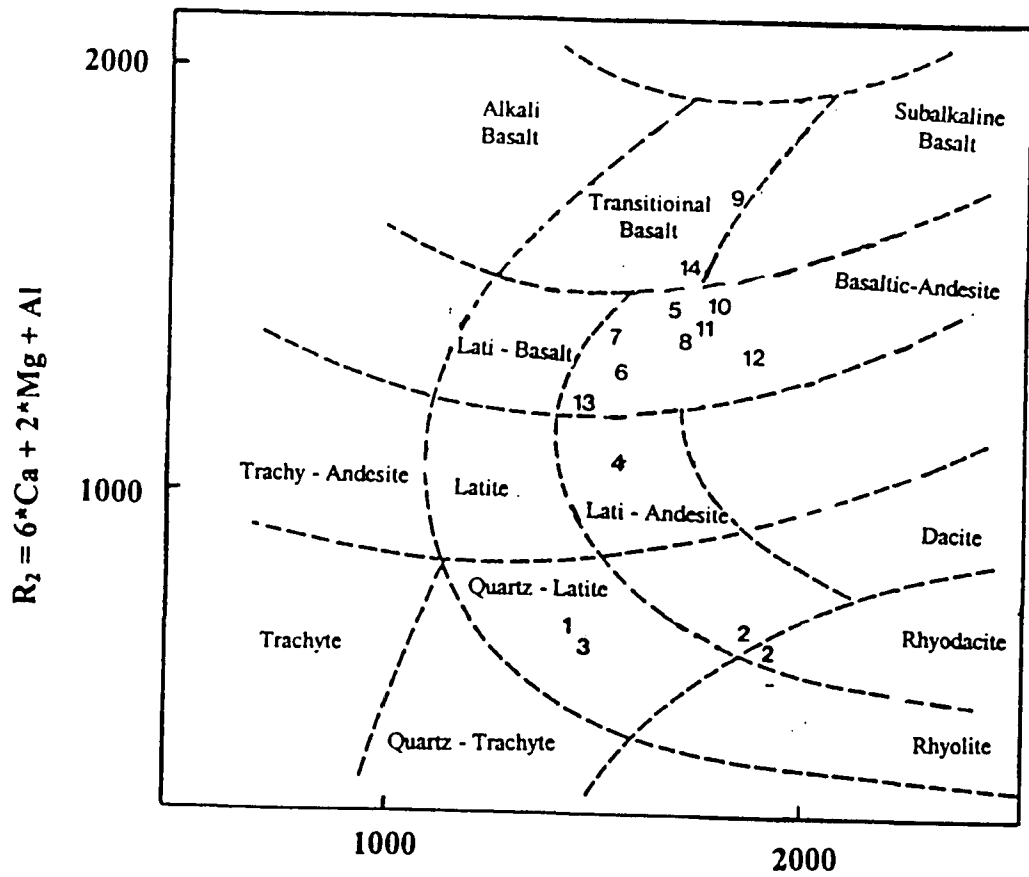


Figure 5.3. Distribution of volcanic rocks in the Paraná River Basin using the classification diagram of De La Roche et al. (1980) from Bellieni et al. (1984b).



$$R_1 = 4 \cdot Si - 11 \cdot (Na + K) - 2 \cdot (Fe + Ti)$$

Symbol	Location
Acid Rocks	
1	Tamarana
2	Faxinal
3	Vitória
4	Guarapuava
Basic Rocks	
5	Tamarana
6	Faxinal
7	Cambará
8	Ibiporã
9	Londrina
10	Maringá
11	Campo Mourão
12	Foz do Iguaçu
13	Pato Branco
14	Toledo

Figure 5.4. Distribution of volcanic rocks collected in the current study using the De La Roche et al. (1980) diagram.

The state of Paraná state should constitute an intermediate position. While most of the basic rocks analyzed in the present study contain 2 - 3% TiO<sub>2</sub> (Table 5.1), there does not appear to be any particular north-south trend in the data.

Magnetic susceptibility of the rocks was not a consistent parameter to separate the rocks. On average the basic rocks had higher magnetic susceptibilities compared to the acid/intermediate rocks due to the presence of magnetite or, more likely, Ti-magnetite (Bellieni et al., 1984a, 1984b; Bellieni et al., 1986, Piccirillo et al., 1988) (Table 5.3). The magnetic susceptibility of the rock sample from Campo Mourão was abnormally low compared with the other basic rocks. A thin section of the rock from this site (not shown) indicated the presence of a large number of opaque phenocrystals that might be ilmenite rather than magnetite (De Jesus Filho et al., 1996). The acid / intermediate rock from Tamarana produced the lowest magnetic susceptibility of all the rocks sampled; however, all magnetic susceptibility measurements remain within the range previously observed for magmatic rocks of the northern hemisphere (Dearing, 1994) (Table 3.3).

Acid/Intermediate Rocks	$\chi_{if}$ ( $10^{-8} \bullet m^3 / Kg$ )
Tamarana	163
Faxinal	800
Vitória	1253
Guarapuava	719
<b>Average</b>	<b>734</b>
Basic Rocks	
Tamarana	891
Faxinal	1582
Cambará	1423
Ibiporã	985
Londrina	1038
Maringá	875
Campo Mourão	291
São Miguel do Iguaçu	1036
Pato Branco	1123
Toledo	805
<b>Average</b>	<b>1005</b>

Table 5.3. Magnetic susceptibility ( $\chi_{if}$ ) of the ground rock samples.

## **5.2. Soil toposequences**

Five toposequences of soils were sampled within the same climatic regime (Cfa - Köppen system) in northern Paraná to study the effects of parent material, weathering intensity, and landscape position on the formation of clay minerals, gibbsite and the Fe oxides. A total of 18 pedons comprising two toposequences developed from acid / intermediate rocks (Tamarana and Faxinal) and three from basic rocks (Ibiporã, Cruzmaltina, and Campo Mourão) were sampled on the Apucarana and Campo Mourão sub-plateaus (Figs. 2.5 and 4.1). It was considered important to include landscapes typical of those occurring throughout the third plateau and to obtain soils representing a wide range of development and chemistry. Complete field morphological descriptions and basic chemical and physical characterization data for all the soils sampled are included in Appendix A. A summary of landscape relationships, the most important chemical and physical characteristics, and soil classification are presented in this section.

### **5.2.1. Morphological characteristics and landscape relationships**

Soil morphological characteristics are dependent on the intensity of the factors and processes of soil formation. In the present case, climate and organisms are treated as fixed parameters, whereas time, parent material and position on the landscape (relief) are the variable factors of soil formation (Buol et al, 1989). In the last thirty years, a number of studies have been conducted to better understand soil-landscape relationships in tropical regions. In Brazil, these include the works of Moniz and Jackson (1967), Moura Filho and Buol (1972), Demattê (1975), Aloisi et al. (1976), Andrade et al. (1976), Resende

(1976), Demattê and Holowaychuk (1977), Demattê et al. (1977), Lepsch et al. (1977a, 1977b), Kämpf and Klamt (1978), Fasolo (1978), Lima (1979), Gallego and Espindola (1979), Rauen (1980), Pötter and Kämpf (1981), Kämpf (1981), Moniz and Buol, (1982), Moniz et al, (1982), Curi (1983), Queiroz and Klamt (1985), Palmieri (1986), Clemente (1988), Demattê and Marconi (1991), Demattê et al. (1994), Rocha and Cerri (1994), Coelho et al. (1994), Moniz et al. (1994), and Kämpf et al. (1995).

Many results from these studies can be used to better understand the distribution of soils and landscapes within the Paraná River Basin. As in temperate regions, landscape position and the intensity of weathering are closely related, and additions, losses, translocations and transformations within the soils ultimately determine their intrinsic properties such as depth, color, texture, structure, and mineralogy. The concept of a catena (Milne, 1935) as a “chain” of soils related to landscape position is also valuable in that it has led to the recognition that “soils are welded together on a landscape and the processes that occur in the soils of the higher portions of the landscape have an influence on soils that occur in lower parts” (Hall, 1983). The development of a catena of soils therefore takes into account not only processes occurring on the surface of the landscape (deposition, losses by erosion, etc.) but also within the soil (lateral flow) and at the contact between the soil and its parent material (basal flow). In this manner, deeply weathered profiles occurring on stable landscape positions may be integrated with younger pedons on less stable landforms (Moniz and Buol, 1982; Moniz et al., 1982).

Erosional landscapes commonly include up to five components: summit, shoulder, backslope, footslope and toeslope (Ruhe, 1960; Buol et al., 1989). The summit is usually

the most stable situation and deep, highly weathered profiles that are homogeneous in color, texture, and structure commonly develop on this landscape element in tropical regions. In these cases, the downward movement of water leaches silica and bases and often gives rise to acid, Al-rich (allic) soils that are composed mostly of 1:1 clay minerals, gibbsite, and Fe oxides with minor amounts of quartz, Ti oxides and resistant, Al-interlayered 2:1 clay minerals (Lepsch et al., 1977b; Moniz and Buol, 1982; Moniz et al., 1982). On shoulder and backslope positions, weathering is less intense and sheet erosion often impedes the development of deep weathering profiles. The lateral and basal movement of water from upper landscape positions also brings abundant supplies of soluble materials (silica, bases) that permit the neoformation (diagenesis) of clay minerals. The moisture regime alternates constantly between wet and dry, and this contributes to the formation of a blocky structure (Moniz and Buol, 1982; Moniz et al., 1982). Tessier (1984) explains that the drying process increases the surface tension within voids, brings particles close to each other, and enhances the cohesion between particles. As a consequence of this process, granular oxic horizons that are usually present in soils of the summit positions are gradually replaced by blocky, high bulk density argillic (or kandic) horizons with or without clay skins in soils occurring on the shoulder and backslope positions (Rauen, 1980; Moniz et al., 1982; Moniz et al., 1994). There is usually also a decrease in the amount of 1:1 clay minerals, gibbsite, and Fe oxides in backslope soils because the lateral flux of silica and bases favors the formation and/or preservation of expandable 2:1 clay minerals such as smectite and vermiculite (Kittrick, 1969; Rai and Kittrick, 1989).

In the lower portion of the backslope and in the footslope/toeslope positions, basal flow over the top of the parent rock becomes more important. At this point, depending on drainage conditions, blocky structure commonly changes to prismatic and compression surfaces and slickensides are present due to an abundance of expandable, 2:1 clay minerals (smectites, vermiculite). These soils are usually fertile but shallow with A / C / R profiles (EMBRAPA, 1984). Poor drainage may also be a factor that must be managed with appropriate drainage or cultural practices.

Landscape cross-sections showing general topographic relationships between the soils sampled for this study are shown in Fig 5.5. The landscapes at Ibiporã, Tamarana, and Cruzmaltina were highly dissected and dominated by bedrock "highs." By contrast, the Campo Mourão and Faxinal landscapes included convex slopes that were long and unbroken. In all cases, the local bedrock was exposed in the footslope/toeslope positions where surfaces were cut by local streams. The soils in these positions were mostly shallow, Solos Litólico (Rd or Re) with A/R or A/Cr/R profiles. Solos Litólico could also be found in the upper backslope/shoulder positions associated with bedrock "highs" in the Ibiporã, Tamarana, and Cruzmaltina toposequences; profile # 15 at Cruzmaltina was sampled to represent this situation. These profiles were usually only 10 to 30 cm thick over lithic or paralithic materials. Colors ranged from yellowish brown (10 YR) to reddish brown (2.5 YR), and the structure was granular to blocky with coarse peds aggregated by organic matter and Fe oxides.

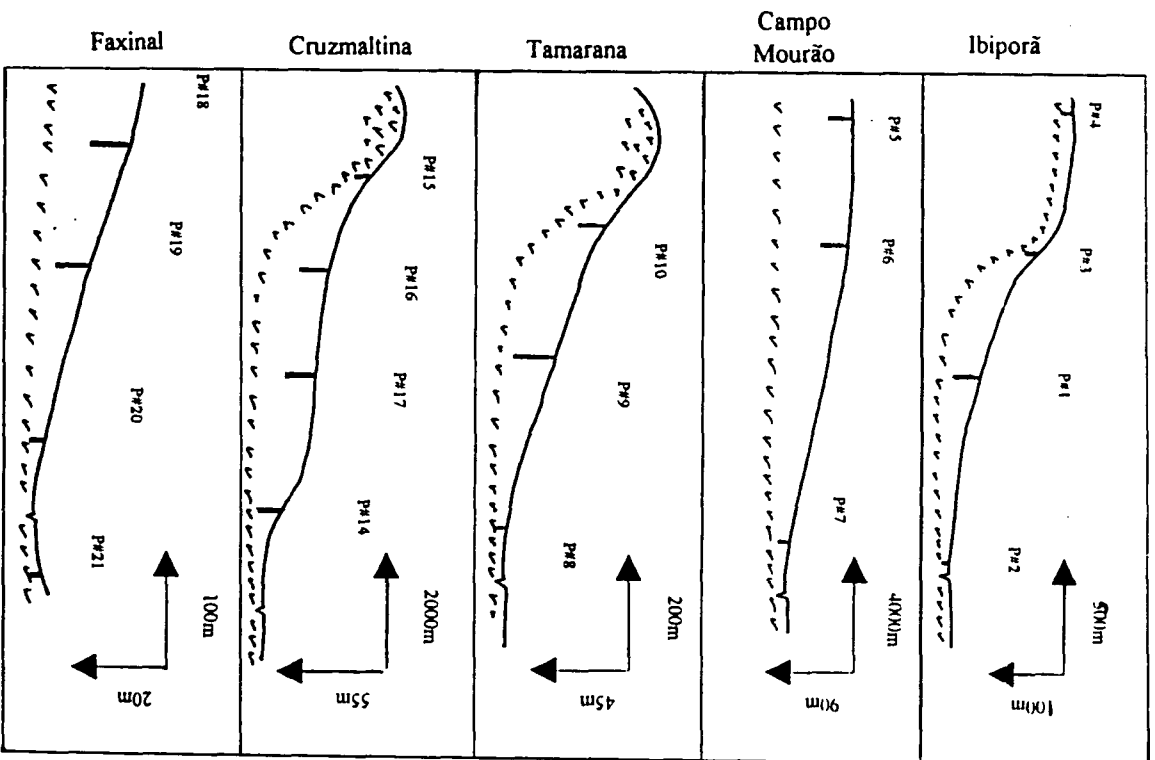


Figure 5.5. Cross sections of the five soil toposequences.

Also included with the "weakly" weathered soils was a Brunizem Avermelhado (BAv) (Profile # 3) in the Ibiporã toposequence and a Cambissolo (C) (Profile # 8) in the landscape from Tamarana. These soils usually occur on landscape positions where soil formation is compromised or offset by erosion processes (EMBRAPA, 1984). The BAv sampled in this study had a thin but well expressed argillic horizon with strong angular blocky structure. Compression features were abundant, especially in the BC horizon, suggesting the presence of expandable 2:1 clay minerals (Moniz and Jackson, 1967; Rauen, 1980; Queiroz and Klamt, 1985; Palmieri, 1986; Demattê and Marconi, 1991, Moniz et al., 1994). Black, Mn-rich coatings and stains were also present on ped surfaces in the BC horizon showing that the profile was still in an early stage of weathering. The Cambissolo from the Tamarana toposequence was also immature and contained abundant weathered rock fragments from the underlying rhyolite-andesite.

The Terra Roxa Estruturada (TR) and Terra Bruna Estruturada (TB) classes of soils contain either an argillic or a kandic (Soil Survey Staff, 1994) sub-surface horizon (Andrade et al., 1976; Aloisi et al., 1976; Galhego and Espindola, 1979; Queiroz and Klamt, 1985; Moniz et al., 1994, Rocha and Cerri, 1994). This horizon is characterized by an accumulation of clays either due to illuviation of colloidal materials from the surface horizons (argillic) or to formation *in situ* (kandic) due to the lateral flow of silica and bases from upslope (Moniz et al., 1982). The TR and TB profiles examined in this study showed the development of clay skins inside voids and cracks and on blocky ped surfaces. Clay contents usually increased with depth to the base of the Bt horizons and then decreased through the transitional BC horizons. The TR soils were consistently reddish

brown (2.5 YR) in color whereas the TB were brown (7.5 YR) to yellowish red (5 YR) and were restricted to the acid / intermediate rock landscapes. The TR and TB are considered to be mature soils within the context of this study. They are not, however, as highly weathered as the Latossolo Roxo (LR) or Latossolo Bruno (LB).

The highly weathered LR and LB soils have a characteristic weak blocky macrostructure that readily breaks to a strong, very fine, granular (coffee powder) microstructure where the Fe oxides are the primary aggregating agents (EMBRAPA, 1984; Galhego and Espindola, 1979; Fasolo, 1978; Rauen, 1980). This type of structure is typical of oxic subsurface horizons in Soil Taxonomy (Soil Survey Staff, 1975). All the LR profiles were developed from basalt and were reddish brown (2.5YR) in color. The single LB pedon (# 18) was developed from acid / intermediate rock and exhibited some yellowish red colors (5 YR) in the upper part of the profile. Color transitions within all the LR / LB profiles were diffuse.

### **5.2.2. Physical and chemical characteristics**

The highly weathered profiles had clay or heavy clay field textures, whereas the less weathered profiles showed more textural variability depending upon the intensity of weathering. Silt/clay ratios tended to be somewhat lower (0.1 to 0.8) (Table 5.4) in the highly weathered profiles as compared to the younger soils (0.4 to 1.4) indicating that as the intensity of weathering increases the silt and sand fractions are altered to form secondary clay minerals, gibbsite and Fe oxides (EMBRAPA, 1984; Rauen, 1980; Kämpf,

1981; Palmieri, 1986; Demattê and Marconi, 1991; Demattê et al., 1994; Kämpf et al, 1995).

The silt / clay ratio has been used as a criterion to distinguish young and old soil materials in some regions. For example, a ratio of 0.15 or less was considered by van Wambeke (1992) to be diagnostic for old, highly weathered profiles. This separation appears to have limited value in the present study (Table 5.4), perhaps due to the fact that the ratio is most applicable to soils with less than 1% C and does not take into account the presence of silt-sized kaolinite, gibbsite or Fe oxides (van Wambeke, 1992). The range of silt / clay ratios found in the literature for LR and LB is around 0.1 to 0.3 (Resende, 1976; Fasolo, 1978; Rauen, 1980; Pötter and Kämpf, 1981; Curi, 1983; Palmieri, 1986).

Soil chemical properties varied markedly between the five toposequences sampled (Table 5.4). All soils in the Ibioporã sequence had pHs > 5.0 and the exchange complexes were dominated by Ca, Mg, and K. No exchangeable Al was detected, and all pedons were eutrophic ( $V\% \geq 50$ ) with the highest base saturation values associated with the youngest profiles (BAv and Re). The CEC's (T values) decreased with increasing weathering (BAv > Re > TRe > LRe), as is typical for soils of this region (EMBRAPA, 1984; Queiroz and Klamt, 1985; Demattê and Marconi, 1991). Organic C contents decreased with depth in all profiles and were highest (4.56 and 3.56%) in the surface horizons of the young profiles (BAv and Re). In general, a base-rich environment favors biological activity and the accumulation of organic matter. The eutrophic character of the soils, their relatively shallow profiles (Appendix A), and the dissected nature of the topography all suggest that the local landscape was not highly stable.

Prof. #	Soil	pH (CaCl <sub>2</sub> )	C (%)	T (cmol <sub>e</sub> /Kg)	V (%)	Al (%)	Silt / Clay
<b>Ibiporã</b>							
1	TRe	5.5 - 5.2	2.00 - 0.26	20.1 - 11.4	65 - 78	0	0.4 - 0.1
2	Re	5.5 - 5.8	3.56 - 2.59	31.6 - 23.7	88 - 86	0	0.7 - 0.4
3	BAv	5.9 - 5.7	4.56 - 0.80	54.5 - 30.2	94 - 89	0	0.8 - 0.3
4	LRe	5.4 - 5.1	3.05 - 0.66	18.4 - 10.9	71 - 65	0	0.5 - 0.2
<b>Campo Mourão</b>							
5	LRd	4.9 - 4.1	4.17 - 0.52	10.2 - 3.6	18 - 4	45 - 0	0.3 - 0.2
6	LRd	4.9 - 4.0	2.30 - 0.53	9.4 - 4.0	27 - 15	40 - 0	0.2 - 0.1
7	Rd	4.5	4.9	18.4	47	9	0.9
<b>Tamarana</b>							
8	Ca	4.1 - 4.0	4.98 - 2.69	16.0 - 14.2	19 - 11	71 - 53	0.4 - 0.6
9	TBa	4.4 - 3.9	2.19 - 0.32	11.6 - 9.5	42 - 9	78 - 0	0.2 - 0.5
10	TBa	4.7 - 3.9	2.70 - 0.46	15.9 - 13.3	63 - 8	80 - 2	0.6 - 0.2
<b>Cruzmalina</b>							
14	TRd	4.5 - 4.0	4.15 - 0.83	22.7 - 6.6	68 - 11	58 - 5	0.8 - 0.2
15	Re	5.6 - 4.1	2.45 - 0.76	25.9 - 11.7	83 - 17	47 - 0	1.4 - 0.4
16	LRa	4.6 - 3.9	3.67 - 0.40	13.8 - 5.4	17 - 5	79 - 24	0.6 - 0.2
17	LRa	4.4 - 4.0	3.48 - 0.27	12.4 - 5.1	11 - 6	80 - 40	0.3 - 0.2
<b>Faxinal</b>							
18	LBa	4.5 - 3.8	2.97 - 0.37	10.3 - 4.4	40 - 9	67 - 9	0.2 - 0.1
19	LBa	4.1 - 3.6	3.09 - 0.92	14.1 - 6.4	45 - 9	71 - 5	0.4 - 0.2
20	Rd	4.5	1.97	10.3	40	9	0.6
21	Re	4.6	5.50	19.6	68	1	0.6

† Data presented show the range of a given parameter for all horizons sampled. C = carbon, T = cation exchange capacity, V = base saturation, Al = aluminum saturation.

Table 5.4. Summary<sup>†</sup> of important soil chemical and physical attributes in the toposequences sampled

The Campo Mourão landscape, by comparison, was dominated by convex surfaces with deep soils (LRd) containing oxic subsurface materials with very low CEC's (4 to 10 cmol/kg). Under such conditions, the soil CEC is highly dependent on the organic matter content (Pavan et al., 1985). Solos Litólicos (Rd) occurring at the base of the hillslope had somewhat higher CECs due, presumably, to the presence of more 2:1 clay minerals (EMBRAPA, 1984; Kämpf et al., 1995). All profiles sampled were dystrophic ( $V\% < 50$ ) but not allic ( $Al \% \leq 50$ ).

The Cruzmaltina toposequence probably typifies the most common association of soils formed from basic rocks of the PFV within the state of Paraná. Specifically, Terra Roxa Estruturada (usually dystrophic) occur on unstable backslopes in association with highly weathered Latossolo Roxo (usually dystrophic or allic) on more stable landscape positions. Solos Litólico are minor landscape components forming wherever local bedrock outcrops occur (Rauen, 1980; EMBRAPA, 1984). As the intensity of weathering increases, the silt/clay ratio, base saturation, CEC, and pH decrease, while the Al saturation increases. Both the LRa pedons sampled at Cruzmaltina were highly allic and the TRd was marginally dystrophic/allic.

The toposequence of soils sampled at Tamarana was developed from acid / intermediate rocks, and the natural deficiency of basic cations in these rocks determined that these soils would have undesirable chemical attributes. Collectively, these were the most acid / intermediate profiles sampled among the five toposequences and the Al saturations were comparable to those observed for the more highly weathered soils at Cruzmaltina and Campo Mourão.

The soils at Faxinal were sampled near the local interface between basic and acid / intermediate extrusive rocks, and the most stable landscape segments were not sampled because they were underlain by basic rocks. Nevertheless, the soils collected for analysis included two highly weathered profiles (LBa) (Fig. 5.5). Both were very acid (allic in the oxic horizon) with low CEC's. One of the associated Solos Litólico (Profile #20) also exhibited an unusually high degree of weathering, as reflected in a low CEC (10.34 cmol/kg) that was mostly associated with the accumulation of organic matter (1.97 %C). Both Solos Litólico profiles had low pHs (4.5 to 4.6), but neither exchange complex was saturated with aluminum. The silt / clay ratio was 0.6 for both profiles and is more typical of young soils in the incipient stage of weathering.

Carbon content was not a good indicator of the intensity of weathering in any of the soils sampled. Among the different toposequences, the lowest C contents in the surface horizons were observed in soils with very different degrees of weathering such as the Terra Roxa Estruturada (Ibiporã), Latossolo Roxo distrófico (Campo Mourão), Terra Bruna Estruturada (Tamarana), and the Solos Litólicos (Cruzmalina and Faxinal). Other chemical characteristics were more closely related to the degree of weathering such as the pH, base saturation (V%) and aluminum saturation (Al). As the degree of weathering increased, the leaching process removed bases (Ca, Mg, and K) and silica (desilication) from the profile while iron (ferritization) and aluminum (allitization) accumulated. The replacement the bases (Ca, Mg, and K) by aluminum is very common in tropical regions (Sanchez, 1976; van Wambeke, 1992).

### 5.2.3. Magnetic properties of the soil fractions

The magnetic character of the soils was observed in the field by the attraction of the soil material to a hand magnet (Resende, 1976; Resende et al., 1986). Laboratory magnetic susceptibility measurements were subsequently performed on both the whole soil samples and the sand, silt and clay fractions. The magnetic susceptibilities of the soil material (<2mm) developed from basic rocks were strongly correlated with the magnetic susceptibility of the clay and silt fractions (Fig 5.6). The correlation was not as good with the sands. The strong, 1:1 relationship between the whole soil materials and the clay fractions can be attributed to the high clay content of these soils (Appendix A and B) and to the accumulation of the clay-sized maghemite during weathering (Resende et al., 1986; Hunt et al., 1995; Singer et al., 1989). Measurements of frequency dependent magnetic susceptibility ( $\chi_{fd}$  %) confirmed that superparamagnetic minerals ( $\chi_{fd} > 10\%$ ) were concentrated in the clay fractions which yield  $\chi_{fd}$  's ranging from 10-18% as compared to 0-10% for the silt and sand fractions (Fig. 5.7). The later values suggest a mixture of superparamagnetic maghemite and coarse, single or multi-domain magnetite (Table 3.2) (Dearing, 1994).

As might be expected, the “weakly” weathered profiles developed from basic rocks had lower magnetic susceptibilities in the clay fraction compared to the highly weathered soils (Fig. 5.8). As weathering intensity increases, the 2:1 clay minerals almost vanish from the soil and are partially replaced by the Fe oxides, including maghemite. The acid / intermediate rock soil clays had even lower magnetic susceptibilities (Fig. 5.8) apparently due to the small concentration of magnetite in the parent rock (section 5.1, Table 5.3).

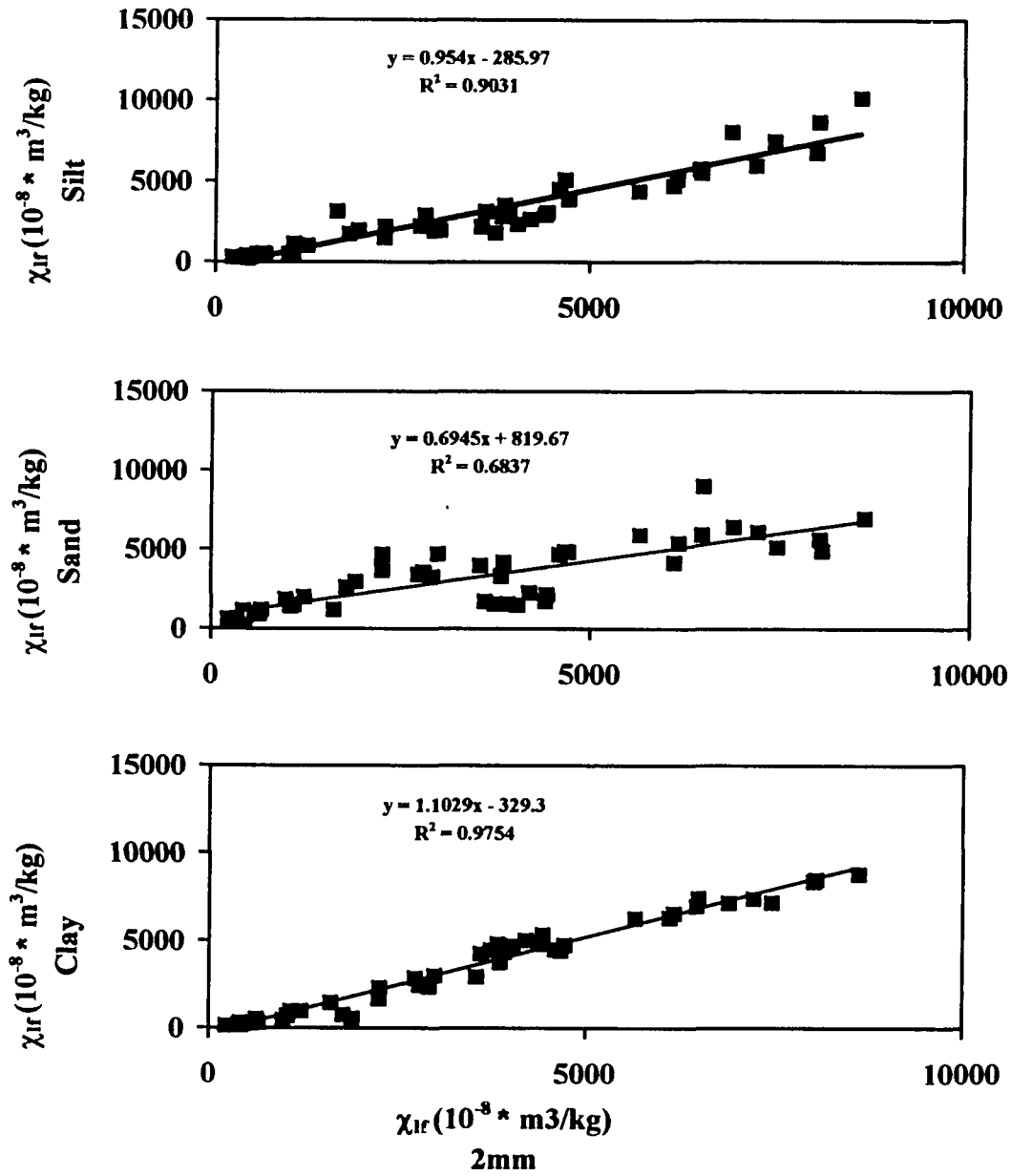


Figure 5.6. Relationship between magnetic susceptibility ( $\chi_{ir}$ ) of the 2mm fraction with the silt, sand and clay size fractions of the basic rock soils.

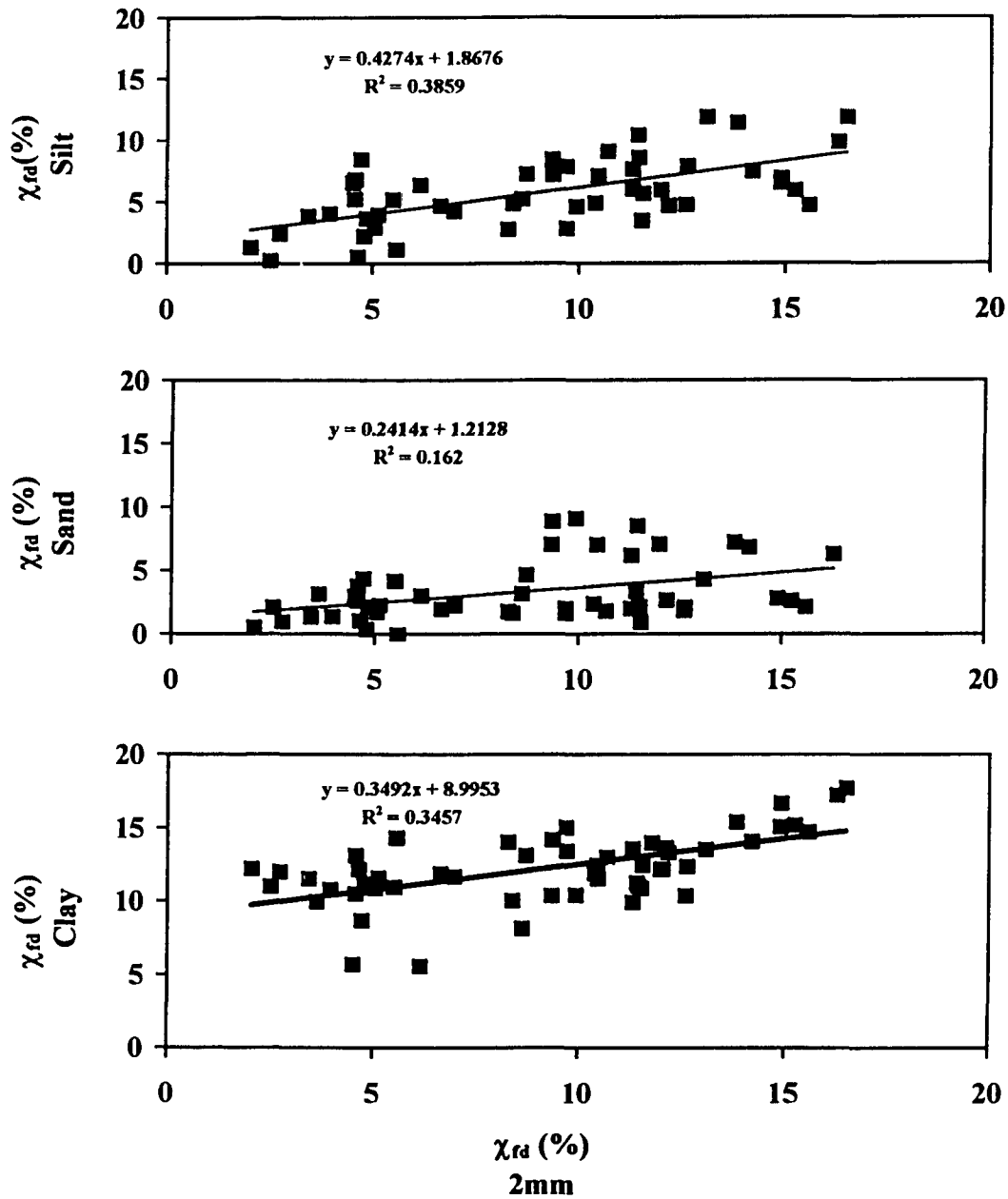


Figure 5.7. Relationship between frequency dependent magnetic susceptibility ( $\chi_{rd}$  %) of the 2mm fraction with the silt, sand and clay size fractions of the basic rock soils.

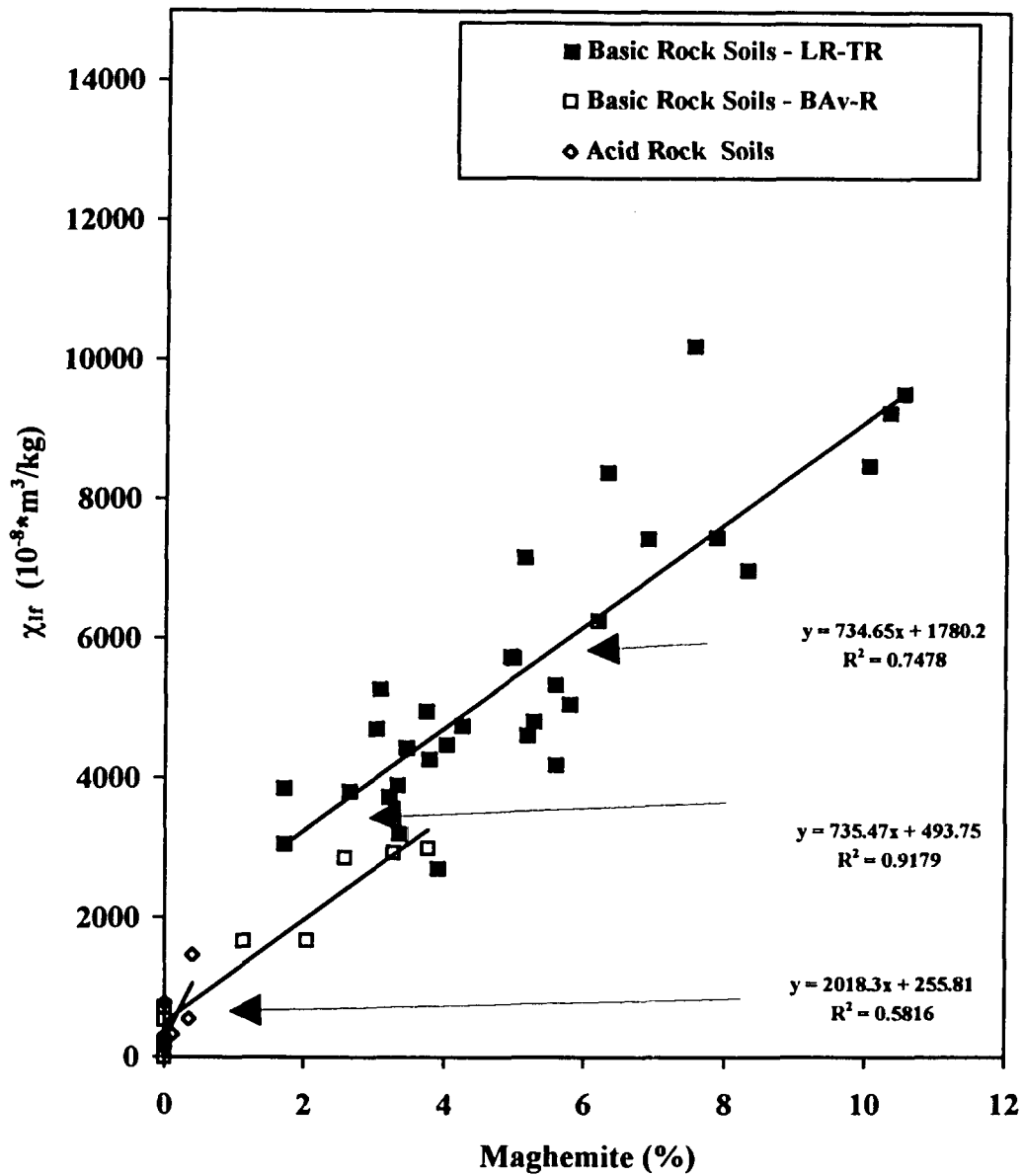


Figure 5.8. Magnetic susceptibility ( $\chi_{lf}$ ) of the 2mm fraction and percentage of maghemite in the clay fraction from basic and acid / intermediate volcanic soils.

These observations also support the idea that magnetite is the primary source of maghemite in soils of the PFV (Resende, 1976; Resende et al., 1986; Coey, 1985; Schwertmann and Taylor, 1989).

#### **5.2.4. Classification of the soils**

The soil morphological descriptions, together with basic chemical, physical and mineralogical (discussed later) characteristics, were used to classify the soils according to both the Brazilian (Camargo et al., 1987) and the United States systems (Soil Survey Staff, 1994) of soil classification (Table 5.5). The two systems require diagnostic data generated using different methods of analysis for basic soil chemical attributes (e.g., CEC, ECEC and base saturation). Data from approved U.S. methods of analysis were not always available; hence, uncertainty exists regarding the appropriate U.S. classification for some pedons. All classifications in the U.S. system were limited to the subgroup level.

All the soils described as Latossolo Roxo and Latossolo Bruno (B -latossólico, Camargo et al., 1987) may be classified as Oxisols in the U.S. system due to the presence of an oxic subsurface horizon (Soil Survey Staff, 1994). The Terra Roxa and Terra Bruna Estruturada (B-textural, Camargo et al., 1987) were classified as either Alfisols or Ultisols according to the presence of an argillic and/or kandic subsurface horizon (Soil Survey Staff, 1994) and the degree of base saturation. The youngest profiles were classified in different orders according to the presence of specific surface and/or subsurface diagnostic horizons. The BA<sub>v</sub> (A - chernozêmico, Camargo et al., 1987) and Re pedons at Ibioporã were classified as Mollisols (mollic epipedon, Soil Survey Staff, 1994), and the

Cambissolo (B - incipiente, Camargo et al., 1987) at Tamarana was identified as an Inceptisol (cambic subsurface horizon, Soil Survey Staff, 1994). The remaining Solos Litólico were classified as Entisols. Detailed mineralogical data from the clay fractions enabled all soils to be placed in either oxidic or kaolinitic mineralogy classes. The LR, TR, and LB pedons were all oxidic. The TB, Ca, BAv, R (except the R from Cruzmaltina) pedons were all kaolinitic.

Prof. #	Brazilian System	American System
1	Terra Roxa Estruturada eutrófica - TRe	Oxidic Rhodic Kandiodalfs
2	Solos Litólicos eutrófico - Re	Kaolinitic Lithic Hapludolls
3	Brunizem Avermelhado - BAv	Kaolinitic Typic Argiudolls
4	Latossolo Roxo eutrófico - LRe	Oxidic Lithic Eutrorthox
5	Latossolo Roxo distrófico -LRd	Oxidic Anionic Acrudox
6	Latossolo Roxo distrófico - LRd	Oxidic Anionic Acrudox
7	Solos Litólicos distrófico - Rd	Kaolinitic Typic Troporthents
8	Cambissolo álico - Ca	Kaolinitic Oxidic Humitropepts
9	Terra Bruna Estruturada álica - TBa	Kaolinitic Typic Kandihumults
10	Terra Bruna Estruturada álica - TBa	Kaolinitic Typic Kandihumults
14	Terra Roxa Estruturada distrófica -TRd	Oxidic Typic Kandihumults
15	Solos Litólicos distrófico - Rd	Oxidic Typic Troporthents
16	Latossolo Roxo álico - LRA	Oxidic Humic Rhodic Hapludox
17	Latossolo Roxo álico - LRA	Oxidic Humic Rhodic Hapludox
18	Latossolo Bruno álico - LBa	Oxidic Humic Hapludox
19	Latossolo Bruno álico - LBa	Oxidic Humic Hapludox
20	Solos Litólicos distrófico - Rd	Kaolinitic Lithic Troporthents
21	Solos Litólicos eutrófico - Re	Kaolinitic Lithic Troporthents

Table 5.5. Classification of the toposequence soils according to the Brazilian (Camargo et al., 1987) and U.S. (Soil Survey Staff, 1994) systems of soil classification

### **5.3. Clay mineralogy of the toposequence soils**

#### **5.3.1. Quantitative analysis of major mineral groups**

The Na - citrate - bicarbonate - dithionite (CBD) method of Mehra and Jackson (1960) was used to concentrate the silicate clay minerals and gibbsite occurring in the natural clays (< 2 $\mu$ m) and to measure the total amount of Fe oxides present. Instead of using the recommended 1 g of Na-dithionite per g of clay, it was necessary to use 3 g to achieve complete dissolution of the secondary Fe oxides. Different authors have already observed that the 1 g treatment is not adequate for many tropical soils (Resende, 1976; Palmieri, 1986; Rauen, 1980) due to the presence of well crystalline hematite (Furtado et al., 1990) and/or the isomorphous replacement of Fe in goethite and hematite by other elements, such as Al, that decrease their solubilities in the presence of a strong reductant (Torrent et al., 1987; Schwertmann, 1991). Resende (1976) reported that 4 to 15 g of Na-dithionite were needed to remove all the Fe oxides from some acid Oxisols of central Brazil.

In contrast to other Fe oxides, magnetite seems to be relatively stable under the reducing conditions promoted by Na-dithionite (Dearing, 1994; Hunt et al., 1995). The possibility of residual magnetite in the CBD-clays can be seen from the magnetic susceptibility data (Table 5.6). The values obtained were less than 5% of those from the total clays (discussed later) but were high compared to standard values of magnetic susceptibility reported for pure kaolinite, gibbsite and hydroxy-Al-interlayered vermiculite (Mullins, 1977, Dearing, 1994).

Prof. #	Soil	Horizon	$\chi_{lf}$ ( $10^{-8} \bullet m^3 / Kg$ )
<b>Ibiporã</b>			
1	TRe	Ap	14
		Bt2	26
		Bt7	26
2	Re	A	32
3	BAv	A	27
		Bt1	23
4	LRe	Bw2	15
<b>Campo Mourão</b>			
5	LRd	Bw2	30
7	Rd	A	29
<b>Tamarana</b>			
8	Ca	A	10
		Bi	8
9	TBa	Bt25	5
		BC2	6
10	TBa	Bt2	24
		BC	15
<b>Cruzmalina</b>			
14	TRd	Ap	16
		Bt2	14
15	Rd	Ap	23
		Cr	8
17	LRa	A	24
		B2	24
		Bw2	28
		Bw4	29
<b>Faxinal</b>			
18	LBa	A	21
		Bw2	28
		Bw4	28
20	Rd	A	12
21	Re	A	7
<b>Average</b>			<b>19</b>

Table 5.6. Magnetic susceptibility ( $\chi_{lf}$ ) of selected CBD - treated clay samples

These results suggest the presence of small amounts (< 1%) of magnetite that were not dissolved by the CBD treatment and that were not detected by XRD. This possibility is also supported by the fact that the CBD clays from the soils developed from basic rocks (richer in magnetite) yielded values of magnetic susceptibility that were generally higher than those for clays weathered from the acid / intermediate rocks (Table 5.6). The range of Fe<sub>2</sub>O<sub>3</sub> extracted by the CBD procedure was 6-25% (Table 5.7) and is typical for soils of this region (Resende, 1976; Rauen, 1980; Kämpf, 1981; Curi, 1983; Palmieri, 1986; Fontes, 1988; Castro Fo, 1988; Peixoto, 1995). The data also show that the soils formed from basic rocks (Ibiporã, Campo Mourão, and Cruzmaltina) yielded higher amounts of CBD-extractable Fe as compared to similar soils developed from the acid / intermediate rocks (Resende, 1976; Rauen, 1980; Kämpf, 1982; Curi, 1983; Palmieri, 1986). Further detailed discussion of the Fe oxide mineralogy will be presented in Section 5.4.

Other minerals identified in the CBD-treated clays were grouped in a gross manner as kaolinite (includes 0.7 nm halloysite), gibbsite and 2:1 clay minerals (mostly hydroxy-Al-interlayered vermiculite or smectite but also includes small amounts of quartz and other resistant minerals) for the purposes of semiquantitative analysis (Table 5.7). The percentage of each major mineral (or mineral group) present in the CBD-treated clays was determined both from XRD peak areas and by TG weight loss. The d<sub>001</sub> kaolinite (0.71 nm), d<sub>002</sub> gibbsite (0.48 nm), and d<sub>001</sub> HIV (1.4 nm) peaks were used for XRD analysis (Fig. 5.9). For example:

$$\% \text{ Kaolinite by XRD} = ((\text{Kao (001)} / (\text{Kao (001)} + \text{Gb (002)} + \text{HIV (001)})) * 100 \quad (5.1)$$

Prof. #	Soil	Horizon	Fe <sub>2</sub> O <sub>3</sub> Kao      Gb      2:1 Clays			
			----- % -----			
<b>Ibiporã</b>						
1	TRe	Ap	22	66	2	9
		Bt2	19	71	2	8
		Bt7	18	60	5	18
2	Re	A	15	51	0	34
		Cr	13	55	0	32
3	BAv	A	10	56	0	34
		Bt1	10	54	0	36
4	LRe	A	21	68	4	6
		Bw2	23	64	5	9
<b>Campo Mourão</b>						
5	LRd	A	24	50	23	3
		Bw2	25	47	23	5
		Bw5	23	46	27	5
7	Rd	A	12	72	8	7
<b>Tamarana</b>						
8	Ca	A	6	87	5	2
		Bi	6	72	4	18
		Cr	7	80	4	10
9	TBa	A	8	72	0	20
		Bt2	10	70	0	20
		BC2	10	69	0	21
10	TBa	A	13	68	4	15
		Bt2	13	65	4	19
		BC	12	54	2	33
<b>Cruzmaltina</b>						
14	TRd	Ap	19	70	10	1
		Bt2	19	63	10	9
15	Rd	Ap	18	80	0	2
		Cr	17	70	4	9
17	LRa	A	21	63	10	6
		B2	22	63	11	5
		Bw2	22	60	13	5
		Bw4	18	66	11	5
<b>Faxinal</b>						
18	LBa	A	17	59	18	6
		Bw2	19	58	21	3
		Bw4	16	59	17	9
20	Rd	A	10	70	11	10
21	Re	A	11	69	4	15

Table 5.7. Proportions of minerals in clays from the toposequence soils. Fe<sub>2</sub>O<sub>3</sub> determined by CBD extraction. Kao and Gb determined by TGA analysis.

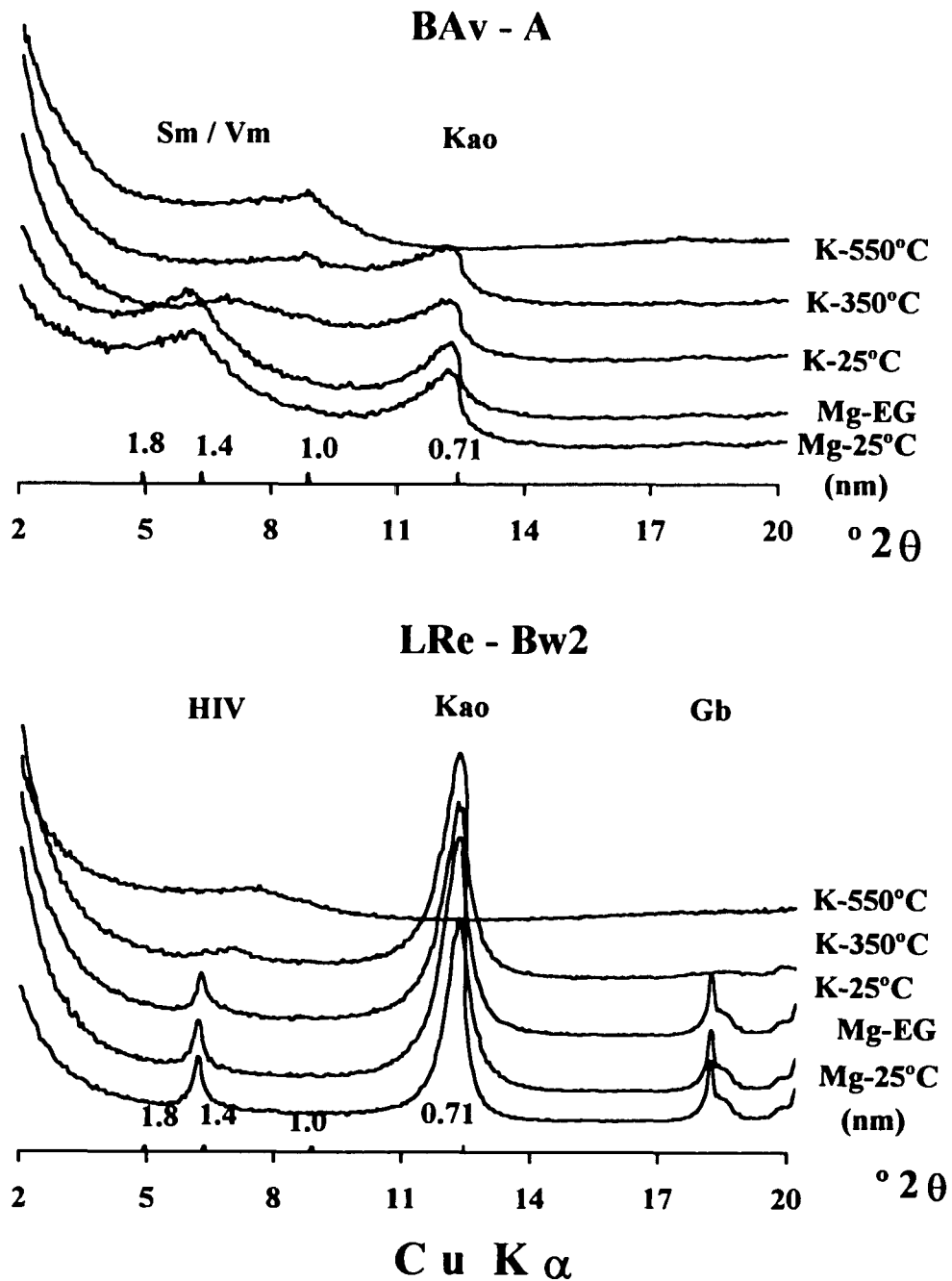


Figure 5.9. X-ray diffraction patterns from selected CBD-treated clays. Ibiporã.

Figure 5.9. Continued. Ibioporã.

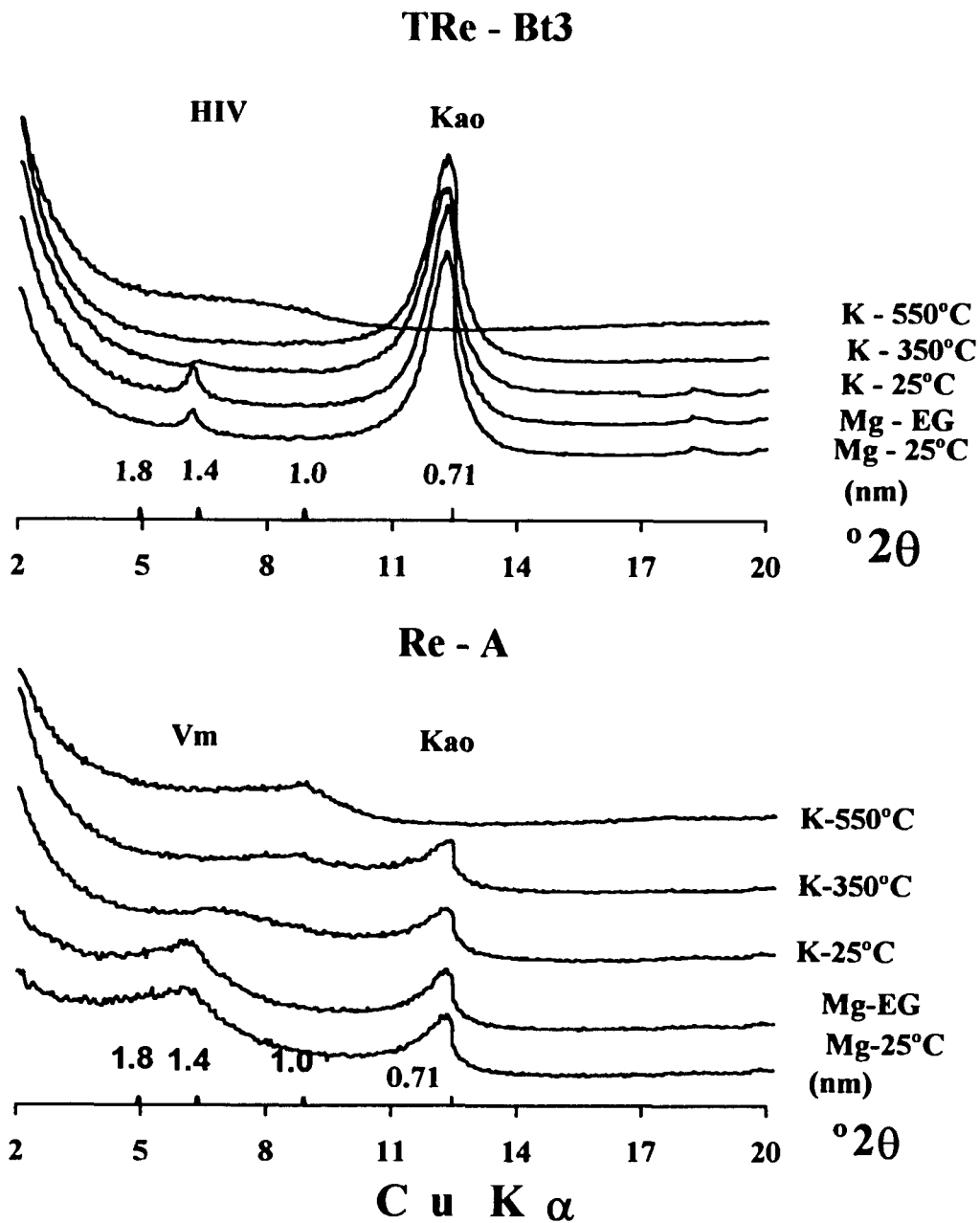


Figure 5.9. Continued. Campo Mourão.

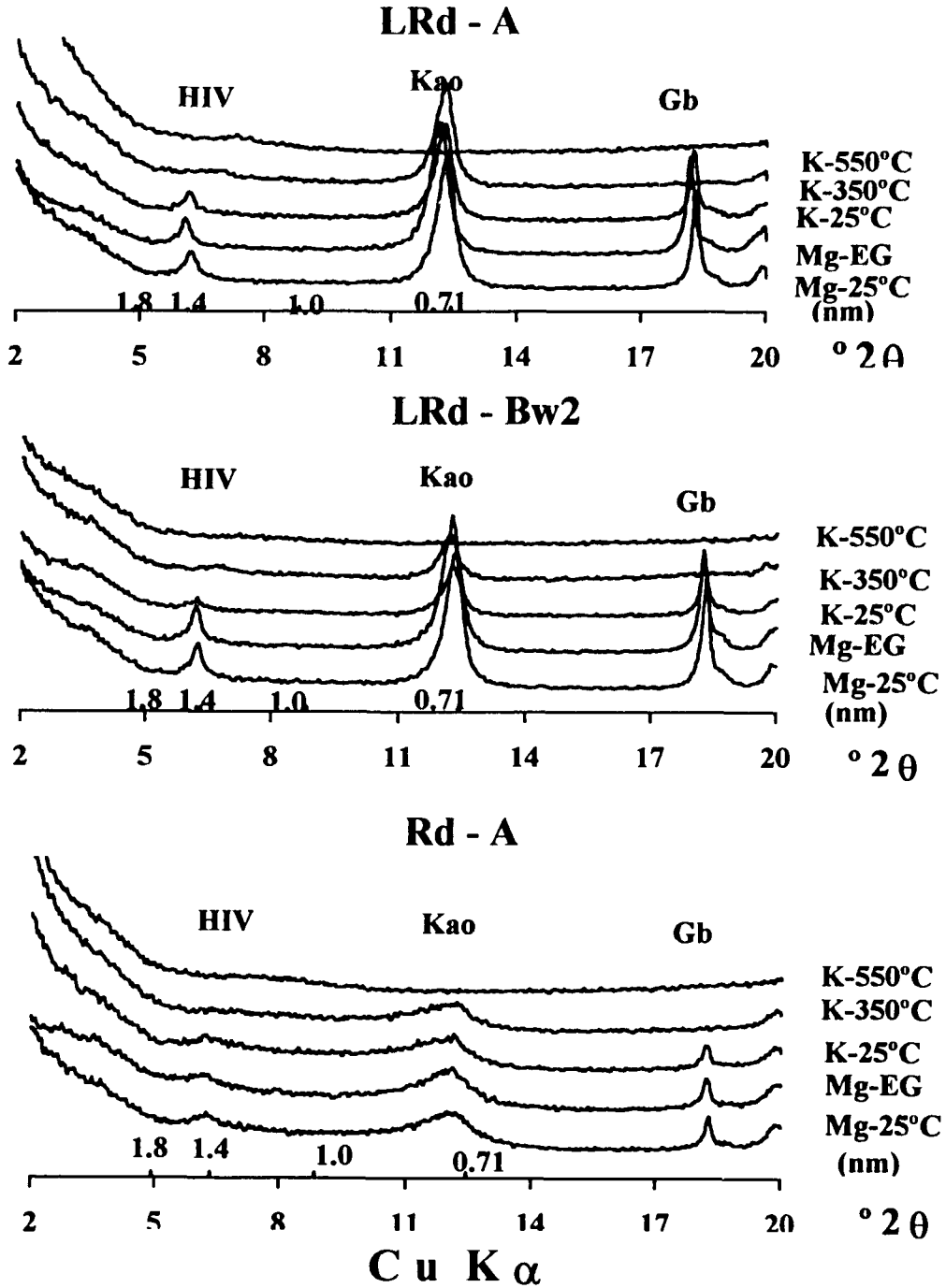


Figure 5.9. Continued. Tamarana.

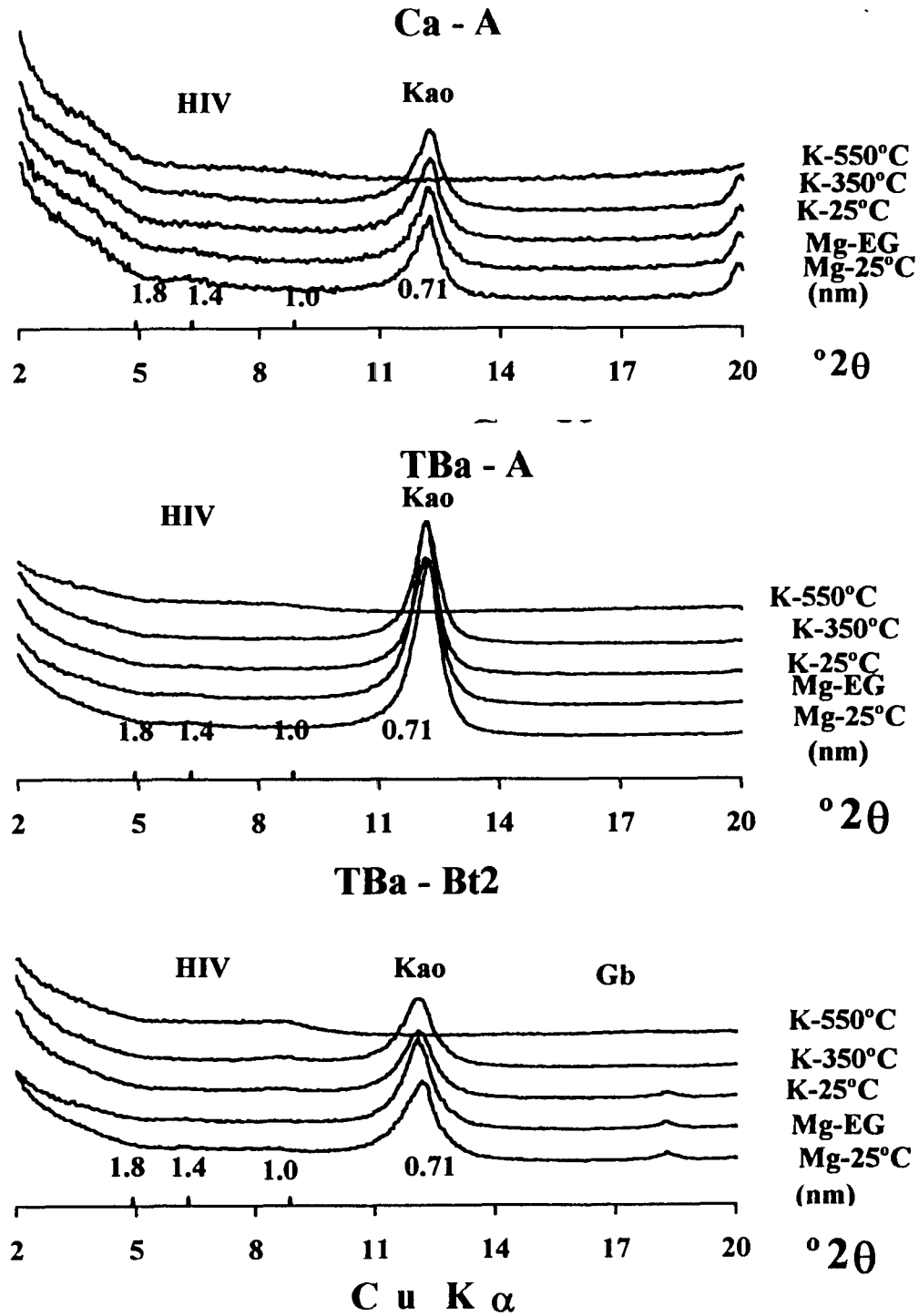


Figure 5.9. Continued. Cruzmaltina.

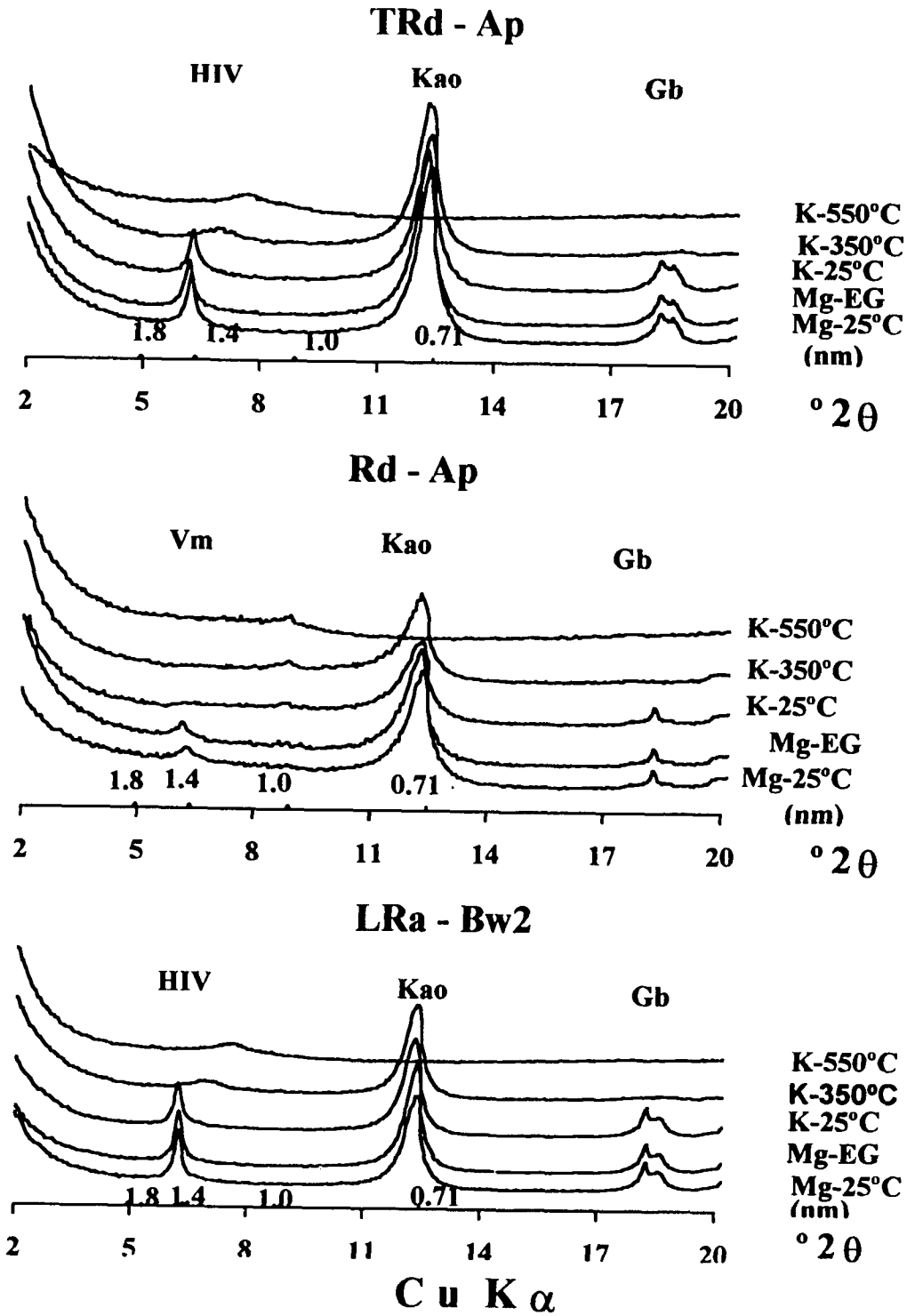
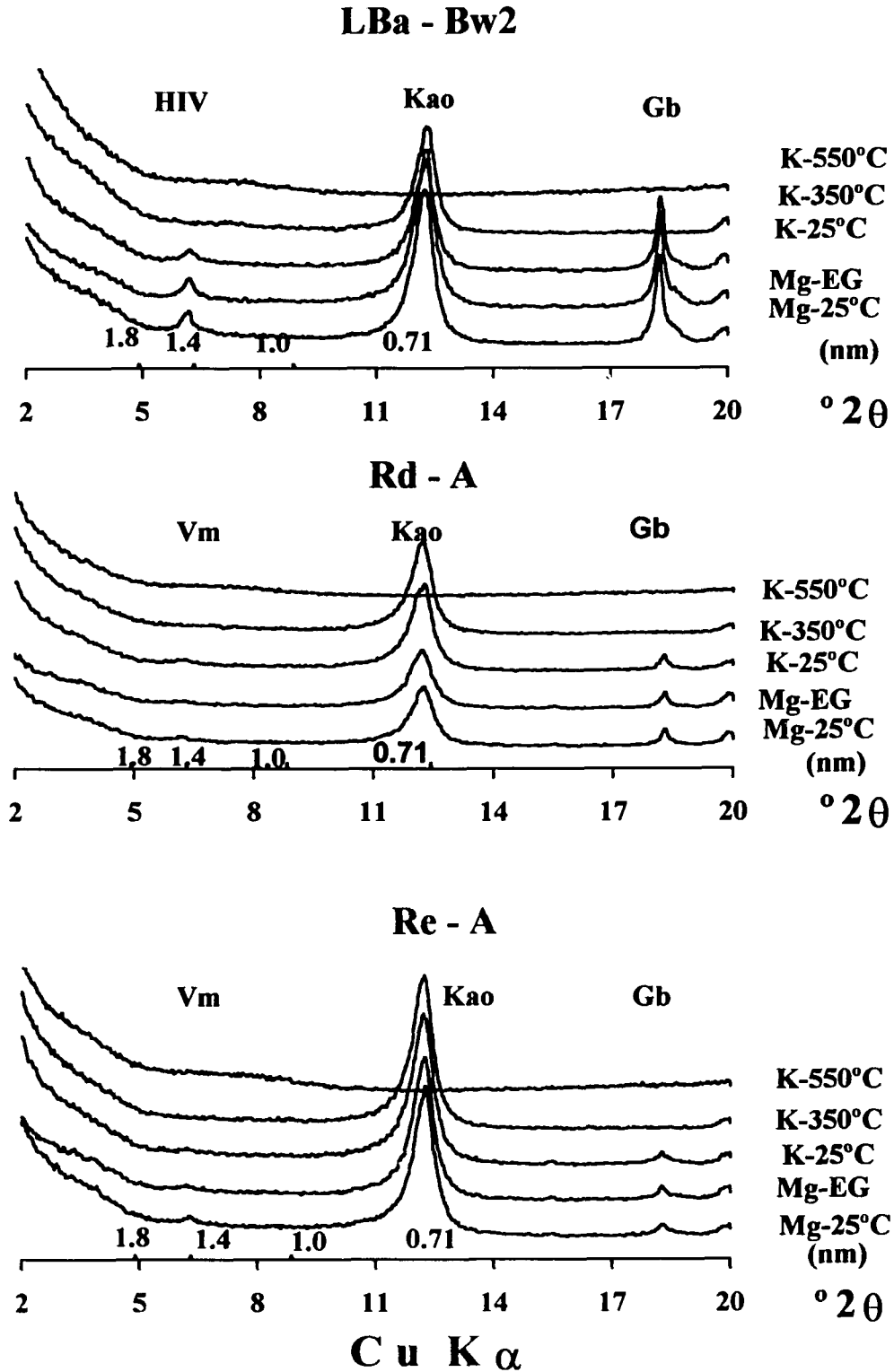


Figure 5.9. Continued. Faxinal.



The qualitative identification of gibbsite and kaolinite by TG/DTA from their characteristic dehydroxylation features at 250 - 300°C and 450 - 550°C, respectively, was straightforward (Fig. 5.10); however, quantification was complicated by the presence of 2:1-type clay minerals. Any weight loss occurring between 50 and 200°C was ignored because the 2:1 clay minerals are effectively dehydrated (cation solvation and interlayer H<sub>2</sub>O) within this temperature range (Tan and Hajek, 1977; Tan et al., 1986). In other words, the weight of the clay at 200°C was used as the reference weight for calculation purposes, and the 2:1 clay minerals were calculated by difference.

A comparison of the two methods of analysis for kaolinite, gibbsite and HIV is presented in Figure 5.11. The limit of detection for any mineral by XRD is in the order of 1 - 5 % (Tettenhorst, 1995), and this limitation makes it practically impossible to measure very low contents of gibbsite in a complex matrix by this method. The data in Figure 5.11 confirm that TG is the preferred method of analysis for small quantities of gibbsite. On the other hand, the TG procedure probably overestimates the amount of kaolinite in some samples because the weight loss may be influenced by dehydroxylation of the polymeric hydroxy-Al compounds in the interlayer regions of HIV and HIS (Harris et al., 1992) (Fig 5.9). This is consistent with the partial collapse of the basal (001) spacing of HIV/HIS between 350-550°C in standard XRD analysis. It is clear that no method of mineral analysis is without problems; however, the TG/ DTA procedure may be most appropriate for clays from tropical soils because of its sensitivity to small amounts of gibbsite in a multimineralic assemblage.

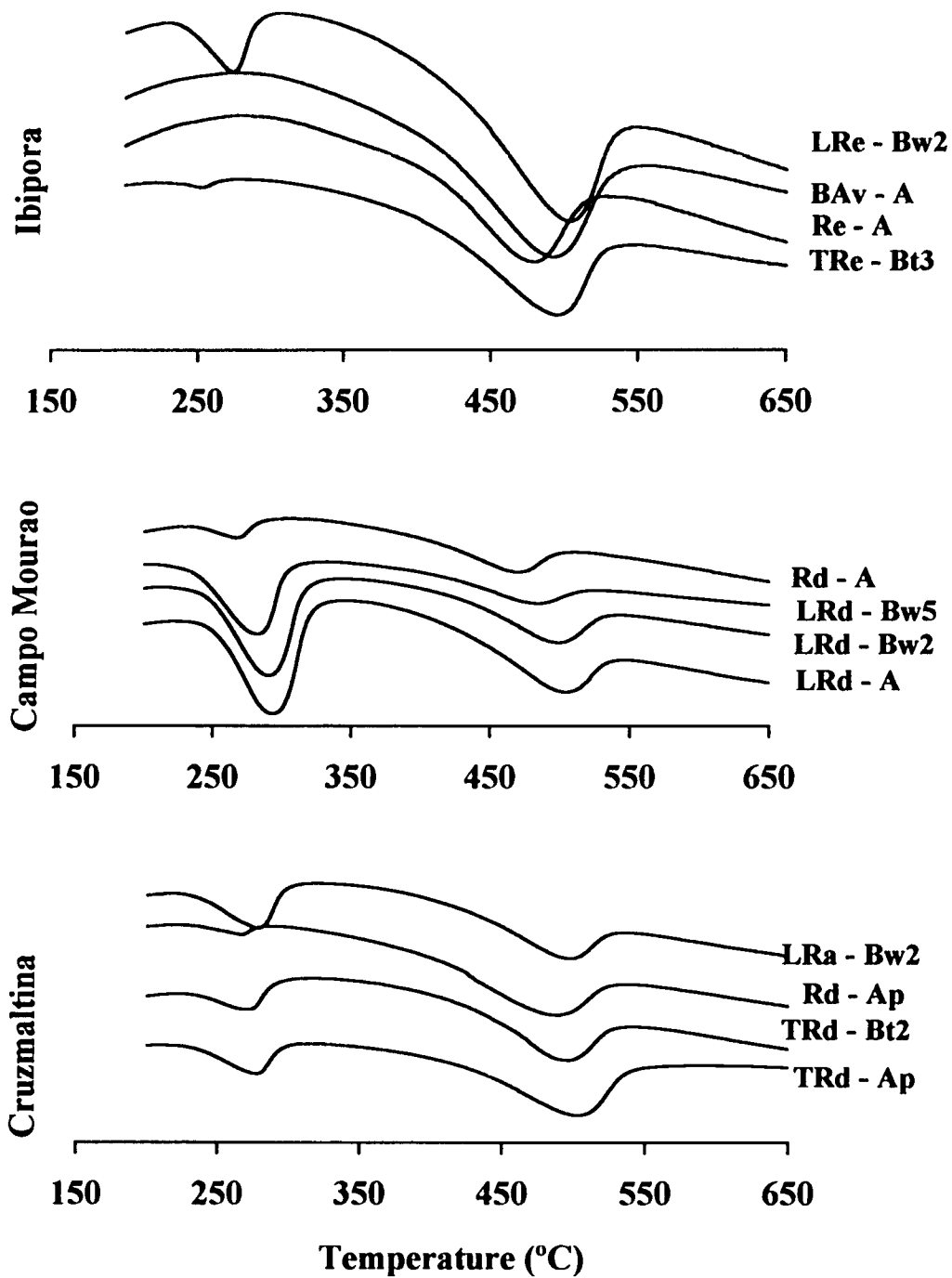
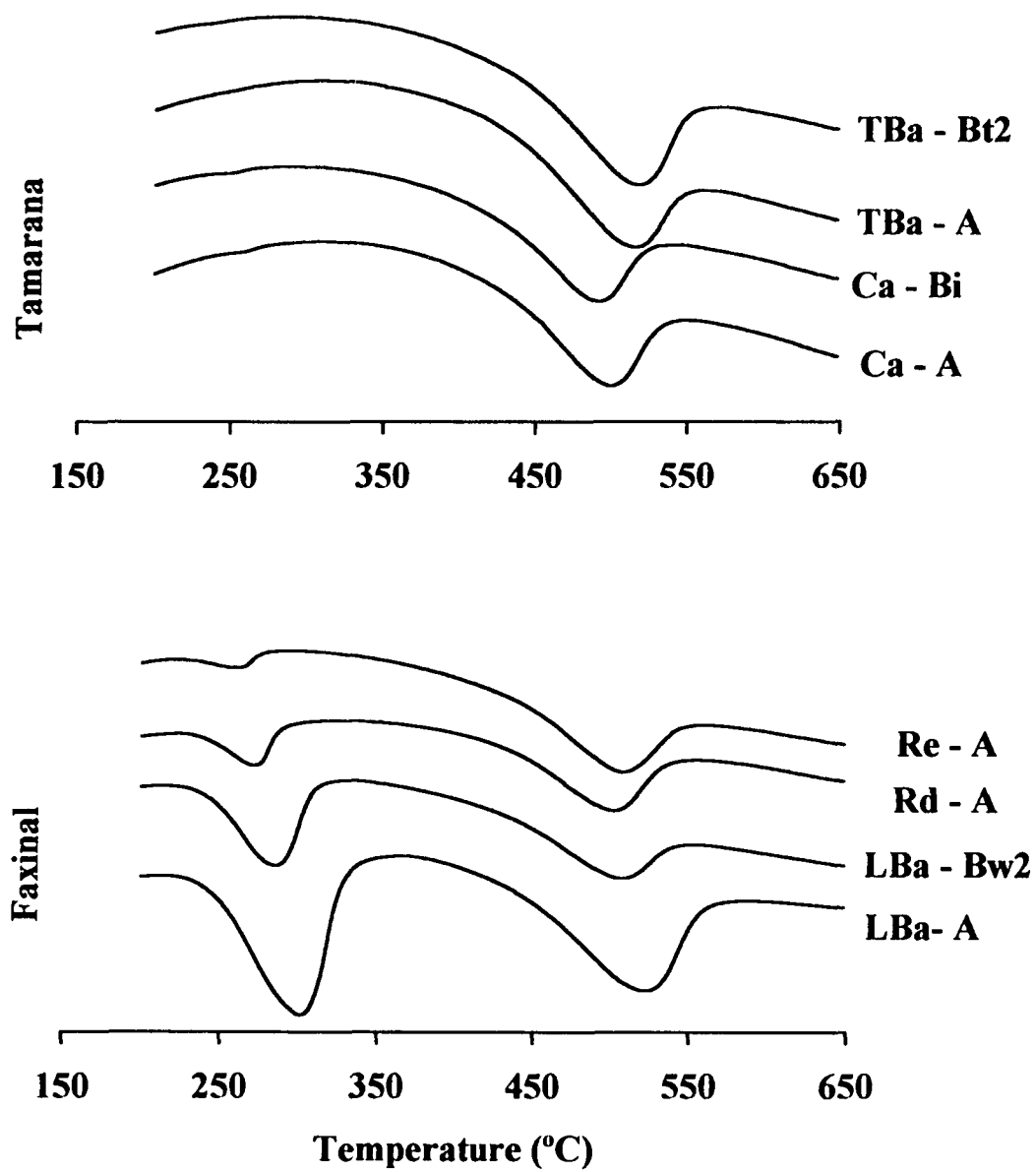


Figure 5.10. DTA patterns from selected CBD-treated clays.

Figure 5.10. Continued.



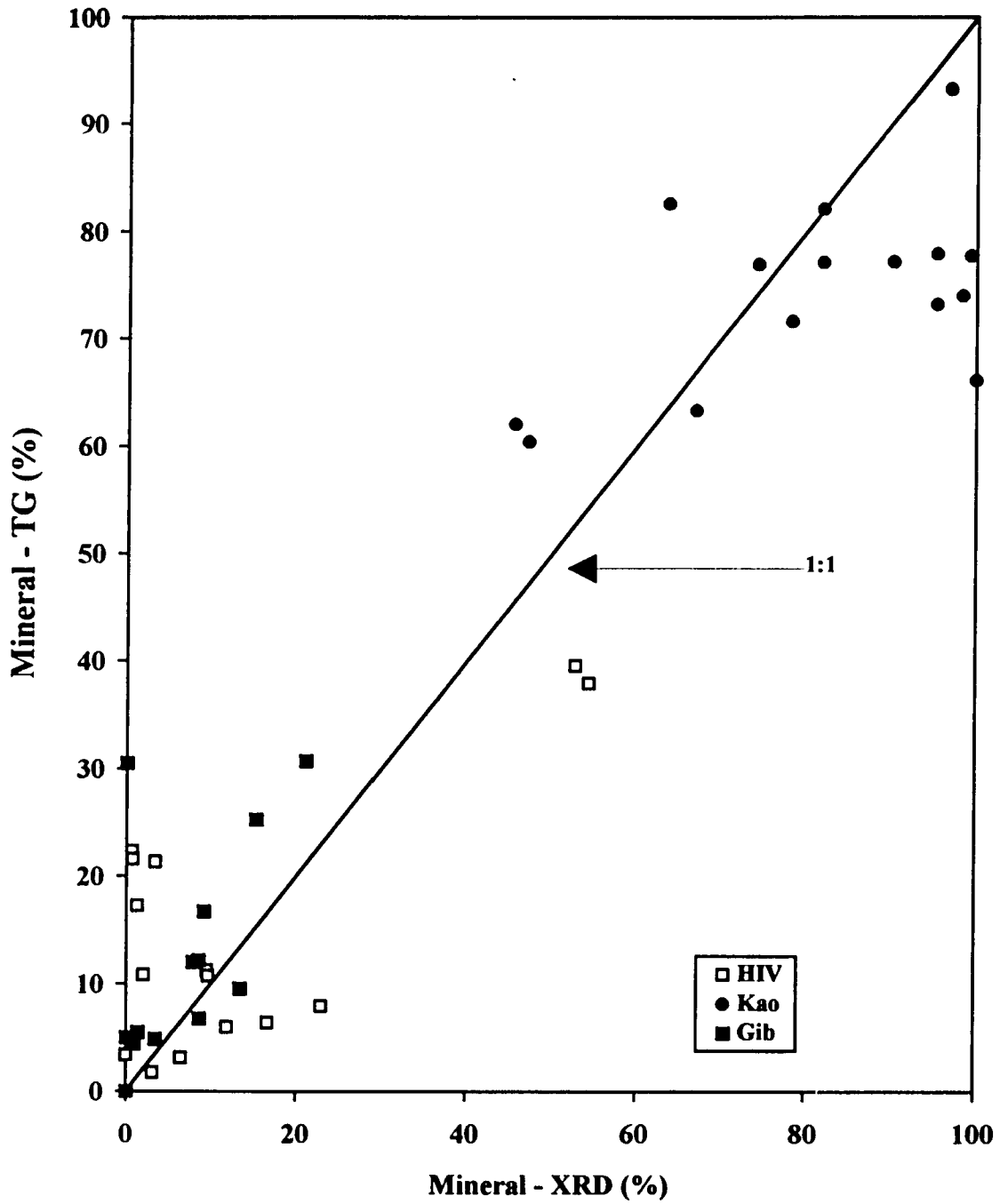


Figure 5.11. Correlation between percentages of kaolinite, gibbsite, and 2:1 clay fraction minerals determined by XRD and TG.

The data presented in Table 5.7. appear to support the idea that a “monotonous mineralogy” is one of the major characteristics of tropical soils (Sanchez, 1976; van Wambeke, 1992); however, subtle differences in clay mineralogical characteristics exist that “may lead to substantial differences in properties affecting soil fertility” (Schwertmann and Herbillon, 1992). These subtleties will now be discussed.

### **5.3.2. The 1:1 clay minerals**

The simple XRD and TG analysis performed in this study suggest that kaolinite is the primary 1:1 clay mineral in soils of the region (Table 5.7). These results are in agreement with all other research papers published on soils from the Paraná River Basin (Resende, 1976; Rauen, 1980; Kämpf, 1981; Curi, 1983; Palmieri, 1986, Clemente, 1988, Fontes, 1988, Castro Fo, 1988; Peixoto, 1995). However, the tests employed do not preclude the possibility that halloysite is also present in some cases, especially since halloysite has already been observed in previous studies of soils from this region (Palmieri, 1986; Almeida et al., 1992; Kämpf et al., 1995). Hydrated halloysite (1.0 nm) was not detected, but dehydrated halloysite (0.7 nm) might be present in association with poorly ordered kaolinite. The later can not be readily differentiated from kaolinite by means of standard cation saturation and thermal treatments. Diagnostic techniques involving intercalation (expansion) of halloysite with formamide or hydrazine are available (Churchman et al., 1984) and will be tested with these clays in future research.

The percentage of kaolinite determined by TG analysis ranged from 46% (LRd - Campo Mourão) to 87% (Ca-Tamarana) (Table 5.7) and was sufficiently high to assign

most of these soils to a kaolinitic mineralogy class (Soil Survey Staff, 1994). The soils developed from the acid / intermediate rock at Tamarana yielded the highest values compared to soils of the same class developed from basic rocks. Similar results were reported by Singh and Gilkes (1992) in Australia. The volcanic rocks contain abundant plagioclase feldspars that either weather directly to kaolinite or produce gibbsite and amorphous materials as precursor phases (Resende, 1976; Clemente, 1988).

The XRD patterns and DTA data for the CBD - treated clays show that the soil kaolinites possess a wide range of crystallinity and, in some cases, are probably interstratified with 2:1 clay minerals (Figs. 5.9 and 5.10). The XRD peak positions and widths at half height (WHH) (Table 5.8), and the position of the endothermic peak from the DTA curves (Table 5.9) were used to assess the degree of crystallinity of the kaolinites. As crystallinity improves, the WHH of the  $d_{001}$  peak should decrease as the peak migrates towards 0.72 nm and the dehydroxylation temperature should increase (Smykatz-Kloss, 1975; Singh and Gilkes, 1992).

Within a given toposequence, the WHH of the kaolinite basal (001) spacing typically increased in the following order: LR, LB > TR, TB > Ca > R , BAv due, most probably, to an increasing degree of interstratification with associated 2:1 clay minerals and/or the presence of halloysite. The highest value ( $1.542^\circ 2\theta$ ) (poorest crystallinity) was found in the Solos Litólicos (Rd) from Campo Mourão, and the lowest value ( $0.495^\circ 2\theta$ ) (best crystallinity) was associated with the Latossolo Roxo (LRd) from the same toposequence.

Prof.#	Soil	Hor.	Treat.	<= WHH (nm) =>			<= Peak (nm) =>		
				2:1	Kao	Gb	2:1	Kao	Gb
<b>Ibiporã</b>									
1	TRe	Bt3	Mg-25	0.323	0.93	0.415	1.450	0.729	0.484
			Mg-EG	0.316	0.919	0.415	1.448	0.729	0.484
			K-550	2.177	n.d.†	n.d.	1.098	n.d.	n.d.
2	Re	A	Mg-25	2.112	1.118	n.d.	1.512	0.734	n.d.
			Mg-EG	2.19	0.99	n.d.	1.511	0.734	n.d.
			K-550	2.294	n.d.	n.d.	1.016	n.d.	n.d.
3	BAv	A	Mg-25	1.958	1.442	n.d.	1.454	0.730	n.d.
			Mg-EG	1.8	1.42	n.d.	1.613	0.727	n.d.
			K-550	2.237	n.d.	n.d.	1.026	n.d.	n.d.
4	LRe	Bw2	Mg-25	0.285	0.63	0.212	1.442	0.723	0.485
			Mg-EG	0.316	0.919	0.205	1.448	0.729	0.484
			K-550	2.502	n.d.	n.d.	1.173	n.d.	n.d.
<b>Campo Mourão</b>									
5	LRd	A	Mg-25	0.353	0.495	0.193	1.420	0.719	0.484
			Mg-EG	0.303	0.713	0.205	1.432	0.724	0.485
			K-550	2.177	n.d.	n.d.	1.098	n.d.	n.d.
7	Rd	A	Mg-25	1.053	1.542	0.270	1.426	0.744	0.485
			Mg-EG	0.61	1.488	0.213	1.435	0.743	0.486
			K-550	1.805	n.d.	n.d.	1.098	n.d.	n.d.
<b>Tamarana</b>									
8	Ca	A	Mg-25	0.642	0.785	n.d.	1.410	0.729	n.d.
			Mg-EG	0.346	0.844	n.d.	1.408	0.727	n.d.
			K-550	2.295	n.d.	n.d.	1.088	n.d.	n.d.
9	TBa	Bt2	Mg-25	0.618	0.756	n.d.	1.391	0.727	n.d.
			Mg-EG	0.7	0.726	n.d.	1.416	0.729	n.d.
			K-550	2.916	n.d.	n.d.	1.112	n.d.	n.d.
10	TBa	Bt2	Mg-25	0.294	1.002	0.571	1.422	0.730	0.485
			Mg-EG	0.71	0.869	0.428	1.435	0.735	0.486
			K-550	2.704	n.d.	n.d.	1.061	n.d.	n.d.

Table 5.8. Width at half height (WHH) and position<sup>†</sup> of diagnostic XRD peaks for the CBD - treated clays

Table 5.8. Continued.

Prof.#	Soil	Hor	Treat.	WHH (nm)			Peak (nm)		
				<= 2:1	Kao	=> Gb	<= 2:1	Kao	=> Gb
Cruzmalina									
14	TRd	Bt2	Mg-25	0.262	0.653	0.443	1.438	0.723	0.484
			Mg-EG	0.292	0.653	0.449	1.453	0.728	0.484
			K-550	1.504	n.d.	n.d.	1.165	n.d.	n.d.
17	LRa	Bw2	Mg-25	0.235	0.61	0.274	1.436	0.723	0.484
			Mg-EG	0.232	0.581	0.274	1.436	0.722	0.484
			K-550	1.156	n.d.	n.d.	1.186	n.d.	n.d.
Faxinal									
18	LBa	Bw2	Mg-25	0.386	0.605	0.215	1.441	0.725	0.486
			Mg-EG	0.309	0.583	0.192	1.433	0.724	0.485
			K-550	1.245	n.d.	n.d.	1.173	n.d.	n.d.
20	Rd	A	Mg-25	0.288	0.706	0.239	1.432	0.725	0.485
			Mg-EG	0.384	0.733	0.247	1.427	0.727	0.485
			K-550	2.808	n.d.	n.d.	1.230	n.d.	n.d.
21	Re	A	Mg-25	0.259	0.64	0.343	1.410	0.724	0.485
			Mg-EG	0.45	0.674	0.308	1.429	0.725	0.485
			K-550	2.475	n.d.	n.d.	1.126	n.d.	n.d.

† d<sub>001</sub> 2:1 peak at 1.4 nm, d<sub>001</sub> kaolinite peak at 0.72 nm, and d<sub>002</sub> gibbsite peak at 0.48 nm.

‡ n.d. = not detected.

The decrease in WHH for these clays was accompanied by a shift of the d<sub>001</sub> XRD peak (Mg-25°C) from 0.744 nm (Rd) to 0.719 nm (Lrd) (Table 5.8). The dehydroxylation temperature also increased from 474 °C (Rd) to 506 °C (LRd) (Table 5.9). The WHH for kaolinites from the soils developed on basic rocks (Ibiporã, Campo Mourão and Cruzmaltina) tended to be larger than those from the acid / intermediate rock kaolinites (Tamarana, Faxinal). This may be due to the abundance of Fe in the former. Singh and Gilkes (1992), for example, characterized kaolinites from Australian laterites and observed a high coefficient of correlation between the degree of crystallinity of the minerals (measured by the WHH), the surface area, and the amount of Fe present within the crystal structure; however, these authors dealt only with kaolinites comparable to those extracted from the most highly weathered profiles in the present study. Most of the observed WHH are large compared with soils that have gone through several cycles of weathering such as those present in the central part of Brazil (Resende, 1976) and Australia (Singh and Gilkes, 1992).

The presence of interstratification between kaolinite and 2:1 clay minerals in clays from the immature soils was suggested by the presence of low angle shoulders on the 0.72 nm peaks that did not collapse with K saturation and heating to 350 °C (Bigham et al., 1982; Jaynes et al., 1989) (Fig. 5.9). The shoulder is most pronounced in the eutrophic profiles where vermiculite / smectite are present (Re and BAv clays from Ibiporã ) but is also apparent in the immature profiles from other locations.

Prof. #	Soil	Horizon	Endothermic Peak (°C)	
			Gibbsite	Kaolinite
Ibiporã				
1	TRe	Bt3	252	495
2	Re	A	n.d. †	487
3	BAv	A	n.d.	493
4	LRe	Bw2	274	504
Campo Mourão				
5	LRd	A	289	506
		Bw2	287	502
		Bw5	280	489
7	Rd	A	268	474
Tamarana				
8	Ca	A	268	500
		Bi	255	495
9	TBa	Bt2	306	519
10	TBa	Bt2	n.d.	517
Cruzmalina				
14	TRd	A	278	504
		Bt2	272	500
15	Rd	A	268	489
17	LRa	A	276	493
		Bw2	278	496
Faxinal				
18	LBa	A	285	508
		Bw2	299	523
20	Rd	A	274	504
21	Re	A	263	508
Average			276	500
SD			13	12

†n.d. = not detected.

Table 5.9. Temperature of diagnostic DTA peaks for the clay size fraction gibbsite and kaolinite.

The presence of interstratification between 1:1 and 2:1 clay minerals, previously thought to be restricted to certain geologic settings (Schultz et al., 1971), is now recognized as being widespread in many pedogenic environments (Wilson and Cradwick, 1972; Herbillon et al., 1981; Bigham et al., 1982; Wada and Kakuto, 1983; Yerima et al., 1985; Jaynes et al., 1989; Breuer and Murad, 1992). Norrish and Pickering (1983) found that interstratified kaolinite/smectite was the primary component of clays from 40 soils developed from basic igneous rocks in Australia. Such a mixed layer mineral is probably a reasonable intermediate in the formation of kaolinite by weathering processes.

### **5.3.3. The 2:1 clay minerals**

The presence of smectite and/or vermiculite in immature soils (BAv, R) and their hydroxy-Al-interlayered counterparts in more highly weathered soils (LR, LB, TB, and TR) of the Paraná River Basin has previously been recognized (Demattê et al., 1977; Galhego and Espindola, 1979; Rauen, 1980, Moniz and Buol, 1982; Moniz et al., 1982; Kämpf, 1981; Queiroz and Klamt, 1985; Palmieri, 1986; Demattê and Marconi, 1991; Demattê et al., 1991 ; Kämpf et al., 1995). The genesis of these minerals in soils derived from volcanic rocks of the PFV is presumably associated with the structural alteration of mica and chlorite and/or formation via the dissolution of plagioclase feldspars and pyroxenes, all of which may be present in the parent materials (Moniz and Jackson, 1967; Moniz et al., 1994; Demattê and Marconi, 1991; Demattê et al., 1991; Kämpf et al., 1995).

Hydroxy-Al-interlayered 2:1 clay minerals (also termed secondary chlorites and Al chlorites), created by the incorporation of polymeric hydroxy Al compounds or "gibbsite islands" in the interlayer regions of expansible clay minerals, have been observed in many soils where acid conditions are prevalent. The introduction of Al into the interlayer region seems to enhance the thermodynamic stability of these minerals relative to "normal" vermiculite and smectite (Karathanasis and Hajek., 1982). Jackson (1963) also noted that hydroxy-Al-interlayered minerals would form in preference to gibbsite until most interlayer sorption sites were consumed; he termed this behaviour the anti-gibbsite effect. Singleton and Harward (1971) suggested that polymeric Fe compounds might also be involved in interlayer formation, and this may be especially true when there is abundant dissolved organic matter in the system to serve as a complexing agent (Singer and Huang, 1993). Early studies of HIV indicated that this mineral is most abundant in the surface or near-surface horizons of soils. It also is commonly enriched in the coarse clay (0.2 - 2  $\mu\text{m}$ ) fraction (Rich, 1968; Jackson, 1963, 1968). The degree of interlayering strongly influences the chemical properties of the host smectite or vermiculite. Generally, as the amount of Al - interlayering increases, the CEC (Helmy et al., 1994), surface area, and K fixation (Rich, 1968) decrease. Anion sorption (e.g., phosphate), on the other hand, increases (Barnhisel and Bertsch, 1989). The qualitative identification of HIV or HIS is usually based on resistance to collapse (or expansion) of the 1.4 nm peak in response to standard XRD pre-treatments and to the appearance of an extra endothermic peak in DTA due to dehydroxylation of the Al - interlayer (Harris et al., 1992).

In the present study, a 1.4 nm XRD peak indicative of smectite, vermiculite, HIS and/or HIV was present in most of the Mg-saturated, water solvated clays at room temperature (Fig. 5. 9). With K-saturation and heating to 500°C, the collapse of this peak varied from 1.23 (Rd - Faxinal) to 1.01 nm (Re - Ibiporã) indicating a wide range of Al - interlayering within the 2:1 clay minerals from the five toposequences (Table 5.8). The range in observed interlayering might be due to the type of 2:1 clay mineral, the nature of the hydroxy - interlayer material (Barnhisel and Bertsch, 1989) or, most likely, the intensity of the local weathering environment. Clays from the young, eutrophic soils of the Ibiporã sequence (BAv and Re) displayed the least evidence of Al-interlayering although it is possible that some Al - interlayer material was removed with the CBD treatment (Yvengar et al., 1981). Expansion of the 1.4 nm peaks in a saturated ethylene glycol atmosphere (60 °C - 24 hrs.) was also observed only in clays from the least weathered profiles. Expansion approached but did not reach 1.71 nm, as would be expected for smectite, indicating that swelling was inhibited by Al-interlayering. Alternatively, the expandable component could be a low charge vermiculite rather than smectite (Walker, 1958; Egashira et al., 1982).

The least developed soils contained the highest amounts of 2:1 clay minerals in all five toposequences (Table 5.7). In some cases (e.g., the BAv and Re profiles from Ibiporã), the formation of these minerals may be attributed to the lateral flow of basic cations and silica in solutions moving downslope from higher points on the landscape (Moniz et al., 1982; Moniz and Buol, 1982). In most instances, however, the 2:1 minerals are probably transient weathering products that are either lost from the system or

preserved as Al-interlayered phases as weathering progresses. The latter scenario is supported by the fact that the abundance of 2:1 minerals generally increased with depth in the more highly weathered soils (LR, LB) of the five toposequences (Table 5.7). The concentrations of HIV/HIS ranged from approximately 3 % in the LRd from Campo Mourão to 9% in the LRe from Ibiporã.

Even when the quantities of 2:1 clay minerals are small, these components could have a major influence on such important soil properties as CEC and coefficient of linear expansion (COLE). The relationship between the CEC (T value) and the % 2:1 minerals in the subsurface clays (Fig. 5.12) of all soils comprising the five toposequences in the present study show a positive correlation ( $R^2 = 0.6835$ ). Kaolinite and gibbsite “strictu sensu” should have small COLEs and CECs under natural soil chemical conditions. Relatively high values of soil CEC previously attributed to kaolinite (Singh and Gilkes, 1992) or halloysite (Palmieri, 1986) may have overlooked the influence of minor amounts of 2:1 clay minerals. For example, Lim et al. (1980) measured the CECs of different standard kaolins and obtained results ranging from 3 to 9 cmol<sub>c</sub>/Kg. After eliminating CEC contributions due to the presence of contaminant illite, vermiculite and montmorillonite, they subsequently calculated a CEC for kaolinite in the range of 0 to 1 cmol<sub>c</sub>/Kg of clay. Isomorphous substitution of Fe for Al in kaolinites has also been frequently reported in the literature (Herbillon et al., 1976; Cuttler, 1980; Angel et al., 1974; Petit and Decarreau, 1990).

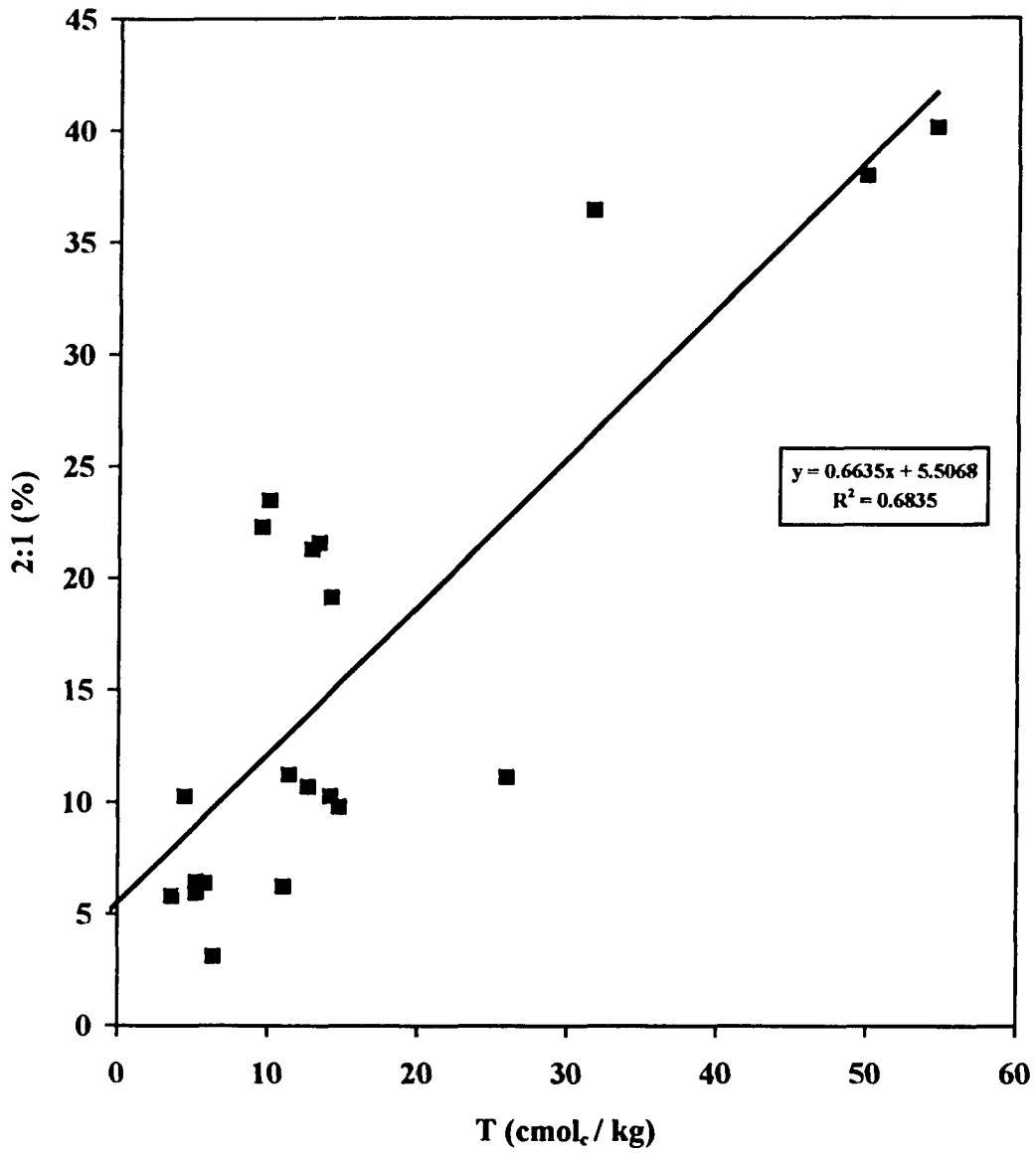


Figure 5.12. Relationship between the cation exchange capacity (T value) and the percentage 2:1 clay fraction minerals in the subsurface horizons from the toposequence soils.

Once again, these studies seem to have ignored the possibility that Fe thought to be present in kaolinite might actually be associated with small amounts of 2:1 clay minerals occurring either as discrete particles or in mixed layers with the kaolinite.

The characterization of 2:1 clay minerals occurring in tropical soils is usually complicated by the abundance of kaolinite, gibbsite and Fe oxides. Preliminary studies indicate that selective dissolution procedures, including the boiling 5M NaOH (Kämpf and Schwertmann, 1982) treatment for removal of kaolinite and gibbsite, do not drastically alter the properties of standard 2:1 clay minerals (Costa et al., 1995). Consequently, the application of these procedures on a more routine basis to soil clays may lead to a better understanding of the chemical and physical properties of highly weathered soils.

#### **5.3.4. Gibbsite**

Jackson (1968) suggested that the stability of clay-sized minerals common to soil environments should increase in the following order: vermiculite < montmorillonite < kaolinite, HIV < gibbsite < hematite, goethite < anatase, rutile, zircon. As the soil pH drops below about 5.5, aluminosilicate clay minerals begin to dissolve releasing  $Al^{3+}$  and Al-hydroxy cations that may precipitate to form gibbsite (McBride, 1994). This phenomenon is clearly reflected in data from three of the five toposequences. The percentage of clay-sized gibbsite in those soils derived from basalt increases in almost linear fashion from 0 - 15% as the soil  $pH_{CaCl_2}$  decreases from 5.5 to 4.5 (Fig. 5.13). Additional weathering continues to yield gibbsite even though the soil system becomes strongly buffered against further decreases in pH.

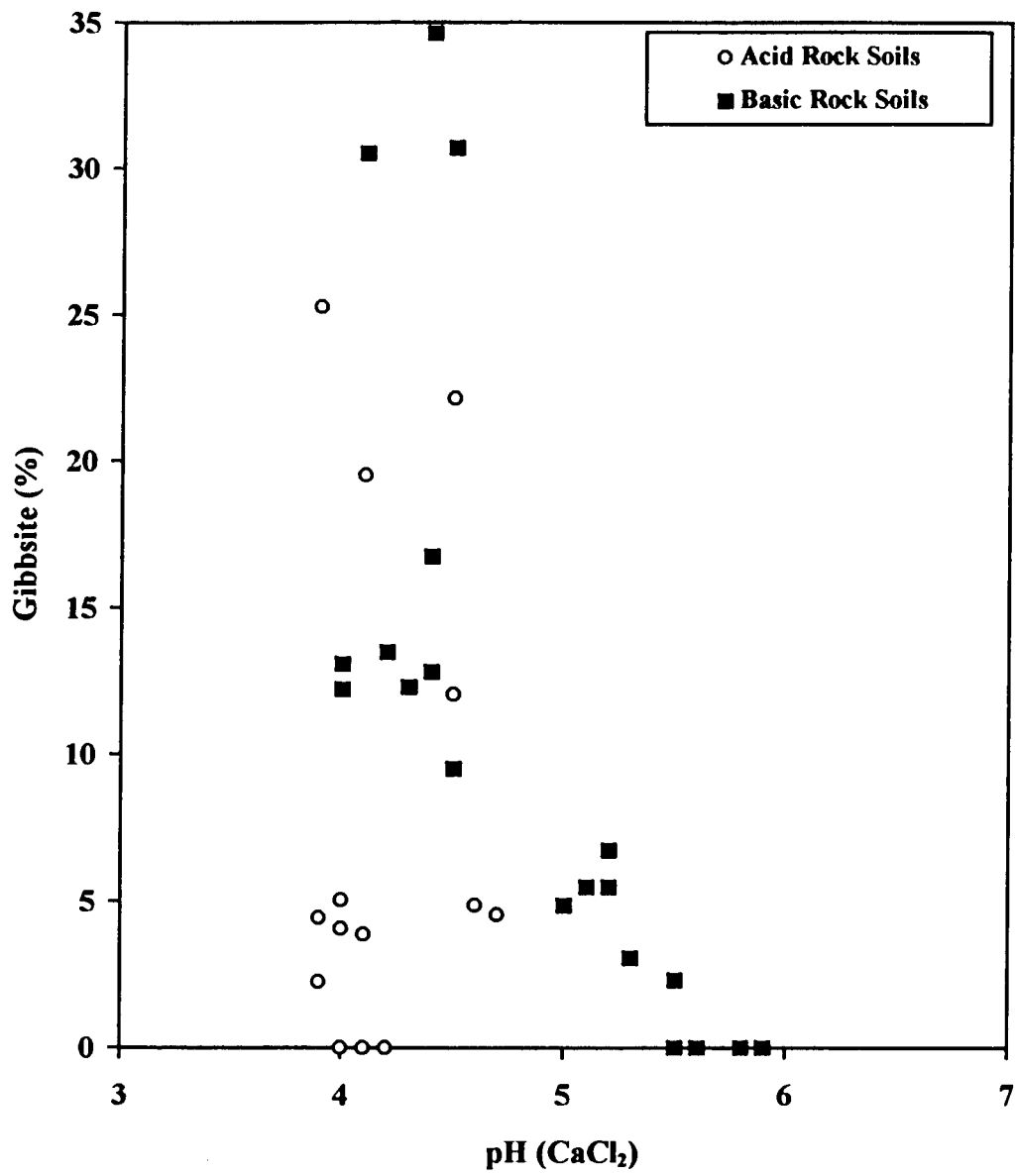


Figure 5.13. Relationship between soil pH (CaCl<sub>2</sub>) and gibbsite content.

The  $\text{pH}_{\text{CaCl}_2}$  of most highly weathered tropical soils, including those of the Paraná River Basin (Resende, 1976; Fasolo, 1978; Rauen, 1980; Kämpf, 1981; Curi, 1983; Palmieri, 1986; Fontes, 1988; Castro Fo, 1988; Peixoto, 1995), seldom falls below 4.0. Characterization of 144 pedons representative of all major soil classes in the state of Paraná revealed that 140 had  $\text{pH}_{\text{H}_2\text{O}}$  values above 3.9; only one had pHs as low as 3.6 (EMBRAPA, 1984). The soils developed from the acid / intermediate rocks at Tamarana and Faxinal were acid even in the incipient stages of weathering and did not present a wide range in pH values. Consequently, no clear relationship exists between soil pH and % gibbsite in these soils (Fig. 5.13). In fact, one TBa pedon (profile #9) contained no detectable gibbsite even though the clay was enriched with well crystalline kaolinite and morphological indicators suggested a fairly advanced stage of weathering.

Gibbsite in the soil clays was identified and quantified primarily on the basis of its endothermic DTA peak in the 250 - 300°C region (Fig. 5.10). The temperature of the dehydroxylation reaction represented by this peak was not constant and was generally lower than reported for standard gibbsite (Hsu, 1989). The highest values of the endothermic peak were obtained for clays from the surface horizons of highly weathered soils of the Latossolo class. The dehydroxylation reaction tended to occur at lower temperatures in samples obtained at depth in the same profiles as well as with all clays extracted from less weathered soils (TR, TB > Ca, BAv > R). In general, the combined XRD and thermal data suggested that gibbsite crystallinity tended to improve with decreasing soil pH.

In the early stages of basalt weathering, goethite and gibbsite appear to be the first minerals formed from the weathering of micas, chlorite and plagioclase feldspars (Moniz and Jackson, 1967; Clemente, 1988; Kämpf et al., 1995), thereby giving rise to weathering rinds that are typically white to yellow in color. Within a few centimeters of the weathering front, kaolinite becomes the dominant mineral and goethite is replaced by hematite/maghemite. Gibbsite initially seems to be unstable due to the competing formation of clay minerals, the interlayering of Al-OH polymers in 2:1 clay minerals (Rich, 1968) (anti-gibbsite effect), and the very slow process of gibbsite crystallization (Hsu, 1989) leading to the formation of small particles. Gibbsite crystallinity may also be negatively affected by the isomorphous replacement of Al by Mg, Fe or other cations as observed by McBride (1978). As weathering intensity increases, the pH decreases and Al is released to solution. After the expandable 2:1 clay minerals become saturated with polymeric Al-hydroxide, gibbsite begins to accumulate. This can be followed in the sequence of soils from Ibiporã (Figs 5.9 and 5.10; Table 5.7). The young profiles have no gibbsite and are rich in 2:1 clay minerals. The gibbsite present in the TRe is poorly crystalline based on its low temperature of dehydroxylation ( $t = 252\text{ }^{\circ}\text{C}$ ) as compared to the LRe ( $T = 274\text{ }^{\circ}\text{C}$ ) (Table 5.9).

## **5.4. Iron oxide mineralogy**

### **5.4.1. Selective dissolution of the iron oxides**

The total Fe content ( $Fe_t$ ) determined after complete dissolution of a sample with strong acids (Bernas, 1968) includes Fe from all possible sources. Selective dissolution techniques have been used for many years to further partition iron compounds into various phases. The well known CBD procedure (Mehra and Jackson, 1960), for example, dissolves all the “free” Fe oxides in a sample by using a strong reducing agent (Na-dithionite); however, the method does not distinguish between oxide species, and the iron removed with the extract ( $Fe_d$ ) is an average of the chemical composition of all phases dissolved. The acid oxalate procedure (Schwertmann, 1973), on the other hand, removes only the most poorly crystalline inorganic phases (e.g., ferrihydrite) as well as organically complexed Fe ( $Fe_o$ ). The ratio of the iron extracted by the two methods ( $Fe_o/Fe_d$ ) has been widely used to assess soil development and age (Alexander, 1974; Blume and Schwertmann, 1969; Fine and Singer, 1989, Borggaard, 1983). In general, highly weathered soils in the tropics yield  $Fe_o/Fe_d$  ratios that are 0.04 or less (Bigam et al., 1978b; Kämpf, 1981; Curi, 1983; Palmieri, 1986; Macedo and Bryant, 1987; Fontes, 1988).

Data from the toposequence clays (Tables 5.10 and 5.11) show that the soils developed from acid / intermediate rocks (Tamarana and Faxinal toposequences) had smaller total Fe contents compared to the soils developed from basic rocks. This result is consistent with the chemistry of the parent rocks (Table 5.1).

Prof.#	Soil	Hor.	Fe <sub>o</sub>	Fed	Fe <sub>o</sub> /Fed	Al <sub>o</sub>	Ald	Al <sub>o</sub> /Ald	Fet	Fed/Fet
<===== % (wt / wt) =====>										
<b>Ibiporã</b>										
1	TRe	Ap	0.43	15.64	0.03	0.24	0.77	0.31	17.19	0.91
		Bt3	0.42	13.48	0.04	0.26	0.75	0.35	13.96	0.97
2	Re	A	1.45	10.65	0.16	0.39	0.91	0.43	13.77	0.77
3	BAv	A	0.97	9.24	0.12	0.39	0.84	0.47	12.16	0.76
		Bt1	0.63	7.24	0.10	0.43	0.94	0.46	11.00	0.66
		Cr	0.28	7.03	0.08	0.29	0.65	0.45	9.15	0.77
4	LRe	A	0.55	14.80	0.04	0.35	1.13	0.31	15.94	0.93
		Bw2	0.57	15.82	0.04	0.36	1.23	0.29	16.81	0.94
<b>Campo Mourão</b>										
5	LRd	A	0.48	16.82	0.03	0.39	1.05	0.37	17.13	0.98
		Bw2	0.38	17.74	0.02	0.33	1.03	0.32	17.98	0.99
7	Rd	A	1.43	8.65	0.16	1.48	3.10	0.48	11.74	0.74
<b>Tamarana</b>										
8	Ca	A	0.99	4.35	0.23	0.89	1.00	0.89	6.43	0.68
		Bi	0.66	4.36	0.15	0.70	1.20	0.59	6.69	0.65
		Cr	0.66	4.57	0.14	0.82	1.26	0.65	6.49	0.70
9	TBa	A	0.29	5.87	0.05	0.17	0.67	0.25	7.18	0.82
		Bt2	0.10	6.66	0.01	0.18	0.77	0.24	8.39	0.79
<b>Cruzmalina</b>										
14	TRd	Ap	0.60	13.27	0.04	0.50	1.74	0.29	13.35	0.99
		Bt2	0.56	13.02	0.04	0.64	2.01	0.32	14.05	0.93
15	Rd	Ap	0.80	12.74	0.06	0.47	1.30	0.36	15.23	0.84
		Cr	0.48	11.97	0.04	0.38	1.17	0.33	12.43	0.96
17	LRa	A	0.90	14.65	0.06	0.70	1.97	0.36	15.91	0.92
		Bw2	0.65	15.64	0.04	0.48	1.34	0.36	16.73	0.93
<b>Faxinal</b>										
18	LBa	A	0.40	10.85	0.04	0.44	1.36	0.32	12.84	0.84
		Bw2	0.44	11.38	0.04	0.33	1.27	0.26	13.58	0.84
20	Rd	A	0.36	5.70	0.06	0.38	1.31	0.29	7.50	0.76
21	Re	A	0.33	6.38	0.05	0.30	1.47	0.21	8.48	0.75

Table 5.10. CBD-extractable iron (Fe<sub>d</sub>) and aluminum (Al<sub>d</sub>), oxalate-extractable iron (Fe<sub>o</sub>) and aluminum (Al<sub>o</sub>), and total iron (Fe<sub>t</sub>) in clays from the toposequence soils.

	Fe <sub>o</sub>	Fed	Fe <sub>o</sub> /Fed	Al <sub>o</sub>	Al <sub>d</sub>	Al <sub>o</sub> /Al <sub>d</sub>	Fet	Fed/Fet
	<===== % (wt / wt) =====>							
	LR - LB - TR - TB							
AV	0,48	13,26	0,04	0,38	1,22	0,31	14,36	0,91
SD	0,18	3,54	0,01	0,16	0,44	0,04	3,24	0,07
	BA <sub>v</sub> - R - C							
AV	0,75	7,74	0,11	0,58	1,26	0,47	10,09	0,75
SD	0,39	2,93	0,06	0,35	0,62	0,18	3,04	0,08

Table 5.11. Average values (AV) and standard deviations (SD) for CBD-extractable iron (Fed) and aluminum (Al<sub>d</sub>), oxalate-extractable iron (Fe<sub>o</sub>) and aluminum (Al<sub>o</sub>), and total iron (Fet) in clays from the highly weathered (LR, LB, TR, TB) and less weathered soils (BA<sub>v</sub>, R, C) of the five toposequences.

As expected, the most mature soils in all five toposequences yielded Fed/Fet ratios that were  $\geq 0.8$  indicating a strong release of Fe from primary silicates through weathering processes. In addition, only a small portion (usually  $< 5\%$ ) of the iron extracted by CBD was also extractable with acid ammonium oxalate. The CBD-extractable iron decreased from the most weathered profiles to the least weathered ones in the following sequence LR, TR > LB > TB > BA<sub>v</sub>, R, and C. An inverse order was observed for the oxalate-extractable iron. These trends support the idea that poorly crystalline Fe phases form early in the weathering process in association with silica and dissolved organic matter (Blume and Schwertmann, 1969; McKeague et al., 1971; Schwertmann, 1973). With continual leaching of the system, the crystallinity of the Fe oxides gradually improves. Aluminum extracted with CBD and acid ammonium oxalate follows similar trends but is more difficult to correlate with the degree of weathering because Al solubility may be

influenced by subtle changes in pH, decomposition of organics (McKeague et al., 1971), the formation of hydroxy-Al-interlayers in 2:1 clay minerals (Barnhisel and Bertsch, 1989), and competing effects from the formation of 1:1 clay minerals (Moniz et al., 1982b)

#### **5.4.2. Identification of iron oxide minerals in the soil clay fraction**

Preliminary XRD analysis showed that it was impossible in some samples (especially clays from the least weathered soils) to distinguish the diffraction peaks of the Fe oxides because of weak intensities and/or overlapping peaks from other minerals (e.g., Brunizem Avermelhado, Fig. 5.14). To eliminate dilution effects from kaolinite and gibbsite, all samples were boiled in 5M NaOH for 1 hr (Norrish and Taylor, 1961; Kämpf and Schwertmann, 1982) (Fig. 5.14). This procedure has been successfully used by several authors and all have reported improved detection of the Fe oxides (Davey et al., 1975; Bigham et al., 1978a; Torrent et al., 1980; Kämpf and Schwertmann, 1982). A few authors have also observed that the 5M NaOH treatment may a) not completely dissolve kaolinite/gibbsite, b) form secondary silicate phases (Singh and Gilkes, 1991), or c) alter the composition or mineral characteristics of the Fe oxides present in a sample (Goodman et al., 1988). The method initially proposed by Norrish and Taylor (1960) was evaluated in detail by Kämpf and Schwertmann (1982). These authors observed that the treatment did, indeed, produce secondary mineral precipitates (sodalite), but these could be eliminated by careful washing of the 5M NaOH residues. They also found no adverse effects on the properties (e.g., Al-substitution) of either synthetic or soil Fe oxides when a source of silica was available in the system.

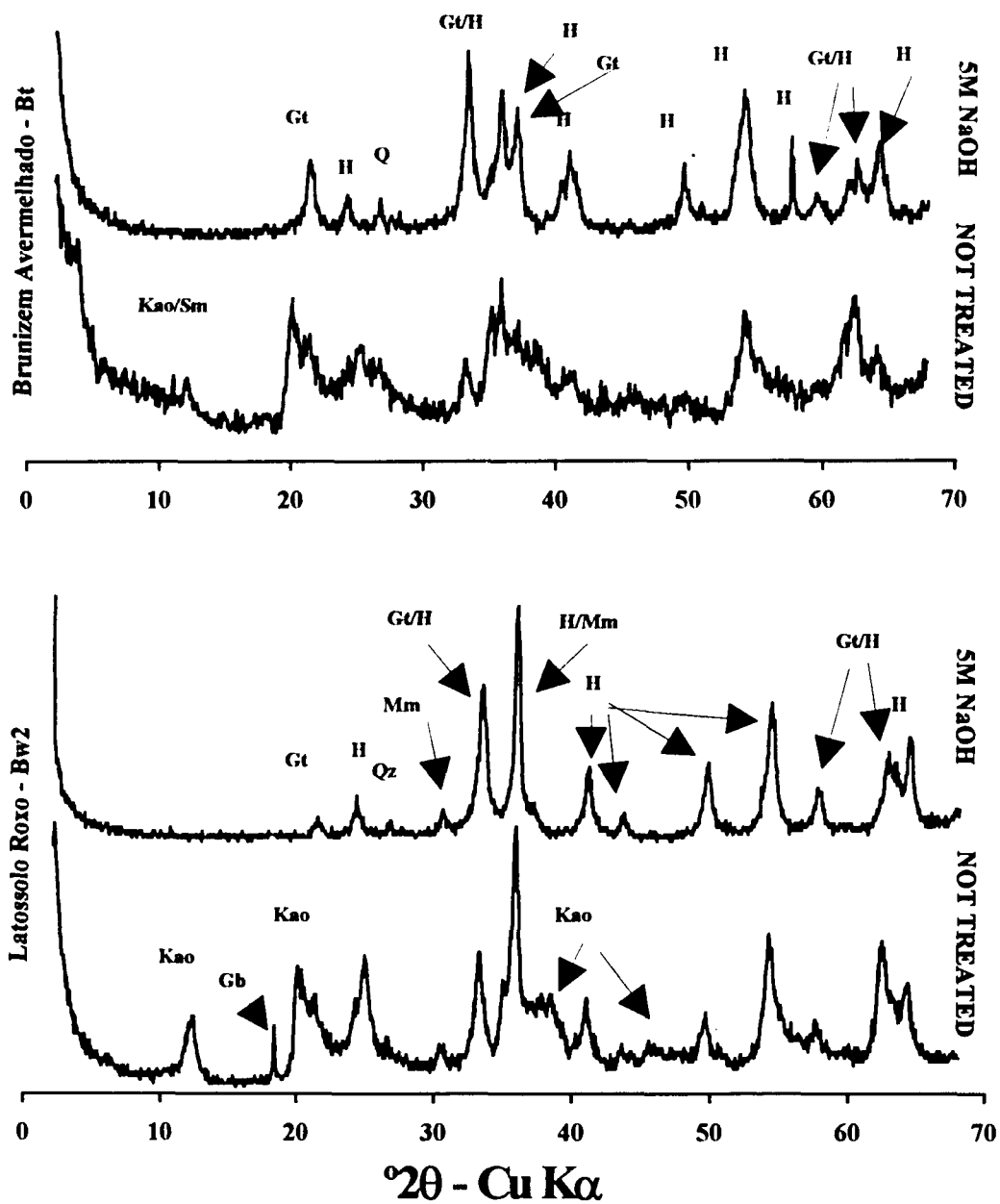


Figure 5.14. Effect of the boiling, 5M NaOH procedure on the dissolution of kaolinite and gibbsite in the Latossolo Roxo-Bw2 and Brunizem Avermelhado-Bt clay fractions from Ibiporã.

Kämpf and Schwertmann (1982) concluded that for tropical soils a natural source of silica is present in the form of kaolinite that promptly dissolves during the treatment.

The degree of concentration of Fe oxides and other resistant minerals in the present study can be inferred from the amount of kaolinite and gibbsite present in the original clays (Table 5.7). Based on these data, the effective concentration factor ranged from four (highly weathered profiles) to almost 10 times (less weathered profiles). Hydroxy-Al-interlayered vermiculite and other 2:1 clay minerals were not dissolved by the boiling 5M NaOH procedure (Costa et al., 1995) and gave a diffraction peak in the 19-20 °2θ range in randomly oriented specimens. This peak has previously been confused with undissolved kaolinite (Kämpf, 1981). In either case, it does not interfere with the diagnostic diffraction peak of goethite at 21.2 °2θ.

#### **5.4.3. Quantification of iron oxide minerals in the soil clay fraction by XRD**

Hematite, goethite and maghemite were the only Fe oxide minerals detected in the clay samples following treatment with 5M NaOH. The proportion of these minerals was estimated using appropriate XRD peak areas. The d<sub>012</sub>, d<sub>110</sub> and d<sub>220</sub> diffraction peaks of hematite, goethite and maghemite, respectively, were used for this purpose because they occur in close proximity to each other and are relatively free of interference from other minerals present in the clay fractions of these soils (Figs. 5.14 and 5.15). The measured peak areas were converted to percentages (Table 5.12) using constant factors (multipliers) derived from the relative intensities of the selected peaks in pure specimens and standard mixtures.

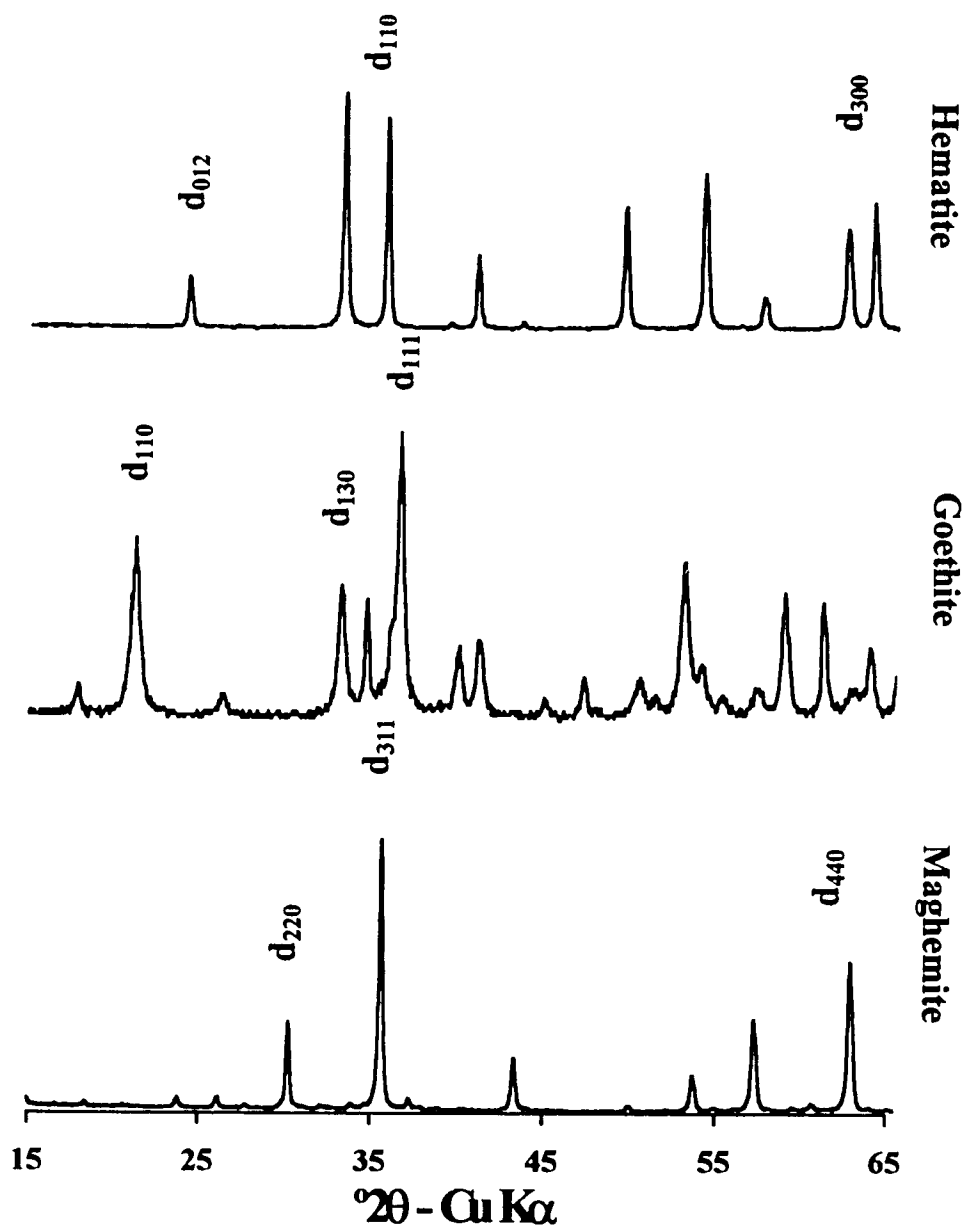


Figure 5.15. X-ray diffraction patterns for synthetic hematite, goethite and maghemite prepared according to the methods of Schwertmann and Cornell (1993).

For the  $d_{012}$  and  $d_{110}$  diffraction lines of hematite and goethite, factors of 3.5 and 1, respectively, have been proposed and successfully tested (Schwertmann and Lathan, 1986). No similar intensity factor has been previously suggested for the  $d_{220}$  diffraction peak of maghemite. The choice of a constant factor of 3.5 for this peak was based on relative intensity information in the ICDD data base and independent measurements using magnetic susceptibility (section 5.4.4).

The types and relative amounts of Fe oxides occurring within the toposequence clays (Table 5.12) depended on the parent material and the landscape position (weathering). The Fe oxide mineralogy of the highly weathered profiles developed from basic rocks was dominated by hematite and maghemite. Goethite was less abundant, and some samples (i.e., LRd - Campo Mourão) actually contained no XRD-detectable goethite. Because it is difficult to measure small amounts (less than 5 wt%) of minerals by XRD, more sensitive methods, such as Mössbauer spectroscopy, should be used to confirm these results. Goethite was more abundant in the less weathered soils (Table 5.12), and it was the dominant Fe oxide in those soils developed from acid / intermediate rocks (except the LBa - Faxinal). The latter were mostly devoid of maghemite. Similar observations were made by Kämpf (1981) and Palmieri (1986) working with soils developed from the same types of rocks in southern Brazil. Both authors reported that the soils formed from acid / intermediate rocks (Cambissolo, Terra Bruna Estruturada, Latossolo Bruno) were dominated by goethite. The youngest profiles examined (Cambissolo) were devoid of hematite.

Prof.#	Soil	Hor	Mm <sup>a</sup>	Gt <sup>b</sup>	Hm <sup>c</sup>
			←===== % =====→		
<b>Ibiporã</b>					
1	TRe	Ap	16.4	18.9	64.7
		Bt3	15.8	16.5	67.7
		Bt7	7.4	20.9	71.7
2	Re	A	0.0	86.8	13.2
3	BAv	A	0.0	57.7	42.3
		Bt	0.0	81.5	18.5
		Cr	0.0	81.2	18.8
4	LRe	A	25.8	16.5	57.7
		Bw2	25.7	21.8	52.5
<b>Campo Mourão</b>					
5	LRd	A	36.3	0.0	63.7
		Bw2	39.5	0.0	60.5
		Bw5	36.2	0.0	63.8
7	R	A	15.9	66.9	17.2
<b>Tamarana</b>					
8	Ca	A	0.0	73.5	26.5
		Bi	0.0	81.0	19.0
9	TBa	A	0.0	79.4	20.6
		B	0.5	72.3	27.2
10	TBa	Bt2	1.5	73.0	25.6
<b>Cruzaltina</b>					
14	TRd	Bt	19.7	47.6	32.6
15	Rd	Ap	9.2	49.6	41.2
17	LRa	Bw2	25.7	12.5	61.8
<b>Faxinal</b>					
18	LBa	Bw2	11.8	35.9	52.3
20	Rd	A	0.0	80.3	19.7
21	Re	A	1.2	89.3	9.6

a=(3.5Mm) / (3.5Mm + 3.5Hm + Gt)x100; b = (Gt) / (Gt + 3.5Mm + 3.5Hm) x 100; c = (3.5Hm) / (3.5Hm + 3.5Mm + Gt) x 100

Table 5.12. Proportions of maghemite (Mm), goethite (Gt), and hematite (Hm) in the 5M NaOH concentrates as measured by X-ray diffraction peak area.

These and other authors (Resende, 1976; Fasolo, 1978; Rauen, 1980; Curi, 1983; Fontes, 1988) also noted the presence of maghemite in some clays and suggested that its occurrence was related to the degree of weathering, parent material, depth (Resende, 1976, Fasolo, 1978, Rauen, 1980), and previous drainage conditions of the soils (Curi, 1983); however, no attempt was made to quantify the distribution of maghemite within or between profiles.

In fact, most previous quantitative work on the distribution of Fe oxides in soils of the Paraná River Basin has focused on hematite and goethite. Kämpf et al. (1986) reviewed the literature of the soils derived from volcanic rocks within the Basin. They observed that the hematite - goethite ratios in these soils ranged from 0 to 0.97 and increased with increasing temperature and decreasing rainfall. From Table 5.12, one can readily see that the parent rock material and degree of weathering are also important factors to be considered since these soils have formed under the same climatic conditions (section 4.2.1).

#### **5.4.4. Quantification of maghemite using magnetic susceptibility**

The magnetic susceptibility of clays from the toposequence and climosequence samples is strongly correlated with their maghemite contents (Fig. 5.16), as calculated from the product of  $Fe_d$  (Table 5.10; Appendix B) and the percentage of maghemite obtained by XRD analysis of the 5M NaOH residues (Table 5.12; Appendix B).

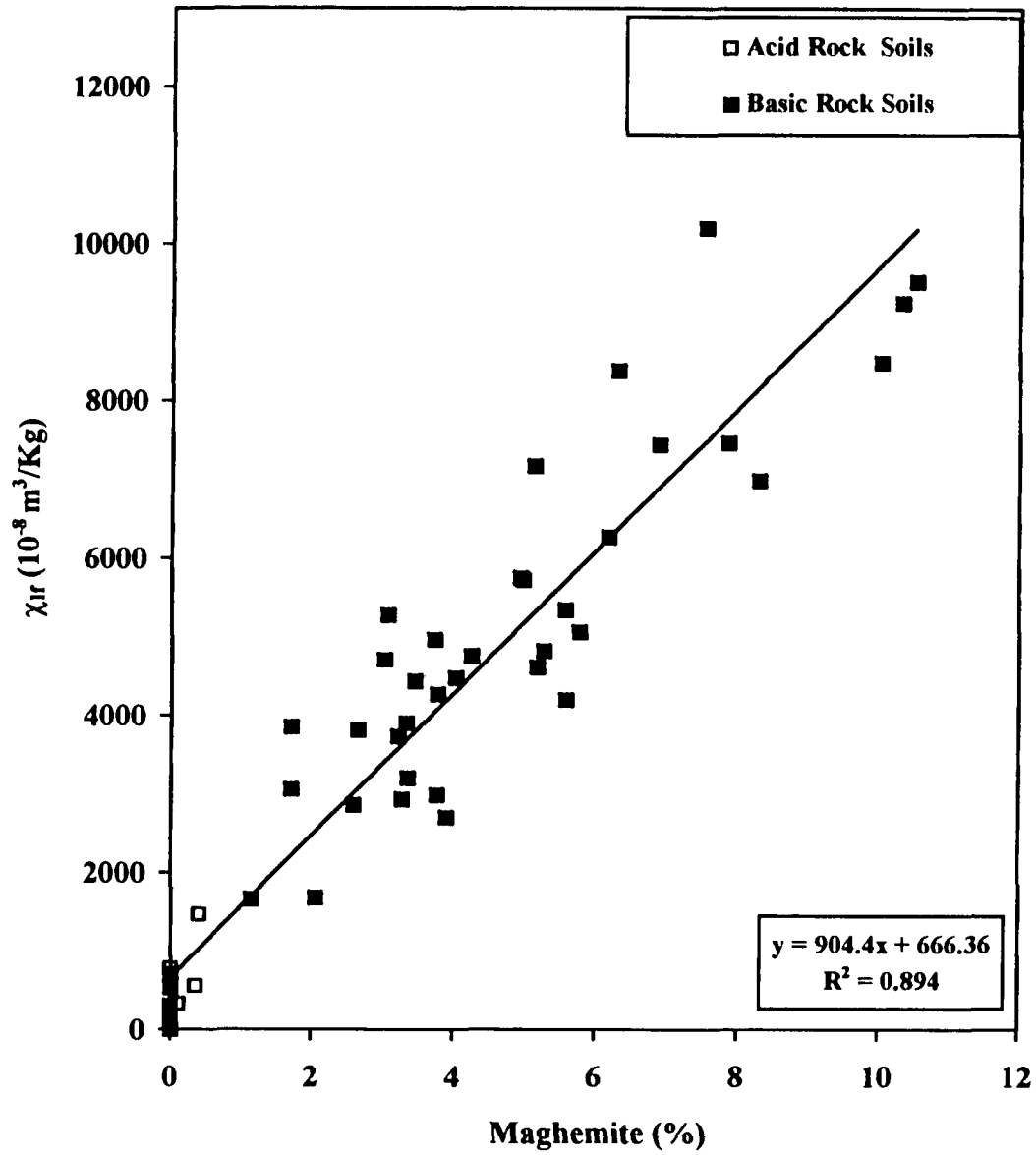


Figure 5.16. Magnetic susceptibility vs. percentage maghemite determined by XRD peak area in the total clays from both the acid and basic rock soils.

Although the correlation statistic is high ( $r^2 = 0.89$ ), the XRD method clearly underestimates the amount of maghemite in clays from the least weathered profiles and those soils developed from acid / intermediate rocks. Small amounts of maghemite (less than 5%) in the clay fractions are difficult to detect by XRD. In addition, the most intense diffraction line of maghemite ( $d_{311}$ - Fig. 5.15) has a very similar d-spacing to the second most intense diffraction line ( $d_{110}$ ) of hematite. Quantification of maghemite and hematite in mixed assemblage is also difficult using Mössbauer spectroscopy because the two minerals yield very similar Mössbauer spectra (Fontes, 1988). These results suggest that magnetic susceptibility may be a more sensitive method for quantifying small amounts of fine-grained maghemite in soil clays.

To test this possibility, mechanical mixtures of maghemite, hematite and goethite synthesized according to the methods of Schwertmann and Cornell (1991) (see XRD patterns, Fig. 5.15) were prepared, and their magnetic susceptibilities were measured as outlined in section 4.6.4. As expected, the relationship between the weight percentage of synthetic maghemite and the magnetic susceptibility was strong, even at low concentrations of maghemite (Fig. 5.17). These results indicate, once again, that magnetic susceptibility can be used for quantification of maghemite in natural samples provided (a) it is the dominant ferrimagnetic mineral present in the samples and (b) the magnetic susceptibility of the maghemite is known. Figure 5.17 shows, for example, that the magnetic susceptibility of the synthetic maghemite was approximately 50000 ( $10^{-8} \cdot \text{m}^3/\text{Kg}$ ).

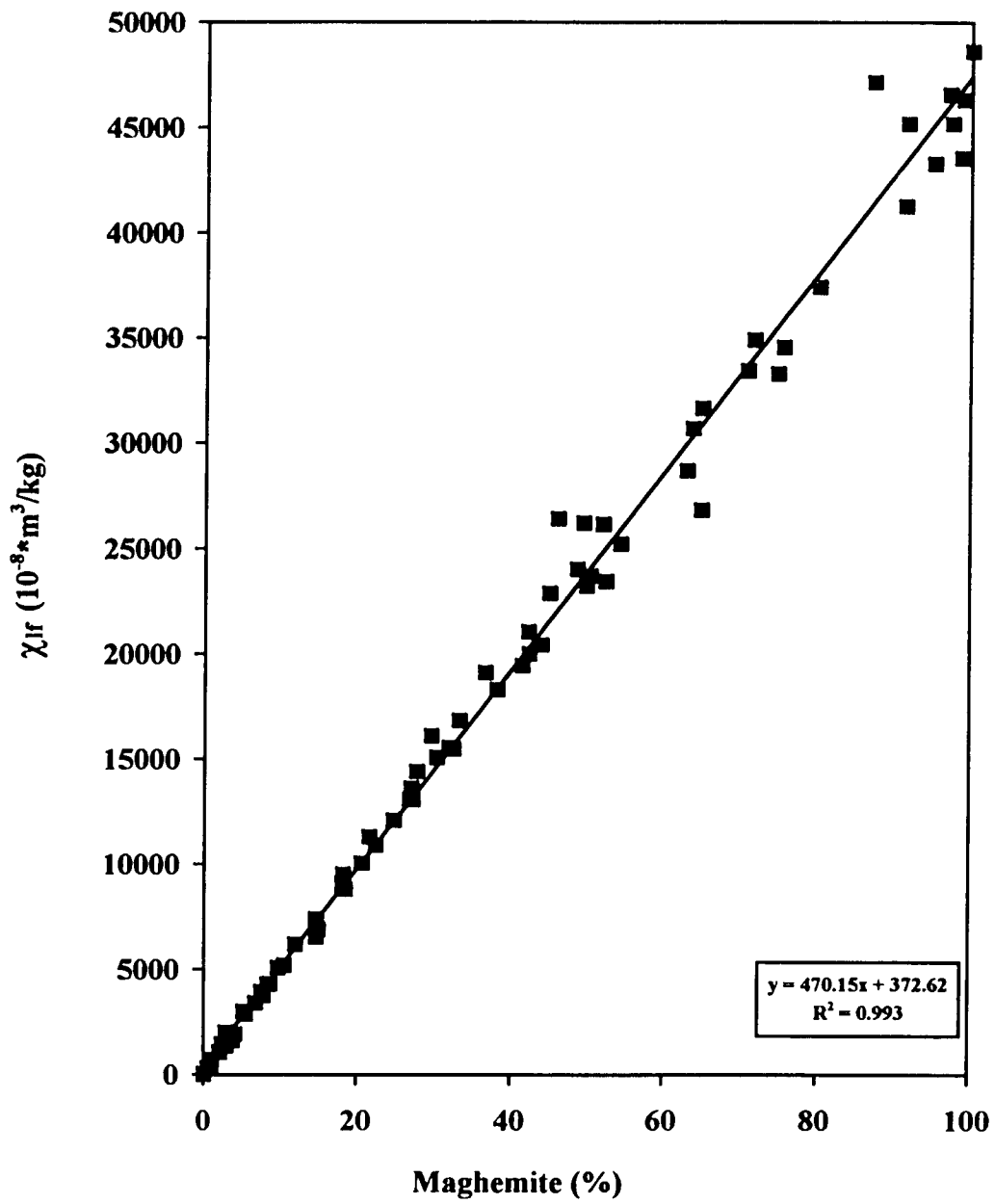


Figure 5.17. Magnetic susceptibility ( $\chi_{f_r}$ ) of artificial mixtures of synthetic maghemite, hematite and goethite.

Values of magnetic susceptibility for maghemite in the literature range from 44000 to 111600 ( $10^{-8} \cdot \text{m}^3/\text{Kg}$ ) (Dearing, 1994; Resende et al, 1986) and vary with particle size and both the degree and type of isomorphous substitution (Coey, 1985). One should expect that the same factors will influence the magnetic susceptibilities of soil maghemites.

Magnetic susceptibilities of the soil maghemites in this study were calculated by allocating the total clay susceptibilities to the mass of maghemite present. The latter was determined from the  $\text{Fe}_d$  contents and the percentages of maghemite obtained by XRD analysis of the 5M NaOH residues (samples without XRD-detectable maghemite were necessarily excluded from this calculation). The average magnetic susceptibility of the soil maghemites was 44000 ( $10^{-8} \cdot \text{m}^3/\text{Kg}$ ) as compared to 50000 ( $10^{-8} \cdot \text{m}^3/\text{Kg}$ ) for the synthetic mixtures where the contents of maghemite were known (Fig. 5.18). In both cases, considerable scatter was observed at low maghemite contents due mostly to the small amount of ferrimagnetic mineral in the  $10 \text{ cm}^3$  sample volume. If a value of 50000 ( $10^{-8} \cdot \text{m}^3/\text{Kg}$ ) is used to back calculate the amount of maghemite present in the original clay fraction, a strong positive correlation is obtained with the amounts measured by the combined XRD-CBD procedures (Fig. 5.19); however, there is a general tendency for the magnetic measurements to yield lower quantities of maghemite. The differences would be aggravated if a lower magnetic susceptibility (e.g., 44000) is used for maghemite.

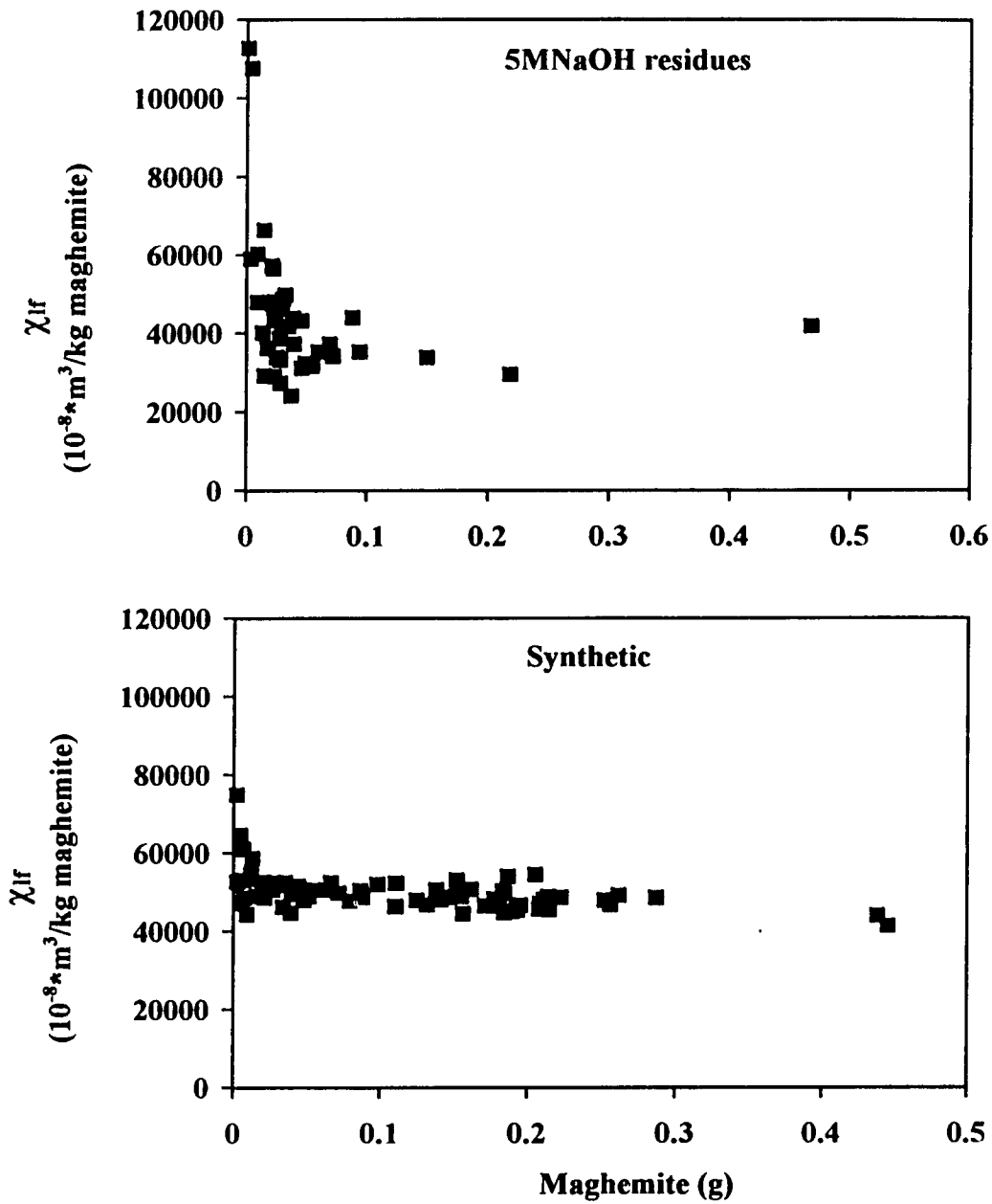


Figure 5.18. Calculated magnetic susceptibilities ( $\chi_{lf}$ ) of the soil and synthetic maghemites.

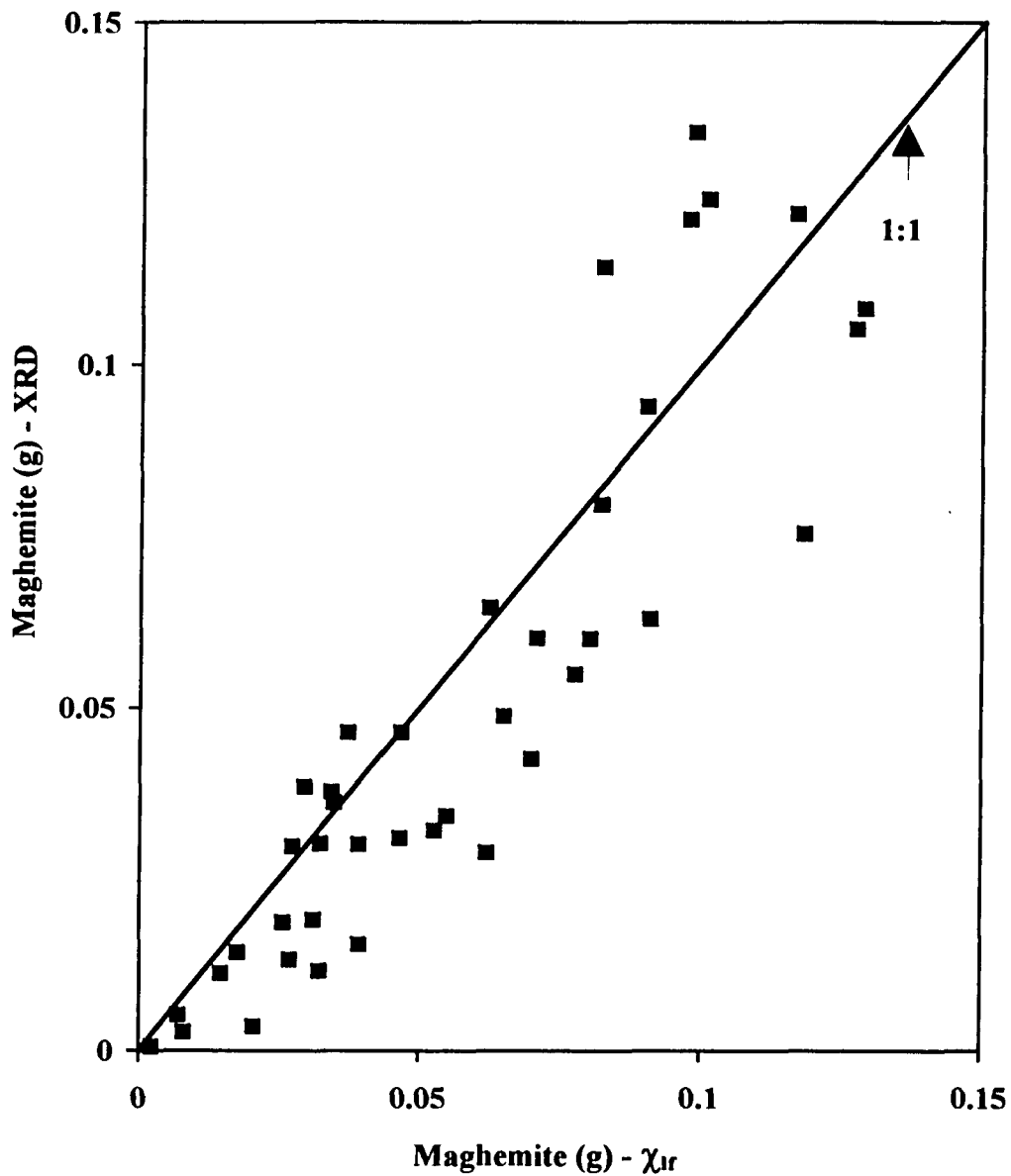


Figure 5.19. Relationship between the mass of maghemite measured by XRD and by magnetic susceptibility using a value of 50000 ( $10^{-8} \bullet \text{m}^3/\text{Kg}$ ) for the magnetic susceptibility of soil maghemite.

Otherwise, these results show that an estimation of the mass of maghemite (or magnetite) present in a sample (soils, clays, rocks, sediments, atmospheric particles, etc.) is feasible by measuring its magnetic susceptibility (a simple and easy measurement) if the specific magnetic susceptibility of the ferrimagnetic component of the sample is known.

Other non destructive techniques such as high density magnetic separation (Jaynes and Bigham, 1986a; Fontes, 1988) are available to concentrate the magnetic fraction of soil materials and could simplify the determination of the magnetic susceptibility of the ferrimagnetic minerals present in complex samples and help to explain how particle size, isomorphous substitution and the boiling 5M NaOH procedure affect this mineral property.

#### **5.4.5. Iron oxides and clay color**

The reddish brown colors of most well drained tropical soils have traditionally been related to the presence of hematite and/or goethite. Hematite is commonly associated with Munsell hues of 5YR and redder (Schwertmann, 1993), and its pigmentation power is strong. Resende (1976) found that the addition of only 1% by weight of hematite to a goethitic Oxisol changed its hue from 10YR to 5YR. Empirical color indices such as the Redness Rating (Torrent et al., 1983) have been effectively used to estimate the hematite content of both soils and clays; however, a universal relationship has not been developed. For example, Torrent et al. (1983) and Kämpf (1981) obtained different relationships between Redness Rating and the hematite contents of soils from Europe and Brazil, respectively. Therefore, it seems that while hematite content may be

well correlated with the colors of soils and clays on a local or regional level, broader correlations may be negatively influenced by factors such as particle size (Schwertmann and Cornell, 1991; Schwertmann, 1993), aluminum substitution (Kosmas et al., 1986), etc.

The relationship between hematite content and Redness Rating observed in the present study differs from those reported by both Torrent et al. (1983) and Kämpf (1981) (Fig. 5.20). This difference may be due to inherent differences in the properties of the hematites or to the fact that the Redness Rating is linearly related to hematite content only to about 4% by weight of the oxide (Torrent et al., 1983). A more important factor may be that many of the current samples contain significant amounts of maghemite which also has a reddish brown color in the 2.5 YR to 5 YR range (Schwertmann, 1993). There appears to be no previous work relating soil/clay color to maghemite content or to the combined effects of maghemite plus hematite. The correlation statistic for Redness Rating vs % oxide decreases slightly ( $r^2 = 0.64$ ) when the sum of hematite and maghemite is used as the independent variable (Fig. 5.21). Clearly, more work is needed to define an appropriate multivariable relationship between color and Fe oxide mineralogy in these soils.

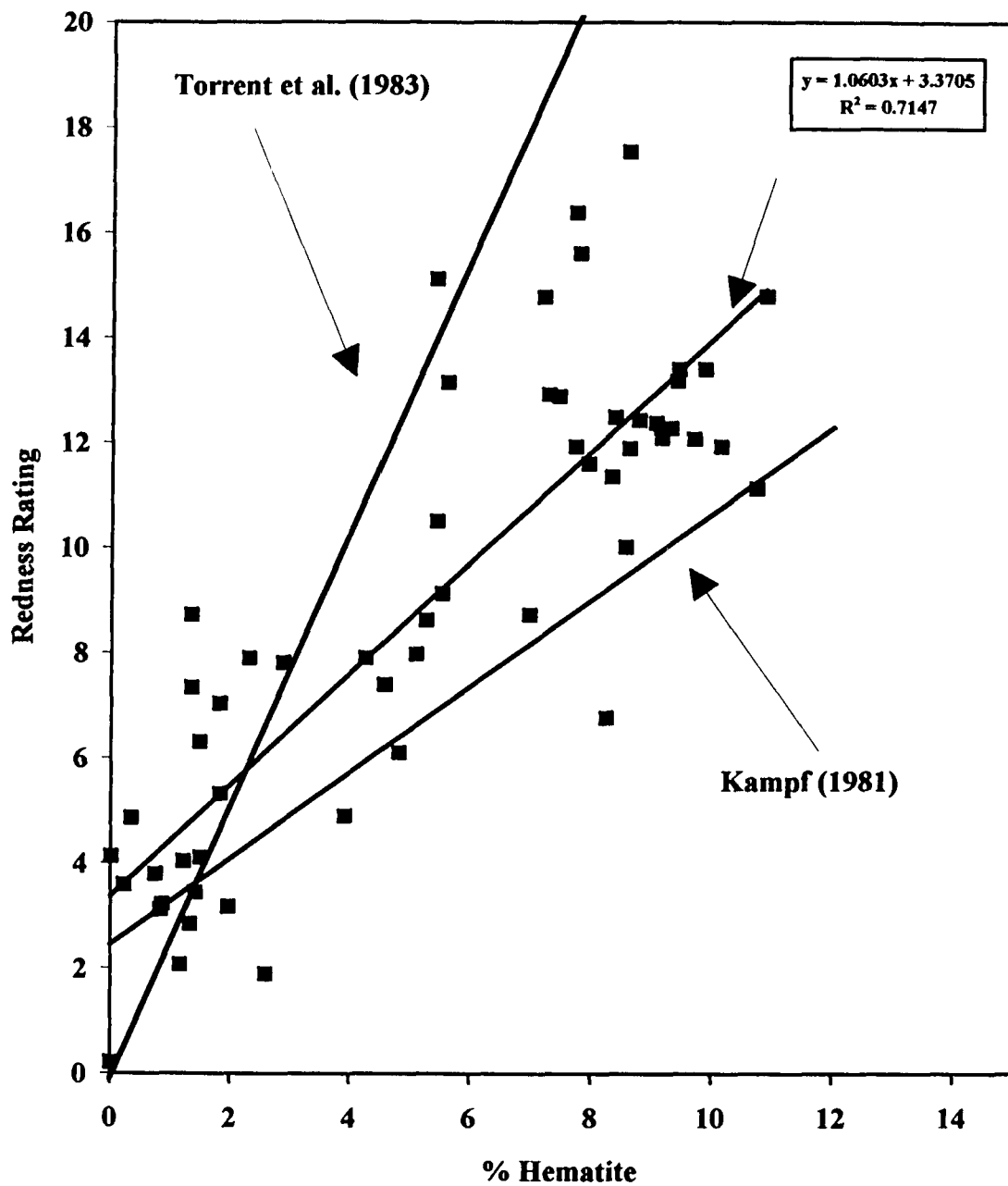


Figure 5.20. Relationship between redness rating of the dry soil clays and the percentage hematite.



#### 5.4.6. Al-substitution in the iron oxides

Aluminum has a smaller ionic radius (0.053 nm) than Fe (0.073 nm); therefore, replacement of Fe by Al systematically influences some crystallographic parameters of the Fe oxides. In most cases, the amount of solid solution can be determined by the displacement of selected XRD peaks with increasing Al substitution. Numerous authors have worked with Al-substituted Fe oxides and have correlated shifts in the position of one or more XRD peaks with the amount of Al substitution. Perhaps the most detailed studies of goethite have been performed by Schulze (1982, 1984). Similar examples for hematite and maghemite include the works of Schwertmann et al. (1979), Schwertmann and Lathan (1986), and Schwertmann and Fechter (1984).

In the case of Al substitution, the displacement of diffraction peaks is usually to higher angles due to the smaller ionic radius of Al as compared to Fe. This effect is shown for the  $d_{110}$  and  $d_{111}$  diffraction lines of hematite and goethite, respectively, in Figure 5.22 which compares the XRD pattern from a soil concentrate (5M NaOH residue from the TRd-Cruzmalina clay) to patterns from pure, synthetic samples of hematite and goethite. For goethite, the  $d_{110}$  and  $d_{111}$  peak positions have commonly been used to calculate Al substitution and the  $a_0$  unit cell dimension. For hematite, similar measurements have been performed using either the  $d_{110}$  or the  $d_{300}$  diffraction peaks. When maghemite is also present in a sample, the hematite  $d_{110}$  peak is overlapped by the  $d_{311}$  peak of maghemite (Fig. 5.15).

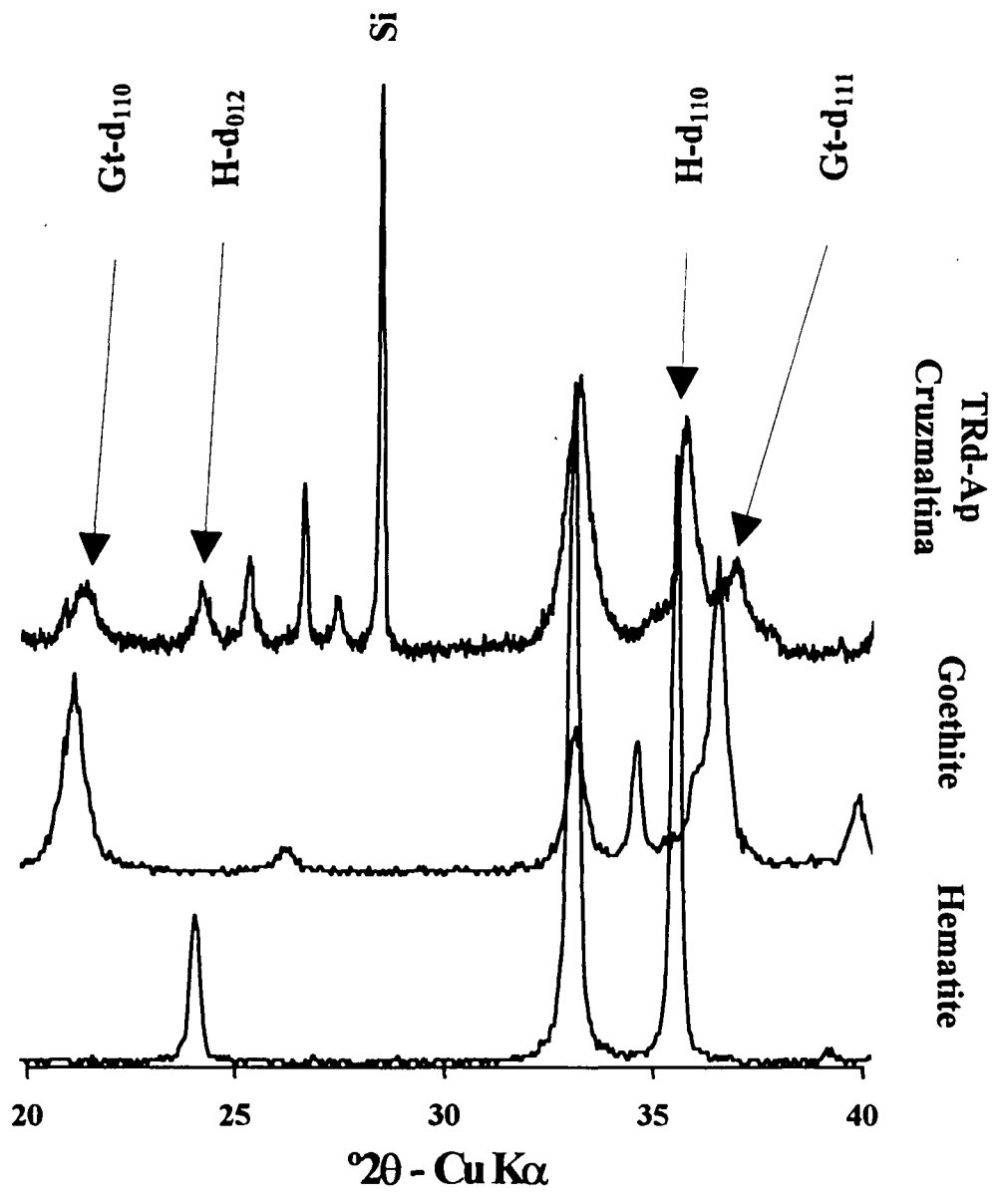


Figure 5.22. XRD patterns from synthetic hematite and goethite compared to that from a residue of the 5M NaOH and 1.8M H<sub>2</sub>SO<sub>4</sub> treatments (TRd- Cruzmalina).

In order to remove this interference, samples containing both hematite and maghemite were treated with  $\text{H}_2\text{SO}_4$  to selectively dissolve maghemite. The procedure used was a modification of the method proposed by Schwertmann and Fechter (1984). Specifically, a kinetic dissolution experiment with two 5M NaOH concentrates from Latosssolo clays (Figs 5.23 and 5.24) showed that after 2 hr contact with a 1.8M  $\text{H}_2\text{SO}_4$  (75°C) solution, most of the maghemite was completely dissolved whereas hematite was preserved. The preferential dissolution of maghemite was monitored by observing the disappearance of the d220 diffraction peak (Fig. 5.23) and by following the ratio of Fe and Al released to solution with increasing time (Fig. 5.24).

Even though it can not be argued that goethite and hematite were unaffected by the acid treatment, the diffraction peaks from both minerals increased in intensity while the d220 and d440 diffraction lines of maghemite disappeared (Fig. 5.23) over a 2 hr period. Schwertmann and Fechter (1984) recommended 7.5 hr for complete dissolution of maghemite. In the present case, 7.5 hr reaction time led to dissolution of not only the maghemite but also much of the associated hematite and goethite, as shown by relative increases in the peak areas of residual anatase, quartz and rutile (Fig. 5.23).

Aluminum substitution in maghemite was measured by using the shift of the d220 diffraction peak in the 5M NaOH residues (Table 5.13) and by the ratio of Fe and Al released to solution after 2 hr of contact with 1.8M  $\text{H}_2\text{SO}_4$  (Fig. 5.24).

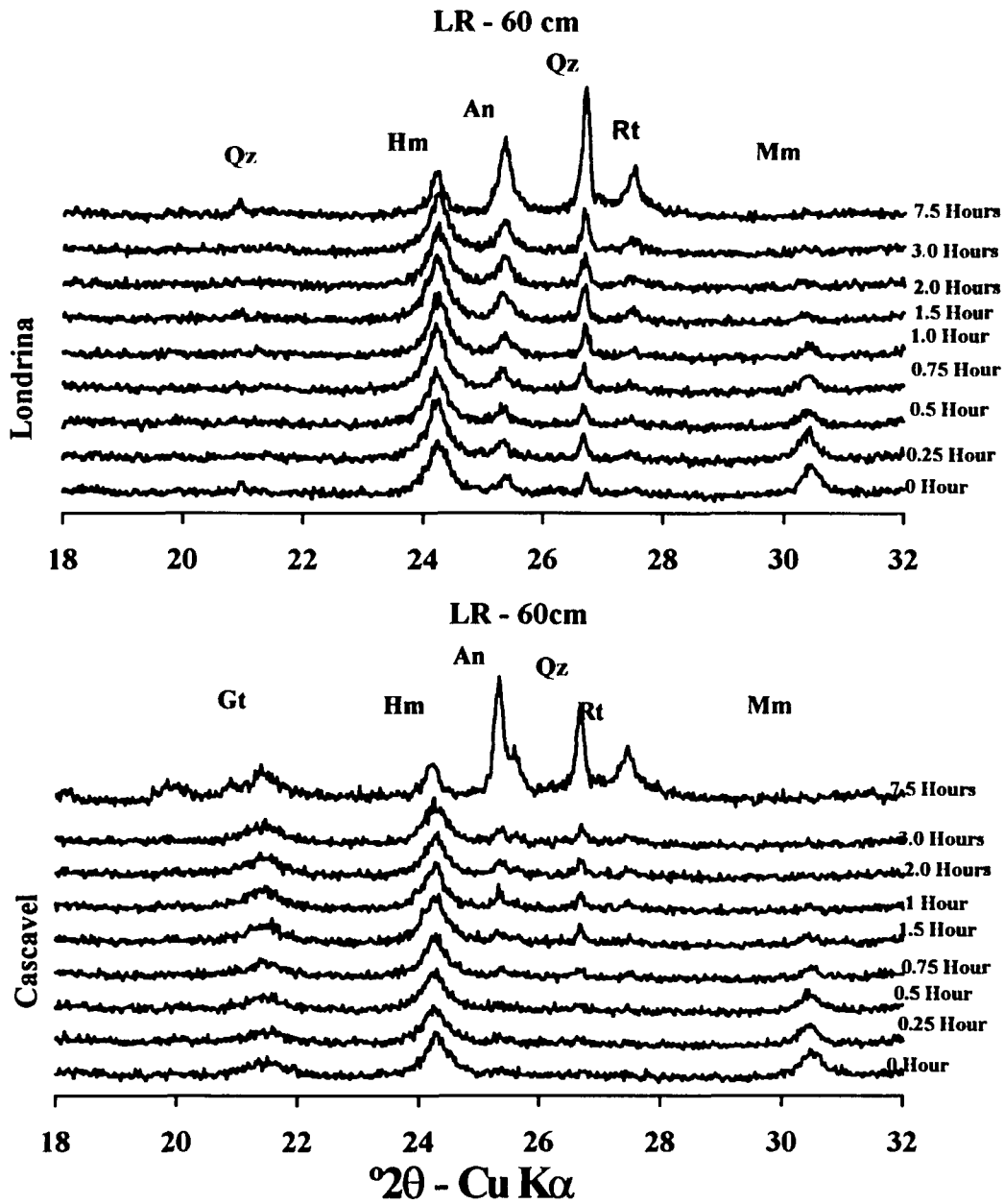


Figure 5.23. Sequential XRD patterns from 5M NaOH residues (LR - Cascavel and LR - Londrina) following exposure to 1.8M H<sub>2</sub>SO<sub>4</sub> (75°C) for up to 7.5 hr.

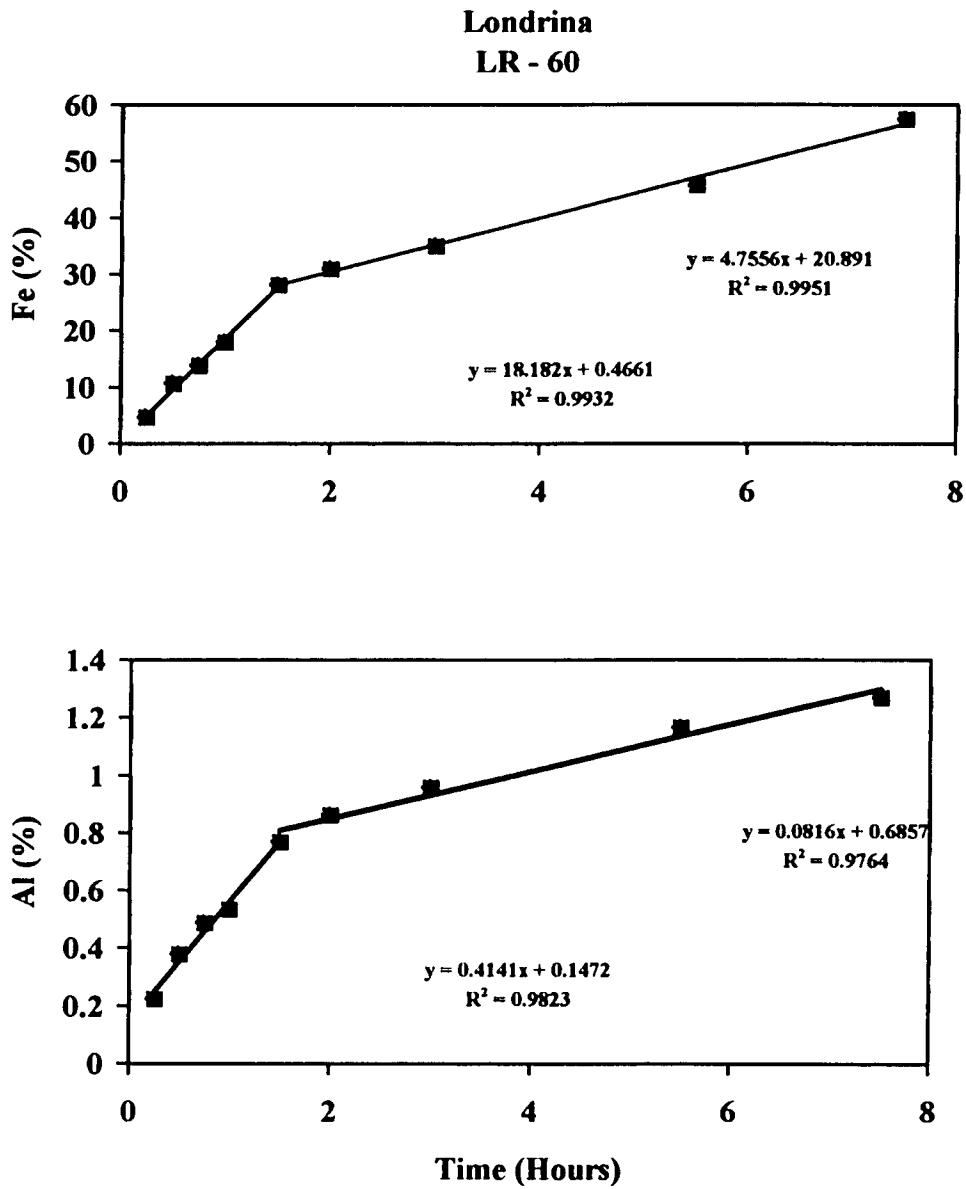
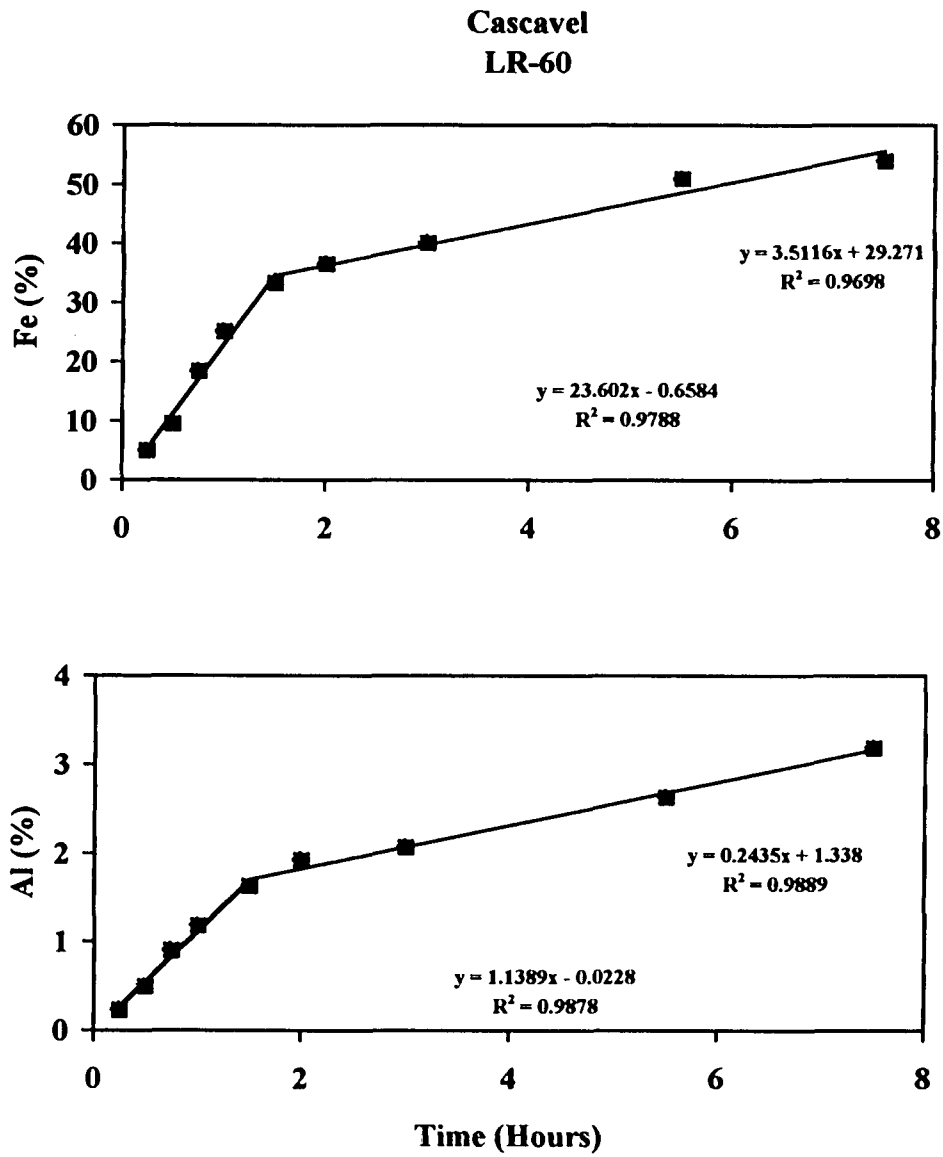


Figure 5.24. Al and Fe in the 1.8M H<sub>2</sub>SO<sub>4</sub> (75°C) extracts expressed as percentages of the CBD-extractable Al and Fe as a function of dissolution time. Londrina.

Figure 5.24. Continued. Cascavel



Prof.#	Soil	Hor.	Goethite		Hematite		Maghemite	
			a	b	b	c	c	d
Al mole %								
Ibiporã								
1	TRe	Ap	15.8	4.1	4.6	7.1	7.5	10.6
		Bt3	28.9	5.6	7.0	8.7	10.2	11.2
		Bt7	nd	5.7	8.8	8.8	12.3	5.2
2	Re	A	18.7	0.9	0.6	3.4	3.1	---
3	BAv	A	14.8	1.9	1.0	4.6	3.6	---
		Bt	21.0	2.4	3.2	5.1	6.1	---
		Cr	21.5	0.9	2.0	3.4	4.7	---
4	LRe	A	20.4	7.5	9.1	10.9	12.5	15.4
		Bw2	22.4	8.2	9.9	11.6	13.5	13.2
Campo Mourão								
5	LRd	A	---	7.4	9.0	10.7	12.5	10.8
		Bw2	---	7.7	9.0	11.0	12.5	10.2
		Bw5	---	7.7	10.1	11.0	13.7	---
7	R	A	39.9	2.9	2.0	5.6	4.7	10.0
Tamarana								
8	Ca	A	23.8	0.5	0.5	3.0	3.0	---
		Bi	22.9	2.2	0.7	4.9	3.3	---
9	TBa	A	14.8	0.1	0.3	2.5	2.8	---
		B	15.7	1.1	1.9	3.7	4.6	---
10	TBa	Bt2	16.8	1.5	1.4	4.2	4.0	---
Cruzmalina								
14	TRd	Bt	20.0	8.8	10.7	12.2	14.4	12.0
15	Rd	Ap	25.8	3.9	4.3	6.8	7.3	10.3
17	LRa	Bw2	26.4	9.2	9.2	12.7	12.7	13.0
Faxinal								
18	LBa	Bw2	24.6	8.5	11.6	11.9	15.4	14.3
20	Rd	A	30.7	3.8	2.3	6.7	5.0	---
21	Re	A	27.1	1.5	2.5	4.2	5.3	13.5

a=Schulze,(1981); b= Schwertmann et al., (1979) ; c= Schwertmann and Lathan (1986); d=Schwertmann and Fechter (1984).

Table 5.13. Mole % Al substitution in goethite, hematite and maghemite determined from XRD peak positions.

Al-substitution in hematite and goethite were determined by shifts in the positions of previously defined peaks following the removal of maghemite (Table 5.13; Fig. 5.25) and by the ratio of Fe and Al released in CBD extracts of the 5M NaOH + 1.8M H<sub>2</sub>SO<sub>4</sub> residues. The d<sub>110</sub> and d<sub>300</sub> peak positions of hematite yielded similar values for Al substitution (Table 5.13); however, the equation derived by Schwertmann et al. (1979) produced lower values compared to those calculated using the equation of Schwertmann and Lathan (1986). Presumably, the differences are related to the fact that the former relationship was derived from natural hematites whereas the latter was obtained using synthetic specimens. Neither equation is as sophisticated as the one derived by Schulze (1982, 1984) for goethite. For example, Schulze (1982, 1984) observed that the particle size of goethite also affected the position of the diffraction peaks and appropriate corrections were considered.

The Al substitutions in hematites from both the toposequence (Table 5.13) and the climosequence clays (Appendix B) were always smaller than those measured for goethite and were within the range usually reported for hematite (0 - 16 mole % Al) (Schwertmann, 1988; Schwertmann and Taylor, 1989). Likewise, the observed range for goethite (0 - 36 mole % Al) was consistent with previous results. The amount of Al substitution calculated from the XRD peak positions of both hematite and goethite also showed a good correlation with the quantities of Al measured in CBD extracts of the 5M NaOH residues following the dissolution of maghemite (Fig. 5.26). The best correlation was observed for hematite because most of the samples were dominated by this mineral, and the presence of small amounts of goethite did not greatly influence the relationship.

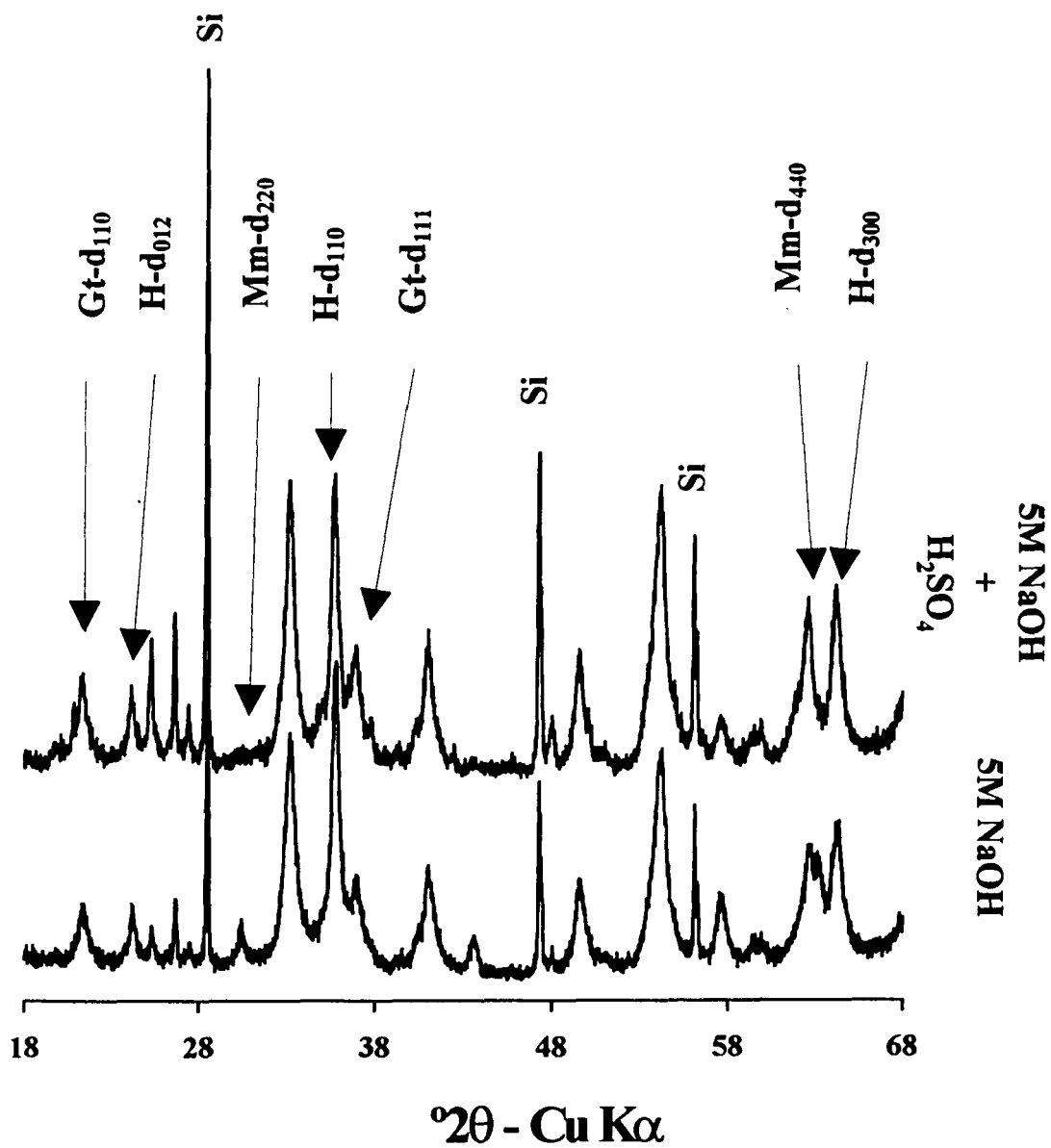


Figure. 5.25. Representative XRD patterns from the 5M NaOH and 5M NaOH plus 1.8M H<sub>2</sub>SO<sub>4</sub> residues (TRd - Cruzmaltina).

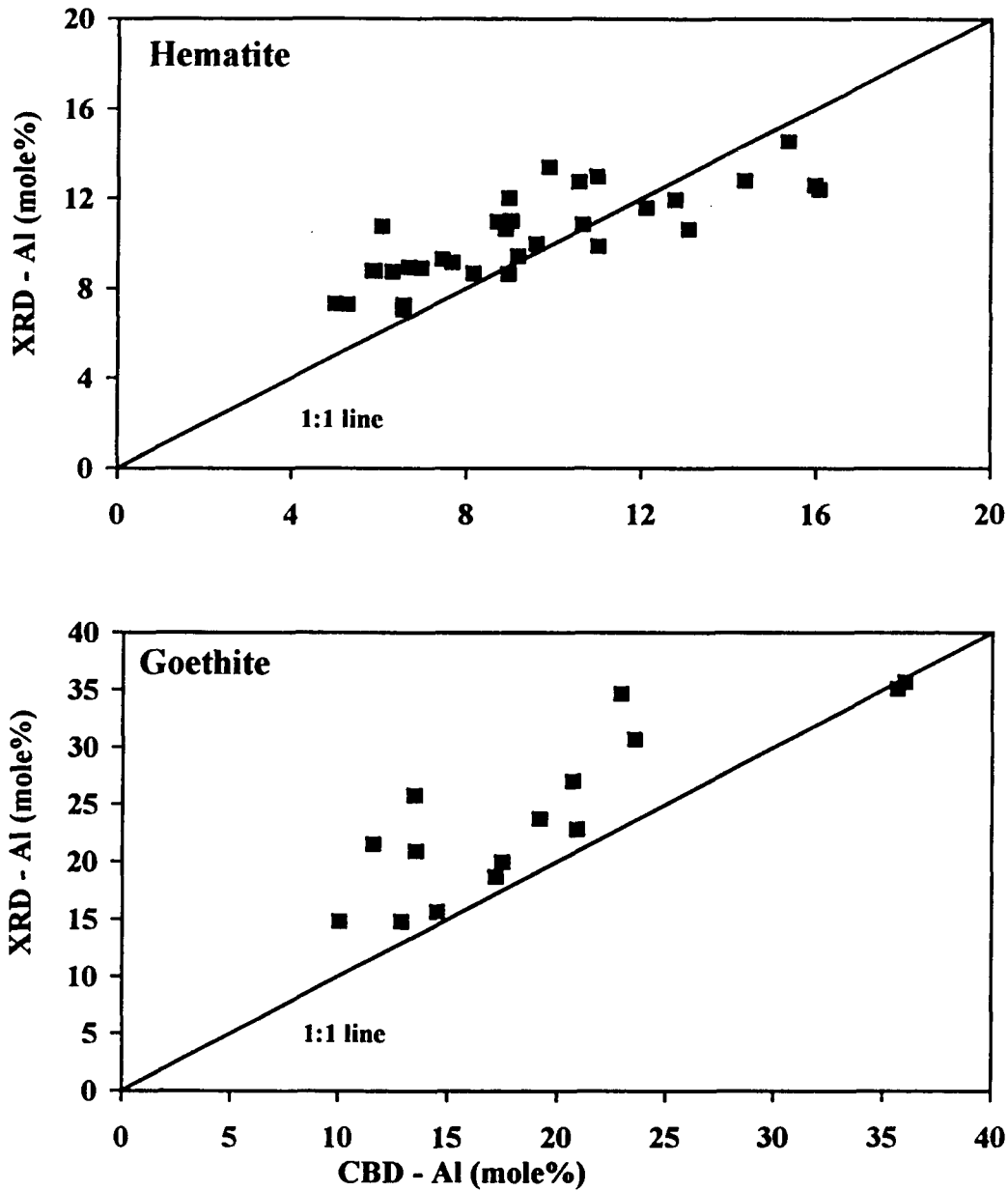


Figure 5.26. Relationship between Al substitution in hematite and goethite measured by XRD vs. selective dissolution using the CBD procedure (maghemite previously removed by dissolution with 1.8M H<sub>2</sub>SO<sub>4</sub>).

On the other hand, the Al mole (%) measured from CBD extracts of the more goethitic samples underestimated the amount of Al substitution because of dilution effects from small but significant amounts of hematite (Table 5.12, Appendix B) in most of the samples. The two points at very high mole % Al that perfectly fit the 1:1 line were from the Latossolo at Guarapuava and Vitória, both of which contained less than 1% hematite (Appendix B). Therefore, chemical dissolution procedures such as the CBD method can be used to quantify the amount of Al substitution within a specific Fe oxide provided the mineral dominates the assemblage of Fe oxides present.

In Oxisols from southern Brazil, goethite has shown Al substitutions in the range of 15 to 36 Al mole (%) while hematite has been observed with 4 to 17 mole % Al (Resende, 1976; Kämpf, 1981; Curi, 1983; Schwertmann and Kämpf, 1985; Palmieri, 1986, Fontes, 1988). In the current study, the highest amounts of Al substitution in hematite were found in the dystrophic and allic soils formed from basalt (Table 5.13). In addition, the Ibiporã toposequence showed a clear increase in the Al substitution of hematite as weathering intensity increased from the young Re and BAv profiles to the highly weathered TRe and LRe. Interestingly, the lowest Al substitutions were observed in those hematites extracted from the acid / intermediate rock soils at Tamarana. The composition of goethite seemed to be less sensitive to soil chemistry and stage of weathering. Even the immature Solos Litólicos profiles yielded goethites with Al substitutions comparable to those observed in the most highly weathered soils.

The degree of Al substitution in the soil maghemites, as calculated by XRD (Table 5.13), ranged from 5 to 16 mole % and did not show any relationship with degree

of weathering or parent rock material. Fontes (1988) calculated the Al substitution in soil maghemites by DXRD and obtained values in the range of 26.1 to 16.4 mole % for four Latossolo derived from basic volcanic rocks. Fontes (1988) also observed that soils derived from sedimentary and metamorphic rocks did not yield detectable XRD peaks for maghemite. The amount of Al dissolved in sulfuric acid extracts of the 5M NaOH residues showed no correlation with the amount of Al substitution calculated by XRD (Fig. 5.27). In general, Al in the sulfuric acid extracts tended to be much higher than would be predicted from XRD results (up to 40 mole % Al). This is probably due to the release of Al from other sources rather than maghemite, such as residual 2:1 phyllosilicates. Additional efforts to properly determine the extent of Al substitution in these maghemites are warranted because the mineral comprises up to 50% of the Fe oxides in some samples, and its importance to physical (aggregation) and chemical (phosphorus retention) properties of soils developed on volcanic rocks has largely been overlooked. Considering all toposequence samples and all Fe oxides, the correlation between soil pH and degree of Al substitution was weak (Fig. 5.28). This reflects not only the diversity of soil conditions but also the buffering capacity of the system which generally does not permit the pH of the soil to drop below pH 3.5 to 4. Slightly better relationships were observed between Al substitution and the percentage of gibbsite present in the clay fraction (Fig. 5.29). The degree of Al substitution in hematite presented the best correlation with the percentage of gibbsite, probably because most of the samples were dominated by this Fe-oxide. Better relationships for maghemite and goethite might be found in a more diverse set of soil samples.

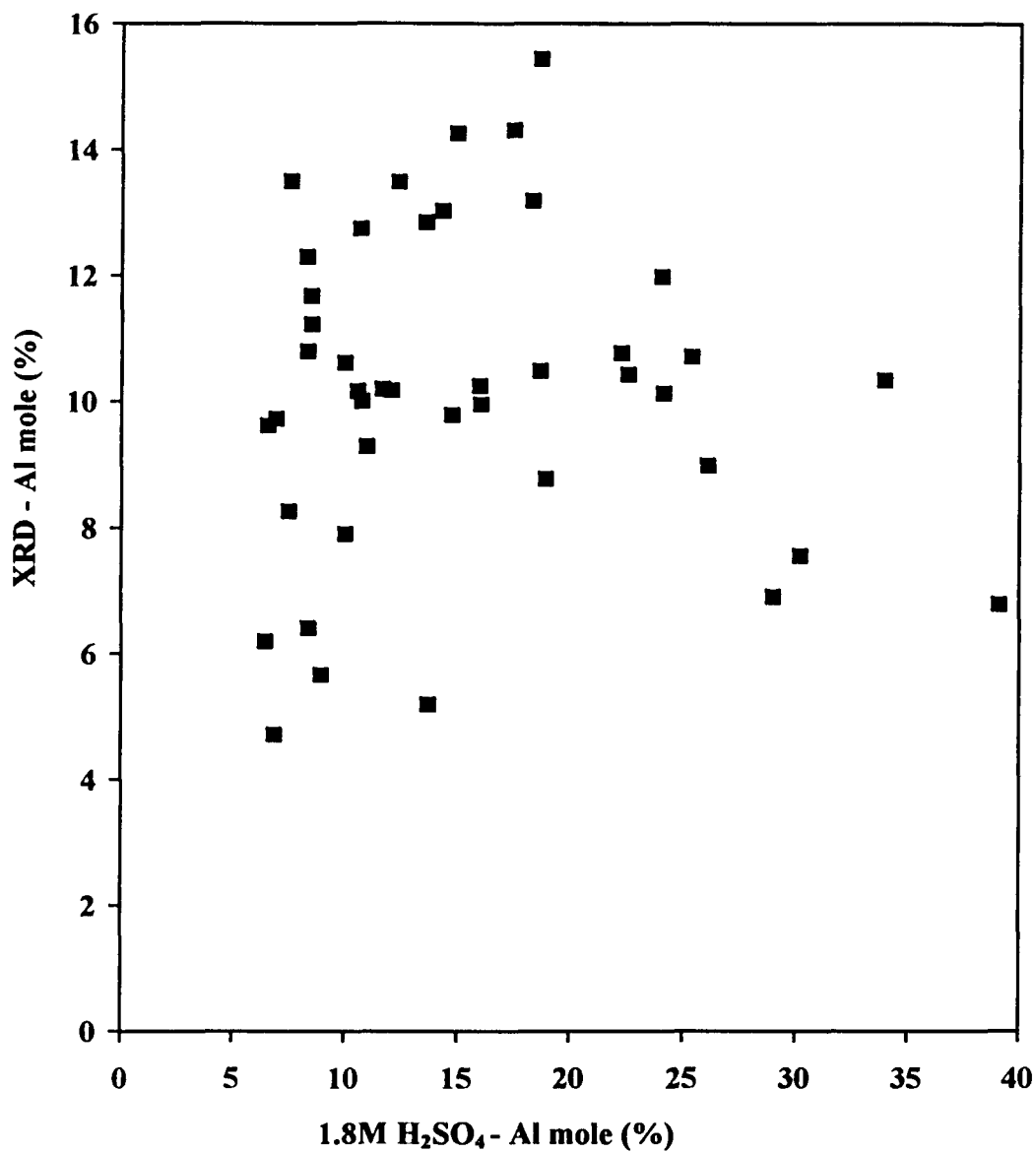


Figure 5.27. Relationship between Al substitution in maghemite measured by XRD peak area vs. extraction with 1.8M H<sub>2</sub>SO<sub>4</sub>.

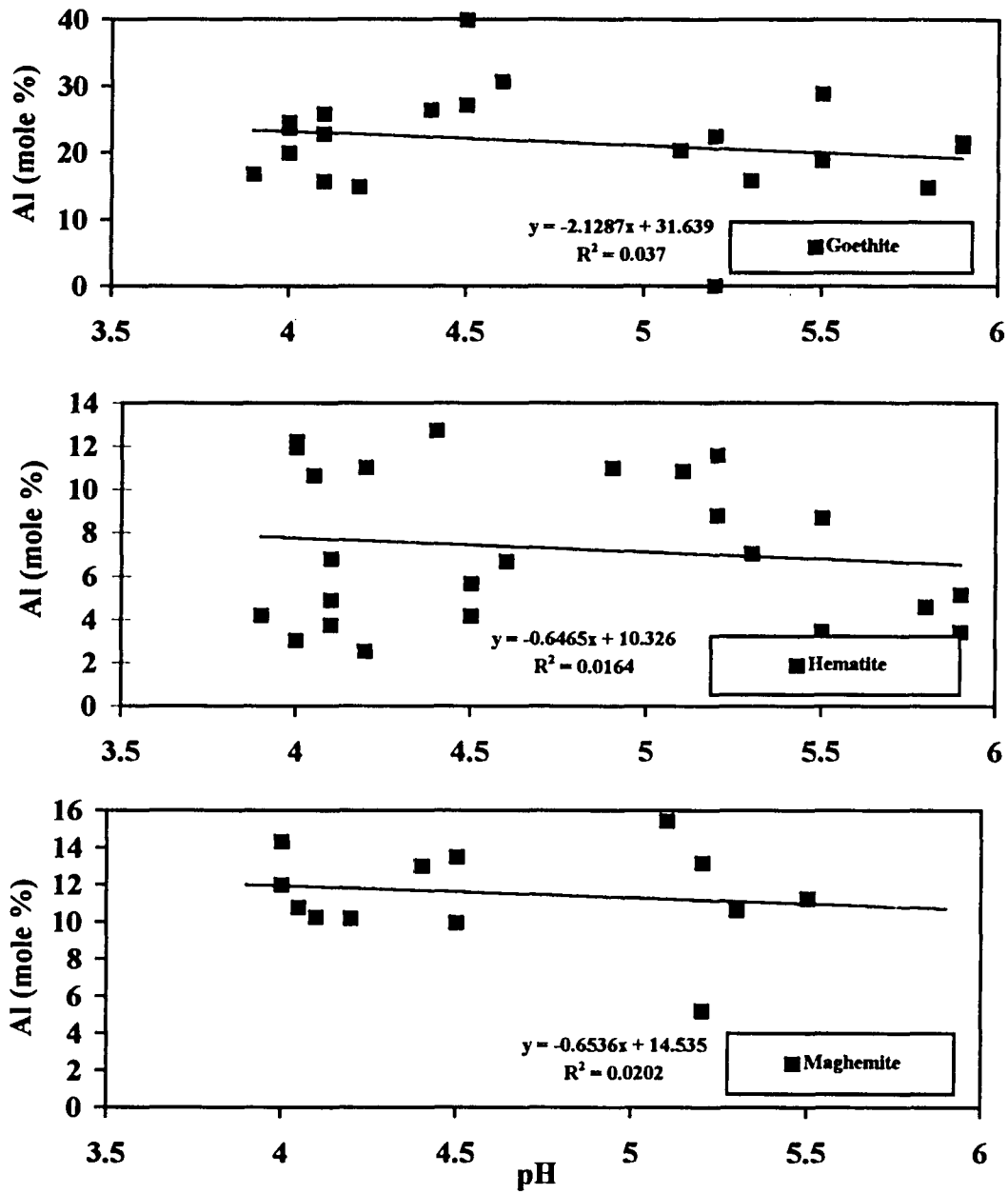


Figure 5.28. Relationship between soil pH (CaCl<sub>2</sub>) and Al substitution in soil hematites, goethites, and maghemites measured by XRD.

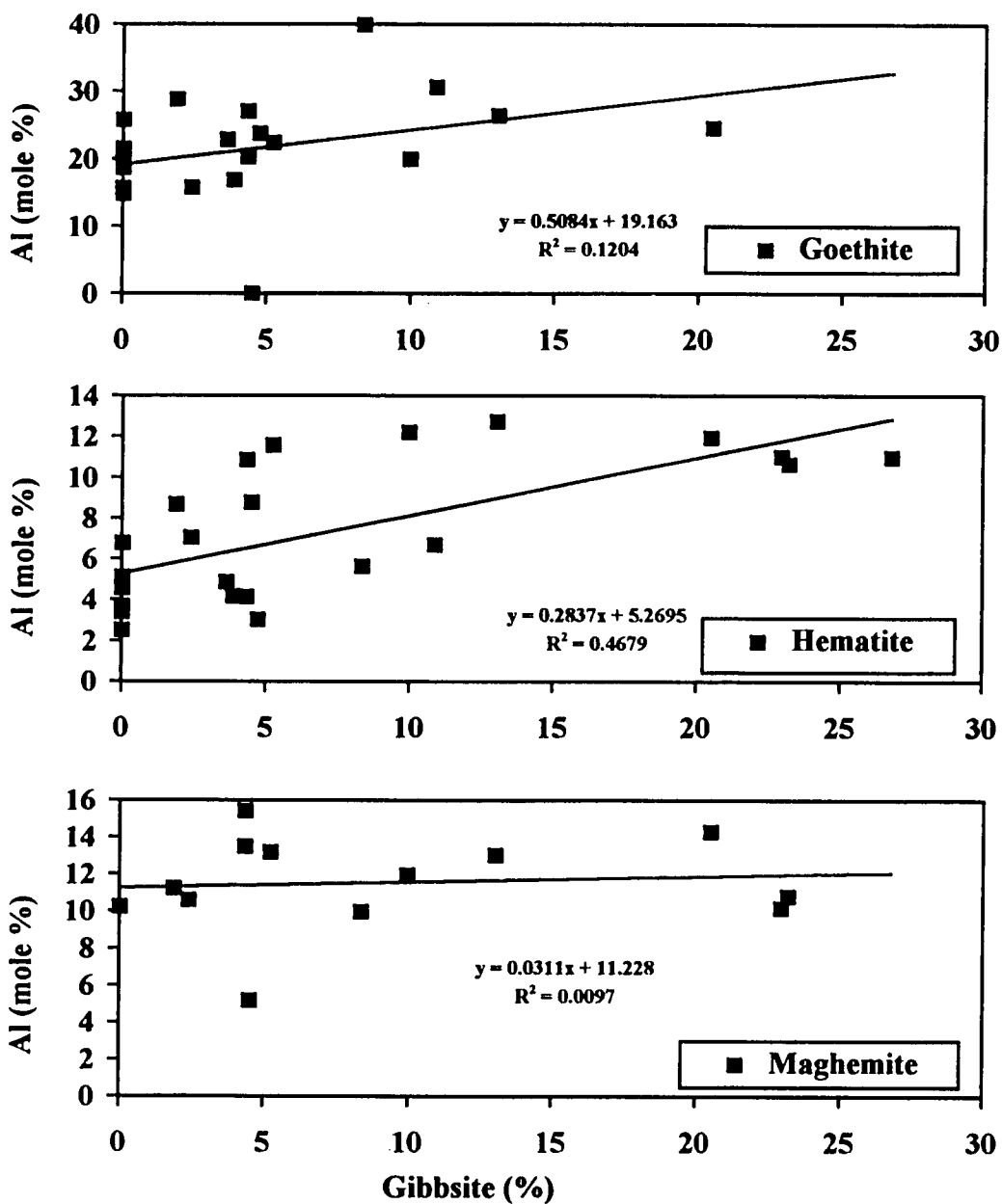


Figure 5.29. Relationship between % gibbsite and Al substitution in soil hematites, goethites, and maghemites measured by XRD peak area.

#### **5.4.7. The influence of lithology on iron oxide mineralogy**

The various factors of soil formation (parent material, time, organisms, topography, and climate) may each have a distinct influence on mineral weathering or genesis. Previous attempts to evaluate the formation of Fe oxides in soils of the Paraná River Basin have usually not isolated the effects of specific factors or processes of soil formation. These studies have also focused almost entirely on the hematite-goethite pair. In the present investigation, the influence of lithology can be evaluated by examining the Fe oxide mineralogy of the most highly weathered soils where the impacts of time, topography, vegetation and climate have been restricted.

In these soils (LR-LB-TR-TB) there is a strong correlation between the ratio of hematite to goethite ( $Hm/Hm + Gt$ ) and parent material as represented by the  $SiO_2$  content of the volcanic rocks (Fig. 5.30). In fact, the data form two mutually exclusive sets. Soils developed from basic rocks yielded  $Hm/Hm + Gt$  ratios ranging between 0.6 and 1.0, whereas those soils formed from acid / intermediate rocks always produced a lower ratio (0 to 0.6). Clays containing no XRD-detectable goethite were separated from Latossolo Roxo formed from basalt at Maringá, Campo Mourão, Juranda, Londrina, São Miguel do Iguaçu, and Palotina (Table 5.12, Appendix B). Well drained soils devoid of goethite have never previously been reported.

Earlier studies have suggested strong correlations between hematite-goethite ratios and both soil pH and total C content; however, these investigations involved soils of varying age, parent material and climatic regime (Kämpf and Schwertmann, 1983; Palmieri, 1986).

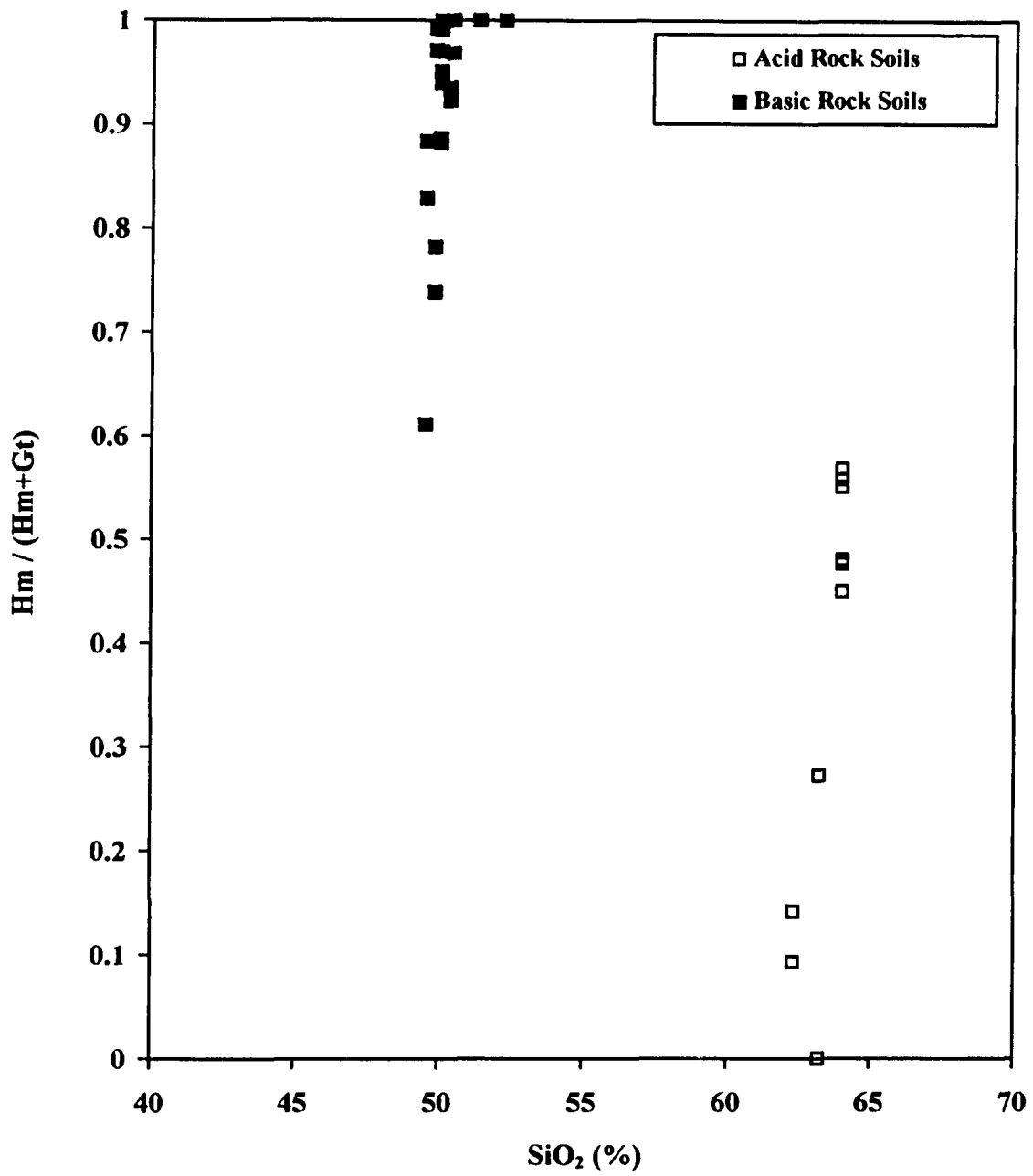


Figure 5.30. Relationship between  $Hm/(Hm+Gt)$  ratios and %  $SiO_2$  in the parent rock material.

In the present case, the proportion of hematite tended to decrease with decreasing pH in soils formed from basic rocks but showed the opposite trend in soils derived from acid / intermediate rocks (Fig. 5.31). No relationship appeared to exist between hematite-goethite ratios and soil carbon (Fig. 5.32).

Maghemite, as determined by XRD, was strongly co-associated with hematite in the basic rock soils, but was virtually absent in those soils derived from acid / intermediate parent materials (Fig. 5.33). The small quantities of maghemite found in clays from the acid / intermediate rock soils may be a product of the burning of vegetation at or near the soil surface (observed in the Ca profile from Tamarana - Appendix A). Burning in the presence of organic matter causes a partial reduction of the Fe in hematite and goethite, thereby producing maghemite (Schwertmann, 1985; Dearing, 1994).

The much stronger link between maghemite and the basic rock soils presumably involves the presence of primary magnetite in the basalts (Coey, 1985). During weathering, the Fe in magnetite may be partially or fully oxidized, thereby forming maghemite (Schwertmann and Taylor, 1989). Recent studies have also suggested that some basalts may contain primary maghemite (Sternthorsson et al., 1992; Helgason et al., 1994; Fabris et al., 1995). Therefore, soils derived from these type of rocks will almost always exhibit a significant magnetic susceptibility unless drainage conditions promote the dissolution of maghemite (and hematite) and lead to the formation of goethite (and/or lepidocrocite) as observed by Curi (1983) in a toposequence of soils developed on basalt in Minas Gerais, Brazil and by Bryant (1981) cited by Cury (1983) in Indiana, US.

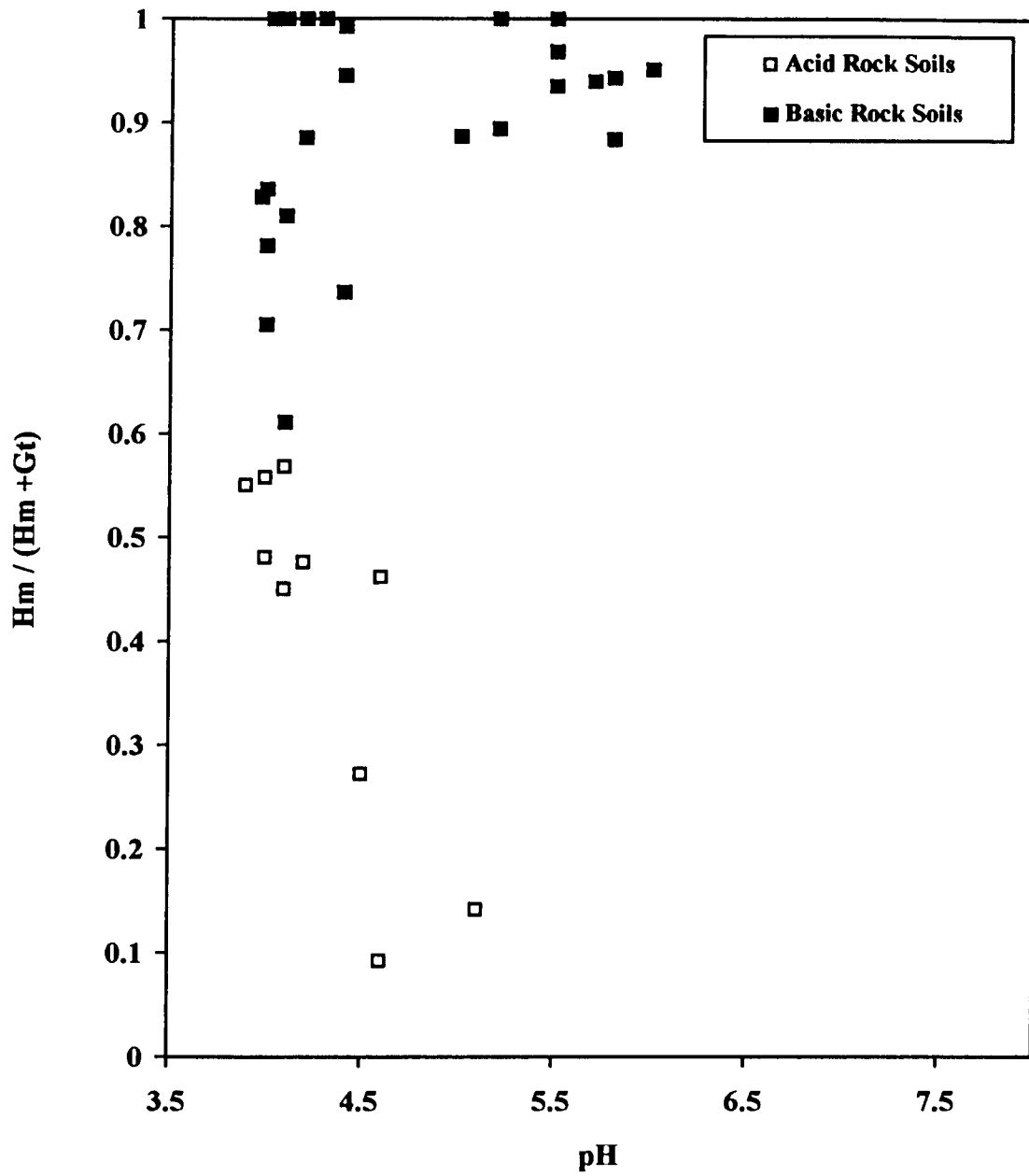


Figure 5.31. Relationship between soil pH and Hm/(Hm+Gt) ratios for the highly weathered soils (LR-LB-TR-TB).

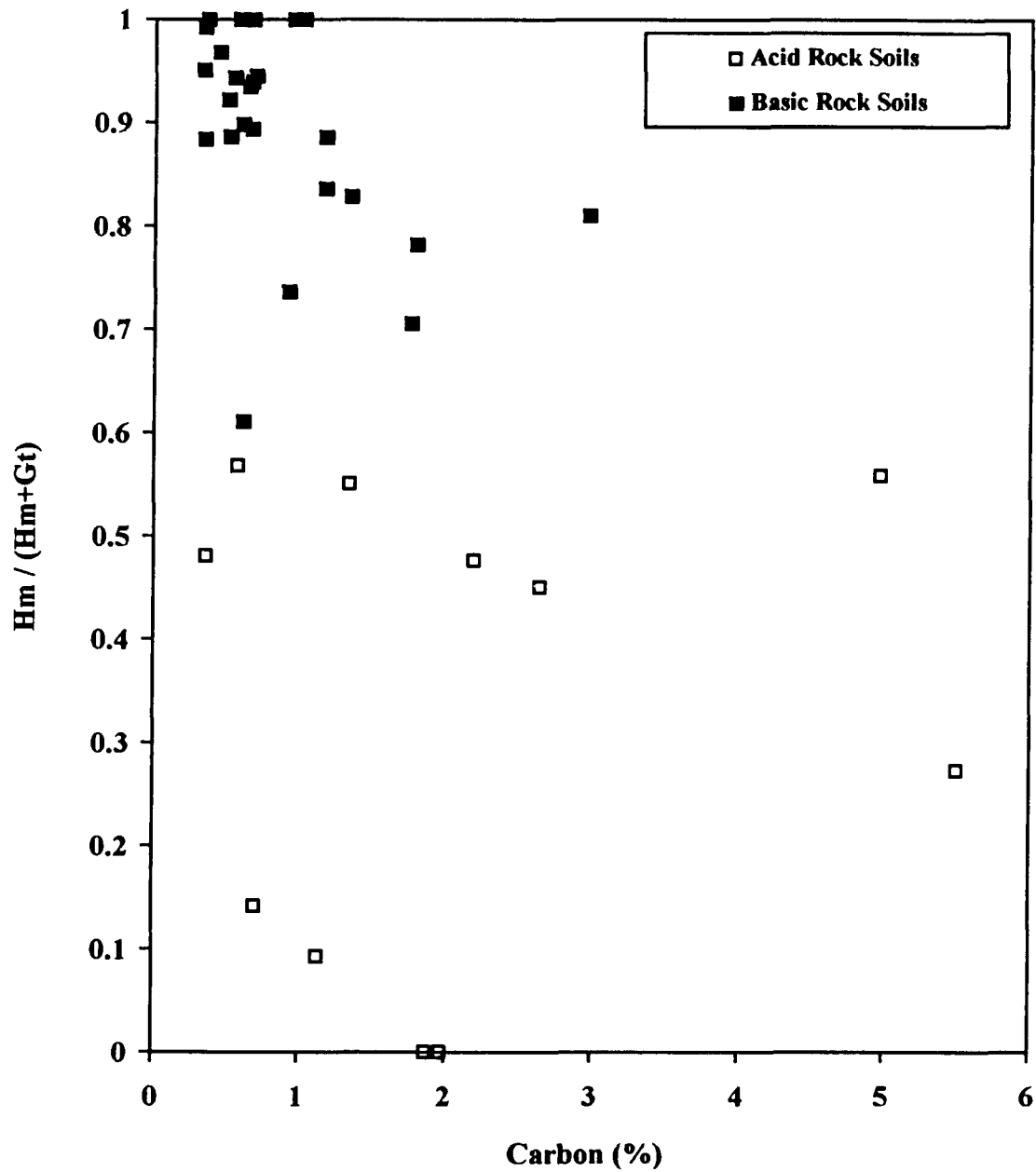


Figure 5.32. Relationship between soil carbon content and Hm/(Hm+Gt) ratios for the highly weathered soils (LR-LB-TR-TB).

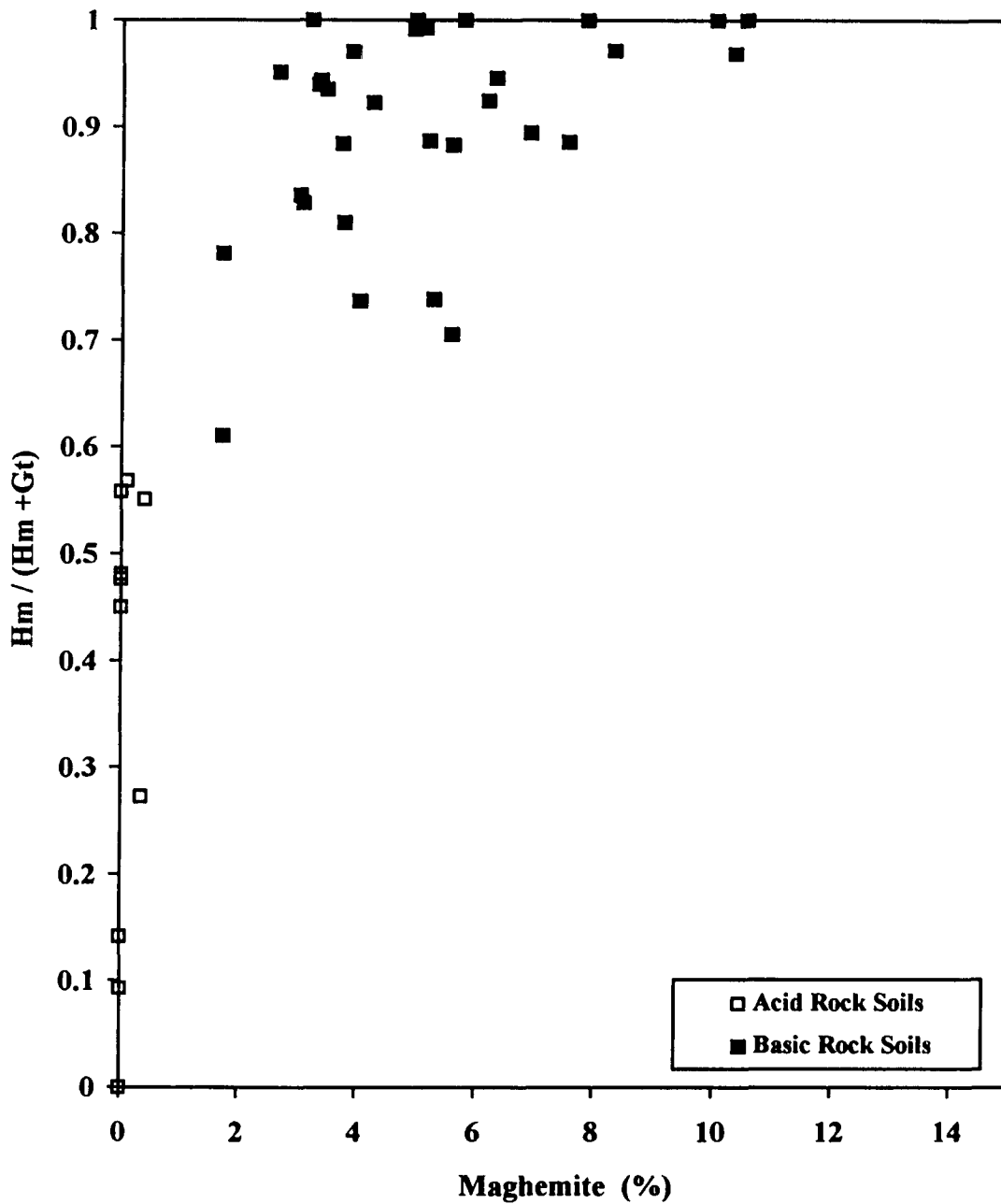


Figure 5.33. Relationship between  $Hm/(Hm+Gt)$  ratios and % maghemite in the highly weathered soils (LR-LB-TR-TB).

The parent rock material seems not to affect the amount of Al substitution within hematite, goethite or maghemite in the most highly weathered profiles (Fig. 5.34). The factors controlling the degree of Al-substitution within hematite and goethite are related to the chemistry of the soil solution, including oxidation - reduction conditions. As noted previously, the most highly weathered soils (LRd, LBa, TRd, TBa) presented the highest amount of Al substitution in the Fe oxides, whereas the eutrophic soils (Ibiporã toposequence), especially those with minimal water deficits (BAv, Re), all had lower degrees of replacement.

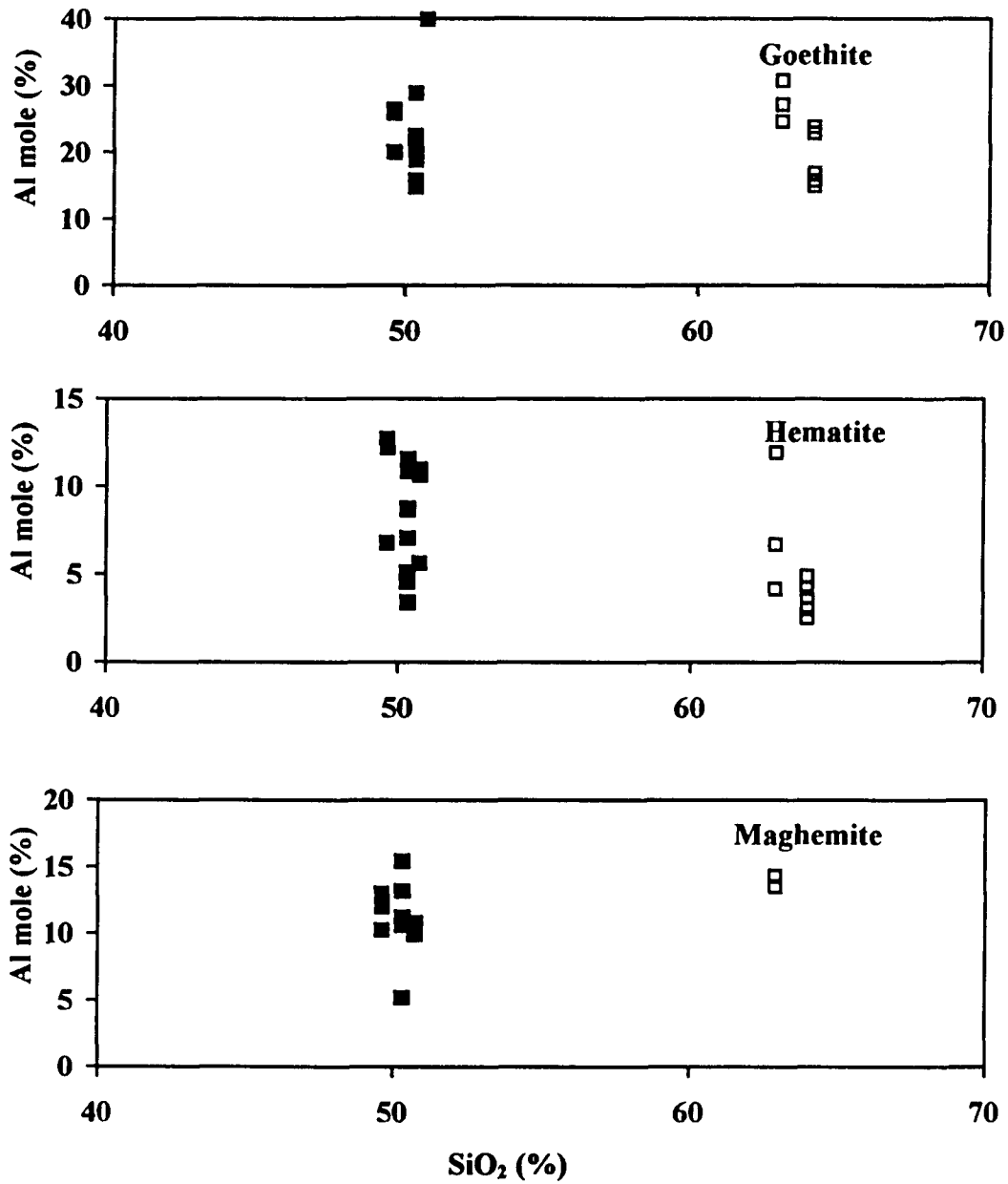


Figure 5.34. Relationship between Al-substitution in goethite, hematite and maghemite in the highly weathered soils (LR-LB-TR-TB) and  $\text{SiO}_2$  content of the parent rocks.

#### **5.4.8. Iron oxides and degree of soil weathering (Basalt soils)**

In the early stages of basalt weathering the saprolite is usually yellowish in color (10 YR to 7.5 YR), and the Fe-oxide fraction is dominated by goethite with high Al substitution (Kämpf and Schwertmann, 1995). As weathering continues, both laterally and with depth, goethite becomes less dominant and is replaced by hematite and maghemite. Thus, transformations of yellow saprolites to red sola have been observed in basalt weathering profiles from all over the world (Schwertmann, 1993) with transition zones ranging in thickness from a few millimeters to meters. Solid state conversions of goethite to hematite under ambient conditions have never been confirmed. Therefore, the observed color (mineralogical) transformations must involve either dilution effects (initial formation of goethite followed by overwhelming accumulation of hematite and maghemite) or the conversion of goethite to hematite via solution processes. Dilution effects could explain the small percentages of goethite present in most of the highly weathered materials examined in the current study, but some of the samples (Table 5.12 and Appendix B) exhibit no XRD detectable goethite. This result suggests that transformations of goethite to hematite via solution must also occur in some cases. Under laboratory conditions, the dissolution of goethite yields ferrihydrite as small rounded particles that coalesce, rearrange and dehydrate to form hematite (Schwertmann and Taylor, 1985; Johnson and Lewis, 1983). The transformation of ferrihydrite to hematite must be rapid because hematite and ferrihydrite have never been detected as co-associated minerals in soils.

Schwertmann (1985) observed that the formation of hematite and goethite are competitive processes wherein high rates of Fe release, neutral to slightly alkaline pH, elevated temperature, and low contents of organic matter and soil moisture favor the production of hematite over goethite. Conversely, laboratory synthesis studies have shown that the presence of dissolved organics, soluble Si, slow release of Fe (Schwertmann, 1985), high water activity (Torrent et al., 1982) and the presence of Na and K in solution (Torrent and Guzman, 1982) favor the formation of goethite over hematite. Most of the latter conditions might be found in the early stages of basalt weathering if plagioclase feldspars are the primary targets of weathering and there is a steady supply of water from base flow (Moniz et al., 1982; Moniz and Buol 1982). As the leaching of Si, Na, and K continues and ferromagnesian silicates begin to decompose, hematite should become the most stable Fe oxide phase. In acid / intermediate rocks dominated by Na, K and low Fe-content minerals (Table 5.1), the rock geochemistry would presumably favor goethite formation. This is especially true in the current study because such rocks occur at higher altitudes where high precipitation and low evapotranspiration rates (Bellieni et al., 1984a, 1984b) favor the accumulation of organic matter (Kämpf, 1981; Palmieri, 1986, Clemente, 1988). This combination of factors should facilitate not only the early formation of goethite but also its dominance throughout the weathering process.

On a landscape scale, the degree of soil weathering is also heavily influenced by time and topographic factors. The soils formed on different landscape positions reflect the combined effects of these factors in terms of both their clay (section 5.3) and Fe oxide

mineralogy (Rauen, 1980; Resende, 1976; Curi, 1983; Clemente, 1988). Whereas soil pH and carbon content had no significant correlation with the distribution of hematite and goethite in the most highly weathered soils (section 5.4.7), the same was not true when the parent rock effect was removed and the full range of basalt soils was examined. Compared to the most highly weathered soils (LR -TR), the younger profiles (BAv - R) exhibited a similar pH range and a slightly higher range of organic C contents (Figs. 5.35 and 5.36). However, the Hm/Hm + Gt ratios in the latter were significantly lower and were similar in magnitude (0 to 0.8) to those observed for the highly weathered soils derived from acid / intermediate volcanic rocks (Figs. 5.31 and 5.32). The more goethitic character of the immature soils derived from basalt reflects not only the earlier stages of weathering (high Si, Na, and K release from the parent rock) but also other environmental factors (e.g., excess water due to lateral flow) that favor the formation of goethite over hematite. Rauen (1980) observed similar variations in the Fe oxide mineralogy of a toposequence of basalt soils in the northern region of Paraná.

Maghemite presented a strong correlation with the % gibbsite in those soils derived from basalt (Fig. 5.37). This does not mean that gibbsite and maghemite formation are somehow related, but it does indicate that maghemite (like gibbsite) accumulates as weathering progresses. As noted previously, the most likely source of maghemite in these soils is the oxidation of magnetite which would tend to accumulate as less resistant minerals (e.g., feldspars) are removed via solution.

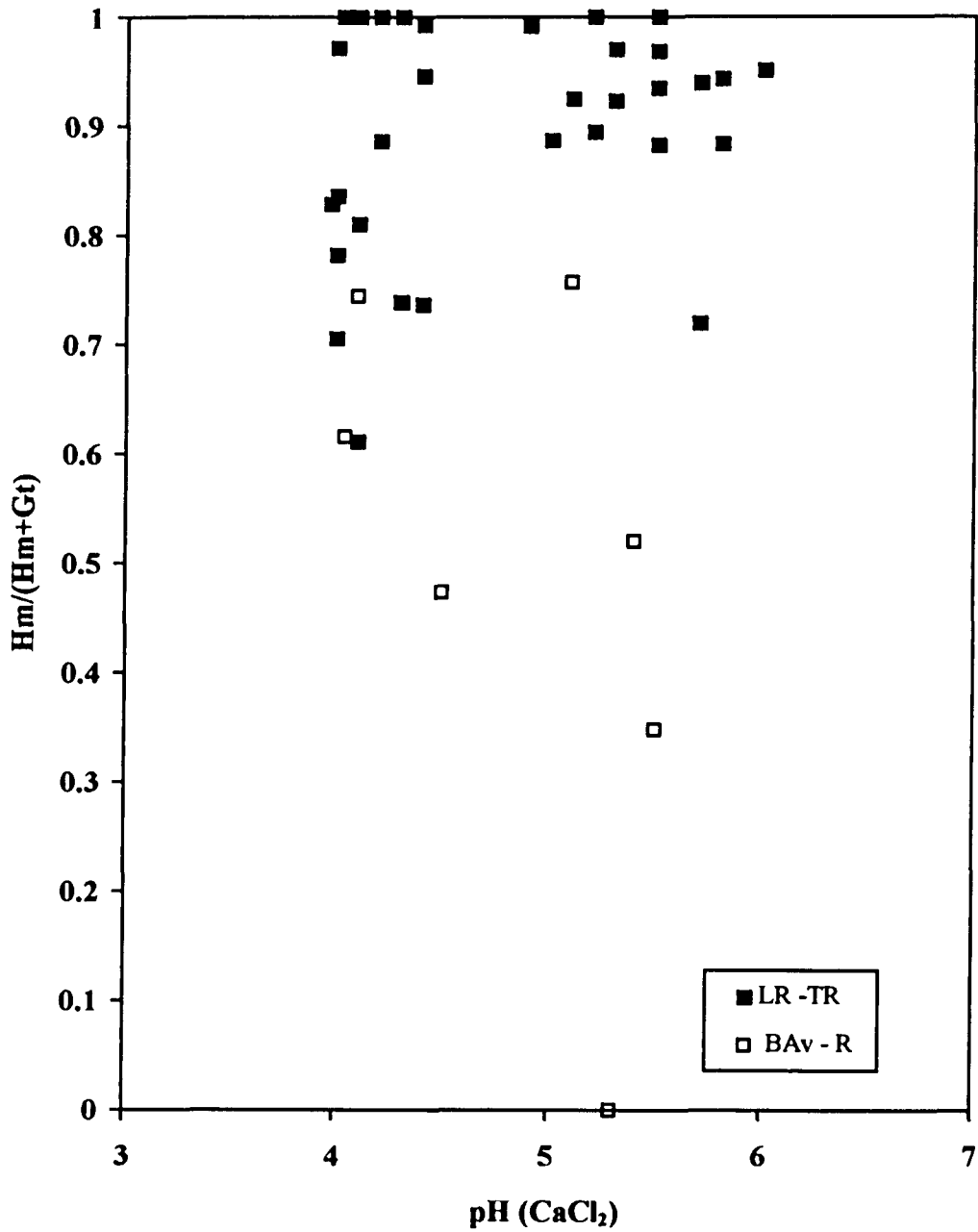


Figure 5.35. Relationship between soil pH and the Hm/(Hm+Gt) ratios of both the highly weathered (LR-TR) and the less weathered soils (BAv-R) derived from basic rocks.

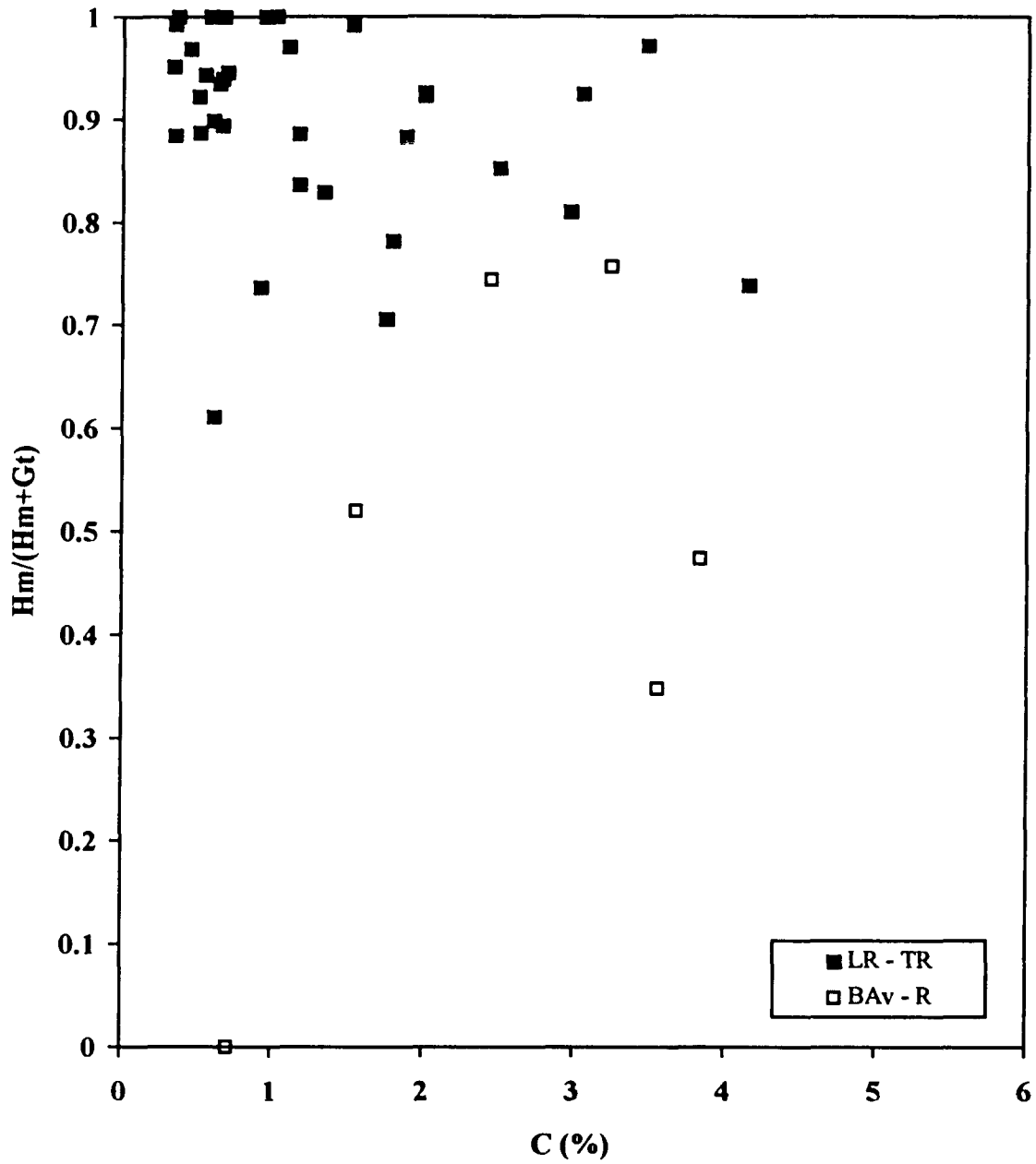


Figure 5.36. Relationship between total C and the Hm/(Hm+Gt) ratios of both the highly weathered (LR-TR) and the less weathered soils (BAv-R) derived from basic rocks.

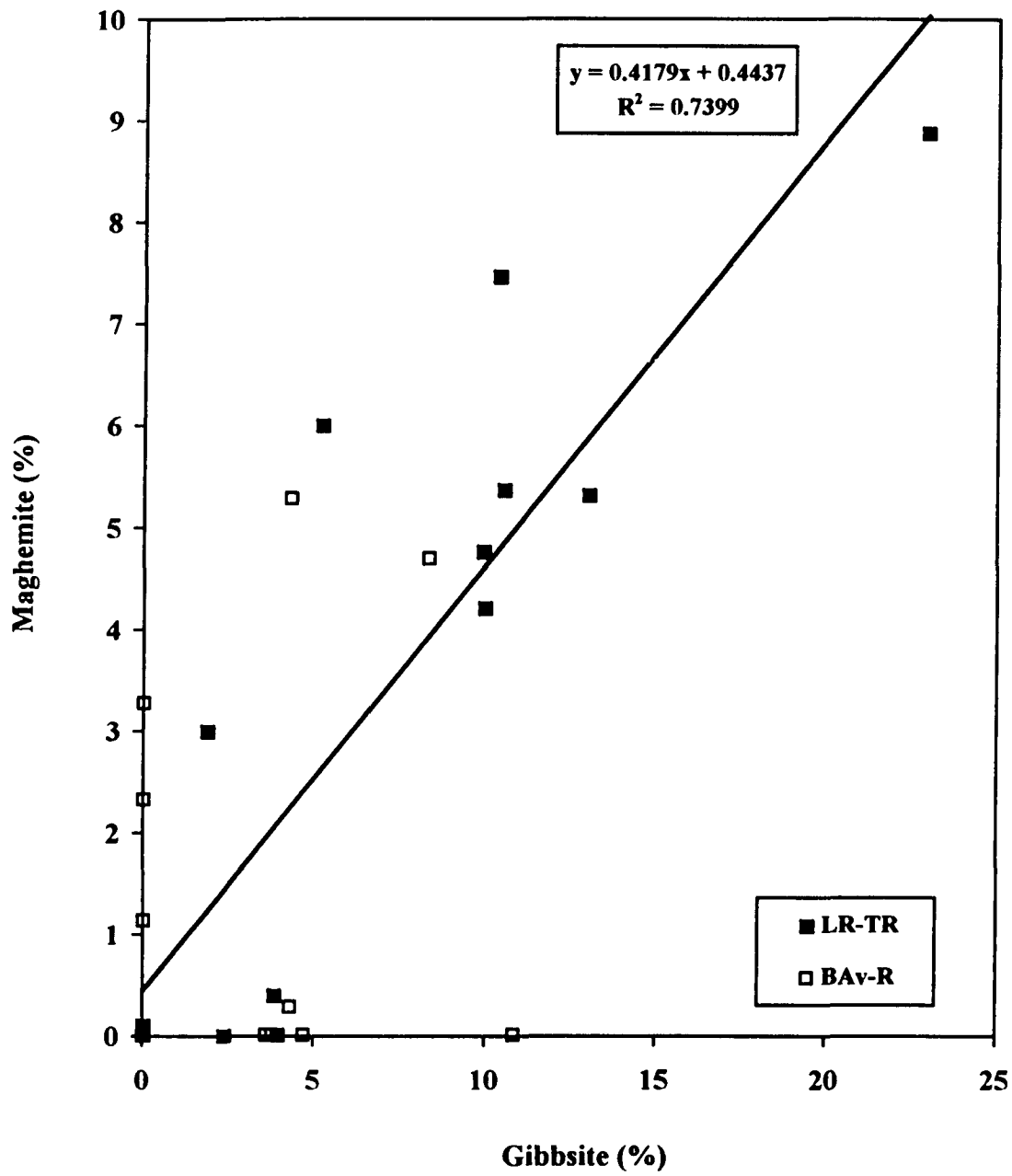


Figure 5.37. Relationship between gibbsite and maghemite contents in clays from the basalt soils.

#### **5.4.9. The influence of climate on iron oxide mineralogy**

The influence of climatic factors on the formation and distribution of Fe oxides (hematite and goethite) in soils of the Paraná River Basin has been the subject of at least two prior studies (Kämpf and Schwertmann, 1983; Palmieri, 1986). In both cases, it was concluded that goethite formation is strongly favored in soils developing under climatic regimes involving low temperature, high precipitation, and associated high organic matter contents; however, both studies involved altitudinal climosequences that included soils with varying degrees of development (e.g., Cambissolo, Vertissolo, and Brunizem Avermelhado vs. Terra Roxa and Latossolo). As noted in section 5.4.8, the degree or stage of weathering can have important influences on the observed proportions of hematite and goethite in soils of this region.

The two earlier studies also compared soils weathered from acid / intermediate volcanic rocks at high altitudes (low temperature, high precipitation, high soil organic C content) with soils formed from basic volcanic rocks at low elevations (higher temperature, lower precipitation and soil organic C content). Therefore, it appears that yet another confounding factor was introduced into the “climosequences” of soils investigated. For example, if one compares the reported Hm/(Hm+Gt) ratios in only the most highly weathered soils (Latossolo) studied by Kämpf (1981) and Palmieri (1986), it appears that the ratio is clearly influenced by mean annual temperature with goethite being heavily favored at lower temperatures (Fig. 5.38). In fact, those data points from Palmieri (1986) in which goethite is the dominant Fe oxide were derived from a Latossolo Bruno found in a region where acid / intermediate parent rocks have now been recognized

(Bellieni et al., 1986a, 1986b; Piccirillo, 1988). As shown in section 5.4.7, goethite formation is naturally favored by the geochemistry of the acid / intermediate volcanic rocks found in this region.

In the present study, it was possible to better isolate the effects of climate on Fe-oxide genesis by focusing on well drained, highly weathered soils (Latosolo) derived only from basalt (Table 5.12, Appendix B). The results indicate that neither temperature (Fig. 5.39) nor excess water ( $P-ET_p$ ) (Fig. 5.40) have affected the distribution of hematite and goethite to the extent previously suggested, nevertheless the data are consistent with the earlier results of Kämpf (1981), Palmieri (1986), and Fontes (1988) (Fig. 5.38) if only the Latosolo Roxo (basalt soils) are considered.

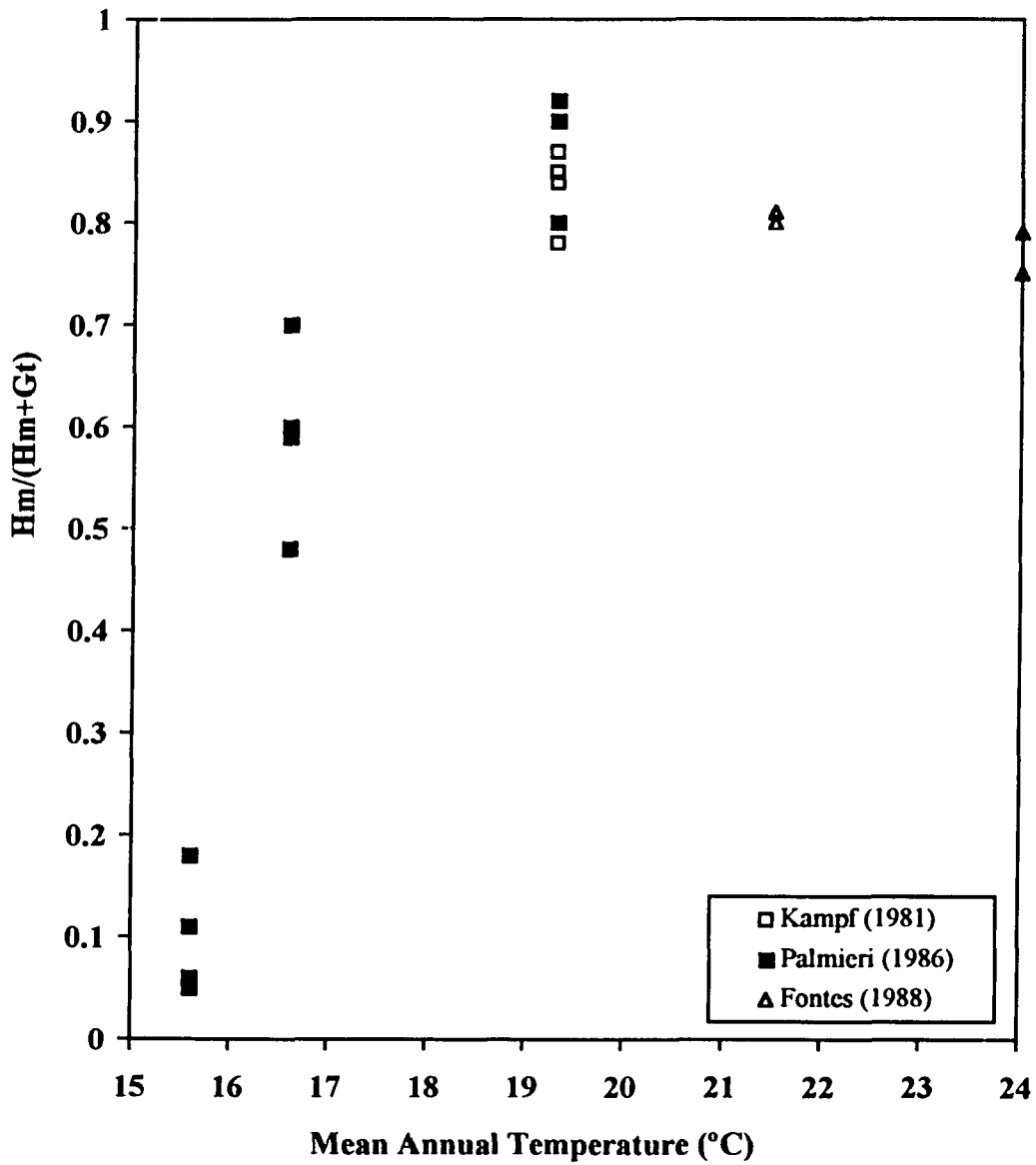


Figure 5.38. Relationship between mean annual temperature and the Hm/(Hm+Gt) ratios of Latossolo investigated by Kämpf (1981), Palmieri (1986) and Fontes (1988).

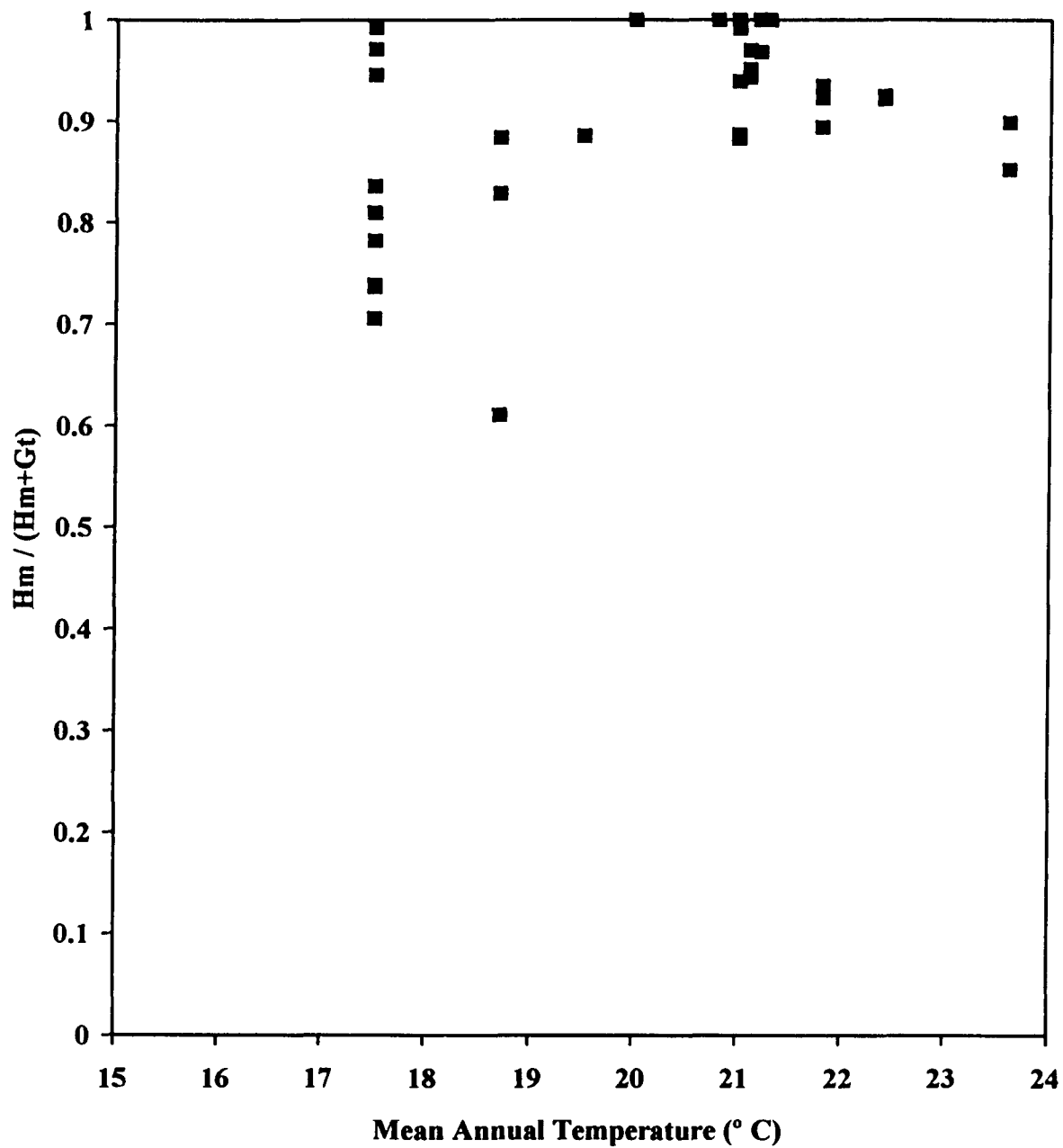


Figure 5.39. Relationship between mean annual temperature and the Hm/(Hm+Gt) ratios of Latossolo Roxo derived from basalt.

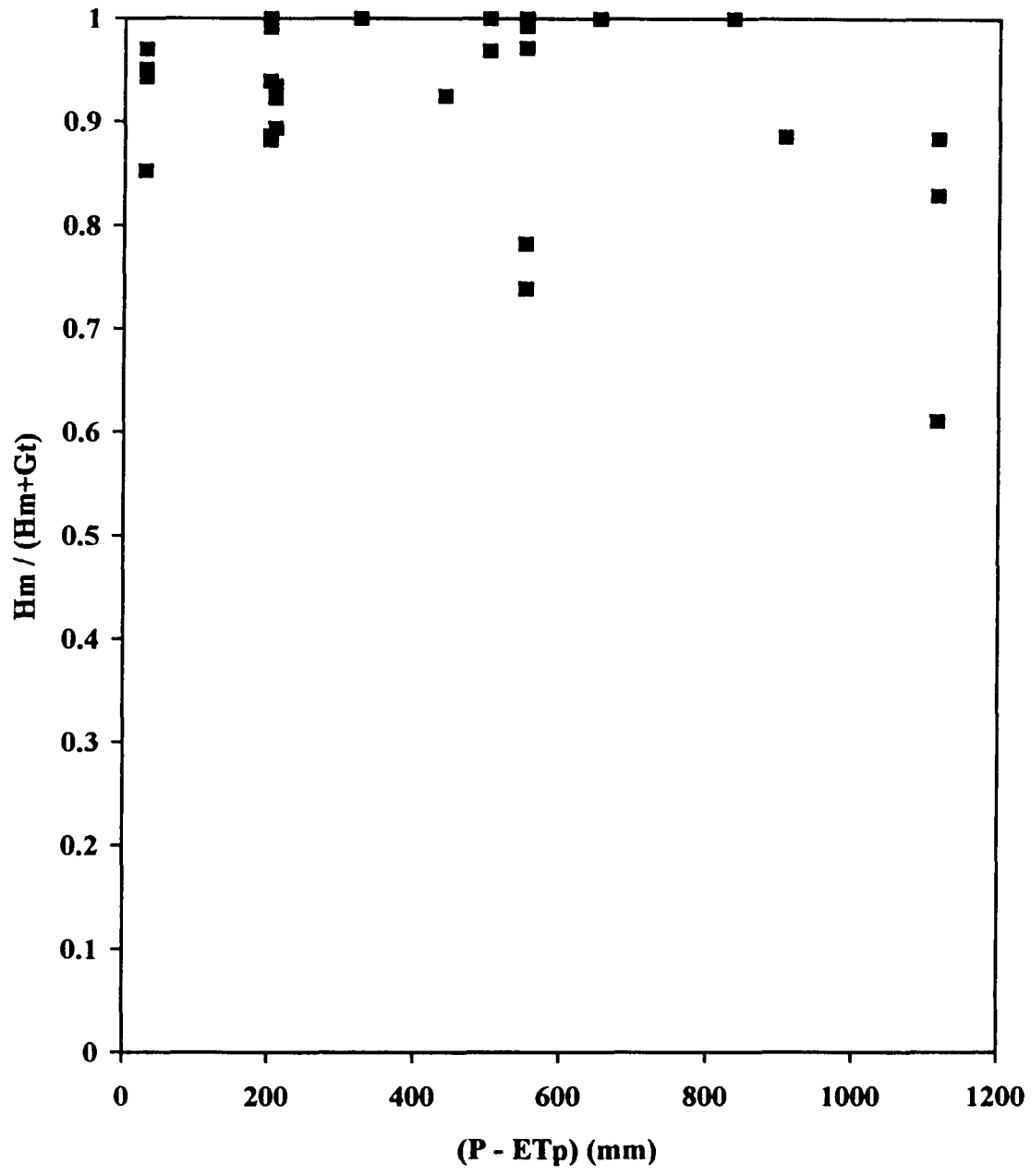


Figure 5.40. Relationship between excess water (P-ETp) and the Hm/(Hm+Gt) ratios of Latossolo Roxo derived from basalt.

## Chapter 6

### CONCLUSIONS

The effects of various soil forming factors on the genesis and profile distribution of Fe oxides and clay minerals in soils developed from volcanic rocks in the Paraná River Basin were investigated. In most cases, unweathered specimens of the parent rock materials were collected with the soil samples. The rock specimens were then ground and analyzed for mineralogy and total chemical composition. The results were used to classify the rocks according to the system of De La Roche (1980). Two major groups, including acid / intermediate rocks with SiO<sub>2</sub> contents greater than 53% (quartz-latitude, rhyodacite and dacite and lati-andesite) and basic rocks with SiO<sub>2</sub> contents less than 53% (basaltic-andesite and transitional basalt) were identified. The acid / intermediate rocks occurred at the highest altitudes on the eastern side of the Paraná River Basin whereas the basic rocks were dominant on the western side.

Two sets of soil materials were used in this research. One set included samples from five toposequences of soils formed from two different types of volcanic rocks (acid/intermediate vs. basic) under similar climatic conditions in the northern region of Paraná state. These soils ranged widely in terms of both development (Solos Litólicos to

Latossolo) and native chemistry (allic to eutrophic). The second set of samples was composed of subsoil materials taken from well drained, Latossolo Roxo profiles formed from basic rocks along a mostly northeast to southwest climatic transect in the state of Paraná. Two additional sites from the state of São Paulo were included to extend the climosequence. All soil samples were characterized to determine basic physical and chemical properties and were classified according to the Brazilian and American systems of soil classification. Surface and subsurface samples representative of diagnostic horizons were then selected for a detailed analysis of clay mineralogy.

The clay fractions were first analyzed using chemical dissolution procedures. These procedures included HF dissolution for total chemical composition, Na-citrate-bicarbonate-dithionite extraction to determine the Fe oxide content, and acid oxalate extraction to quantify the amounts of poorly crystalline and organically complexed Fe. Following the removal of Fe oxides with CBD, selected clay samples were further analyzed to estimate the proportions and characteristics of kaolinite, gibbsite and 2:1 clay minerals using a combination of XRD and thermal analysis techniques.

Iron oxides in the toposequence and climosequence clays were concentrated using boiling, 5M NaOH to dissolve kaolinite and gibbsite (Norrish and Taylor, 1960; Kämpf and Schwertmann, 1982). The proportions of goethite, hematite and maghemite in the residues were then quantified by XRD. Maghemite was not detected in residues from some of the youngest basalt soils or in most of the soil clays derived from acid/intermediate rocks. These results suggest that XRD analysis of the 5M NaOH concentrates underestimated the amounts of maghemite present because almost all the soil

clays had a positive magnetic susceptibility when exposed to a low intensity magnetic field. The magnetic susceptibility decreased to near zero after CBD extraction, thereby indicating that fine-grained maghemite was removed by the treatment.

An attempt was made to determine the magnetic susceptibility of the pure soil maghemites. This was accomplished by assigning the magnetic susceptibility of the total clay fraction to maghemite. The mass of maghemite present in the clay was then estimated as the product of the Fe<sub>d</sub> content of the total clay and the % maghemite obtained, as previously described, by XRD analysis of the 5M NaOH concentrates. The average magnetic susceptibility of the soil maghemites was about 44000 ( $10^{-8} \cdot \text{m}^3/\text{Kg}$ ) but ranged from 25000 to more than 80000 for different soils due, presumably, to particle size effects, degree and type of isomorphous substitution, analytical error, and/or artifacts created by the 5M NaOH procedure. If a suitable magnetic susceptibility value can be obtained for maghemite, this technique could provide a sensitive method for measuring the maghemite contents of soil clays. Better analytical methods are needed to quantify and characterize maghemite because this mineral represents, for some basalt soils, almost 50% of the total Fe oxides present. The influence of maghemite on soil physical and chemical characteristics has mostly been overlooked.

A dissolution technique was developed to selectively remove maghemite from the 5M NaOH residues and thereby provide further concentration of goethite and hematite. This procedure was a modification of a method originally proposed by Schwertmann and Fechter (1984) and involved a 2-hr extraction of the residues with 1.8M

H<sub>2</sub>SO<sub>4</sub> at 75°C. The extraction dissolved more than 90% of the maghemite without any apparent degradation of residual hematite and goethite.

Determinations of dissolved Al and Fe in the sulfuric acid extracts and measurements of the position of the d<sub>220</sub> diffraction peak of maghemite (prior to dissolution) were used to evaluate the degree of Al substitution within this mineral. XRD results indicated that Al-substitution in the soil maghemites ranged from 5.2 to 15.4 mole %. The correlation with Al dissolved in the 1.8M H<sub>2</sub>SO<sub>4</sub> extracts was poor, probably due to removal of Al from other sources (e.g., residual 2:1 clay minerals). More detailed analysis need to be performed to better understand the effects of Al-for-Fe substitution in maghemite.

The Al - substitutions in hematite and goethite were determined from the positions of selected XRD peaks following the removal of maghemite with 1.8M H<sub>2</sub>SO<sub>4</sub>. The removal of maghemite was critical to obtain proper measurements from hematite because of overlapping peaks from these two minerals. The Al-substitution in hematite varied from 0.1 to 15.4 mole % and was usually lowest in the most weakly weathered profiles from a given toposequence. Interestingly, the lowest Al substitutions in hematite were observed in those soils derived from acid/intermediate rocks. Some variation in individual results was observed depending upon which XRD spacings and which equations were used to calculate Al substitution (Schwertmann et al., 1979; Schwertmann and Lathan, 1986). The degree of Al-substitution in goethite varied from 14.8 to 39.9 mole % and showed a weak positive correlation with soil gibbsite content, and a weak negative correlation with increasing pH. The amount of Al substitution determined from CBD

extracts of the 5M NaOH + 1.8M H<sub>2</sub>SO<sub>4</sub> residues were highly correlated with values obtained by XRD analysis when samples were segregated so that hematitic (< 20% goethite) and goethitic (< 20% hematite) samples were evaluated separately.

Studies of the toposequence samples showed that the amount, distribution and characteristics of the silicate clay minerals, gibbsite, and Fe oxides were related to the parent material, landscape position, and degree of weathering. The most highly weathered Latossolo (LR, LB) occurring on stable, well drained segments of the landscape always yielded the highest concentrations of Fe and Al oxides and the smallest amounts of 2:1 clay minerals. The somewhat less weathered Terra Roxa (TR) and Terra Bruna (TB) soils contained the largest amounts of kaolinite due, presumably, to landscape positions that facilitated the removal of silica and nutrients through lateral and basal flow and thereby favored the diagenesis of 1:1 clay minerals (Moniz et al., 1982; Moniz and Buol, 1982). The kaolinites in these soils also showed the best crystallinity as reflected in narrow widths at half height (WHH) for basal XRD peaks and high dehydroxylation temperatures during thermal analysis.

Clay minerals of the 2:1 type were observed in all profiles, especially those derived from basalt, and semiquantitative estimates of their abundance was achieved by a combination of selective dissolution procedures and thermogravimetric analysis. X-ray diffraction patterns from oriented aggregates showed that the 2:1 clay minerals in the less weathered profiles derived from basalt (BAv, R) were often interstratified with kaolinite and/or halloysite. Less interstratification but more hydroxy-Al-interlayering was observed in 2:1 clay minerals occurring in the highly weathered profiles (LR, LB, TR, and TB).

Even though present in small amounts (less than 10%), such minerals are probably responsible for most of the cation exchange capacity of these soils. Gibbsite contents were highly correlated with pH and degree of weathering of the soils derived from basalt. Immature profiles with pH above 5.5 had no detectable gibbsite in the clay fractions, but gibbsite content increased in an almost linear fashion as the pH decreased from 6 to 4 in the more highly weathered soils. A  $\text{pH}_{\text{CaCl}_2}$  of 3.9 to 4 was the lowest value attained by soils derived from either the acid/intermediate or basic rocks in this region. This pH "barrier" must be related to their mineralogy and the buffering capacity of the soil organic matter (complexing Al and H). No correlation between soil  $\text{pH}_{\text{CaCl}_2}$  and gibbsite content was observed for those soils derived from acid/intermediate rocks. On comparable landscape positions and at similar stages of weathering, the acid/intermediate rock soils usually contained less Fe oxides and more kaolinite than those soils derived from basalt.

The distribution of Fe oxides varied not only with the parent rock material but also with the degree of weathering of the soils within a given toposequence. Maghemite was detected by XRD in most of the soils derived from basic rocks, where its abundance was clearly related to the degree of weathering. Maghemite in these soils was most likely produced by oxidation of magnetites or titanomagnetites found in the parent rocks. Most of the soils developed from acid/intermediate rocks contained no XRD-detectable maghemite in the clay fractions; however, the clays did yield positive magnetic susceptibilities indicative of minor amounts of fine-grained maghemite. This maghemite was presumably formed by burning of vegetative matter at or near the soil surface during profile development.

Maghemite has seldom been included in previous studies of Fe oxide genesis, which have typically focused on the hematite-goethite pair. In this investigation, clays separated from the most highly weathered materials formed from basic rocks were always dominated by hematite ( $Hm/(Hm+Gt) > 0.6$ ), whereas less weathered soils yielded  $Hm/(Hm+Gt)$  ratios ranging from 0 to 0.8. The lowest values in the latter were associated with BC and C horizons where geochemical conditions in the early stages of rock weathering apparently favor the formation of a highly Al-substituted goethite that subsequently either dissolves as weathering intensity increases or is diluted by the formation of hematite (and maghemite). Some Latossolo Roxo clays (basic rock soils) were identified that contained no XRD-detectable goethite. The Fe oxide mineralogy of soils developed from acid/intermediate volcanic rocks was consistently dominated by goethite but hematite became more abundant with weathering. The combined toposequence and climosequence data showed no apparent relationship between hematite-goethite ratios and climatic factors (average annual temperature or excess water), soil pH, or organic C content as reported in previous studies from this region (Kämpf and Schwertmann, 1983; Palmieri, 1986). Parent material and stage of weathering were clearly the primary forces affecting Fe oxide genesis and distribution in the current study.

## LIST OF REFERENCES

- Alexander, E. B. 1974. Extractable iron in relation to soil age on terraces along the Truckee River, Nevada. *Soil Sci. Soc. Am. Proc.* 38:121-124.
- Alexander, J. D. 1969. A color chart for organic matter. *Crops and Soils* 21:15 - 17.
- Alleoni, L. R. F., and O. A. Camargo. 1994a. Pontos de efeito salino nulo de Latossolos ácidos. *R. bras. Ci. Solo* 18:175 - 180.
- Alleoni, L. R. F., and O. A. Camargo. 1994b. Potencial elétrico superficial e carga elétrica líquida de Latossolos ácidos. *R. bras. Ci. Solo* 18:181 - 185.
- Almeida, J. A., N. Kämpf, and E. Klamt. Amidas e hidrazina na identificação de caulinita desordenada em solo brunos subtropicais do Rio Grande do Sul e de Santa Catarina. *R. bras. Ci. Solo* 16:169 - 175.
- Aloisi, R. R., G. Ranzani, J.L.I. Demattê, and C.C. Cerri. 1976. Mineralogia da fração argila de alguns solos do município de Jaboticabal, SP. pp. 518-523. **In:** Congresso Brasileiro de Ciência do Solo, 15°. *Anais da Sociedade Brasileira de Ciência do Solo.*
- Amaral, G., U. G. Cordani, K. Kawashita, and J. H. Reynolds. 1966. Potassium-argon dates of basaltic rocks from southern Brazil. *Geochim. Cosmochim. Acta* 30:159 - 189.
- Anand, R. R., and R. J. Gilkes. 1987. Variations in the properties of iron oxides within individual specimens of laterite duricrust. *Aust. J. Soil Res.* 25:287 - 302.
- Andrade, S. S. de, A. C. Moniz, H. G. dos Santos, and H. C. Almeida. 1976. Sequência de evolução de solos bem drenados originados de rochas eruptivas básicas da região fisiográfica de Campo Grande, M.T. pp. 518-523. **In:** Congresso Brasileiro de Ciência do Solo, 15°. *Anais da Sociedade Brasileira de Ciência do Solo.*
- Angel, B. R., J. P. E. Jones, and P. L. Hall. 1974. Electron spin resonance studies of doped synthetic kaolinite. *Clay Miner.* 10:247 - 255.

Ashaye, T. J. 1969. Sesquioxide status and particle size distribution in twelve Nigerian soils derived from sandstone. *African Soils* 14:85-86.

Barnhisel, R. I.; P. M. Bertsch. 1989. Chlorites and hydroxy-interlayered vermiculite and smectite. pp. 729 - 788. In: J. B. Dixon, and S. B. Weed (eds). *Minerals in soil environments*. 2nd ed. Pub. n° 1. Soil Sci. Soc. Am., Madison, WI.

Barrón, V., and J. Torrent. 1986. Use of the Kubelka-Munk theory to study the influence of iron oxides on soil color. *J. Soil Sci.* 37:499 - 510.

Barrow, N. J. 1992. A brief discussion on the effect of temperature on the reaction of inorganic ions with soil. *J. Soil Sci.* 43:37 - 45.

Bas, M. J. Le, R. W. Le Maitre, and A. R. Wooley. The construction of the total alkali-silica chemical classification of volcanic rocks. *Miner. Petrol.* 46:1 - 22.

Bellieni, G., P. Brotzu, P. Comin-Chiaramonti, M. Ernesto, A. Melfi, I. G. Pacca, and E. M. Piccirillo. 1984a. Flood basalt to rhyolite suites in the southern Paraná plateau (Brazil): Paleomagnetism, petrogenesis and geodynamic implications. *J. Petrol.* 25:579 - 618.

Bellieni, G., P. Comin-Chiaramonti, L. S. Marques, A. J. Melfi, E. M. Piccirillo, A. J. R. Nardy, and A. Roisemberg. 1984b. High and low TiO<sub>2</sub> flood basalts from the Paraná plateau (Brazil): Petrology and geochemical aspects bearing on their mantle origin. *Neues Jahrbuch Miner. Abh.* 150:273- 306.

Bellieni, G, P. Comin-Chiaramonti, L. S. Marques, A. J. Melfi, A. J. R. Nardy, C. Papatrechas, M. Piccirillo, A. Roisemberg, and D. Stolfa. 1986. Petrogenetic aspects of acid and basaltic lavas from the Paraná plateau (Brazil): Geological, mineralogical and petrochemical relationships. *J. Petrol.* 27:915 - 944.

Bernas, B. 1968. A new method for decomposition and comprehensive analysis of silicates by atomic absorption spectrometry. *Anal. Chem.* 40:1682 - 1686.

Bernstein, L. R., and G. A. Waychunas. 1987. Germanium crystal chemistry in hematite and goethite from the Apex Mine, Utah, and some new data on germanium in aqueous solution and in stottite. *Geochim. Cosmochim. Acta* 51:623 - 630.

Bigham, J. M., L. Carlson, and E. Murad. 1994. Schwertmannite, a new iron oxyhydroxy-sulphate from Pyhäsalmi, Finland, and other localities. 1994. *Miner. Mag.* 58 : 641 - 648.

Bigham, J. M., and E.J. Ciolkosz (ed.). 1993. *Soil Color. Spec. Publ. N° 41.* Soil Sci. Soc. Am., Madison. WI. 159p.

Bigham, J. M., D. C. Golden, L. H. Bowen, S. W. Buol and S. B. Weed. 1978a. Iron oxide mineralogy of well drained Ultisols and Oxisols. I. Characterization of iron oxides in soil clays by Mössbauer spectroscopy, x-ray diffractometry, and selected chemical techniques. *Soil Sci. Soc. Am. J.* 42:816-825.

Bigham, J. M., D. C. Golden, S. W. Buol, S. B. Weed and L. H. Bowen. 1978b. Iron oxide mineralogy of well drained Ultisols and Oxisols. II. Influence on color, surface area, and phosphate retention. *Soil Sci. Soc. Am. J.* 42:825-830.

Bigham, J. M., U. Schwertmann, L. Carlson, and E. Murad. 1990. A poorly crystallized oxyhydroxysulphate of iron formed by bacterial oxidation of Fe(II) in acid mine waters. *Geochim. Cosmochim. Acta* 54 : 2743 - 2758.

Bigham, J. M., N. E. Smeck, W. F. Jaynes, and M. J. Shipitalo. 1982. Interstratification of 1: 1 and 2 :1 layer silicates in a Crider soil of southwestern Ohio. p. 273. In: *Agron. Abst., Am. Soc. Agron., Madison, WI.*

Bjork, S. J., A. Dearing, and A. Jonsoon. 1982. Magnetic susceptibility of late Weichselian deposits in southeastern Sweden. *Boreas* 1:99-111.

Blume, H. P., and U. Schwertmann. 1969. Genetic evaluation of profile distribution of aluminum, iron, and manganese oxides. *Soil Sci. Soc. Am. Proc.* 33: 438 - 444.

Boero, V., and U. Schwertmann. 1987. Occurrence and transformations of iron and manganese in a colluvial terra rossa toposequence of northern Italy. *Catena* 14:519-531.

Borggaard, O. K. 1983. Effect of surface area and mineralogy of iron oxides on their surface charge and anion adsorption properties. *Clays Clay Miner.* 31:230 - 232.

Brasil, 1973. Levantamento de reconhecimento dos solos do Estado do Rio Grande do Sul. Min. Agr., DNPA, DPP. Bol. Técn. 30, Recife. 431p.

Brasil, 1977. Mapa geológico do Brasil. Min. Agr., DNPA, DPP.

Breuer, J., and E. Murad. 1992. Mineralogy of soil kaolinites from Cameron. *Z. Pflanzenernähr. Bodenk.* 155:379 - 383.

Brown, G. 1990. Understanding the continents, tectonic and thermal processes of the lithosphere. Open Univ. Milton Keynes.

Bryant, R. B. 1981. Genesis of the Ryker and associated soils in southern Indiana. Ph.D. Thesis. Purdue Univ. West Lafayette, IN.

Bryant, R. B., and J. Macedo. 1990. Differential chemoreductive dissolution of iron oxides in a Brazilian Oxisol. *Soil Sci. Soc. Am. J.* 54:819 - 821.

Bui, E. N., J. B. Dixon, H. Shafdan, and L. P. Wilding. 1990. Geomorphic features and associated iron oxides of the Dallol Bosso of Niger (West Africa). *Catena* 17:41 - 54.

Buol, S. W., F. D. Hole, and R. J. McCracken. 1989. *Soil genesis and classification*, 3rd ed. Iowa State Univ. Press. Ames, IA. 446 p.

Cady, J. C., L. P. Wilding, and L. R. Drees. 1986. Petrographic microscope techniques. pp. 185 - 198. In: A. Klute (ed.) *Methods of Soil Analysis, Part I.*, 2nd ed. Am. Soc. Agron., Madison, WI.

Camargo, N. M., E. Klant and J. H. Kaufman. 1987. Classificação de solos em levantamentos pedológicos no Brasil. *Rev. bras. Ci. Solo* 12:11-33.

Camargo, M. N., P. Klinger, F. H. Beinroth, H. Eswaran, C. S. Holzhey, and J. Olmos. 1986. Tour guide. VIIIth Int. Soil Class. Work. Brazil. SMSS/Embrapa/UPR. 285p.

Camargo, O.A., A. C. Moniz, J. A. Jorge, and J. M. A. S. Valadares. 1986. Métodos de análise química, mineralógica e física de solos do Instituto Agronômico de Campinas. Campinas, Instituto Agronômico. B.T. n° 106, 94 pp.

Carlson, L. and U. Schwertmann. 1981. Natural ferrihydrites in surface deposits from Finland and their association with silica. *Geochim. Cosmochim. Acta* 45:421 - 429.

Carter, D. L., M. D. Heilman, C. L. Gonzales. 1965. The ethylene glycol monoethyl ether (EGME) technique for determining soil surface area. *Soil Sci.* 100:409-413.

Castro Fo, C. de. 1988. Effects of liming on characteristics of a Brazilian Oxisol at three levels of organic matter. Ph.D. Thesis, The Ohio State University, Columbus, OH. 261 pp.

Charlet, L., and G. Sposito. 1987. Monovalent ion adsorption by an Oxisol. *Soil Sci. Soc. Am. J.* 51:1155-1160.

Churchman, G. J., J. S. Whitton, G. G. C. Claridge, and B. K. G. Theng. 1984. Intercalation method using formamide for differentiating halloysite from kaolinite. *Clays Clay Miner.* 32:241 - 248.

Clemente, C. A. 1988. Alterações e solos desenvolvidos sobre rochas vulcânicas ácidas da Formação Serra Geral nos Planaltos de Guarapuava e Palmas, região centro sul do Estado do Paraná. Ph.D. Thesis, Escola Superior de Agricultura Luiz de Queiroz. Piracicaba, SP, 211pp.

Coelho, R. M., I. F. Lepsch, and J. R. F. Menck. 1994. Relações solo - relevo em uma encosta com transição arenito - basalto em Jaú (SP). *Rev. bras. Ci. Solo* 18:125 - 138.

Coey, J. M. D. 1986. Magnetic properties of iron in soil oxides and clay minerals. pp. 65 - 84. In: J.W. Stucki, B.A. Goodman, and U. Schwertmann (eds.) *Iron in soils and clay minerals*. NATO ASI Series, Vol. 217, D. Reidel Publ., Dordrecht.

Comin-Chiaramonti, P., C. B. Gomes, E. M. Piccirillo, and G. Rivalenti. 1983. High TiO<sub>2</sub> dikes in the coastline of São Paulo and Rio de Janeiro states (Brazil). *Neus Jahr. Miner. Abh.* 146:133 - 150.

Commission Internationale de l'Eclairage. 1931. *Proceedings of the Eighth Session*, Cambridge, England. 1931. Bureau Central de la CIE, Paris.

Cordani. U. G. P., L. P. Sartori, and K. Kawashita. 1980. Geoquímica dos isótopos de estrôncio e a evolução da atividade vulcânica na Bacia do Paraná (sul do Brasil) durante o Cretaceo. *An. Acad. bras. Ci.* 52:811 - 818.

Cornell, R. M. 1991. Simultaneous incorporation of Mn, Ni, and Co in the goethite ( $\alpha$ -FeOOH) structure. *Clay Miner.* 26:427 - 430.

Cornell, R. M., and R. Giovanoli. 1987. Effect of manganese on the transformation of ferrihydrite into goethite and jacobsite in alkaline media. *Clays Clay Miner.* 35:11 - 20.

Costa, A. C. S., J. M. Bigham, and S. J. Traina. 1995. Mineralogy of Oxisols after application of sequential dissolution procedure. p. 39. In: V. M. Goldschmidt Conf. Abst.

Curi, N. 1983. Lithosequence and toposequence of Oxisols from Goiás and Minas Gerais, Brazil. Ph. D. Thesis, Purdue University. West Lafayette, IN.

Curi, N., and D. F. Franzmeier. 1984. Toposequence of Oxisols from the central plateau of Brazil. *Soil Sci. Soc. Am. J.* 48:341-346.

Curi, N., and D. F. Franzmeier. 1987. Effect of parent rocks on chemical and mineralogical properties of some Oxisols in Brazil. *Soil Sci. Soc. Am. J.* 51:153-158.

Curry, N.A., G.B. Johnston, P.J. Besser, and A.H. Morrish. 1965. Neutron diffraction measurements on pure and doped synthetic hematite crystals. *Phil. Mag.* 12:221-228.

Cuttler, A. H. 1980. The behaviour of a synthetic <sup>57</sup>Fe-doped kaolin, Mössbauer and electron paramagnetic resonance studies. *Clay Miner.* 15:429 - 444.

Davey, B. G., J. D. Russel, and M. J. Wilson. 1975. Iron oxide and clay minerals and their relation to colors of red and yellow podzolic soils near Sydney, Australia. *Geoderma* 14:125-138.

Dearing, J. 1992. Sediment yields and sources in a Welsh lake-catchment during the past 800 years. *Earth Surf. Proc. Land*. 17:1 - 22.

Dearing, J. 1994. Environmental magnetic susceptibility. Using the Bartington MS2 system. Chi Publ., Kenilworth, England. 104 pp.

De Jesus Filho, M. F., J. D. Fabris, A. T. Goulart, J. M. D. Coey, B. A. Ferreira, and M. C. F. Pinto. 1996. Ilmenite and magnetite in a tholeiitic basalt. *Clays Clay Miner.* 43:641-642.

De La Roche, H. J. Leterrier, P. Grandclaude, and M. Marchal. 1980. A classification of volcanic and plutonic rocks using R1R2-diagram and major-element analysis - its relationships with current nomenclature. *Chem. Geol.* 29:183 - 210.

Demattê, J. L. I. 1975. Characteristics and classification of a toposequence of soils near Piracicaba. Ph.D. Thesis, The Ohio State University. 298 pp.

Demattê, J. L. I., N. Holowaychuk. 1977. Solos da região de São Pedro - Estado de São Paulo. II. Mineralogia. *R. bras. Ci. Solo* 1:99-103.

Demattê, J. L. I., A. Marconi. 1991. A drenagem na mineralogia de solos desenvolvidos de diabásio em Piracicaba (SP). *R. bras. Ci. Solo*. 15:1 - 8.

Demattê, J. L. I., A. Marconi, G. Sparovek, and P. Vidal Torrado. 1994. Estimativa da evolução do intemperismo mediante ganhos e perdas de ions numa sequência de solos desenvolvidos de diabásio e influenciados pela drenagem em Piracicaba (SP). *R. bras. Ci. Solo*. 15:69 - 73.

Demattê, J. L. I., A. C. Moniz, and J. E. S. Pessoti. 1977. Solos originados de sedimentos do Grupo Estrada Nova, Município de Piracicaba. I. Análise granulométrica quantitativa da fração argila. *Rev. bras. Ci. Solo*. 1: 43 - 47.

Deshpande, T. L., D. L. Greenland, and J. P. Quirk. 1968. Changes in soil properties associated with the removal of iron and aluminum oxides. *J. Soil Sci.* 19:108 - 122.

Dixon, J. B. 1966. Quantitative analysis of kaolinite and gibbsite in soils by differential thermal and selective dissolution methods. *Clays Clay Miner.* 14:83 - 89.

Drits, V. A., B. A. Sakharov, A. L. Salyn, and A. Manceau. 1993. Structural model for ferrihydrite. *Clay Miner.* 28:185 - 207.

Dzomback, D. A., and F. M. M. Morel. 1990. Surface complexation modeling: hydrous ferric oxide, John Wiley and Sons, New York, NY.

Egashira, K., J. B. Dixon, and L. R. Hossner. 1982. High-charge smectite from lignite overburden of east Texas. pp. 335 - 345. In: H. van Olphen and F. Veniale (ed.) Proc. Int. Clay Conf., Bologna and Pavia, Italy. Elsevier Sci. Publ. Co., Amsterdam

Eggleton, R. A., and R. W. Fitzpatrick. 1988. New data and a revised structural model for ferrihydrite. *Clays Clay Miner.* 36:111 - 124.

El-Swaify, S. A., and H. Sayeg. 1975. Charge characteristics of an Oxisol and an Inceptisol from Hawaii. *Soil Sci.* 120:49-56.

EMPRESA BRASILEIRA DE PESQUISA AGROPECUÁRIA. SERVIÇO NACIONAL DE LEVANTAMENTO E CONSERVAÇÃO DO SOLO. 1979. Manual de métodos e análises de solos. Rio de Janeiro.

EMPRESA BRASILEIRA DE PESQUISA AGROPECUÁRIA. SERVIÇO NACIONAL DE LEVANTAMENTO E CONSERVAÇÃO DO SOLO. INSTITUTO AGRONÔMICO DO PARANÁ. 1984. Levantamento de Reconhecimento dos Solos do Estado do Paraná. Vol. I and II. 791pp.

EMPRESA BRASILEIRA DE PESQUISA AGROPECUÁRIA. SERVIÇO NACIONAL DE LEVANTAMENTO E CONSERVAÇÃO DO SOLO. 1988. Critérios para distinção de classes de solos e de fases de unidades de mapeamento. Rio de Janeiro. 43 pp.

Fabris, J. D., J. M. D. Coey, Q. Qi, and W. N. Mussel. 1995. Characteristics of Mg - rich maghemite from tuffite. *Am. Miner.* 80:664 - 669.

Fassbinder, J. W. E., H. Stanjek, and H. Vali. 1990. Occurrence of magnetic bacteria in soil. *Nature* 343:256 - 258.

Fasolo, P. J. 1978. Mineralogical identification of four igneous extrusive rock derived Oxisols from the State of Paraná, Brazil. MS Thesis, Indiana University, IN. 109 pp.

Faure, G. 1991. Principles and applications of inorganic geochemistry. MacMillan Publ. Co. New York, NY. 626 pp.

Fernández, R. N., and D. G. Schulze. 1987. Calculation of soil color from reflectance spectra. *Soil Sci. Soc. Am. J.* 51:1277 - 1282.

Fey, M. V. 1983. Hypothesis for the yellowing of red soil materials. Tech. Communication, S. African Dept. of Agric. Fish. 180:130 - 136.

Fine, F., and M. J. Singer. 1989. Contribution of ferrimagnetic minerals to oxalate and dithionite extractable iron. *Soil Sci. Soc. Am. J.* 53:191- 196.

Fitzpatrick, R.W., J. Le Roux, and U. Schwertmann. 1978. Amorphous and crystalline titanium and iron-titanium oxides in synthetic preparations, at near ambient conditions, and in soil clays. *Clays Clay Min.* 26:189-201.

Fitzpatrick, R. W., and U. Schwertmann. 1982. Al-substituted goethite: an indicator of pedogenic and other weathering environments in South Africa. *Geoderma* 27: 335 - 347.

Floyd, J. D., and A. Trench. 1988. Magnetic susceptibility contrasts in Ordovician greywackes of the southern uplands of Scotland. *J. Geol. Soc. London.* 145:77-83.

Fodor, R. V. 1987. Low- and high-TiO<sub>2</sub> flood basalts of southern Brazil: Origin from picritic parentage and a common mantle source. *Earth Planet. Sci. Letters* 84:423 - 430.

Fodor, R.V., C. Corwin, and A. Roisemberg. 1985. Petrology of Serra Geral (Paraná) continental flood basalts, southern Brazil: crustal contamination, source material, and South Atlantic magmatism. *Contrib. Mineral. Petrol.* 91: 4 - 65.

Fodor, R. V., E. H. McKee, and A. Roisemberg. 1989. Age distribution of Serra Geral (Paraná) flood basalts, southern Brazil. *J. South Amer. Earth Sci.* 2:343 - 349.

Fontes, M. P. F. 1988. Iron oxide mineralogy in some Brazilian Oxisols. Ph.D. Thesis. N. C. State Univ., Raleigh, NC.

Fontes, M. P. F., J. D. Fabris, M. Resende, and E. Galvão da Silva. 1985. Concreções ferruginosas de alguns solos brasileiros. I. Caracterização química. *R. bras. Ci. Solo* 9 : 119 - 123.

Furtado, A., M. Madeira, and E. Jeanroy. 1990. Mineralogy of soils from Madeira island (Portugal). Solubility of the iron oxides. *Sci. Géol. Bull.* 43:139 - 149.

Galagher, K. J., W. Feitknecht, and U. Mannweiler. 1968. Mechanism of oxidation of magnetite to  $\gamma$ -Fe<sub>2</sub>O<sub>3</sub>. *Nature* 217:1118 - 1121.

Galhego, H. R., and C. R. Espindola. 1979. Mineralogia da fração argila de solos desenvolvidos de produtos de alteração de rochas eruptivas básicas em Botucatu (SP). *R. bras. Ci. Solo* 3:131-135.

Gallez, A. A., S.R. Juo, and A.J. Herbillon. 1976. Surface and charge characteristics of selected soils in the tropics. *Soil Sci. Soc. Am. J.* 40:601-608.

Gehring, A. U., and A. M. Hofmeister. 1994. The transformation of lepidocrocite during heating: A magnetic and spectroscopy study. *Clays Clay Miner.* 42:409 - 415.

Gillman, G. P. 1974. The influence of the net charge on water dispersible clay and sorbed sulfate in six weathered soils from tropical north Queensland. *Aust. J. Soil. Res.* 14:351 - 360.

Gillman, G. P., and G. Uehara. 1980. Charge characteristics of soils with variable and permanent charge. II. Experimental. *Soil Sci. Soc. Am. J.* 44 :252 - 255.

Goodman, B. A., M. L. Berrow, and J. D. Russell. 1988. Transformation of poorly - crystalline oxides during boiling with NaOH to concentrate iron oxides from soils. *J. Soil Sci.* 39:87 - 98.

Grim, R. E. 1968. *Clay mineralogy*, 2nd ed. McGraw-Hill. New York, NY. 596 pp.

Grohmann, F. 1977. Correlação entre a superfície específica e outras propriedades de solos de São Paulo. *Rev. bras. Ci. Solo* 1:9 - 12.

Gualberto, V. 1984. Caracterização física, química e mineralógica de alguns latossolos, com altos teores de ferro. da Amazônia e do Planalto Central. M. Sc. Thesis. Univ. Federal de Viçosa.

Hall, G. F. 1983. Pedology and geomorphology. pp. 117 - 140. **In:** L. P. Wilding, N. E. Smeck, and G. F. Hall (eds.) *Pedogenesis and Soil Taxonomy. I. Concepts and Interactions.* Elsevier, Amsterdam.

Harris, W. G., K. A. Hollen, S. R. Bates, and W. A. Acree. 1992. Dehydration of hydroxy - interlayered vermiculite as a function of time and temperature. *Clays Clay Miner.* 40:335 - 340.

Hawksworth, C., M. Mantovani, and D. Peate. 1988. Lithosphere remobilization during Paraná CFB magmatism. *J. Petrol.* 205 - 223.

Helgason, Ö, H. P. Gunnlaugsson, and S. Steinhörsson. 1994. Maghemite in basalt studied by Mössbauer spectroscopy in an external magnetic field. *Hyperfine Interactions* 91:583 - 587.

Helmy, A. K., E. A. Ferreira, and S. G. de Busseti. 1994. Cation exchange capacity of hydroxy-Al montmorillonite. *Clays Clay Miner.* 4:444 - 450.

Hendershot, W. H., and L. M. Lavkulich. 1978. The use of zero point of charge (ZPC) to assess pedogenic development. *Soil Sci. Soc. Am. J.* 42:468-472.

Herbillon, A. J., R. Frankart, and L. Vielvoye. 1981. An occurrence of interstratified kaolinite-smectite minerals in a red-black soil toposequence. *Clay Miner.* 16:195 - 201.

Herbillon, A. J., M. M. Metsdagh, L. Virevoye, and E. G. Derouane. 1976. Iron in kaolinite with special reference to tropical soils. *Clay Miner.* 11:201- 220.

Holmgren, G. G. S., R. L. June, and R. C. Geschwender. 1977. A mechanically controlled variable rate leaching device. *Soil Sci. Soc. Am. J.* 41:1207-1208.

Hsu, P. H. 1989. Aluminum hydroxides and oxyhydroxides. pp. 331 - 379. **In:** J. B. Dixon, and S. B. Weed (eds.) *Minerals in soil environments*, 2nd ed. Book Ser. n° 1. Soil Sci. Soc. Am., Madison, WI.

Hunt, A. 1986. The application of mineral magnetic methods to atmospheric aerosol discrimination. *Phys. Earth Planet. Interiors* 42:10 - 21.

Hunt, C. P., M. J. Singer, G. Kletetschka, J. TenPas, and K. L. Verosub. 1995. Effect of citrate-bicarbonate-dithionite treatment on fine grained magnetite and maghemite. *Earth Planet. Sci. Letters* 130:87 - 94.

Hurst, V. J. 1977. Visual estimation of iron in saprolite. *Geol. Soc. Am. Bull.* 88:174 - 176.

Ibanga, I. J., S. W. Buol, S. B. Weed, and L. H. Bowen. 1983. Iron oxides in petroferric materials. *Soil Sci. Soc. Am. J.* 47:1240 - 1246.

Innes, R. P., and D. J. Pluth. 1970. Thin section preparation using epoxy impregnation for petrographic and electron microprobe analysis. *Soil Sci. Soc. Am. Proc.* 34:483 - 485.

Instituto Agronômico do Paraná. 1994. *Cartas climáticas do estado do Paraná*. Documento 18, Londrina, Pr, Brazil. 49 pp.

Jackson, M. L. 1963. Interlayering of expandable layer silicates in soils by chemical weathering. *Clays Clay Miner.* 11:29 - 46.

Jackson, M. L. 1968. Weathering of primary and secondary minerals in soils. *Trans. 9th Int. Congr. Soil Sci.* 4:281 - 292.

Jaynes, W. F. 1988. Characterization and separation of soil clay minerals using ion exchange, lithium charge reduction, and density gradient techniques. Ph.D. Dissertation. The Ohio State University, Columbus, OH. 230 pp.

Jaynes, W. F., and J. M. Bigham. 1986a. Concentration of iron oxides from soil clays by density gradient centrifugation. *Soil Sci. Soc. Am. J.* 50:1633 - 1639.

Jaynes, W.F., and J. M. Bigham. 1986b. Multiple cation-exchange capacity measurements on standard clays using a commercial mechanical extractor. *Clays Clay Miner.* 34:93 - 98.

Jaynes, W. F., J. M. Bigham, N. E. Smeck, and M. J. Shipitalo. 1989. Interstratified 1:1 - 2:1 mineral formation in a polygenetic soil from southern Ohio. *Soil Sci. Soc. Am. J.* 53:1888 - 1894.

Johnson, J. H., and D. G. Lewis. 1983. A detailed study of the transformation of ferrihydrate to hematite in an aqueous medium at 92°C. *Geochim. Cosmochim. Acta* 47:1823 - 1831.

Jones, R. C., and G. Uehara. 1978. Amorphous coatings on mineral surfaces. *Soil Sci. Soc. Am. Proc.* 37:792-798.

Juo, A. S. R., and R. L. Fox. 1977. Phosphate sorption capacity of some benchmark soils. *West Africa Soil Service* 124:370-376.

Kämpf, N. 1981. Die Eisenoxidmineralogie einer klimasequenz von böden aus eruptiva in Rio Grande do Sul, Brasilien. Ph.D. Dissertation, Techn. Univ. München, Weihenstephan.

Kämpf, N., A. C. Azevedo, and M. I. da Costa Jr. 1995. Estrutura básica de argilomineral 2:1 com hydroxi-Al entrecamadas em latossolo bruno do Rio Grande do Sul. *R. bras. Ci. Solo* 19:185 - 190.

Kämpf, N., and E. Klamt. 1978. Mineralogia e Gênese de Latossolos (Oxisols) and solos podzólicos da região noroeste do Planalto Sul - Riograndense. *Rev. bras. Ci. Solo* 2:68 - 73.

Kämpf, N., M. Resende, and N. Curi. 1988. Iron oxides in Brazilian Oxisols. pp 71 - 78. In: F. H. Beinroth, M., N. Camargo, and H. Eswaran (eds). *Proc. Eighth Int. Soil Classification Workshop. Classification, Characterization and Utilization of Oxisols.* Rio de Janeiro.

Kämpf, N., P. Schneider, and P. F. Mello. 1995. Alterações mineralógicas em sequência vertissolo - litossolo na região da campanha no Rio Grande do Sul. *R. bras. Ci. Solo* 19:349 - 357.

Kämpf, N., and U. Schwertmann. 1982. The 5M NaOH concentration method for iron oxides in soils. *Clays Clay Miner.* 30:401 - 408.

Kämpf, N., and U. Schwertmann. 1983. Goethite and hematite in a climosequence in southern Brazil and their application in classification of kaolinitic soils. *Geoderma* 29:27-39.

Kämpf, N., and U. Schwertmann. 1995. Goethitas na interface solo - rocha em amostras do Rio Grande do Sul e Minas Gerais. *R. bras. Ci. Solo* 19:359 - 366

Karathanasis, A. D., and B. F. Hajek. 1982. Revised methods for rapid quantitative determination of minerals in soil clays. *Soil Sci. Soc. Am. J.* 46:419 - 425.

Karathanasis, A. D., and B. F. Hajek. 1983. Transformation of smectite to kaolinite in naturally acid soil systems: Structural and thermodynamic considerations. *Soil Sci. Soc. Am. J.* 47:158 - 163.

Kinjo, I., and P.F. Pratt. 1971. Nitrate adsorption. II. In competition with chloride, sulfate and phosphate. *Soil Sci. Soc. Am. Proc.* 35:725 - 728.

Kittrick, J.A. 1969. Soil minerals in the system  $Al_2O_3$ - $SiO_2$ - $H_2O$  and a theory to their formation. *Clays Clay Miner.* 17:157 - 167.

Kosmas, C. S., N. Curi, R. B. Bryant, and D. P. Franzmeier. 1984. Characterization of iron oxide minerals by second - derivative visible spectroscopy. *Soil Sci. Soc. Am. J.* 48:401 - 405.

Kosmas, C. S., D. P. Franzmeier, and D. G. Schulze. 1986. Relationship among derivative spectroscopy, color, crystalline dimensions, and Al substitution of synthetic goethites and hematites. *Clays Clay Miner.* 34:625 - 634.

Lagaly, G., and A. Weiss. 1976. The layer charge of smectitic layer silicates. pp 157 - 172. In: S. W. Bailey (ed.) *Proc. Int. Clay Conf., Mexico City. 1975.* Applied Publ., Wilmette, IL.

Leger, R. G., G. J. F. Millette, and S. Chomchan. 1979. The effects of organic matter, iron oxides and moisture on the color of two agricultural soils of Quebec. *Can. J. Soil Sci.* 59:191 - 202.

Leinz, V. 1949. Contribuição a geologia dos derrames basálticos do sul do Brasil. *Bol. Fac. Ci. Lt. USP.* 103 pp.

Leinz, V., A. Bartorelli, G. R. Sadowski, and G. A. L. Isolta. 1966. Sobre o comportamento espacial do Trapp basaltico da Bacia do Paraná. *Soc. Bras. Geol.* 15:809.

Lemos, R. C., and R. D. Santos. 1984. Manual de descrição e coleta de solo no campo. Campinas, Soc. Brasileira de Ciência do Solo, Serviço Nacional de Levantamento e Conservação de Solo, 46 pp.

Lepsch, I., S. W. Buol, and R. B. Daniels. 1977a. Soil landscape relationship in the occidental plateau of São Paulo, Brazil. I. Geomorphic surfaces and soil mapping units. Soil Sci. Soc. Am. J. 41:104 - 109.

Lepsch, I., S. W. Buol, and R. B. Daniels. 1977b. Soil landscape relationship in the occidental plateau of São Paulo, Brazil. II. Soil, morphology, genesis and classification. Soil Sci. Soc. Am. J. 41:109 - 115.

Lim, C. H., M. L. Jackson, R. D. Koons, and P. A. Helmke. 1980. Kaolins: sources of differences in cation exchange capacities and cesium retention. Clays Clay Miner. 28:125 - 129.

Lima, J. C. 1979. Estudo de uma sequência de solos desenvolvidos de rochas básicas do sudoeste do Estado do Paraná. MS Thesis. Escola Superior de Agricultura Luiz de Queiroz-USP. 123 pp.

Lim - Nunez, R., and R. J. Gilkes. 1987. Acid dissolution of synthetic metal containing goethites and hematites. pp. 197 - 204. In: L. G. Schultz, H. van Olphen, and F.A. Mumpton (eds.) Proc. Int. Clay Conf., Denver (1985). The Clay Miner Soc. Bloomington, IN.

Llanillo, R. F. 1989. Regionalização do estado do Paraná. pp. 41-50. In: Paraná Rural. Manual técnico do subprograma de manejo e conservação do solo. Secretaria de Agricultura e Abastecimento.

Lucas, Y., F. J. Luizão, A. Chauvel, J. Rouiller, and D. Nahon. 1993. The relation between biological activity of the rain forest and mineral composition of soils. Science 260:521 - 523.

Maack, R. 1968. Geografia física do Estado do Paraná. Banco de Desenvolvimento Econômico do Paraná. Universidade Federal do Paraná.

Macedo, J., and R. B. Bryant. 1987. Morphology, mineralogy and genesis of a hydrosequence of Oxisols in Brazil. Soil Sci. Soc. Am. J. 51:690 - 698.

Macedo, J., and R. B. Bryant. 1989. Preferential microbial reduction of hematite over goethite in a Brazilian Oxisol. Soil Sci. Soc. Am. J. 53:1114 - 1118.

- Mackenzie, R. C. 1964. The thermal investigation of soil clays. pp. 200 - 244. **In:** C. I. Rich and G. W. Kunze (eds.) Soil clay mineralogy. Univ. North Car. Press, Chapel Hill, NC.
- Maher, B. A. 1986. Characterization of soils by mineral magnetic measurements. *Phys. Earth Planet. Interiors* 42:76 - 92.
- Manceau, A., and V. A. Drits. 1993. Local structure of ferrihydrite and ferroxhite by EXAFS spectroscopy. *Clay Miner.* 28:165 - 184.
- Mares, S. 1984. Geophysical well-logging. pp. 474 - 525. **In:** Introduction to applied geophysics.
- Matsusaka, Y., and G. D. Sherman. 1964. Lime requirement of Hawaiian soils. *Hawaii Farm Sci.* 13:5 - 7.
- McBride, M. B. 1978. Retention of Cu, Ca, Mg and Mn by amorphous alumina. *Soil Sci. Soc. Am. J.* 42 : 27 - 31.
- McBride, M.B. 1994. Environmental Chemistry of Soils. Oxford Univ. Press, New York. 406 pp.
- McKeague, J .A. 1967. An evaluation of 0.1M pyrophosphate and pyrophosphate-dithionite in comparison with oxalate as extractants of the accumulation products in Podzols and some others soils. *Can J. Soil Sci.* 47:95 - 99.
- McKeague, J .A., J. E. Brydon, and N. M. Miles. 1971. Differentiation of forms of extractable iron and aluminum in soils. *Soil Sci. Soc. Am. Proc.* 35:33 - 38.
- McKeague, J. A., and J. H. Day. 1966. Dithionite- and oxalate-extractable Fe and Al as aids in differentiating various classes of soils. *Can J. Soil Sci.* 46:13 - 22.
- Mehra, O. P., and M. L. Jackson. 1960. Iron oxide removal from soils by a dithionite-citrate system buffered with sodium bicarbonate. pp. 317 - 327. **In:** A. Swineford (ed.) Proc. 7th Natl. Clay Conf. (1958). Washington, D.C., Pergamon Press, New York, NY.
- Mekaru, T., and G. Uehara. 1972. Anion adsorption in ferruginous tropical soils. *Soil Sci. Soc. Am. Proc.* 36:296 - 300.
- Melfi, A. J. 1966. Potassium-argon dates for core samples of basaltic rocks from Southern Brazil. *Geochim. Cosmochim. Acta* 31:1079-1089.

Melfi, A. J. 1978. Natureza e origem dos constituintes secundários dos solos desenvolvidos sobre rochas básicas da Bacia do Paraná. *Cerâmica* 24:347 - 354.

Milne, G. 1935. Some suggested units for classification and mapping, particularly for East African soils. *Soil Res.* 4:183 - 198.

Mineropar. 1986. Mapa geológico do Estado do Paraná. Curitiba, Pr.

Mohr, E. C. J., and F. A. van Baren. 1954. Tropical soils. A critical study of soil genesis as related to climate and vegetation. The Royal Tropical Institute. Interscience. 498 pp.

Mohr, E. C. J., F. A. van Baren, and J. van Schuylenborgh. 1973. Tropical soils. 3rd ed. The Hague. 481 pp.

Moniz, A. C., and S. W. Buol. 1982. Formation of an Oxisol - Ultisol transition in São Paulo-Brazil. I. Double - water flow model of soil development. *Soil Sci. Soc. Am. J.* 46:1228 - 1233.

Moniz, A. C., S. W. Buol, and S. B. Weed. 1982. Formation of an Oxisol - Ultisol transition in São Paulo-Brazil. II. Lateral flow dynamics of chemical weathering. *Soil Sci. Soc. Am. J.* 46:1234 - 1239.

Moniz, A. C., and M. L. Jackson. 1967. Quantitative mineralogy of Brazilian soils derived from basaltic rocks and slate. *Soil Sci. Rep.* 212., Univ. Wisconsin. Madison, WI. 74 pp.

Moniz, A. C., S. Manfredini, and J. L. I. Demattê. 1994. Variações morfológicas mineralógicas e hídricas em terra roxa estruturada ao longo de uma vertente em Rio das Pedras (SP). *R. bras. Ci. Solo* 18:513 - 520.

Moniz, A. C., and J. B. Oliveira. 1974. Estudo mineralógico de solos derivados de rochas ígneas básicas da estação experimental de Ribeirão Preto, SP. pp. 591-601. In: 14º Congresso Brasileiro de Ciência do Solo. Anais Soc. Bras. Ci. do Solo.

Mooney, H. M., and R. Bleifus. 1952. Magnetic susceptibility measurements in Minnesota. Part II. Analysis of field measurements. *Geophysics* 17:531 - 543.

Moore, D. M., and R. C. Reynolds, Jr. 1989. X-ray diffraction and the identification and analysis of clay minerals. Oxford Univ. Press. NY. 332 pp.

Morais, F. I., A. L. Page, and L. J. Lund. 1976. The effect of pH, salt concentration and nature of electrolytes on the charge characteristics of Brazilian tropical soils. *Soil Sci. Soc. Am. J.* 40:521 - 527.

Morelli, M., and E. B. Ferreira. 1987. Efeito do carbonato de cálcio e do fosfato diamônico em propriedades eletroquímicas e físicas de um Latossolo. *Rev. bras. Ci. Solo* 11:1 - 6.

Morrish, A.H. and J.A. Eaton. 1971. Magnetic transition in rhodium-doped hematite single crystals. *J. Appl. Phys.* 42:1495-1496.

Moura Filho, W., and S.W. Buol. 1972. Studies of a Latosol Roxo (Eutruxox) in Brazil. I. Clay mineralogy. *Experientia* 13:218 - 234.

Mullins, C. E. 1977. Magnetic susceptibility of the soil and its significance in soil science - A review. *J. Soil Sci.* 28:223 - 246.

Munsell Color Company. 1975. Munsell soil color charts. 1975 ed. Munsell Color Co. Baltimore, MD.

Murad, E., and J. H. Johnston. 1987. Iron oxides and oxyhydroxides. pp. 507 - 582. In: G. J. Long (ed.) *Mössbauer spectroscopy applied to inorganic chemistry*. Vol. 2. Plenum Publ. Corp., New York, NY.

Nalovic, L., G. Pedro, and C. Janot. 1975. Demonstration by Mössbauer spectroscopy of the role played by transitional trace elements in the crystallogenesis of iron hydroxides (III). pp. 601 - 610. In: S. W. Bailey (ed.) *Proc. Int. Clay Conf., Mexico City*. 1975. Applied Publ., Wilmette, IL.

Nardy, A. J. N. 1988. Petrologia e paleomagnetismo das rochas vulcânicas da região Centro-sul do estado do Paraná: Formação Serra Geral. MS Thesis. Instituto Astronômico e Geofísico- USP. São Paulo. 186 pp.

Norrish, K., and J. G. Pickering. 1983. Clays minerals. pp. 281 - 308. In: *Soils: An Australian viewpoint*. CSIRO, Melbourne. Academic Press, London.

Norrish, K., and R. M. Taylor. 1961. The isomorphous replacement of iron by aluminium in soil goethites. *J. Soil Sci.* 12:294 - 306.

Oldfield, F., R. Thompson, and D. P. E. Dickson. 1981. Artificial enhancement of stream bedload: A hydrological application of superparamagnetism. *Physics Earth Planet Int.* 26: 107 - 124.

Palmieri, F. 1986. A study of a climosequence of soils derived from volcanic rock parent material in Santa Catarina and Rio Grande do Sul States, Brazil. Ph.D. Thesis. Purdue Univ., West Lafayette, IN.

PARANÁ. 1989. Paraná Rural. Manual técnico do subprograma de manejo e conservação do solo. Secretaria de Agricultura do Estado do Paraná. 306 pp.

Parks, G. A. 1967. Aqueous surface chemistry of oxides and complex oxide minerals. *Adv. Chem* 67:121 - 160.

Pavan, M. A. 1981. Toxicity of Al(III) to coffee (*Coffea arabica*, L.) in nutrient solution culture and in Oxisols and Ultisols amended with  $\text{CaCO}_3$ ,  $\text{MgCO}_3$  and  $\text{CaSO}_4 \cdot 2\text{H}_2\text{O}$ . Ph.D. Thesis. University of California, Riverside, CA. 214 pp.

Pavan, M. A., F.T. Bingham, and P. F. Pratt. 1985. Chemical and mineralogical characteristics of selected acid soils of the State of Paraná, Brazil. *Turrialba* 35:131 - 139.

Peixoto, R. T. G. 1995. Chemical properties of Oxisols derived from Paraná Basalt (Brazil). Ph.D. Thesis. The Ohio State University, Columbus, OH.

Pena, F., and J. Torrent. 1984. Relationship between phosphate sorption and iron oxides in Alfisols from a river terrace sequence of Mediterranean Spain. *Geoderma* 33:283-296.

Petit, S., and A. Decarreau. 1990. Hydrothermal (200°C) synthesis and crystal chemistry of iron-rich kaolinites. *Clay Miner.* 25:181 - 196.

Petri, S., and V. S. Fúlfaro. 1983. *Geologia do Brasil*. EDUSP. 631 pp.

Piccirillo, E. M., A. J. Melfi, P. Comin-Chiaramonti, G. Bellieni, M. Ernesto, L. S. Marques, A. J. R. Nardy, I. G. Pacca, A. Roisemberg, and D. Stolfa. 1988. pp. 195-238. In: J. D. MacDougall (ed.) *Continental flood basalts*. Kluwer Academic Publishers.

Pombo, L. E. Klamt, I. Kunrath and D. Gianluppi. 1982. Identificação de óxidos de ferro na fração argila de Latossolo Roxo. *R. bras. Ci. Solo* 6:13 - 17.

Post, D. F., S. J. Levine, R. B. Bryant, M. D. Mays, A. K. Batchilly, R. Escadafal, and A. R. Huete. 1993. Correlations between field and laboratory measurements of soil color. pp. 35 - 49. In: J. M. Bigham and E. J. Ciolkosz (eds.) *Soil Color*. Sp. Pub n° 31. Soil Sci. Soc. Am. Madison, WI.

Pötter, R. O., and N. Kämpf. 1981. Argilo - minerais e óxidos de ferro em cambissolos e latossolos sob regime climático térmico údico no Rio Grande do Sul. *R. bras. Ci. Solo* 5:153 - 159.

Queiroz, S. B., and E. Klamt. 1985. Mineralogia e gênese de brunizém avermelhado e terra roxa estruturada similar na encosta inferior do nordeste do Rio Grande do Sul. *R. bras. Ci. Solo* 9:51 - 57.

Rai, D., and J. Kittrick. 1989. Mineral equilibria and the soil system. pp. 161- 198. **In:** J. B. Dixon and S. B. Weed (eds). Minerals in soil environments, 2nd ed., Book Ser. n°1. Soil Sci. Soc. Am., Madison, WI.

Rauen, M. J. 1980. Mineralogical identification of a toposequence of soils from basaltic rocks in the state of Paraná, Brazil. MS Thesis. Purdue Univ., West Lafayette, IN.

Renne, P. R., M. Ernesto, I. G. Pacca, R. S. Coe, J. M. Glen, M. Prévot, and M. Perrin. 1992. The age of Paraná flood volcanism, rifting of Gondwanaland, and the jurassic-cretaceous boundary. *Science* 258:975 - 979.

Rocha, G. C., and C. C. Cerri. 1994. Características e organização de uma toposequência de solos sobre rocha básica na amazônia brasileira. *R. bras. Ci. Solo* 18:117 - 123.

Resende, M. 1976. Mineralogy, chemistry, morphology and geomorphology of some soils of the Central Plateau of Brazil. Ph.D. Thesis. Purdue Univ., West Lafayette, IN. 237 pp.

Resende, M., J. E. M. Allan, and J. M. D. Coey. 1986. The magnetic soils of Brazil. *Earth and Planetary Sci. Letters* 78 : 322 - 326.

Resende, M., D. P. Santana, D. P. Franzmeier, and J. M. Coey. 1986. Magnetic properties of Brazilian Oxisols. pp 78-108. **In:** F. H. Beinroth, M. N. Camargo, and H. Eswaran (eds). Proc. 8th. Int. Soil Class. Workshop. Classification, Characterization and Utilization of Oxisols. Rio de Janeiro.

Resende, M., D. P. Santana, and S. B. Rezende. 1985. Susceptibilidade magnética em latossolos do Sudeste e Sul do Brasil. **In:** M. C. Camargo (ed.). Anais da III reunião de correlação e classificação de solos. Embrapa, Rio de Janeiro.

Rich, C. I. 1968. Hydroxy interlayers in expandible layer silicates. *Clays Clay Miner.* 16:15 - 30.

Rodrigues, T. E. 1984. Caracterização e genese de solos brunos do macico alcalino de Polços de Caldas (MG). Ph.D. Thesis. Escola Superior de Agricultura Luiz de Queiroz. 235 pp.

Ruhe, R. V. 1960. Elements of soil landscapes. Trans. 7th Int. Congr. Soil Science, Madison, WI. 4:165 - 170.

Rutledge, E. M., L. P. Wilding and M. Elfield. 1967. Automated particle size separation by sedimentation. *Soil Sci. Soc. Am. Proc.* 31:287 - 288.

Sanchez, P.A. 1976. Properties and management of soils in the tropics. John Wiley and Sons, NY. 618 pp.

Santana, D. P. 1984. Soil formation in a toposequence of Oxisols from Patos de Minas region, Minas Gerais state, Brazil. Ph.D. Thesis. Purdue Univ., West Lafayette, IN.

Sartori, P. L. P., and C. B. Gomes. 1980. Composição química - mineralógica das últimas manifestações vulcânicas da região de Santa Maria, RS. An. Acad. Bras. Ci. Lt. 52:125 - 133.

Sartori, P. L. P., C. M. Filho, and E. Menegotto. 1975. Contribuição ao estudo das rochas vulcânicas da Bacia do Paraná na região de Santa Maria, RS. Rev. bras. Geoc. 5:141 - 159.

Schellmann, W. 1978. Behaviour of nickel, cobalt and chromium in ferruginous lateritic nickel ores. Bull. BRGM (2), II. 3:275-282

Schneider, A. W. 1964. Contribuição à petrologia dos derrames basálticos da Bacia do Paraná. Esc. Geol. Porto Alegre. Univ. Fed. Rio Grande do Sul. Pub. nº1.

Schofield, R.K. 1949. The effect of pH on electric charges carried by clay particles. Soil Sci. 1:1 - 8

Schultz, L. G., A. O. Shepard, P. D. Blackmon, and H. C. Starkey. 1971. Mixed - layer kaolinite - montmorillonite from the Yucatan Peninsula, Mexico. Clays Clay Miner. 19:137 - 150.

Schulze, D. G. 1981. Identification of soil iron oxide minerals by differential x-ray diffraction. Soil Sci. Soc. Am. J. 45:437-440.

Schulze, D. G. 1982. The identification of iron oxides by differential x-ray diffraction and the influence of aluminum substitution on the structure of goethite. Ph.D. Thesis Technische Universität München. Weihenstephan, FRG. 166p.

Schulze, D. G. 1984. The influence of aluminum on iron oxides. VIII. Unit cell dimensions of Al - substituted goethites and estimation of Al from them. Clays Clay Miner. 32:36 - 44.

Schulze, D.G., J. L. Nagel, G. E. van Scoyoc, T. L. Henderson, M. F. Baumgardner, and D. E. Stott. 1993. pp 71 - 90. In: J. M. Bigham, and E. J. Ciolkosz (eds). Soil color. Spec. Pub nº 31. Soil Sci. Soc. Am. Madison, WI.

Schwertmann, U. 1973. Use of oxalate for Fe extraction from soils. *Can J. Soil Sci.* 53:244 - 246.

Schwertmann, U. 1985. The effect of pedogenic environments on iron oxide minerals. pp. 171-200. **In:** B.A. Stewart (ed). *Advances in Soil Science*. Vol. 1.

Schwertmann, U. 1988. Some properties of soil and synthetic iron oxides. pp. 203 - 250. **In:** J. W. Stucki, B. A. Goodman, and U. Schwertmann (eds.). 1985. *Iron in soils and clay minerals*. NATO ASI Ser. D. Reidel Publ. Co., Dordrecht.

Schwertmann, U. 1991. Solubility and dissolution of iron oxides. pp. 3 - 27. **In:** Y Chen, and Y. Hadar (eds.) *Iron nutrition and interactions in plants*. Kluwer Acad. Publ.

Schwertmann, U. 1993. Relationships between iron oxides and soil color. pp. 51 - 70. **In:** J. M. Bigham, and E. J. Ciolkosz (eds). *Soil color*. Spec. Pub n° 31. Soil Sci. Soc. Am. Madison, WI.

Schwertmann, U., J. M. Bigham, and E. Murad. 1995. The first occurrence of schwertmannite in a natural stream environment. *Eur. J. Mineral.* 7:547 - 552.

Schwertmann, U., and L. Carlson. 1994. Aluminum influence on iron oxides: XVII. Unit-cell parameters and aluminum substitution of natural goethites. *Soil Sci. Soc. Am. J.* 58: 256 - 261.

Schwertmann, U., and R. M. Cornell. 1991. *Iron oxides in the laboratory. Preparation and characterization*. VCH Publ. Inc. NY. 137 pp.

Schwertmann, U., and H. Fechter. 1984. The influence of aluminum on iron oxides: XI. Aluminum - substituted maghemite in soils and its formation. *Soil Sci. Soc. Am. J.* 48:1462 - 1463.

Schwertmann, U., R. M. Fitzpatrick, R. M Taylor, and D. G. Lewis. 1979. The influence of aluminum substitution on iron oxides: 2. Preparation and properties of Al-substituted hematites. *Clays Clay Min.* 27:105-122.

Schwertmann, U., and A. J. Herbillon. 1992. Some aspects of fertility associated with the mineralogy of highly weathered tropical soils. pp. 47 - 60. **In:** R. Lal and P.A Sanchez (eds). *Myths and science of soils of the tropics*. Special Publ. n° 29. Soil Sci. Soc. Am. Madison, WI.

Schwertmann, U., and N. Kämpf. 1985. Properties of goethite and hematite in kaolinitic soils of southern and central Brazil. *Soil Sci.* 139:344 - 350.

Schwertmann, U., and M. Lathan. 1986. Properties of iron oxides in some New Caledonian Oxisols. *Geoderma* 39:105 - 123.

Schwertmann, U., and E. Murad. 1983. The effect of pH on the formation of goethite and hematite from ferrihydrite. *Clays Clay Miner.* 31:277 - 284.

Schwertmann, U., E. Murad, and D.G. Schulze. 1982a. Is there holocene reddening (hematite formation) in soils of axeric temperate areas? *Geoderma* 27:209-223.

Schwertmann, U., D. G. Schulze, and E. Murad. 1982b. Identification of ferrihydrite in soils by dissolution kinetics, differential x-ray diffraction and Mössbauer spectroscopy. *Soil Sci. Soc. Am J.* 46:869 - 875.

Schwertmann, U., and R. M. Taylor. 1989. Iron oxides. pp. 379 - 438. **In:** J.B. Dixon, and S. B. Weed (eds). *Minerals in soil environments*, 2nd Ed., Book Ser. n° 1. Soil Sci. Soc. Am. Madison, WI.

Setzer, J. 1966. *Atlas climático e ecológico do Estado de São Paulo*. Comissão Interestadual da Bacia Paraná-Uruguai. CESP, São Paulo.

Singer, M. J., and P. Fine. 1989. Pedogenetic factors affecting magnetic susceptibility of northern Californian soils. *Soil Sci. Soc. Am. J.* 53:1119 - 1127.

Singer, A., and P. M. Huang. 1993. Humic acid effect on aluminum interlayering in montmorillonite. *Soil Sci. Soc. Am. J.* 57:271 - 279.

Singh, B., and R. J. Gilkes. 1991. Concentration of iron oxides from soil clays by 5M NaOH treatment: The complete removal of sodalite and kaolin. *Clay Minerals* 26:463 - 472.

Singh, B., and R. J. Gilkes. 1992. Properties of soil kaolinites from south-western Australia. *J. Soil Sci.* 43:645 - 667.

Singleton P. C., and M. E. Harward. 1971. Iron hydroxy interlayering in clays. *Soil Sci. Soc. Am. Proc.* 35:838 - 842.

Siqueira, C., J. R. Leal, A. C. X. Velloso, and G. A. Santos. 1990. Eletro - química de solos tropicais de carga variável: II: Quantificação do efeito da matéria orgânica sobre o ponto de carga zero. *Rev. bras. Ci. Solo* 14:13-17.

Smykatz-Kloss, W. 1975. The DTA determination of the degree of (dis-) order of kaolinites: Method and application to some kaolin deposits of Germany. pp. 429 - 438. **In:** S.W. Bailey (ed.) *Proc. Int. Clay Conf.*, Mexico City, Wilmette, IL.,

- Soil Survey Staff. 1951. Soil survey manual. USDA-SCS. U.S. Govt. Printing Office, Washington, D.C.
- Soil Survey Staff. 1972. Soil survey laboratory methods and procedures for collecting soil samples. USDA-SCS, U.S. Govt. Printing Office, Washington, D.C.
- Soil Survey Staff. 1975. Soil Taxonomy. A basic system of soil classification for making and interpreting soil survey. Agricultural Handbook 436. U.S. Govt. Printing Office, Washington, D.C.
- Soil Survey Staff. 1994. Keys to soil taxonomy. AID/USDA-SCS/SMSS. Pocahontas Press, Blacksburg, VA..
- Sposito, G. 1984. The surface chemistry of soils. Oxford Univ. Press, NY.
- Stanjek, H., and U. Schwertmann. 1992. The influence of aluminum on iron oxides. part XVI: Hydroxyl and aluminum substitution in synthetic hematites. *Clays Clay Min.* 40:347 - 354.
- Steinhorsson, S., Ö Helgason, M. B. Madsen, C. Bender Koch, M. D. Bentzon, and S. MØrup. 1992. Maghemite in Iceland basalts. *Miner. Mag.* 56:185 - 199.
- Stoop, W. A. 1980. Ion adsorption mechanics in oxidic soils, implications for point of zero charge determinations. *Geoderma* 23:303 - 314.
- Stucki, J. W., B. A. Goodman, and U. Schwertmann (eds.). 1985. Iron in Soils and Clay Minerals. NATO ASI Ser., Vol. 217. D. Reidel Publ. Co., Dordrecht. 893 pp.
- Svab, E. and E. Kren. 1979. Neutron diffraction study of substituted hematite. *J. Magnetism Magnetic Mater.* 14:184-186.
- Szubert, E. C., C. A. Kirchner, and I. Shintaku. 1978. Vulcanismo ácido no planalto meridional do Rio Grande do Sul. *Anais XXX Congresso Brasileiro de Geologia* 3:1350 - 1356.
- Tan, K. H., and B. F. Hajek. 1977. Thermal analysis of soils. pp. 865 - 884. **IN:** J. B. Dixon, and S. B. Weed (eds) *Minerals in soil environments*. Soil Sci. Soc. Am., Madison, WI.
- Tan, K. H., B. F. Hajek, and I. Barshad. 1986. Thermal analysis techniques. pp. 151 - 184. **In:** A. Klute (ed). *Methods of soil analysis. Part.I. Physical and mineralogical methods*. Monograph nº9, Am. Soc. Agron., Madison, WI.

- Taylor, R. M., and A. M. Graley. 1967. The influence of ionic environments on the nature of iron oxides. *J. Soil Sci.* 18:341 - 348.
- Taylor, R. M., and U. Schwertmann. 1974a. Maghemite in soils and its origin I. Properties and observations on soil maghemites. *Clay Min.* 10:289 - 298.
- Taylor, R. M. and U. Schwertmann. 1974b. Maghemite in soils and its origin II. Maghemite syntheses at ambient temperature and pH 7. *Clay Miner.* 10:299 - 310.
- Tessier, D. 1984. Méthode d'approche de l'organisation des argiles et des matériaux argileux. Comportement physique et mécanique des sols. Département Science du Sol ed.
- Tettenhorst, R. 1995. X-ray diffraction class notes. The Ohio State University. Columbus, OH.
- Theng, B.K.G. (ed.) 1980. Soils with variable charge. New Zealand Soc. Soil Sci., Offset Publ., Palmerston North. 447 pp.
- Tite, M. S., and R. E. Lington. 1986. The magnetic susceptibility of soils from central and southern Italy. Estratto da *Prospezioni Archeologiche*, 10, Fondazione Lerici, 25 - 36.
- Tite, M. S., and C. Mullins. 1971. Enhancement of the magnetic susceptibility of soils on archaeological sites, *Archaeometry* 13 : 209 - 219.
- Torrent, J., and V. Barrón. 1993. Laboratory measurement of soil color: theory and practice. pp. 21 - 34. In: J. M. Bigham, and E. J. Ciolkosz (eds). *Soil color. Spec. Publ. n°31. Soil Sci. Soc. Am., Madison, WI.*
- Torrent, J., and A. Cabedo. 1986. Sources of iron oxides in reddish brown soil profiles from calcarenites in southern Spain. *Geoderma* 37:57 - 66.
- Torrent, J., and R. Guzman. 1982. Crystallization of Fe(III) - oxides from ferrihydrite in salt solutions: Osmotic and specific ion effects. *Clay Miner.* 17:463 - 469.
- Torrent, J., R. Guzman., and M. A. Parra. 1982. Influence of relative humidity on the crystallization of Fe(III) oxides from ferrihydrite. *Clays Clay Miner.* 30:337 - 340.
- Torrent, J., U. Schwertmann, and V. Barrón. 1987. The reductive dissolution of synthetic goethite and hematite in dithionite. *Clay Min.* 22:329 - 337.
- Torrent, J., U. Schwertmann, H. Fechter, and F. Alferez. 1983. Quantitative relationships between soil color and hematite content. *Soil Sci.* 136:354 - 358.

Torrent, J., U. Schwertmann, and D. G. Schulze. 1980. Iron oxide mineralogy of some soils of two river terrace sequences in Spain. *Geoderma* 23:191-208.

Thiry, M. and J.F. Sornein. 1983. Petrologie d'une sequence d'alteration de carbonate de fer - le chapeau de fer du gisement de siderite de batere (Pyrenees orientales). Int. Colloquium CRNS 4-7, Paris, France.

Uehara, G., and G. Gilman. 1981. The mineralogy, chemistry and physics of tropical soils with variable charge. Westview Tropical Agric. Ser., No. 4. Westview Press, Boulder, CO. 170 pp.

van Raij, B., and M. Peech. 1972. Electrochemical properties of some Oxisols and Alfisols of the tropics. *Soil Sci. Soc. Am. Proc.* 36:587 - 593.

van Wambeke, A. 1992. Soils of the tropics: properties and appraisal. McGraw Hill, Inc. New York, NY. 343 pp.

Vandenberghe, R.E., A.E. Verbeeck, E. DeGrave, and W. Stiers. 1986. <sup>57</sup>Fe Moessbauer effect study of Mn-substituted goethite and hematite. *Hyperfine Interactions* 29:1157-1160.

Volkoff, B. 1978. Os produtos ferruginosos que determinam a cor dos Latossolos da Bahia. *Rev. bras. Ci. Solo.* 2:55 - 59.

Wada, K., and Kakuto, Y. 1983. A new intergradient vermiculite - kaolin mineral in 2:1 to 1:1 mineral transformation. *Sci. Géol. Mém.* 123 - 131.

Walker, G. F. 1958. Reactions of expandible - lattice clay minerals with glycerol and ethylene glycol. *Clay Miner. Bull.* 3:302 - 313.

Walling, D. E., M. R. Peart, F. Oldfield, and R. Thompson. 1979. Suspended sediment sources identified by magnetic susceptibility. *Nature* 281:110-113.

Wann, S. S., and G. Uehara. 1978. Surface charge manipulations of constant surface potential colloids. I: Relation to sorbed phosphorus. *Soil Sci. Soc. Am. J.* 42:565 - 580.

Wechsler, B., D. H. Lindsley, and C. T. Prewitt. 1984. Crystal structure and cation distribution in titanomagnetites (Fe<sub>3-x</sub>Ti<sub>x</sub>O<sub>4</sub>). *Am. Miner.* 69:754 - 770.

Whitting, L. D. 1965. X-Ray techniques for mineral identification and mineralogical composition. pp. 671- 698. In: C.A. Black et al. (eds). *Methods of soil analysis. Part I. Monograph n° 9. Am. Soc. Agron., Madison, WI.*

Williams, H., F. J. Turner., and C. M. Gilbert. 1982. Petrography: An introduction to the study of rocks in thin sections, 2nd ed. W. H. Freeman and Co., San Francisco, CA.

Williams, J., and R. J. Coventry. 1979. The contrasting soil hydrology of red and yellow earths in a landscape of flow relief. In: The hydrology of areas of low precipitation. Proc. Canberra Symp. Int. Assoc. Hy. Sci. Publ. n°128. Washington D.C.

Wilson, M. J., and P. D. Cradwick. 1972. Occurrence of interstratified kaolinite - montmorillonite in some Scottish soils. *Clay Miner.* 9:435 - 437.

Wolska, E., and U. Schwertmann. 1989. The vacancy ordering and distribution of aluminum ions in  $\gamma$ -(Fe-Al)<sub>2</sub>O<sub>3</sub>. *Solid State Ionic* 32/33:214 - 218.

Wolska, E., and A. Wolniewicz. 1987. On the aluminum-substituted magnetites. *Phys. Status Solid.* 104:569 - 574..

Yerima, B. P. K., F. G. Calhoun, A. L. Senkayi, and J. B. Dixon. 1985. Occurrence of interstratified kaolinite - smectite in El Salvador Vertisols. *Soil Sci. Soc. Am.* 49: 462 - 466.

Yvengar, S. S. , L. W Zelazny, and D. C. Martens. 1981. Effect of photolytic oxalate treatment on soil hydroxy -interlayered vermiculites. *Clays Clay Min.* 29:429 - 434.

**APPENDIX A**  
**Soil morphological descriptions**

Abbreviations used in soil field description tables.

Soil characteristic		Soil characteristic	
<b>1. Boundary (Bd)</b>		<b>6. Consistence</b>	
1.1 Distinctness	Cl - Clear Gr - Gradual Df - Diffuse	6.1. Dry	So - Soft DSH - Slightly hard DH - Hard DVH - Very hard
1.2 Topography	Pl - Plane Sm - Smooth Wv - Wavy	6.2. Moist	MVF - Very friable MFr - Friable MFm - Firm
2. Color - Munsell notation		6.3 Wet	WSt - Sticky WVS - Very sticky WPI - Plastic WVP - Very plastic
3. Texture (Tr)		<b>7. Clayskin</b>	
3.1 Modifier (Md)	Hv - Heavy	7.1. Abundance (Ac)	VF - Very few F - Few C - Common M - Many
3.2 Class (Cl)	Cl - Clay Lm - loam St - silt	7.2. Grade	1 - Weak 2 - Moderate 3 - Strong
4. Structure		<b>8. Consistence</b>	
4.1 Grade (Gd)	0-Structureless 1 - Weak 2 - Moderate 3 - Strong	8.1. Dry	So - Soft DSH - Slightly hard DH - Hard DVH - Very hard
4.2 Size (Sz)	VF - Very fine Fn - Fine Md - Medium Cr - Coarse VC - Very coarse	8.2. Moist	MVF - Very friable MFr - Friable MFm - Firm
4.3 Shape (Sh)	Gr - Granular SB - Subangular Blocky AB - Angular Blocky	8.3. Wet	WSt - Sticky WVS - Very sticky WPI - Plastic WVP - Very plastic
<b>5. Clayskin</b>			
5.1 Abundance (Ac)	VF - Very few F - Few C - Common M - Many		
5.2. Grade	1 - Weak 2 - Moderate 3 - Strong		

Profile: 1  
 Date: 10-11-93  
 Local: Ibioporã, IAPAR's crops experimental station  
 Classification: Terra Roxa Estruturada eutr6fica (TRe) - Rhodic Kandiudalfs  
 Situation: Trench in the middle part of the backslope. Altitude 460m. Declivity 8%.  
 Soil parent material: Colluvium and weathered products of underlying rocks  
 Underlying rock: Basalt  
 Local relief: Gently sloping  
 Regional relief: Nearly level to steep  
 Erosion: Sheet erosion, frequent, superficial, slightly eroded  
 Drainage: Well drained  
 Vegetation: Tropical forest  
 Actual use: Sorghum  
 Climate: Cfa  
 Described by: Antonio C. S. Costa

Horizon		Depth	Color		Texture		Structure			Clay		Consistence			Boundary
Br*	USA**		Moist		MD Class	Sh	Sz	Gd	Skin	Dry	Moist	Wet			
Ap	Ap	0-10	2.5YR3/4	Hv	Cl	Gr	Md-Cr	2	0	MSH	WFr	WSt-WPl	Cl-Pl		
AB	AB	10-28	2.5YR3/4	Hv	Cl	SB	Cr	3	F 1	DH	WFr	WSt-WPl	Cl-Pl		
Bt1	Bt1	28-46	2.5YR3/4	Hv	Cl	SB	Md-Cr	3	C 2	DH	WFr	WVS-WVP	Cl-Pl		
Bt2	Bt2	46-70	2.5YR3/4	Hv	Cl	SB	Md-Cr	3	M 3	DH	WFr	WVS-WVP	Cl-Pl		
Bt3	Bt3	70-100	2.5YR3/4	Hv	Cl	SB	Md-Cr	3	M 3	DH	WFr	WVS-WVP	Gr-Pl		
Bt4	Bt4	100-150	2.5YR3/4	Hv	Cl	SB	Md-Cr	3	M 3	DH	WFr	WVS-WVP	Gr-Pl		
Bt5	Bt5	150-170	Auger sampling												
Bt6	Bt6	170-190	Auger sampling												
Bt7	Bt7	190-210	Auger sampling												
Bt8	Bt8	210-230	Auger sampling												

\* Br (SNLCS, 1988); \*\* USA (Soil Survey Staff, 1993)

#### Chemical and Physical Characteristics of the Soil.

pH		Exchangeable										Particle Size Distribution			
CaCl <sub>2</sub>	H <sub>2</sub> O	C	Ca+Mg	K	Al+H	Al	S	T	V	Al	P	Sand	Silt	Clay	
		%	cmol/Kg										% <----->		
5.3	5.9	2.00	14.65	0.75	4.61	0	15.39	20.00	77	0	27	16	22	62	
5.4	5.7	1.70	15.00	0.53	4.61	0	15.53	20.14	77	0	10	13	26	61	
5.4	5.8	1.07	13.62	0.16	3.97	0	13.78	17.75	78	0	2	10	14	76	
5.5	6.0	0.75	11.12	0.08	3.55	0	11.20	14.75	76	0	2	6	9	85	
5.5	5.9	0.64	12.06	0.09	3.70	0	12.15	15.84	77	0	3	6	8	86	
5.3	5.8	0.46	10.15	0.07	3.68	0	10.22	13.90	74	0	3	6	10	84	
5.2	5.4	0.34	7.30	0.05	3.97	0	7.35	11.32	65	0	2	6	6	88	
5.2	5.4	0.28	7.68	0.05	3.68	0	7.73	11.41	68	0	1	5	12	83	
5.3	5.5	0.25	10.00	0.10	3.68	0	10.10	13.78	73	0	1	4	8	88	
5.2	5.6	0.26	9.10	0.06	3.68	0	9.16	12.84	71	0	3	5	9	86	

Profile: 2  
 Date: 10-11-93  
 Local: Ibioporã. IAPAR's crops experimental station  
 Classification: Solo Litólico eutrófico (Re) - Lithic Hapludolls  
 Situation: Trench in the lower part of the footslope. Altitude 420m. Declivity 15%.  
 Soil parent material: Colluvium and weathered products of underlying rocks  
 Underlying rock: Basalt  
 Local relief: Strongly sloping  
 Regional relief: Nearly level to steep  
 Erosion: Sheet erosion, frequent, superficial, moderately eroded  
 Drainage: Somewhat poorly drained  
 Vegetation: Tropical forest  
 Actual use: Grasses  
 Climate: Cfa  
 Described by: Antonio C. S. Costa

Horizon		Color	Texture	Structure	Consistence			Boundary	
Br*	USA**	Depth	Moist	MD Class	Sh	Sz	Gd	Dry Moist Wet	
A	A	0-18	7.5YR3/2	Cl	Gr	Md	3	DSH MFr MPI Mst	Cl Sm
Cr	Cr	18-40	weathered material of the basic rock						
R	R	40+							

\* Br (SNLCS, 1988); \*\* USA (Soil Survey Staff, 1993)

#### Chemical and Physical Characteristics of the Soil.

pH		Exchangeable									Particle Size Distribution			
CaCl <sub>2</sub>	H <sub>2</sub> O	C	Ca+Mg	K	Al+H	Al	S	T	V	Al	P	Sand	Silt	Clay
		%	cmol <sub>c</sub> /Kg						%		ppm	%		
5.5	6.0	3.56	19.80	0.44	3.42	0	20.24	23.66	86	0	1	27	29	44

Profile: 3

Date: 11-11-93

Local: Ibioporã. IAPAR's crops experimental station

Classification: Brunizem Avermelhado eutrófico (BAv) - Typic Argiudolls

Situation: Road cut in the upper part of the backslope. Altitude 480m. Declivity 20%.

Soil parent material: Colluvium and weathered products of underlying rocks

Underlying rock: Basalt

Local relief: Moderately steep

Regional relief: Nearly level to steep

Erosion: Sheet erosion, frequent, superficial, severely eroded

Drainage: Somewhat poorly drained

Vegetation: Tropical forest

Actual use: Grasses

Climate: Cfa

Described by: Antonio C. S. Costa

Horizon	Depth	Color	Texture	Structure	Clay	Consistence	Boundary	
Br*	USA**	Moist	MD Class	Sh Sz Gd	Skin	Dry Moist Wet		
Od	Oae	3-0	decomposed and semidecomposed root grasses					
A	A	0-28	5YR 3/2	Hv	Cl	SB Cr 3	NIL DSH MFm WPI/WSt Gr/Pl	
Bt	Bt	28-67	5YR 3/3	Hv	Cl	SB/AB VC 3	M 3 DH MFm WVP/WVS Cl/Pl	
BC	BC	67-85	5YR 3/4		Cl	SB/AB Cr 2	C 2 DSH MFm WPI/WSt Cl/Pl	
Cr	Cr	85-100	weathered material of the basic rock					

\* Br (SNLCS, 1988); \*\* USA (Soil Survey Staff, 1993)

### Chemical and Physical Characteristics of the Soil.

pH		Exchangeable										Particle Size Distribution		
CaCl <sub>2</sub>	H <sub>2</sub> O	C	Ca+Mg	K	Al+H	Al	S	T	V	Al	P	Sand	Silt	Clay
		%	cmol <sub>c</sub> /Kg						%>		ppm	%>		
5.7	6.3	4.56	44.30	0.85	4.61	0	45.15	49.76	91	0	42	21	35	44
5.9	6.5	1.55	26.88	0.10	3.18	0	26.98	30.16	89	0	2	9	22	69
5.9	6.4	0.80	35.72	0.16	3.42	0	35.88	39.30	91	0	1	31	20	49
5.9	6.8	nd	50.90	0.17	3.42	0	51.07	54.49	94	0	1	35	28	37

nd = not determined

Profile: 4  
 Date: 11-11-93  
 Local: Ibioporã. IAPAR's crops experimental station  
 Classification: Latossolo Roxo eutrófico (LRe) - Lithic Eutradox  
 Situation: Trench in the summit of the landscape. Altitude 520m. Declivity 5%.  
 Soil parent material: Weathered products of underlying rocks  
 Underlying rock: Basalt  
 Local relief: Nearly level to gently sloping  
 Regional relief: Nearly level to steep  
 Erosion: Sheet erosion, sparse, superficial, slightly eroded  
 Drainage: Excessively drained  
 Vegetation: Tropical forest  
 Actual use: Pasture  
 Climate: Cfa  
 Described by: Antonio C. S. Costa

Horizon	Depth (cm)	Color Moist	Texture MD Class	Structure						Consistence			Boundary
				Primary			Secondary			Dry	Moist	Wet	
Br*	USA**			Sh	Sz	Gd	Sh	Sz	Gd				
Od	Oae	1-0	decomposed and semi	decomposed roots of the pasture									
A	A	0-17	2.5YR 3/4 Hv Cl	AB Cr 3						DH	MFr	WPI/WSt	Gr/Pl
AB	AB	17-33	2.5YR 3/4 Hv Cl	SB VC 2						DH	MFr	WPI/WSt	Df/Pl
Bw1	Bo1	33-57	2.5YR 3/4 Hv Cl	SB VC 1			Gr VF 3			DSH	MVF	WPI/WSt	Df/Pl
Bw2	Bo2	57-112	2.5YR 3/4 Hv Cl	SB VC 1			Gr VF 3			DSH	MVF	WPI/WSt	Df/Pl
R	R	112+	Weathered Basalt										

\* Br (SNLCS, 1988); \*\* USA (Soil Survey Staff, 1993)

#### Chemical and Physical Characteristics of the Soil.

pH	CaCl <sub>2</sub> H <sub>2</sub> O	C	Exchangeable										Particle Size Distribution		
			Ca+Mg	K	Al+H	Al	S	T	V	Al	P	Sand	Silt	Clay	
		%	cmol <sub>c</sub> /Kg	ppm	%	%	%								
5.1	5.6	3.05	12.42	0.64	5.35	0.00	13.06	18.41	71	0	2	19	26	55	
5.1	5.7	1.47	10.00	0.30	4.28	0.00	10.30	14.58	71	0	1	10	21	69	
5.4	6.0	0.98	7.16	0.09	3.68	0.00	7.25	10.93	66	0	2	9	15	76	
5.2	5.7	0.66	7.30	0.07	3.97	0.00	7.37	11.34	65	0	2	10	17	73	

Profile: 5

Date: 11-19-93

Local: Campo Mourao. COAMO's crops experimental station

Classification: Latossolo Roxo distrófico (LRd) - Anionic Acrudox

Situation: Trench in the summit of the landscape. Altitude 645m. Declivity 3%.

Soil parent material: Weathered products of underlying rocks

Underlying rock: Basalt

Local relief: Nearly level to gently sloping

Regional relief: Nearly level to gently sloping

Erosion: Not apparent

Drainage: Excessively drained

Vegetation: Tropical forest

Actual use: Pine forest

Climate: Cfa

Described by: Antonio C. S. Costa

Horizon	Depth	Color	Texture	Structure						Consistence			Boundary		
				Br*	USA**	(cm)	Moist	MD Class	Primary	Secondary	Dry	Moist		Wet	
						Sh	Sz	Gd	Sh	Sz	Gd				
A	A	0-15	5YR 3/3	Hv	Cl	SB	Cr	1	Gr	Md	2	So	MVF	WPI/WSt	Cl/Pl
AB	AB	15-32	2.5YR 3/4	Hv	Cl	SB	Cr	1	Gr	Md	2	So	MVF	WPI/WSt	Cl/Pl
Bw1	Bo1	32-58	2.5YR 3/4	Hv	Cl	SB	VC	1	Gr	Fn	3	So	MVF	WPI/WSt	Df/Pl
Bw2	Bo2	58-145	2.5YR 3/4	Hv	Cl	SB	VC	1	Gr	VF	3	So	MVF	WPI/WSt	Df/Pl
Bw3	Bo3	145-210	2.5YR 3/4	Hv	Cl	SB	VC	1	Gr	VF	3	So	MVF	WPI/WSt	Df/Pl
Bw4	Bo4	210-250	auger sampling												
Bw5	Bo5	250-300	auger sampling												

\* Br (SNLCS, 1988); \*\* USA (Soil Survey Staff, 1993)

#### Chemical and Physical Characteristics of the Soil.

pH	CaCl <sub>2</sub> H <sub>2</sub> O	Exchangeable										Particle Size Distribution		
		C	Ca+Mg	K	Al+H	Al	S	T	V	Al	P	Sand	Silt	Clay
		%	cmol/Kg							%>		%>		
4.1	4.7	4.17	1.50	0.30	8.36	1.47	1.80	10.16	18	45	4	10	16	74
4.1	4.7	1.77	0.64	0.11	6.45	0.59	0.75	7.20	10	44	1	7	21	72
4.2	5.1	1.30	0.84	0.03	5.35	0.36	0.87	6.22	14	29	1	8	19	73
4.2	4.7	0.95	0.58	0.02	4.61	0.24	0.60	5.21	12	29	2	8	14	78
4.5	5.0	0.71	0.42	0.01	3.97	0.00	0.43	4.40	10	0	1	8	15	77
4.5	5.0	0.61	0.18	0.01	3.97	0.00	0.19	4.16	5	0	1	8	14	78
4.9	5.0	0.52	0.14	0.01	3.42	0.00	0.15	3.57	4	0	1	7	15	78

Profile: 6

Date: 11-20-93

Local: Campo Mourao. COAMO's crops experimental station

Classification: Latossolo Roxo distrófico (LRd) - Anionic Acrudox

Situation: Trench in the lower third part of the backslope. Altitude 619m. Declivity 9%.

Soil parent material: Weathered products of underlying rocks

Underlying rock: Basalt

Local relief: Gently sloping

Regional relief: Nearly level to gently sloping

Erosion: Sheet erosion, sparse, superficial, slightly eroded

Drainage: Excessively drained

Vegetation: Tropical forest

Actual use: Cotton crop

Climate: Cfa

Described by: Antonio C. S. Costa

Horizon	Depth (cm)	Color Moist	Texture MD Class	Structure						Consistence			Boundary
				Primary			Secondary			Dry	Moist	Wet	
Br*	USA**			Sh	Sz	Gd	Sh	Sz	Gd				
Ap	Ap	0-21	2.5YR 3/2 Hv Cl	Gr Md 3						DSH MFm WPI/WSt			Cl/Pl
AB	AB	21-39	2.5YR 3/4 Hv Cl	SB Cr 1			Gr Fn 2			DSH MFm WPI/WSt			Cl/Pl
Bw1	Bo1	39-75	2.5YR 3/4 Hv Cl	SB VC 1			Gr VF 3			So MVF WVP/WVS			Df/Pl
Bw2	Bo2	75-180	2.5YR 3/4 Hv Cl	SB VC 1			Gr VF 3			So MVF WVP/WVS			Df/Pl
Bw3	Bo3	180-210	2.5YR 3/4 Hv Cl	SB VC 1			Gr VF 3			So MVF WVP/WVS			Df/Pl

\* Br (SNLCS, 1988); \*\* USA (Soil Survey Staff, 1993)

#### Chemical and Physical Characteristics of the Soil.

pH		Exchangeable										Particle Size Distribution		
CaCl <sub>2</sub> H <sub>2</sub> O	C	Ca+Mg	K	Al+H	Al	S	T	V	Al	P	Sand	Silt	Clay	
	%	cmol <sub>c</sub> /Kg				%				ppm	%			
4.1	4.6	2.30	2.07	0.48	6.86	0.84	2.54	9.40	27	25	4	23	11	66
4.2	4.8	1.52	1.28	0.07	6.23	0.90	1.35	7.57	18	40	1	18	10	72
4.3	4.8	1.10	0.96	0.03	4.79	0.31	0.99	5.77	17	24	1	16	6	78
4.9	5.2	0.74	0.92	0.01	4.61	0.06	0.93	5.54	17	6	1	6	15	79
4.9	5.2	0.53	0.59	0.01	3.42	0.00	0.61	4.03	15	0	1	6	13	81

Profile: 7  
 Date: 11-21-93  
 Local: Campo Mourão. Inside "Pedreira Casale"  
 Classification: Solo Litólico distrófico (Rd) - Typic Troprothents  
 Situation: Road cut the lower third part of the backslope. Altitude 555m. Declivity 25%.  
 Soil parent material: Weathered products of underlying rocks  
 Underlying rock: Basalt  
 Local relief: Moderately steep  
 Regional relief: Nearly level to moderately steep  
 Erosion: Sheet erosion, frequent, superficial, moderately eroded  
 Drainage: Moderately well drained  
 Vegetation: Tropical forest  
 Actual use: Grass  
 Climate: Cfa  
 Described by: Antonio C. S. Costa

Horizon	Depth	Color	Texture	Structure	Consistence	Boundary
Br* USA**	cm	Moist	MD Class	Sh Sz Gd	Dry Moist Wet	
A	0-30	2.5YR 3/2	Lm	SB Cr 3	DVH MFm WPI/WSt	CL/Sm
Cr	30-100	weathered material of the basic rock				
R	100+	Basalt				

\* Br (SNLCS, 1988); \*\* USA (Soil Survey Staff, 1993)

#### Chemical and Physical Characteristics of the Soil.

pH		Exchangeable										Particle Size Distribution		
CaCl <sub>2</sub>	H <sub>2</sub> O	C	Ca+Mg	K	Al+H	Al	S	T	V	Al	P	Sand	Silt	Clay
		%	cmol <sub>c</sub> /Kg			----->			<--- % --->		ppm	<----- % ----->		
4.5	4.9	3.84	8.42	0.25	9.70	0.84	8.67	18.37	47	9	3	36	30	34

Profile: 8  
 Date: 19/11/93  
 Local: Tamarana. Inside the Caiaganqui indian reserve.  
 Classification: Cambissolo álico (Ca) - Oxic Humitropepts  
 Situation: Road cut. Lower third part of the backslope. Altitude 640m. Declivity 10%.  
 Soil parent material: Weathered products of underlying rocks  
 Underlying rock : Rhyolite - andesite  
 Local relief: Rolling  
 Regional relief: Very steep to strongly sloping  
 Erosion: Sheet erosion, frequent, superficial, moderately eroded  
 Drainage: Moderately well drained  
 Vegetation: Tropical forest  
 Actual use: Grasses recently burned.  
 Climate: Cfa  
 Described by: Antonio C. S. Costa

Horizon	Depth	Color	Texture	Structure	Consistence	Boundary	
Br* USA**	cm	Moist	MD Class	Sh Sz Gd	Dry Moist Wet		
Oo	Oi	1-0	ashes and decomposed roots of the grasses				
A	A	0-18	7.5YR 3/2	Lm	Gr Md 2	So MFr WPI/WSt Cl/Sm	
Bi	B	18-35	7.5YR 4/4	Lm	SB Cr 3	DSH MFr WPI/WSt Cl/Sm	
Cr	Cr	35-55	weathered material of the acid rock				

\* Br ( SNLCS, 1988); \*\* USA (Soil Survey Staff, 1993)

#### Chemical and Physical Characteristics of the Soil.

pH		Exchangeable										Particle Size Distribution		
CaCl <sub>2</sub>	H <sub>2</sub> O	C	Ca+Mg	K	Al+H	Al	S	T	V	Al	P	Sand	Silt	Clay
		%	cmol/Kg						% --->		ppm	% ----->		
4.0	5.0	4.98	2.82	0.16	13.06	3.36	2.98	16.04	19	53	6	18	25	57
4.1	4.9	2.64	1.46	0.08	13.06	3.78	1.54	14.60	11	71	1	32	23	45

Profile: 9

Date: 12-22-93

Local: Tamarana. Inside the Caiaganqui indian reserve.

Classification: Terra Bruna Estruturada álica (TBa) - Typic Kandihumults

Situation: Road cut. Middle part of the backslope. Altitude 650m. Declivity 15%.

Soil parent material: Weathered products of underlying rocks

Underlying rock: Rhyolite - andesite

Local relief: Strongly sloping

Regional relief: Very steep to strongly sloping

Erosion: Not apparent

Drainage: Well drained

Vegetation: Tropical forest

Actual use: Grasses

Climate: Cfa

Described by: Antonio C. S. Costa

Horizon	Depth	Color	Texture	Structure	Clay	Consistence	Boundary	
Br* USA**	cm	Moist	MD Class	Sh Sz Gd	Skin	Dry Moist Wet		
Oo	Oi	1-0	decomposed and semidecomposed roots of the grasses					
A	A	0-23	5YR 4/3	Cl	Gr VC 2	NIL	DSH MFm WPI/WSt CI/PI	
BA	BA	23-38	5YR 4/4	Cl	SB Cr 2	NIL	DSH MFm WPI/WSt CI/PI	
Bt1	Bt1	38-62	5YR 4/4	Hv Cl	SB VC 3	C 2	DSH MFm WVP/WVS Df/PI	
Bt2	Bt2	62-101	5YR 4/6	Hv Cl	SB VC 3	M 3	DSH MFm WVP/WVS Df/PI	
Bt3	Bt3	101-124	5YR 4/6	Hv Cl	SB VC 2	M 3	DSH MFm WVP/WVS Df/PI	
BC1	BC1	124-160	2.5YR 4/8	Cl	SB VC 1	F 2	DSH MFr WPI/WSt CI/PI	
BC2	BC2	160+	2.5YR 4/8	Cl	SB VC 1	VF 1	DSH MFr WPI/WSt Df/PI	

\* Br ( SNLCS, 1988); \*\* USA (Soil Survey Staff, 1993)

#### Chemical and Physical Characteristics of the Soil.

pH	Exchangeable											Particle Size Distribution		
	CaCl <sub>2</sub> H <sub>2</sub> O	C	Ca+Mg	K	Al+H	Al	S	T	V	Al	P	Sand	Silt	Clay
	%	<-----	cmol <sub>e</sub> /Kg	<-----	<-----	<-----	<-----	<-----	<--- % --->	ppm	<-----	%	<----->	
4.2	4.8	2.19	4.00	0.16	5.76	0.80	4.16	9.92	42	16	2	28	25	47
4.4	4.8	1.38	2.40	0.08	8.36	1.70	2.48	10.84	23	41	1	26	22	52
4.4	4.8	1.09	1.82	0.07	9.70	1.98	1.89	11.59	16	51	2	21	23	56
4.1	5.1	0.58	1.00	0.12	8.36	2.50	1.12	9.48	12	69	1	20	15	65
3.9	4.4	0.34	0.82	0.07	9.00	3.20	0.89	9.89	9	78	2	19	17	64
4.0	5.0	0.32	1.82	0.04	8.36	1.90	1.86	10.22	18	51	2	18	25	57
4.0	4.6	0.36	2.00	0.75	7.20	0.00	2.75	9.95	28	0	2	20	27	53

Profile: 10  
 Date: 12-23-93  
 Local: Tamarana. Inside the Caiacangui indian reserve  
 Classification: Terra Bruna Estruturada álica (TBa) - Typic Kandihumults  
 Situation: Road cut. Upper part of the backslope. Altitude 685m. Declivity 15%  
 Soil parent material: Colluvium and weathered products of underlying rocks  
 Underlying rock: Rhyolite - andesite  
 Local relief: Strongly sloping  
 Regional relief: Very steep to strongly sloping  
 Erosion: Not apparent  
 Drainage: Well drained  
 Vegetation: Tropical forest  
 Actual use: Secondary forest  
 Climate: Cfa  
 Described by: Antonio C. S. Costa

Horizon	Depth	Color	Texture	Structure	Clay	Consistence	Boundary
Br*	USA**	Moist	MD Class	Sh Sz Gd	Skin	Dry Moist Wet	
A	A	0-10	5YR 3/4	Cl	Gr Cr 2	NIL	Gr/Pl
AB	AB	10-30	7.5YR 4/4	Cl	SB Cr 2	F 1	Gr/Pl
Bt1	Bt1	30-50	5YR 4/4	Hv Cl	SB VC 3	C 2	Gr/Pl
Bt2	Bt2	50-75	5YR 4/4	Hv Cl	SB VC 3	C 3	Gr/Pl
Bt3	Bt3	75-100	5YR 4/6	Hv Cl	SB VC 2	C 2	Gr/Pl
BC	BC	100+	2.5YR 4/3	Cl	SB VC 1	F1	Gr/Pl

\* Br (SNLCS, 1988); \*\* USA (Soil Survey Staff, 1993)

#### Chemical and Physical Characteristics of the Soil.

pH		Exchangeable										Particle Size Distribution		
CaCl <sub>2</sub>	H <sub>2</sub> O	C	Ca+Mg	K	Al+H	Al	S	T	V	Al	P	Sand	Silt	Clay
		%	cmol/Kg		----->			<--- % --->		ppm		<----- % ----->		
4.7	5.4	2.70	9.24	0.39	5.76	0.16	9.63	15.39	63	2	2	37	21	42
4.3	4.8	2.28	7.66	0.13	6.21	0.90	7.79	14.00	56	10	2	38	22	40
4.4	4.9	1.41	4.50	0.12	11.26	3.02	4.62	15.88	29	40	1	30	19	51
3.9	4.6	1.34	2.00	0.08	11.26	3.80	2.08	13.34	16	65	1	16	11	73
4.1	4.6	0.57	1.72	0.10	14.08	7.00	1.82	15.90	11	79	1	15	13	72
3.9	4.3	0.46	1.16	0.12	14.08	5.20	1.28	15.36	8	80	2	15	22	63

Profile: 14  
 Date: 12-22-93  
 Local: Cruzmaltina  
 Classification: Terra Roxa Estruturada distrófica (TRd) - Typic Kandihumults  
 Situation: Road cut. Upper third part of the backslope. Altitude 655m. Declivity 18%.  
 Soil parent material: Colluvium and weathered products of underlying rocks  
 Underlying rock: Basalt  
 Local relief: Strongly sloping  
 Regional relief: Rolling to moderately steep  
 Erosion: Sheet erosion ,sparse, superficial , slightly eroded  
 Drainage: Well drained  
 Vegetation: Tropical forest  
 Actual use: Soybeans  
 Climate: Cfa  
 Described by: Antonio C. S. Costa

Horizon	Depth	Color	Texture	Structure	Clay	Consistence	Boundary
Br*	USA**	cm	Moist	MD Class	Sh Sz Gd	Dry Moist Wet	
Ap	Ap	0-17	5YR 3/2	Cl	Gr Md 2	So MVF WPI/WSt	Cl/Pl
Bt1	Bt1	17-32	2.5YR 3/4	Hv Cl	SB Md 2	So MFr WVP/WVS	Cl/Pl
Bt2	Bt2	32-90	2.5YR 3/4	Hv Cl	SB Md 3	DSH MFm WVP/WVS	Df/Pl
Bt3	Bt3	90-130	2.5YR 3/4	Hv Cl	SB Cr 3	DSH MFm WVP/WVS	Df/Pl
Bt4	Bt4	130-160	2.5YR 3/4	Hv Cl	SB Cr 3	DSH MFm WVP/WVS	Df/Pl
Bt5	Bt5	160-220	2.5YR 3/4	Hv Cl	SB Cr 2	DSH MFm WVP/WVS	Df/Pl

\* Br ( SNLCS, 1988); \*\* USA (Soil Survey Staff, 1993)

#### Chemical and Physical Characteristics of the Soil.

pH		Exchangeable										Particle Size Distribution		
CaCl <sub>2</sub>	H <sub>2</sub> O	C	Ca+Mg	K	Al+H	Al	S	T	V	Al	P	Sand	Silt	Clay
		%	cmol./Kg						% <--->		ppm	% <--->		
4.3	5.1	4.15	13.79	1.69	7.20	0.84	15.48	22.68	68	5	2	17	38	45
4.3	4.9	2.29	6.59	0.24	4.26	0.90	6.83	11.09	62	12	2	9	24	67
4.0	4.9	1.75	2.87	0.06	9.70	1.10	2.93	12.63	23	27	2	5	23	72
4.5	5.0	1.54	1.35	0.04	7.20	1.60	1.39	8.59	16	54	1	8	22	70
4.4	5.1	0.92	0.76	0.04	6.69	1.10	0.80	7.49	11	58	1	7	18	75
4.2	4.8	0.83	0.78	0.04	5.76	1.10	0.82	6.58	12	57	1	7	19	74

Profile: 15  
 Date: 11-24-93  
 Local: Cruzmaltina  
 Classification: Solo Litólico distrófico (Rd) - Typic Troporthents  
 Situation: Road cut. Shoulder. Altitude 710m. Declivity 30%.  
 Soil parent material: Weathered products of underlying rocks  
 Underlying rock: Basalt  
 Local relief: Steep  
 Regional relief: Very steep to strongly sloping  
 Erosion: Sheet erosion, frequent, superficial, moderately eroded  
 Drainage: Well drained  
 Vegetation: Tropical forest  
 Actual use: Soybeans  
 Climate: Cfa  
 Described by: Antonio C. S. Costa

Horizon	Depth	Color	Texture	Structure	Consistence	Boundary
Br* USA**	cm	Moist	MD Class	Sh Sz Gd	Dry Moist Wet	
Ap	Ap	0-10	5YR 3/4	Cl	Gr Cr 2	DSH MFr WPI/WSt Cl/Sm
Cr	Cr	10-70	weathered material of the basic rock			
R	R	70+	basalt			

\* Br (SNLCS, 1988); \*\* USA (Soil Survey Staff, 1993)

#### Chemical and Physical Characteristics of the Soil.

pH	CaCl <sub>2</sub> H <sub>2</sub> O	Exchangeable										Particle Size Distribution		
		C	Ca+Mg	K	Al+H	Al	S	T	V	Al	P	Sand	Silt	Clay
		%	cmol <sub>c</sub> /Kg		----->			<--- % --->		ppm	<----- % ----->			
4.1	4.9	2.45	2.00	0.03	9.70	1.82	2.03	11.73	17	47	2	21	21	58

Profile: 16  
 Date: 11-26-93  
 Local: Cruzmaltina  
 Classification: Latossolo Roxo álico (LRa) - Humic Rhodic Hapludox  
 Situation: Road cut. Summit. Altitude 678m. Declivity 3%.  
 Soil parent material: Weathered products of underlying rocks  
 Underlying rock: Basalt  
 Local relief: Gently sloping  
 Regional relief: Rolling  
 Erosion: no erosion  
 Drainage: Excessively well drained  
 Vegetation: Tropical forest  
 Actual use: Grasses  
 Climate: Cfa  
 Described by: Antonio C. S. Costa

Horizon	Depth	Color	Texture	Structure			Consistence			Boundary
				Primary	Secondary		Dry	Moist	Wet	
Br*	USA**	(cm)	Moist	MD Class	Sh Sz Gd	Sh Sz Gd				
A	A	0-18	2.5YR 3/2	Hv Cl	Gr Md 2			DH MFm	WPI/WSt	Cl/Pl
AB1	AB1	18-35	2.5YR 3/4	Hv Cl	SB CR 2			DH MFm	WPI/WSt	Cl/Pl
AB2	AB2	35-65	2.5YR 3/4	Hv Cl	SB CR 2			DSH MFm	WPI/WSt	Cl/Pl
AB3	AB3	65-105	2.5YR 3/4	Hv Cl	SB CR 1	Gr VF 3		DSH MFr	WPI/WSt	Df/Pl
Bw1	Bo1	105-150	2.5YR 3/4	Hv Cl	SB VC 1	Gr VF 3		DSH MVF	WPI/WSt	Df/Pl
Bw2	Bo2	150-220	2.5YR 3/4	Hv Cl	SB VC 1	Gr VF 3		DSH MVF	WPI/WSt	Df/Pl
Bw3	Bo3	220-300	2.5YR 3/6	Hv Cl	SB VC 1	Gr VF 3		DSH MVF	WPI/WSt	Df/Pl

\* Br (SNLCS, 1988); \*\* USA (Soil Survey Staff, 1993)

#### Chemical and Physical Characteristics of the Soil.

pH	CaCl <sub>2</sub> H <sub>2</sub> O	Exchangeable										Particle Size Distribution		
		C	Ca+Mg	K	Al+H	Al	S	T	V	Al	P	Sand	Silt	Clay
		%	cmol/Kg							% <--- % --->		% <----- % ----->		
4.1	4.8	3.67	2.18	0.17	11.26	1.96	2.35	13.61	17	45	12	17	23	60
4.0	4.8	3.18	0.72	0.04	11.26	2.92	0.76	12.02	6	79	4	11	22	67
3.9	4.6	3.18	0.70	0.05	13.06	2.74	0.75	13.81	5	79	5	15	19	66
4.2	5.0	1.89	1.00	0.02	8.36	1.20	1.02	9.38	11	54	2	8	21	71
4.1	4.9	1.45	0.56	0.02	8.36	1.34	0.58	8.94	7	70	2	9	18	73
4.3	5.0	0.77	0.78	0.02	8.21	0.80	0.80	9.01	9	50	1	7	16	77
4.6	5.2	0.40	0.80	0.01	4.61	0.26	0.81	5.42	15	24	1	17	19	64

Profile: 17  
 Date: 11-27-93  
 Local: Cruzmaltina  
 Classification: Latossolo Roxo álico (LRa) - Anionic Acrudox  
 Situation: Road cut. Summit. Altitude 675m. Declivity 2%.  
 Soil parent material: Weathered products of underlying rocks  
 Underlying rock: Basalt  
 Local relief: Gently sloping  
 Regional relief: Rolling  
 Erosion: Sheet erosion, sparse, superficial, slightly eroded  
 Drainage: Excessively well drained  
 Vegetation: Tropical forest  
 Actual use: Grasses  
 Climate: Cfa  
 Described by: Antonio C. S. Costa

Horizon	Br*	USA**	Depth (cm)	Color Moist	Texture MD Class	Structure			Consistence			Boundary
						Primary Sh Sz Gd	Secondary Sh Sz Gd		Dry	Moist	Wet	
A	A		0-10	2.5YR 3/2	Hv Cl	Gr Md 2			DH	MFm	WPI/WSl	Cl/Pl
AB1	AB1		10-30	2.5YR 3/2	Hv Cl	SB Md 3			DH	MFm	WPI/WSr	Cl/Pl
AB2	AB2		30-60	2.5YR 3/4	Hv Cl	SB Cr 2			DSH	MFm	WPI/WSl	Df/Pl
Bw1	Bo1		60-100	2.5YR 3/4	Hv Cl	SB VC 1	Gr	VF 3	DSH	MFr	WVP/WVS	Df/Pl
Bw2	Bo2		100-150	2.5YR 3/4	Hv Cl	SB VC 1	Gr	VF 3	DSH	MFr	WVP/WVS	Df/Pl
Bw3	Bo3		150-210	2.5YR 3/4	Hv Cl	SB VC 1	Gr	VF 3	DSH	MFr	WVP/WVS	Df/Pl
Bw4	Bo4		210-250	2.5YR 3/4	Hv Cl	SB VC 1	Gr	VF 3	DSH	MFr	WVP/WVS	Df/Pl
Bw5	Bo5		250-300	2.5YR 3/4	Hv Cl	SB VC 1	Gr	VF 3	DSH	MFr	WVP/WVS	Df/Pl

\* Br (SNLCS, 1988); \*\* USA (Soil Survey Staff, 1993)

Note : Intense pedoturbation throughout the profile. The profile was dry when sampled.

#### Chemical and Physical Characteristics of the Soil.

pH	CaCl <sub>2</sub> H <sub>2</sub> O	C	Exchangeable									Particle Size Distribution		
			Ca+Mg	K	Al+H	Al	S	T	V	Al	P	Sand	Silt	Clay
		%	cmol/Kg									% ----->		
4.0	4.6	3.48	0.94	0.15	11.26	0.72	1.09	12.35	9	40	3	13	17	70
4.0	4.7	2.84	0.76	0.06	11.26	3.22	0.82	12.08	7	80	1	8	20	72
4.2	4.9	1.94	1.30	0.02	9.70	1.80	1.32	11.02	12	58	1	9	15	76
4.2	5.0	1.10	0.46	0.02	7.20	0.80	0.48	7.68	6	63	1	7	16	77
4.4	4.9	0.69	0.40	0.03	5.35	0.82	0.43	5.78	7	66	2	7	14	79
4.4	4.9	0.53	0.62	0.02	4.98	0.84	0.64	5.62	11	57	1	7	12	81
4.4	4.9	0.34	0.56	0.03	4.61	0.74	0.59	5.20	11	55	1	5	15	80
4.3	4.9	0.27	0.50	0.03	4.61	0.76	0.53	5.14	10	59	2	5	21	74

Profile: 18  
 Date: 01/05/94  
 Local: Faxinal  
 Classification: Latossolo Bruno álico (L.Ba) - Humic Hapludox  
 Situation: Road cut. Lower third part of the backslope. Altitude 755m. Declivity 12%.  
 Soil parent material: Colluvium and weathered products of underlying rocks  
 Underlying rock: Rhyolite - andesite  
 Local relief: Strongly steep  
 Regional relief: Rolling  
 Erosion: Sheet erosion, sparse, superficial, not apparent  
 Drainage: Somewhat excessively drained  
 Vegetation: Tropical forest  
 Actual use: Grasses and small trees  
 Climate: Cfa  
 Described by: Antonio C. S. Costa

Horizon	Depth (cm)	Color Moist	Texture MD Class	Structure						Consistence			Boundary		
				Primary			Secondary			Dry	Moist	Wet			
Br*	USA**			Sh	Sz	Gd	Sh	Sz	Gd						
A	A	0-18	5YR 3/4	Hv	Cl	Gr	Cr	2				DSH	DFm	WPI/WSt	CI/PI
AB	AB	18-43	5YR 3/4	Hv	Cl	Sb	Md	2				So	DFr	WPI/WSt	CI/PI
Bw1	Bo1	43-93	2.5YR 4/4	Hv	Cl	SB	Cr	1	Gr	VF	3	So	DFr	WVP/WVS	Df/PI
Bw2	Bo2	93-200	2.5YR 4/4	Hv	Cl	SB	VC	1	Gr	VF	3	DSH	DFr	WVP/WVS	Df/PI
Bw3	Bo3	200-250	auger sampling												
Bw4	Bo4	250-300	auger sampling												

\* Br (SNLCS, 1988); \*\* USA (Soil Survey Staff, 1993)

#### Chemical and Physical Characteristics of the Soil.

pH		Exchangeable										Particle Size Distribution		
CaCl <sub>2</sub>	H <sub>2</sub> O	C	Ca+Mg	K	Al+H	Al	S	T	V	Al	P	Sand	Silt	Clay
		%	cmol <sub>c</sub> /Kg						%		ppm	%		
4.5	5.0	2.97	4.00	0.13	6.21	0.40	4.13	10.34	40	9	2	30	5	65
4.1	4.6	2.82	2.29	0.29	6.69	0.68	2.58	9.27	28	21	1	28	8	64
3.8	4.2	1.43	0.90	0.05	7.20	1.90	0.95	8.15	12	67	1	32	6	62
3.9	4.4	1.17	0.54	0.03	5.76	0.79	0.57	6.33	9	58	1	28	8	64
4.0	4.5	0.73	0.54	0.02	4.61	0.29	0.56	5.17	11	34	2	34	10	54
4.2	4.6	0.42	0.54	0.02	3.97	0.22	0.56	4.53	12	28	1	29	9	62

Profile: 19  
 Date: 01/04/94  
 Local: Faxinal. Inside Pedreira Faxinal Ltd.  
 Classification: Latossolo Bruno álico (LBa) . (Humic Hapludox)  
 Situation: Lower third part of the backslope. Altitude 740m. Declivity 30%.  
 Soil parent material: Colluvium and weathered products of underlying rocks  
 Underlying rock: Rhyolite - andesite  
 Local relief: Strongly sloping  
 Regional relief: Rolling  
 Erosion: Sheet erosion, sparse, superficial, moderately eroded  
 Drainage: Moderately well drained  
 Vegetation: Tropical forest  
 Actual use: Grasses and small trees  
 Climate: Cfa  
 Described by: Antonio C. S. Costa

Horizon Br*	Depth (cm)	Color Moist	Texture MD Class	Structure						Consistence			Boundary	
				Primary			Secondary			Dry	Moist	Wet		
				Sh	Sz	Gd	Sh	Sz	Gd					
	0-20													
	20-40													
	40-60													
	60-80													
	80-100													
	100-120													

\* Br (SNLCS, 1988); \*\* USA (Soil Survey Staff, 1993)

#### Chemical and Physical Characteristics of the Soil.

pH		Exchangeable										Particle Size Distribution			
CaCl <sub>2</sub>	H <sub>2</sub> O	C	Ca+Mg	K	Al+H	Al	S	T	V	Al	P	Sand	Silt	Clay	
		%	cmol <sub>c</sub> /Kg										% <----->		
4.1	4.5	3.09	5.92	0.40	7.76	0.33	6.32	14.08	45	5	8	25	10	65	
3.8	4.2	2.07	2.66	0.09	8.36	1.44	2.75	11.11	25	34	1	22	12	66	
3.6	4.0	1.53	0.82	0.05	9.00	2.10	0.87	9.87	9	71	1	28	11	59	
3.7	4.1	1.36	0.92	0.05	7.20	1.51	0.97	8.17	12	61	1	25	13	62	
3.8	4.2	1.09	0.72	0.05	6.21	0.92	0.77	6.98	11	55	1	27	14	59	
3.9	4.4	0.92	0.60	0.07	5.76	0.50	0.67	6.43	10	43	1	28	19	53	

Profile: 20  
 Date: 01/04/94  
 Local: Faxinal. Inside "Pedreira Faxinal LTD".  
 Classification: Solo Litólico distrófico (Rd) - Lithic Troprothents  
 Situation: Trench on the footslope. Altitude 735m. Declivity 18%.  
 Soil parent material: Colluvium and weathered products of underlying rocks  
 Underlying rock: Rhyolite - andesite  
 Local relief: Strongly sloping  
 Regional relief: Rolling  
 Erosion: Sheet erosion, sparse, superficial, severely eroded  
 Drainage: Moderately well drained  
 Vegetation: Tropical forest  
 Actual use: Grasses and small trees  
 Climate: Cfa  
 Described by: Antonio C. S. Costa

Horizon	Depth	Color	Texture	Structure	Consistence	Boundary
Br* USA**	cm	Moist	MD Class	Sh Sz Gd	Dry Moist Wet	
A	0-20	10YR 6/4	Lm	Gr Md 2	DSH MFr WPI/WSt	Cl/Sm
R	20+	weathered acid rock				

\* Br ( SNLCS, 1988); \*\* USA (Soil Survey Staff, 1993)

#### Chemical and Physical Characteristics of the Soil.

pH	Exchangeable										Particle Size Distribution			
	CaCl <sub>2</sub> H <sub>2</sub> O	C	Ca+Mg	K	Al+H	Al	S	T	V	Al	P	Sand	Silt	Clay
	%		cmol <sub>c</sub> /Kg						%	ppm		%		
4.5	5.0	1.97	4.00	0.13	6.21	0.40	4.13	10.34	40	9	2	25	29	46

Profile: 21  
 Date: 01/04/94  
 Local: Faxinal. "Inside Pedreira Faxinal LTD".  
 Classification: Solo Litólico eutrófico (Re) - Lithic Troporthents  
 Situation: Trench in the backslope. Altitude 735 m. Declivity 25%.  
 Soil parent material: Colluvium and weathered products of underlying rocks  
 Underlying rock: Rhyolite - andesite  
 Local relief: Moderately steep  
 Regional relief: Rolling  
 Erosion: Sheet erosion, sparse, superficial  
 Drainage: Moderately well drained  
 Vegetation: Tropical forest  
 Actual use: Grasses and small trees  
 Climate: Cfa  
 Described by: Antonio C. S. Costa

Horizon	Depth	Color	Texture	Structure	Consistence			Boundary
					Dry	Moist	Wet	
Br* USA**	cm	Moist	MD Class	Sh Sz Gd				
A	A	0-10	7.5YR 6/4	Lm	Gr Md 2	DSH MFr	WPI/WSt	Cl/Sm
R	R	10+	weathered acid rock					

\* Br ( SNLCS, 1988); \*\* USA (Soil Survey Staff, 1993)

#### Chemical and Physical Characteristics of the Soil.

pH	CaCl <sub>2</sub> H <sub>2</sub> O	C	Exchangeable								Particle Size Distribution			
			Ca+Mg	K	Al+H	Al	S	T	V	Al	P	Sand	Silt	Clay
		%	cmol/Kg					% --->		ppm	% ----->			
4.6	5.1	5.50	12.88	0.55	6.21	0.19	13.43	19.64	68	1	3	22	29	49

## **APPENDIX B**

**Soil chemical, physical and mineralogical data**

Soil	Local	Hor	pH CaCl <sub>2</sub>	C (%)	S <==cmol <sub>c</sub> /Kg==>	T	V <==%==>	Al <==%==>	Fed
LR	Cambará-Pr	A	5.3	1.1	7.5	12.11	62	5	12.1
LR	Cambará-Pr	Bw	6	0.33	4.57	8.85	52	8	12.63
LR	Cambará-Pr	60	5.8	0.54	5.92	9.34	63	0	12.49
LR	Campo Mourão-Pr	175	5.5	0.44	nd	nd	nd	nd	17.39
LR	Cascavel-Pr	B22	4.8	0.93	0.52	4.59	11	9	19.20
LR	Cascavel-Pr	60	4.2	1.17	0.19	8.15	2	75	15.69
LR	Faxinal-Pr	60	4	1.79	0.15	10.87	1	87	11.47
LR	Guaira-SP	125	5.1	0.6	0.12	1.82	7	0	nd
LR	Guarapuava-Pr	0-20	4.8	2.74	nd	nd	nd	nd	8.75
LR	Guarapuava-Pr	110	4.6	1.13	nd	nd	nd	nd	7.70
LR	Juranda-Pr	175	5.2	0.58	nd	nd	nd	nd	17.21
LR	Londrina-Pr	60	4.1	0.67	1.74	8.4	21	13	16.37
LR	Londrina-Pr	B22	4.1	0.53	0.72	9.24	8	69	19.58
LR	Maringá-Pr	Ap	4.9	1.53	4.61	10.26	45	9	11.56
LR	Maringá-Pr	Bw	4.5	0.95	0.96	8.19	12	33	10.01
LR	Maringá-Pr	0-20	5.5	1.88	nd	nd	nd	nd	13.74
LR	Maringá-Pr	200	5	0.51	nd	nd	nd	nd	13.75
LR	Palotina-Pr	60	4.0	0.59	2.76	9.62	29	25	9.95
LR	Pato Branco-Pr	Bw	4.1	0.61	2.5	8.71	29	26	9.93
LR	Pato Branco-Pr	200	5.8	0.34	nd	nd	nd	nd	14.31
LR	Pato Branco-Pr	60	3.9	1.34	0.35	11.34	3	85	11.22
LR	Ribeirão Preto-SP	100	5.3	0.5	0.82	2.22	37	0	nd
LR	São Miguel do Iguaçu-Pr	0-20	4.9	2.17	nd	nd	nd	nd	16.29
LR	São Miguel do Iguaçu-Pr	175		0.36	nd	nd	nd	nd	13.42
LR	Vitória-Pr	60	3.9	1.87	0.49	15.68	3	84	7.21

nd = not determined

Chemical characteristics of soil samples. Terms are defined in section 4.2.

Soill	Location	Hor	Mm Gt H			Gt Hm Mm					
			%			Al mole %					
			a	b	c	d	e	e	f	f	g
						d110	d300	d110	d300		
LR	Cambará-Pr	A	21.3	7.6	71.0	nd	4.4	6.9	7.3	10.1	4.7
LR	Cambará-Pr	Bw	13.3	13.2	73.5	20.2	6.2	7.1	9.3	10.4	6.8
LR	Cambará-Pr	60	16.9	14.4	68.7	14.1	4.3	7.1	7.3	10.4	6.2
LR	Campo Mourão-Pr	175	39.7	6.2	54.1	27.2	9.9	9.1	13.4	12.5	10.0
LR	Cascavel-Pr	B22	25.4	26.2	48.4	28.0	9.0	10.3	12.4	13.9	nd
LR	Cascavel-Pr	60	28.2	22.3	49.5	27.4	9.3	11.4	12.8	15.1	12.7
LR	Faxinal-Pr	60	7.0	45.9	47.1	26.7	9.1	11.5	12.6	15.2	10.4
LR	Guafra-SP	125	27.0	10.0	63.0	29.3	10.9	11.4	14.5	15.1	13.5
LR	Guarapuava-Pr	0-20	0.0	98.5	1.5	31.1	nd	nd	nd	nd	nd
LR	Guarapuava-Pr	110	0.0	97.2	2.8	35.7	nd	nd	nd	nd	nd
LR	Juranda-Pr	175	42.8	0.0	57.2	nd	8.6	9.7	12.0	13.3	10.2
LR	Londrina-Pr	60	33.6	0.0	66.4	nd	4.3	7.4	7.3	10.7	6.4
LR	Londrina-Pr	B22	34.9	0.0	65.1	nd	7.5	6.1	10.8	9.2	nd
LR	Maringá-Pr	Ap	29.4	0.0	70.6	nd	5.8	8.2	8.9	11.6	7.6
LR	Maringá-Pr	Bw	31.1	0.0	68.9	nd	5.7	7.5	8.8	10.8	8.3
LR	Maringá-Pr	0-20	23.5	24.3	52.2	23.2	5.6	7.3	8.7	10.6	5.7
LR	Maringá-Pr	200	21.8	24.2	54.0	28.4	6.8	8.0	10.0	11.3	8.8
LR	Palotina-Pr	60	22.6	0.0	77.4	20.3	5.7	6.6	8.8	9.8	6.9
LR	Pato Branco-Pr	Bw	6.5	29.0	64.5	28.3	8.4	9.6	11.8	13.2	14.3
LR	Pato Branco-Pr	200	14.7	26.9	58.4	22.7	6.7	8.8	9.9	12.2	9.3
LR	Pato Branco-Pr	60	14.2	36.0	49.8	23.5	7.3	11.0	10.6	14.7	10.7
LR	Ribeirão Preto-SP	100	34.0	6.0	60.0	27.1	9.5	9.8	13.0	13.4	9.6
LR	São Miguel do Iguaçú-Pr	0-20	28.2	0.0	71.8	nd	5.8	7.8	9.0	11.1	nd
LR	São Miguel do Iguaçú-Pr	175	30.1	0.0	69.9	nd	6.0	8.0	9.2	11.4	7.9
LR	Vitória-Pr	60	0.0	100.0	0.0	35.1	nd	nd	nd	nd	nd

a= (3.5Mm/(3.5Mm+3.5Hm+Gt)); b=(Gt/(3.5Mm+3.5Hm+Gt)); Hm= (3.5Hm/(3.5Mm+3.5Hm+Gt)); d=Schulze (1982, 1984); e = Schwertmann et al., (1979); f= Schwertmann and Lathan (1986); g = Schwertmann and Fechter (1984); nd = not determined

Relative proportion of maghemite (Mm); Goethite (Gt) and Hematite (Hm). Al-substitution within the iron oxides based on X-ray diffraction.